Effect of the overhang length of a recurve seawall in reducing wave overtopping

Estelle Swart

Thesis presented in partial fulfilment of the requirements
for the degree Master of Engineering in the
Faculty of Civil Engineering at Stellenbosch University

Supervisor: Prof JS Schoonees

December 2016

DECLARATION

By submitting this thesis electronically, I declare that the entirety of the work contained therein is my own, original work, that I am the sole author thereof (save to the extent explicitly otherwise stated), that reproduction and publication thereof by Stellenbosch University will not infringe any third party rights and that I have not previously in its entirety or in part submitted it for obtaining any qualification.

Name ……

Date ……

ABSTRACT

With the slow but steady rise in sea level, which is due to global warming, the pressure on the coastal zone across the world has greatly increased. In the past coastal developments have frequently encroached onto the shore, therefore progressively more of these developments have recently come under increasing wave and storm attack, with large portions of the world's coastlines needing protection.

A solution to adequately protect the coastlines under threat would be to increase the crest height of existing seawalls. However, since this would often obstruct the sea view, such a solution would be unacceptable to seaside property owners. The construction of recurve seawalls to reduce overtopping provides a solution, while limiting the obstruction of the sea view.

Historically, seawalls have been used to protect coastlines. Recurve seawalls, where the sea-facing side of the wall is shaped concavely forward to re-direct wave attack back out to sea, were first designed in the 1980s. However, very few guidelines for the design of recurve seawalls are currently available.

Against this background, the current physical model study was conducted with the objectives of quantifying the reduction in wave overtopping in terms of the various geometrical properties of the recurve seawall, such as the overhang length and freeboard height (being the difference between the crest level and water level), and developing design curves for recurve seawalls.

To achieve the objectives of this study, a 2D physical model was designed and built. More than 200 tests were undertaken in order to cover a wide range of water levels and wave periods for nine different recurve seawall designs.

The study found that as the overhang length increases, the reduction in overtopping increases up to a certain point, after which a longer overhang length has no further significance. However, under certain conditions, the 0.3 m overhang length produced worse overtopping reduction results than the vertical wall. Further, a recurve seawall with a parapet angle greater than 50º will not improve the reduction in overtopping, when compared to the results for a vertical wall under similar conditions.

It was concluded that the crest level, in combination with the freeboard level, are critical parameters in the determination of overtopping. It is recommended that the freeboard should be

sufficient so that the incoming wave hits the vertical part of recurve wall. If sufficient freeboard is not available, the recurve wall will be drowned and will not provide any overtopping reduction. A combination of high freeboard and low water levels can produce up to 100% reduction in overtopping.

The repeatability of the tests showed that the accuracy is very good, and significantly better than the data in the CLASH database. Comparison of the measured overtopping with the prediction of the most referenced database, the EurOtop dataset, showed that the EurOtop method should be used with caution.

Additional tests should be conducted to investigate the influence that the beach slope, as well as the wave height, will have on the effectiveness of the recurve wall. Further overhang lengths in a critical area (for example the 0.2 m and 0.4 m overhang lengths), are also required to expand the usefulness of the design guidelines. The stability of the recurve seawalls and of their foundations should also be considered in greater detail.

OPSOMMING

Met die seevlak wat as gevolg van aardverwarming stadig maar geleidelik styg, is daar algaande meer druk uitgeoefen op kussones reg oor die wêreld. Terwyl daar in die verlede dikwels kusontwikkelings tot binne die dinamiese kussone ingedring het, word baie van die ontwikkelings aan toenemende golf- en storm-aanvalle blootgestel en benodig groot dele van wêreld se kuslyne beskerming.

'n Oplossing om die kuslyne in gevaar te beskerm, is om die kruinhoogte van bestaande seemure te verhoog. Alhoewel aangesien so 'n oplossing die see-uitsig in baie gevalle sal belemmer, sal dit onaanvaarbaar wees vir die eienaars van eiendom aangrensend aan die kuslyn. Die bou van terugkaatsmure om die golfoorslag te verminder voorsien 'n oplossing sonder om see-uitsig te belemmer.

Seemure is geskiedkundig gebruik om kuslyne te beskerm. Terugkaatsmure, waar die seewaartse kant van die muur konkaaf vorentoe gevorm is om die golf aanval seewaarts te stuur, is eerste in die 1980s ontwerp. Desnieteenstaande is baie beperkte riglyne vir die ontwerp van terugkaatsmure tans beskikbaar.

Die huidige navorsingsprojek is teen die agtergrond uitgevoer met die doelwit om die vermindering van golfoorslag te kwantifiseer in terme van die meetkundige eienskappe van die terugkaatsmuur – soos die oorhanglengte en die vryboordhoogte (wat die verskil tussen die kruinvlak en die watervlak is) en om ontwerpsriglyne vir terugkaatsmuur te ontwikkel.

Om die bogenoemde doelwitte te bereik, is 'n 2D fisiese model ontwerp en gebou. Meer as 200 toetse is uitgevoer, wat 'n wye reeks watervlakke en golfperiodes insluit vir nege terugkaatsmuur-ontwerpe.

In die studie is daar bevind dat, soos die oorhanglengte van die terugkaatsmuur verleng, verhoog die vermindering in oorslag, maar net tot op 'n punt, waarna die verlenging van oorhanglengte geen verdere effek sal hê op die vermindering van oorslag nie. Vir sekere omstandighede het die 0.3 m oorhanglengte egter 'n kleiner vermindering in oorslag gelewer as die vertikale muur. Verder sal 'n terugkaatsmuur met 'n borswering hoek groter as 50º by dieselfde golftoestande en watervlak nie die vertikale muur se vermindering in oorslag verbeter nie.

Daar is tot die gevind dat beide die kruinhoogte en die vryboordhoogte kritiese parameters is in die bepaling van oorslag. Daar word verder aanbeveel dat die vryboordhoogte voldoende moet wees sodat die inkomende golf die vertikale deel van die terugkaatsmuur sal tref. Indien voldoende vryboord nie reeds beskikbaar is of verskaf kan word nie, sal die terugkaatsmuur versuip en sal dan geen vermindering in oorslag plaasvind nie. ŉ Kombinasie van hoë vryboord en lae watervlak kan egter tot 100% vermindering in oorslag lewer.

Die herhaalbaarheid van die toetse het gewys dat die akkuraatheid baie goed is, en aansienlik beter is as die CLASH data. ŉ Vergelyking van die gemete oorslag met die voorspelling van die mees verwysde datastel, die EurOtop datastel, het getoon dat die EurOtop metode versigtig gebruik moet word.

Addisionele toetse moet gedoen word om die invloed van die strandhelling te ondersoek, asook die invloed wat die golfhoogte sal hê op die effektiwiteit van die terugkaatsmuur. Verder moet oorhanglengtes in ŉ kritiese gebied (byvoorbeeld 0.2 m en 0.4 m) beskou word om die bruikbaarheid van die ontwerpsriglyne uit te brei. Laastens moet die stabiliteit en fondasie van die terugkaatsmure in ag geneem word en in meer detail bestudeer word.

ACKNOWLEDGEMENTS

I would like to acknowledge the contribution of the following people. Without the support and encouragement this would not have been possible.

- My study leader, Prof Koos Schoonees, for your guidance, knowledge and open door throughout my post graduate studies;
- My father, Harry Swart, without your support and guidance I would not have succeeded;
- My mother, Jean Swart, for your continuous moral support;
- Kishan Tulsi, and Talia Schoonees for your willingness to give advice, excitement and motivation to undertake this project;
- Johann Nieuwoudt, Iliyaaz Williams and Marvin Lindoor, for your time, understanding and humour. Thank you for making the laboratory something to look forward to each day.
- Lastly, I thank my friends and family for the support, motivation and assistance in and out of this study.

TABLE OF CONTENTS

LIST OF TABLES

LIST OF FIGURES

LIST OF ABBREVIATIONS AND GLOSSARY

2D	–	Two dimensions
3D	–	Three dimensions
CLASH	–	Crest Level Assessment of coastal Structures and Hazard analysis on permissible overtopping
CPS	–	Circular cum Parabolic Seawall
DWA	–	Dynamic Wave Absorption
Drowned	–	When the freeboard level is low, the recurve wall will not behave as designed.
EPP	–	Equivalent Paddle Position
FSS	–	Flaring Shaped Seawall
Freeboard	–	The difference between the crest level and the water level
JONSWAP	–	Joint North Sea Wave Project
MSE	–	Mean Square Error
NN	–	Neural Network
RMS	–	Root Mean Square
Stratifying water	–	The process of defining layers of different temperatures at various depths in a body of water.
SWL	–	Still water level

NOMENCLATURE

$\propto$	–	Equilibrium coefficient
β	–	Parapet angle as in Table 2.11
γ	–	JONSWAP peak enhancement factor
σ	–	Dimensionless spectral width parameter
σ_0	–	Wave run-up height
λ	–	Height ratio
A, B	–	Empirical coefficients dependent on wave return wall profile in Table 2.5
A_{C*}	–	Dimensionless crest freeboard (m)
A_C	–	Freeboard to the base of the recurve seawall (m)
A_f	–	Adjustment factor
B_r	–	Overhang length
d	–	Diameter of the FSS
D_f	–	Discharge factor
F	–	Fetch length
g	–	Gravitational acceleration (m/s^2)
h_*	–	Impulsiveness parameter
$H_{2\%}$	–	2% wave height (m)
h	–	Water depth of the toe of FSS
h_A	–	Layer thickness at SWL
H_i	–	Incident wave height (m)
H_{MAX}	–	Maximum wave height (m)
H_{m0}	–	Significant wave height (m)

H_r	–	Reflected wave height (m)
H_s	–	Significant wave height at the toe of recurve seawall (m)
h_t	–	Height of parapet
k-factor	–	A factor used to indicate/evaluate the effectiveness of the recurve wall, as defined in Equation 2.12
K_r	–	Bulk reflection factor
L_O	–	Deep water wavelength (m)
P_c	–	Height of vertical part of the wall above SWL (m)
P_s*	–	Dimensionless pressure parameter
ρ_w	–	Density of a fluid
q	–	Mean discharge per metre of seawall [l/s/m]
Q_c	–	Mean discharge per metre of seawall at crest of armoured slope [m^3/s/m]
r	–	Roughness coefficient
R	–	Wave run-up height
R_c	–	Freeboard (m)
R_{cw}	–	Freeboard to the top of recurve seawall (m)
T_m	–	Mean wave period at the toe of recurve seawall (s)
T_P	–	Wave period (s)
v	–	Kinematic viscosity
v_A	–	Wave run-up velocity at SWL
W_*	–	Dimensionless wall height
W_h	–	Height of recurve seawall (m)
WL_{paddle}	–	Water level at the wave paddle (m)
WL_{toe}	–	Water level at toe of structure (m)
X_*	–	Adjusted crest berm freeboard

CHAPTER 1

INTRODUCTION

1.1 Background

In preceding decades, environmental considerations including setback lines were not always deemed important. Structures and roads were often built on sites that today would be classified as environmentally sensitive or vulnerable areas. Furthermore, developers and architects have always wanted to build as close to the water as possible. Consequently, these structures and roads now need to be protected against coastal processes.

In addition, the sea level has been rising in recent decades. These structures already mentioned, as well as structures that were built in sites acceptable in the past, could now be in increasing danger along the coastline. Amongst other threats, these structures are now exposed to wave overtopping, that occurs as the incoming waves hit coastal structures and water travels over the crest of the structure originally built to keep the sea at bay.

Engineering measures are needed to protect these endangered properties and roads. To reduce the wave overtopping at a structure, the initial design approach was to decrease overtopping horizontally, in order to reduce the wave height reaching the structure. There are numerous alternative methods in doing this. For example, the construction of a berm, breakwater, or horizontal reef; or increasing the height of the terrain level. If this cannot be achieved, the alternative is to limit the overtopping in the vertical plane, namely by either increasing the crest level or constructing a recurve seawall.

However, there is pressure from coastal communities to retain the sea view from their properties as far as possible. Although there are more factors that endanger coastal structures, one possible approach to ameliorate this process where space is limited is the construction of a recurve seawall structure. The recurve seawall can either be added to an existing seawall, or incorporated in the design of new protection measures.

This study specifically focused on the reduction of overtopping by means of the optimisation of the recurve seawall design at the back of a beach (Type 3), as further discussed in Chapter

2. Recurve seawalls have been designed to reduce overtopping and limit the amount of water flowing over the crest structure. As the wave hits the structure and water is thrown upward, the wind can cause the uprush and fine spray to be carried over the crest of the structure. For the purpose of this study the effect of wind is excluded.

The application of the recurve structure can be only as successful as the amount of attention given to this area of research. Limited research has been done on the influence that the shape of the recurve wall would have on the rate of reduction of overtopping. Only limited or incomplete design curves are currently available that could assist in the design process for recurve walls (EurOtop, 2007).

1.2 Objectives

The following objectives of this study were identified:

- To quantify the reduction in overtopping on seawalls on beaches by the use of recurve seawalls that do not obstruct the sea view;
- To determine the effect that the overhang length of the recurved seawall has on the reduction of wave overtopping;
- To create design curves for different overhang lengths of the recurve walls;
- To determine to what freeboard height, difference between the crest level and water level, the designs are feasible.

1.3 Methodology

A literature review has been completed in order to obtain a comprehensive understanding of previous and current research on the reduction of overtopping on coastal structures, the design of seawalls and more specifically the design of recurve seawalls.

A set of experiments was undertaken to test the influence of the sea-facing slope of the seawall on the reduction of overtopping rates. An existing curve of the influence of recurve overhang versus overtopping reduction rates was refined by testing more recurve seawall overhang lengths. This was done for a range of maritime conditions during which the wave height was kept constant and the water level, seabed slope, wall height and wave period were varied. For

each slope the maximum functional freeboard height was determined, which would provide a guideline to the height of the recurve seawall structure that had to be constructed.

A few experiments were repeated to ensure that data obtained was accurate and reliable. The results obtained from the experiments were analysed to create a design curve to aid in the process of future design of recurve seawalls, showing the influences the overhang length of the recurve wall has on the overtopping reduction rate. The results obtained have been evaluated against previous research (Allsop, Bruce, Pearson & Besley, 2005); (Schoonees, 2014) to assess whether this comparison has led to insights that can add value to the findings of the present study.

1.4 Report layout and structure

In *Chapter 2*, a literature review is conducted to achieve a comprehensive understanding of wave overtopping, the function of recurved seawalls, the available research on design guidelines and physical modelling of wave overtopping. With the added knowledge gained, the physical model setup is discussed in *Chapter 3*. This includes the measuring equipment, design parameters, testing schedule and scaling procedure. Chapter 4 discusses the results obtained from the physical models, followed by a detailed discussion and analysis of the data in Chapter 5. The proposed design procedure is introduced in Chapter 6. Finally, the conclusions of the research study and recommendations for further research are discussed in Chapters 7 and 8.

CHAPTER 2

LITERATURE REVIEW

2.1 Introduction

This literature study was undertaken, in order to understand all aspects related to wave overtopping, recurve seawalls and physical modelling. The design guidelines for recurve seawalls may be divided into the fundamental principles and recent research.

2.2 Recurve seawalls

2.2.1 Types of seawalls

Recurved walls are used in various cases and in wide application. These were roughly categorised in three groups by Schoonees (2014) namely: large recurved walls, recurve walls on top of sea defence, structures as part of composite sea defences and finally recurved seawall on top of vertical seawalls.

A recurved seawall is also referred to in the literature as a wave return wall, a parapet wall or a bullnose; however, it will be further referred to in this study as a recurve seawall. This investigation focuses on Type 3, as demonstrated in Figure 2.1.

	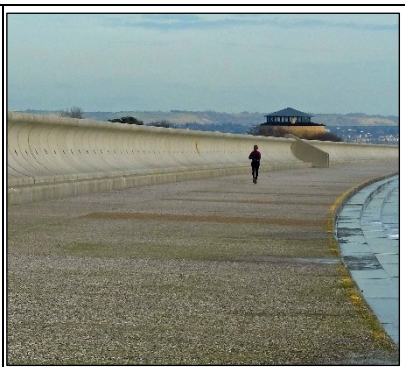	
Type 1: Large recurve wall (Evans, 2015)	Type 2: Recurve wall on top of a structure (Hill, 2014)	Type 3: Recurve wall on top of a vertical wall (Schoonees, 2014)

Figure 2.1: Examples of recurve seawall classification

Further combinations of recurve seawalls in composite structures for example on top of breakwaters, or as used in of erosion protection, are not considered. Practical examples are provided in Annexure A.

Although recurve seawalls are frequently used in sea defence, available research provides limited guidance on the design guidelines to apply or the optimal shape of the recurve seawall.

2.2.2 Recreational uses of recurve wall

The construction of recurve walls occurs typically in environments where a solution is required, which will disrupt the aesthetic as little as possible. This introduces the secondary recreational function of the recurve seawall.

With the use of recurve wall (Type 3) on top of a dike or at the top of seaward a slope, the recurve top functions as a bench, as demonstrated in Figure 2.2.

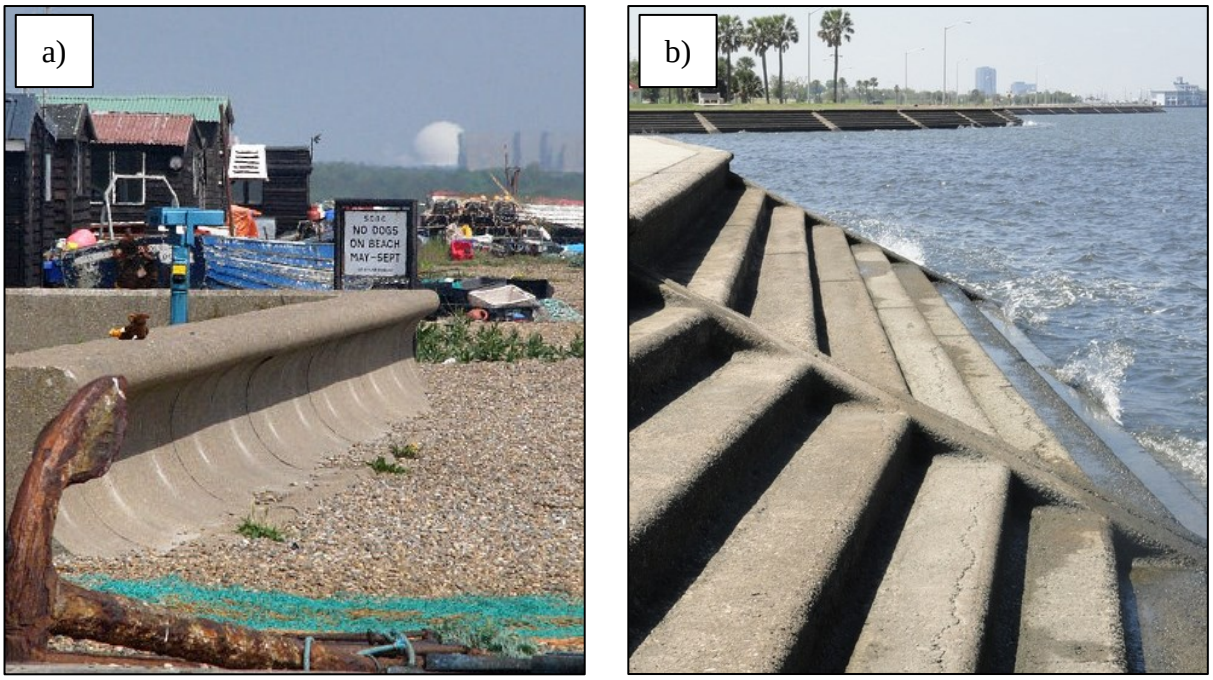

Figure 2.2a: Aldeburgh, UK (Stacey, 2009)
b: New Orleans, USA (Lake Pontchartrain Basin Foundation, 2015)

The large surface on top of the structure can be used for fishing activities. These structures are also designed with a face sloping to the landward side, so that pedestrians can lean over easily without endangering their lives. In case of the Flaring Shaped Seawall it is possible to use the top surface as a promenade for the recreational use of the community.

As this is not the primary function, not much attention is given to additional functions. However, when the structure is required to blend with the environment, additional recreational uses may be considered.

2.3 Overtopping

The purpose of the recurve wall is to reduce the wave overtopping generated by waves colliding with the seawall. This works according to the concept that the wall should project the water volume colliding with it seawards. This results in a more feasible alternative than designing a structure to stop the wave mass. There three types of overtopping are now further discussed (EurOtop, 2007).

2.3.1 Overtopping types

The first type of overtopping occurs when the wave run-up is high enough that the water flows over the crest of the structure, commonly referred to as ‘green water’. The second and most common type occurs with vertical seawalls, as the wave breaks against the seawall, generating large volumes of water splashes also referred to as ‘white water’. The water then either falls back into the ocean or is carried over the crest of the structure by the wind blowing onshore (EurOtop, 2007).

The third type of overtopping, which is often disregarded, is overtopping in the form of spray. The wind carries the fine spray landward over the crest of the structure, as the wave breaks against the seawall.

It should be noted that the water spray can cause local hazards when it occurs with a strong onshore wind (EurOtop, 2007). Extra care should be taken as for water spray is often excluded from estimates of overtopping and adjustment should be made accordingly. Examples of the types of overtopping types are provided in Figure 2.3.

		
Type 1: Green water (Swarzenski, 2014)	Type 2: White water (EurOtop, 2007)	Type 3: Water spray (Mail Online, 2014)

Figure 2.3: Examples of overtopping

According to Bruce, van der Meer, Pullen, and Allsop (2009), when considering vertical walls, three wave conditions occur: non-impulsive/pulsating, impulsive/breaking and broken wave overtopping conditions.

The non-impulsive/pulsating conditions occur when the wave height is relatively small in comparison to the water depth, and they are not easily influenced by the toe or bed slope (Bruce *et al.*, 2009). Figure 2.4 shows the non-impulsive wave sequence.

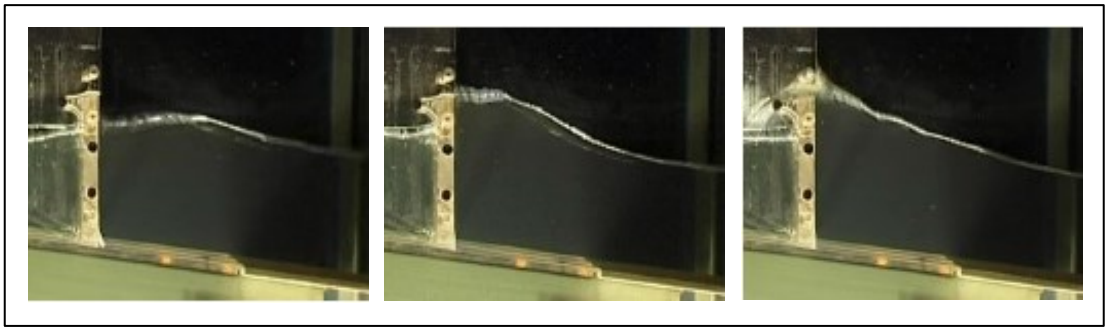

Figure 2.4: Non-impulsive/pulsating wave sequence (Bruce *et al.*, 2009)

The non-impulsive wave sequence results in non-impulsive green water overtopping over the crest of the structure.

Figure 2.5 shows the impulsive/breaking wave sequence, which occurs when the waves are larger in comparison with the water depth at the toe of the structure.

Figure 2.5: Impulsive wave sequence (Bruce *et al.*, 2009)

The impulsive wave sequence, the waves collide violently against the vertical wall. This causes impulsive overtopping condition, as the wave is thrown upward. These conditions can cause forces 10 to 40 times greater than the forces of non-impulsive conditions (Bruce *et al*., 2009).

Finally, the cases that fall between the impulsive and non-impulsive conditions are classified as near-breaking conditions, illustrated in Figure 2.6.

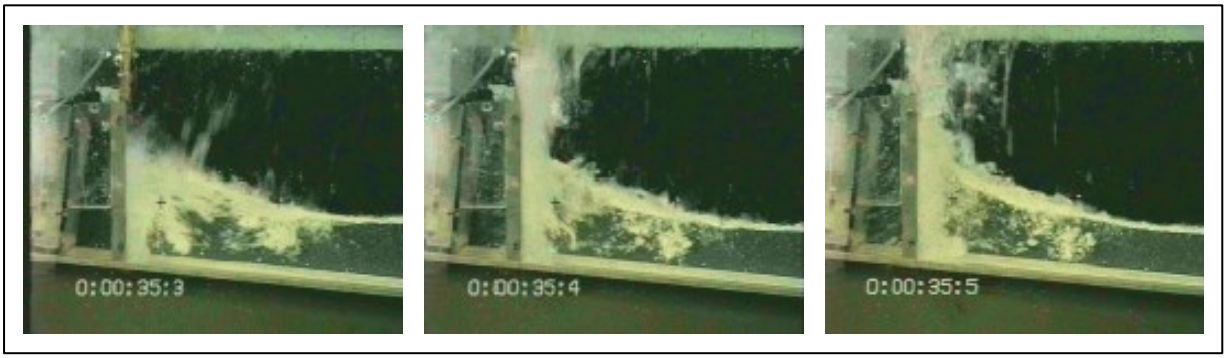

Figure 2.6: Near-breaking sequence (Bruce *et al.*, 2009)

As demonstrated in the figure, the wave breaks before it reaches the vertical wall. These conditions are caused by high-speed waves that are a water mass filled with a high concentration of air. This is treated as impulsive condition as it results in the same magnitude overtopping rate (Bruce *et al.*, 2009).

2.3.2 Overtopping limits

EurOtop (2007) stated that the discharge rate alone is not a good indication as to whether the overtopping is safe or unsafe for pedestrians walking along the seawall. Discharge volume as

an alternative would be a better indicator. However, there is little information available on hazard levels for the wide range of structures used to control overtopping.

Most research on overtopping limits, however, are expressed as discharge, therefore this measure will be used in this study.

The allowable overtopping rates or limits provided in Table 2.1 give a general guidance to what overtopping discharges are tolerable in the specified conditions.

Table 2.1: Permissible overtopping: Pedestrians (EurOtop, 2007)

Pedestrians	**Mean unit discharge q [l/s/m]**
Unsafe for unaware pedestrians relatively easily upset or frightened, with no clear view of the sea, on a narrow walkway or to close proximity to the edge of seawall	q > 0.03
Unsafe for aware pedestrians not easily upset or frightened, that can tolerate getting wet, on a wider walkway with clear view of the sea	q > 0.1
Unsafe for trained staff, well shod and protected, expecting to get wet. Overtopping flows at lower levels only, no falling jet, with a low danger of falling from the walkway	q > 10

The overtopping rate limits for the unaware pedestrians are only applicable if all the conditions are as specified; however, if a few descriptive conditions are missing the general limit should be considered unsafe for unaware pedestrians.

For buildings and infrastructure, the overtopping limits before damage occurs are as demonstrated in Table 2.2.

Table 2.2: Permissible overtopping: Buildings and infrastructure (EurOtop, 2007); (CIRIA, 2007)

Buildings and infrastructure	**Mean unit discharge q [l/s/m]**
No damage	q < 0.001
Minor damage to fittings etc.	0.001 < q < 0.03
Structural damage	q > 0.03
Damage to grassed or lightly protected promenade behind seawall	q > 50
Damage to paved or armoured promenade behind seawall	q > 200

For vehicles, the recommended limits given in Table 2.3 are for two cases delivering a higher and lower limit. The higher limits apply for the case where overtopping causes gradually varying fluvial flow over the road surface.

The lower limits, as given is derived from site data by considering more impulsive flows, with overtopping volumes projected at a speed with abruptness. These should, however, be used cautiously.

Table 2.3: Permissible overtopping: Vehicles (EurOtop, 2007)

Vehicles	**Mean unit discharge q [l/s/m]**
Unsafe for driving at moderate or high speed, impulsive overtopping giving falling or high velocity jets	q > 0.01 - 0.05
Unsafe for driving at low speed, overtopping by pulsating flows at low levels only, no falling jets	q > 10-50

2.3.3 Effects of wind

The wind has an effect not only on the water spray generated in type 3 overtopping, but can also influence the water volume. The wind can dampen or amplify the water jet, change the incident wave profile or modify the shape or angle of physical jet (Allsop, Bruce, Pearson & Besley, 2005).

These processes are difficult to recreate in small-scale tests and, while little information is available on the actual effect, they were omitted for the purposes of this study. The effect of wind on overtopping volume is an additional design constraint that should be carefully considered, for it can cause significant offset if onshore wind is present, or cause over design if offshore wind present (Allsop *et al.*, 2005).

2.4 Design guidelines for recurve seawalls: Fundamental research

2.4.1 Owen and Steele (1993)

Owen and Steele (1993) performed research on two recurve seawall profiles, one profile recommended by Berkeley-Thorn and Roberts (1981) and a second recommended by Owen and Steele (1993). Provided below is the profile developed by Berkeley-Thorn and Roberts (1981) with typical dimensions.

Table 2.4: Berkeley-Thorn and Roberts (1981) recurve wall geometry

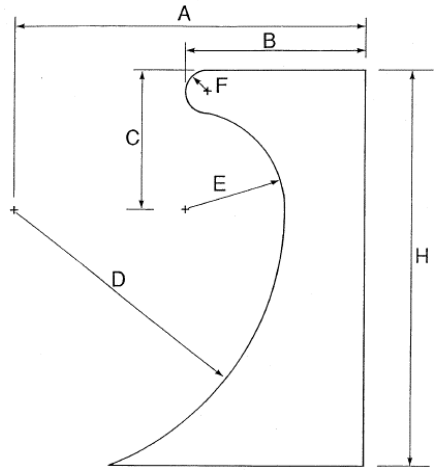

	Prototype parameters (m)				
H	0.61	0.91	1.22	1.52	1.83
A	0.53	0.79	1.05	1.33	1.63
B	0.38	0.5	0.61	0.72	0.84
C	0.33	0.42	0.52	0.6	0.67
D	0.31	0.52	0.75	0.99	1.24
E	0.15	0.23	0.3	0.38	0.46
F	0.1	0.1	0.11	0.11	0.11

This shape is valuable since the curve shoots back the incipient wave at a shallow angle (measuring from the SWL), which reduces the probability of the wave being carried over the crest of the structure in the form of spray (Owen & Steele, 1993).

Incoming waves break on the slope, or on the wall, and reflect back seaward. In reality, these two functions are not mutually exclusive and generally, when both occur, an erosive force, which results in toe protection problems, is found to occur (Berkeley-Thorn & Roberts, 1981). This can be prevented in the design phase, by designing to protect the wall and toe by incorporating a dissipating feature.

Berkeley-Thorn and Roberts (1981) developed a dimensionless height, freeboard and discharge parameter to take into account the varying parameters of each test, to be able to compare the tests against each other. This parameter is derived by Equations (2.1) and (2.2) with specific parameters for site and profile specific constants.

Dimensionless wall height

$$W_* = \frac{W_h}{R_c} \tag{2.1}$$

Dimensionless freeboard on top of recurve seawall

$$R_{*w} = \frac{R_{cw}}{T_m}\sqrt{g\,H_s} \tag{2.2}$$

Owen and Steele (1993) concluded that a recurve seawall is a more efficient alternative to raising the crest of a vertical seawall to the same height. It was also determined that the effectiveness of the recurve seawall is dependent on the dimensionless height and freeboard.

2.4.2 Banyard and Herbert (1995)

The research of Banyard and Herbert (1995) built on the work undertaken by Owen and Steele (1991) on the effectiveness of a recurve seawall. Banyard and Herbert identified that the discharge factor of the recurve seawall is the parameter that has the greatest influence on the overtopping ratio. The seawalls can be grouped in recurve seawalls on impermeable and on permeable slopes.

The process used to obtain the mean overtopping for recurve seawalls on impermeable seawalls is developed by Banyard and Herbert and is shown in Equations (2.3) to (2.8).

$$A_{C*} = \frac{A_C}{T_m\sqrt{g\ H_s}} \quad (2.3)$$

$$Q_{b*} = A\exp(-BA_{c*}) \quad (2.4)^{**}$$

$$Q_b = Q_{b*}T_m\ g\ H_s \quad (2.5)$$

$$W_* = \frac{W_h}{A_C} \quad (2.6)$$

**It should be noted that these equations are only valid when $0.02 < A_{c*} < 0.30$

Where:

A_C – Freeboard to the base of the recurve seawall (m)

H_s – Significant wave height at the toe of recurve seawall (m)

T_m – Mean wave period at the toe of recurve seawall (s)

g – Gravitational acceleration (m/s^2)

A, B – Empirical coefficients dependent on the recurve seawall profile in Table 2.5

W_* – Dimensionless wall height

W_h – Height of recurve seawall (m)

Table 2.5: Banyard and Herbert's (1995) empirical coefficients

Empirical coefficients derived for uniform slope seawalls		
Seaward slope	**A**	**B**
1:1	0.0794	20.1
1:1.5	0.0884	19.9
1:2	0.0939	21.6
1:2.5	0.103	24.5
1:3	0.109	28.7
1:3.5	0.112	34.1
1:4	0.116	41
1:4.5	0.12	47.7
1:5	0.131	55.6

The freeboard is adjusted for the distance of the wall behind the top of the seaward slope by means of applying Equation (2.7). With the adjusted freeboard calculated, the discharge factor is acquired with the use the graph illustrated in Figure 2.7.

$$X_* = A_f A_{C*} \tag{2.7}$$

$$Q = Q_b D_f \tag{2.8}$$

Where:

Q_b – Base discharge ($m^3/s/m$)

A_f – Adjustment factor, refer to Table 2.6

D_f – Discharge factor in Figure 2.7

Research by Besley (1999) determined that if the dimensionless relative wave return height W_* is 0.55 and, at high A_{C*}, the recurve wall provides good reduction in overtopping rate. However, at a low A_{C*}, the water level will raise to the curved section of the recurve wall. The recurve wall will not be as effective and become *drowned* (Besley, 1999).

Table 2.6: Banyard and Herbert's (1995) adjustment factors

$W_h/A_C \geq 0.6$			$W_h/A_C < 0.6$		
Seawall Slope	**Crest berm width (C_W)**	**A_f**	**Seawall Slope**	**Crest berm width (C_W)**	**A_f**
1:2	0	1	1:2	0	1
1:2	4	1.07	1:2	4	1.34
1:2	8	1.1	1:2	8	1.38
1:4	0	1.27	1:4	0	1.27
1:4	4	1.22	1:4	4	1.53
1:4	8	1.33	1:4	8	1.67

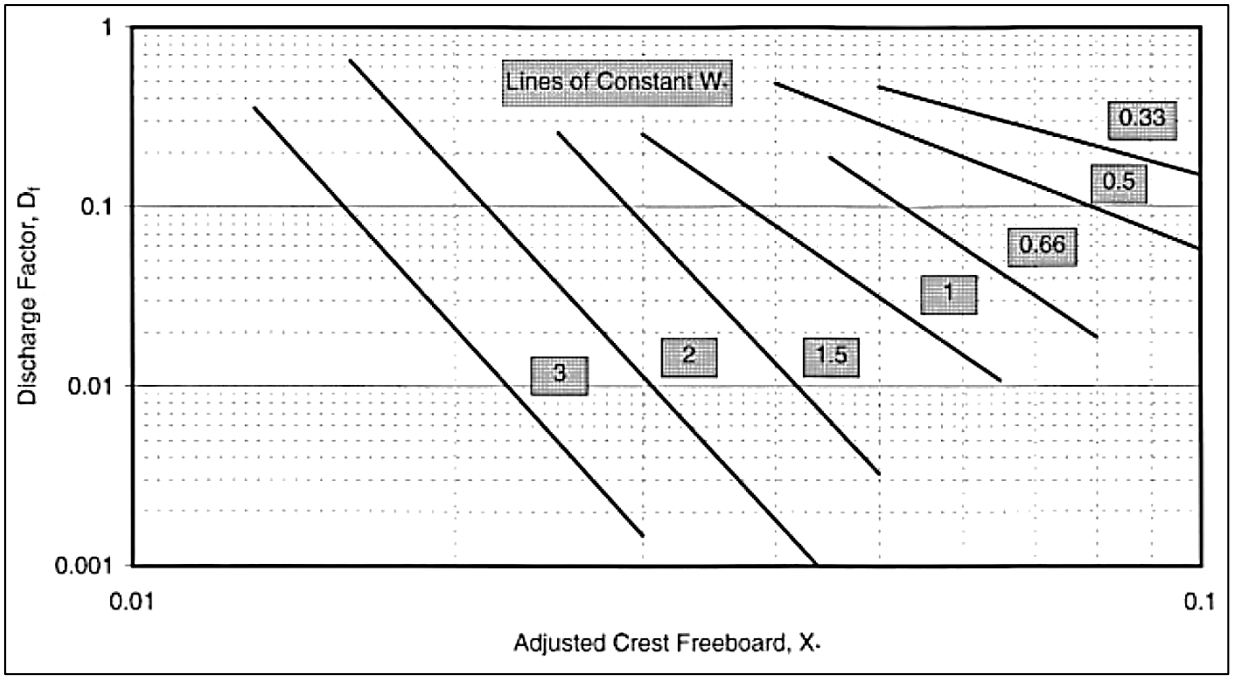

Figure 2.7: Discharge factor for impermeable slopes (Banyard & Herbert, 1995)

Research by Bradbury and Allsop (1988) proved that a crown wall on top of a permeable crest is more effective than an impermeable crest. The datasets were reanalysed, which resulted in a design graph plotting the discharge factor (D_f) against the base discharge (Q_C^*), which comprises of various factors. This follows the similar process to that used to determine the discharge factor for impermeable slopes and makes use of Equations (2.3), (2.5) and (2.6).

The process to obtain the mean overtopping for recurve seawalls on impermeable seawalls is developed by Banyard and Herbert (1995) in Equation (2.9) to (2.11).

$$Q_{b*} = A \exp\left(\frac{-BA_{c*}}{r}\right) \quad (2.9)^{**}$$

$$Q_c = C_r Q_b \quad (2.10)$$

$$Q = Q_c D_f \quad (2.11)$$

** It should be noted that these equations are only valid when $0.02 < A_{c*} < 0.30$

Where:

r – Roughness coefficient

D_f – Discharge factor in Figure 2.8

Q_c – Mean discharge per metre of seawall at crest of armoured slope [$m^3/s/m$]

These two processes may be followed in reverse to determine what reduction in overtopping can be expected with any selected design for a wave return recurve wall.

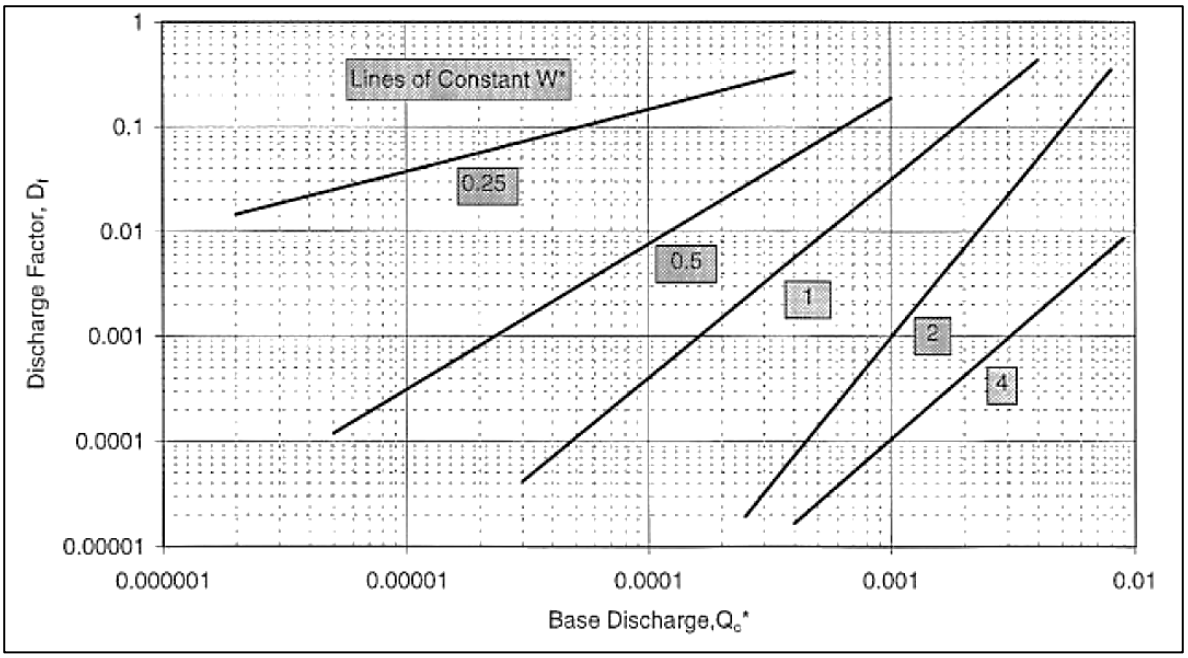

Figure 2.8: Discharge factor for permeable slopes (Banyard & Herbert, 1995)

2.4.3 Clifford (1996)

The recurve profile developed by Berkeley-Thorn and Roberts (1981) was used in this study. The parameters are provided in the definition sketch, Figure 2.9 (Clifford, 1996).

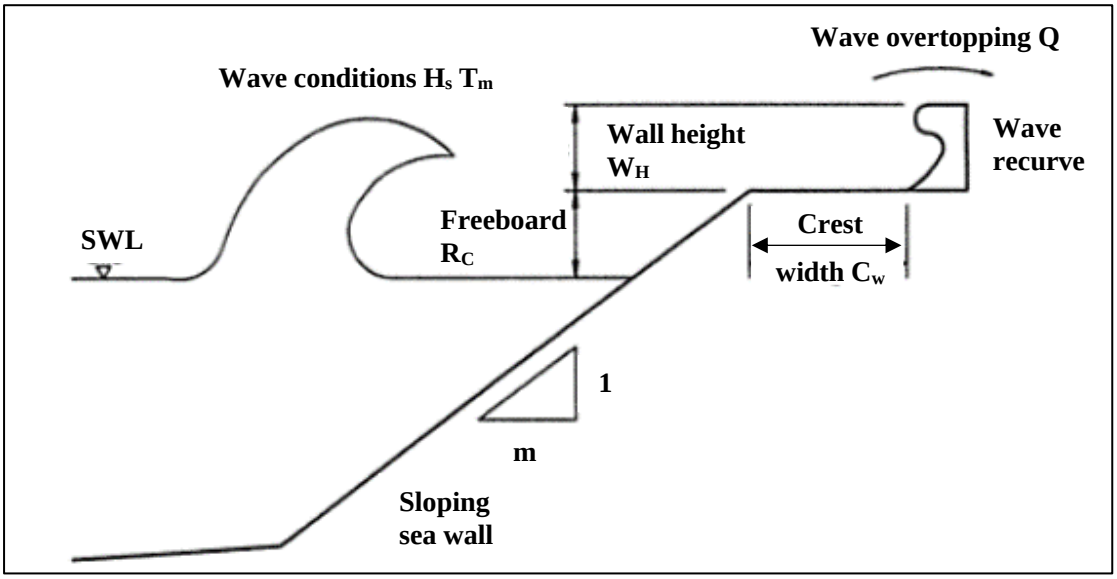

Figure 2.9: Clifford (1996) definition sketch

The recurve walls can be located either on top of the seaward slope (with C_W = 0), or a few meters to the back of it, to create a promenade on the width of the crest. The tests were performed with two different seaward slopes, 1:2 and 1:4.

The adjustments to the crest berm freeboard (R_*) necessary to correlate the various tests, depending on the ratio of wall height (W_h) to freeboard height (R_c) are provided in Table 2.7.

Table 2.7: Crest berm freeboard adjustment factors (Clifford, 1996)

Seawall slope	**Crest width C_w**	$\frac{W_h}{R_C} \geq \frac{2}{3}$	$\frac{W_h}{R_C} \leq \frac{1}{2}$
		Adjustment factor A_f	**Adjustment factor A_f**
1:2	0	1	1
1:2	4	1.07	1.34
1:2	8	1.1	1.38
1:4	0	1.27	1.27
1:4	4	1.22	1.53
1:4	8	1.33	1.67

The adjusted crest berm freeboard (X_*) is plotted against the discharge factor in Figure 2.10 as illustrated in Equations (2.1) and (2.7). The result graphs are setup with the known parameters for the ease of the designer.

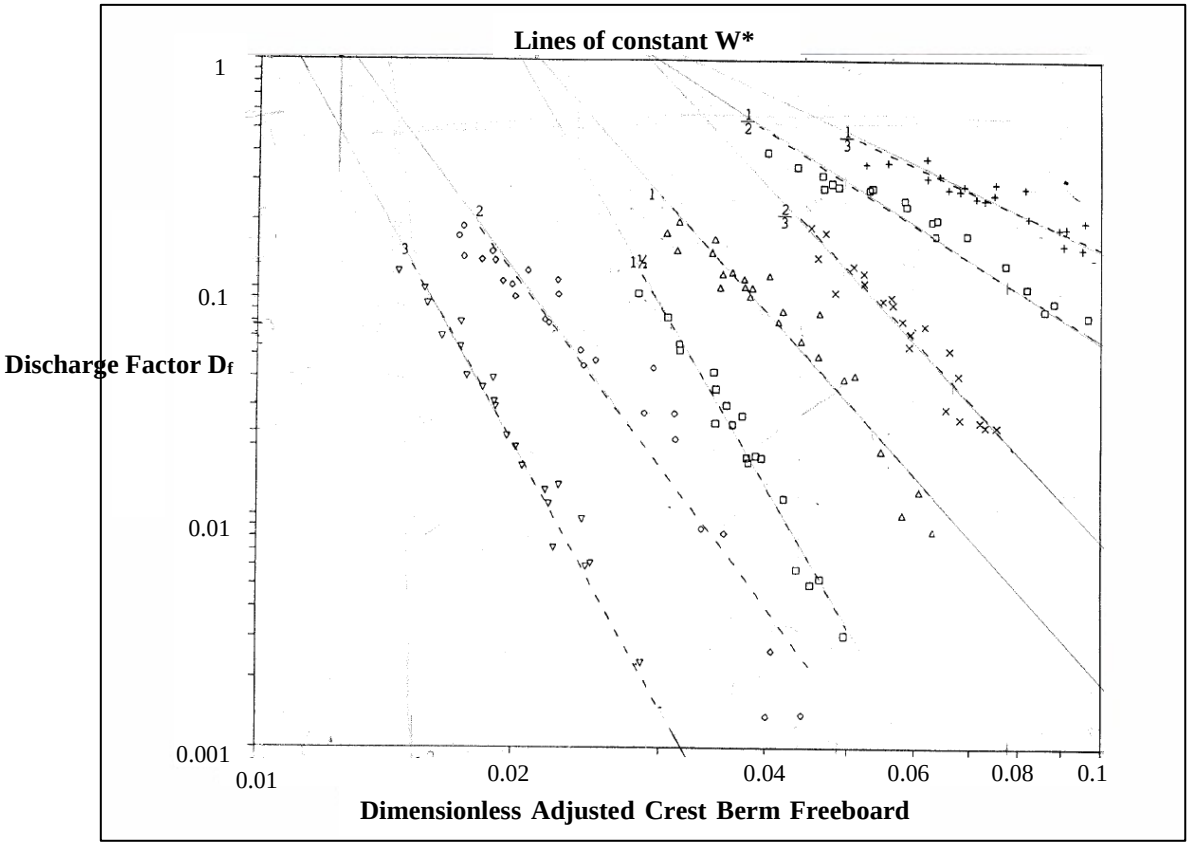

Figure 2.10: Adjustment discharge factors (Clifford (1996) adapted by author)

2.5 Design guidelines for recurve seawalls: Recent studies

2.5.1 CLASH

The Crest Level Assessment of coastal Structures by full-scale monitoring, neural network prediction and Hazard analysis on permissible wave overtopping (CLASH) project, was initiated by the European Union to gather information regarding wave overtopping. The focus is on the prediction and the actual behaviour of overtopping in physical models, for a wide range of coastal structures. These investigations were done both on large scale and in laboratory conditions.

The main objectives are to determine scale effects and to create an overtopping prediction method based on Neural Networks (Van Gent, Pozueta, Van den Boogaard & Medina, 2005).

The CLASH database comprises of 31 parameters: 17 structural parameters, 11 hydraulic parameters and three general parameters, which were all screened before being included in the database. Approximately 1000 tests were excluded by the screening process, which was a crucial process designed to ensure data entered in the databases is accurate in order to achieve

the best possible results. The CLASH database now consists of 10 000 wave overtopping test results performed on a wide range of structures.

This has resulted in certain tests being used to generate an empirical method to predict wave overtopping. This prediction was made by an artificial neural network (NN), an algorithm that uses a large database to estimate the overtopping generated by specified wave conditions. The use of a neural network is recommended when a large amount of data needs to be analysed and when the dataset is dependent on more than one parameter (Allsop, Pullen, van der Meer, Bruce, Schüttrumpf & Kortenhaus, 2008).

If not enough data is available, the NN would extrapolate between the two available data points. This would deliver an unreliable overtopping estimation and not the preferred method.

Similarly, the quality and accuracy of the input parameters determine the quality and the accuracy of the output (Allsop *et al.*, 2008). Allsop, *et al.* (2005) recommended that a minimum of 15 parameters be used for input to deliver a reliable overtopping estimation.

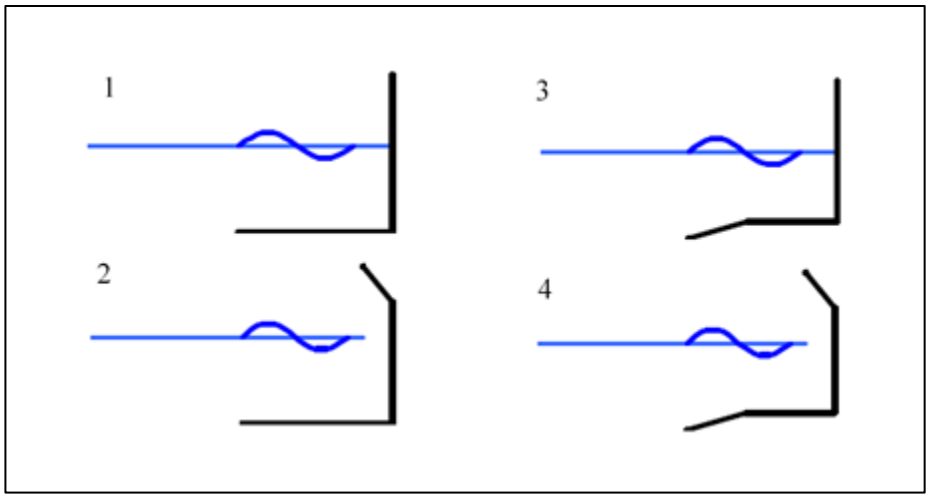

Figure 2.11: Neural Network structure configurations (Allsop *et al.*, 2008)

Demonstrated in Figure 2.11 are the types of structure configurations a neural network is based on. Kortenhaus, Haupt and Oumeraci (2002) investigated the influence the recurve has on the overtopping reduction (Figure 2.11 Structure 1 and 2), with the aim of developing a generic method. Overtopping analyses were performed with input from a wide variety of types of recurve seawall structures.

Another method to estimate wave overtopping is the empirical method developed by the VOWS project by Allsop *et al.* (2008). The EurOtop Overtopping Manual (2007) provides the public with an online estimation tool to determine the overtopping rate that can be expected for certain composite seawalls.

On the online form, the user provides similar geometric parameters to those required for the use of the neural network. The interface of the vertical wall and the vertical wall with wave return is demonstrated in Annexure E.

A k-factor is used to evaluate the effectiveness of the recurve wall, which is defined by equation (2.12).

$$k = \frac{q_{with\ recurve}}{q_{without\ recurve}} \tag{2.12}$$

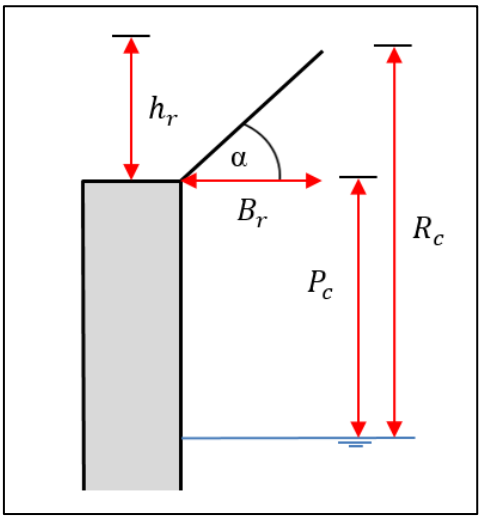

Figure 2.12: CLASH parapet definition sketch
Regenerated by author (Kortenhaus, Haupt & Oumeraci, 2002)

Initial research by Kortenhaus, Haupt and Oumeraci (2002), adjusted by the k-factor, produced good results for the recurve walls tests that were conducted for lower freeboard cases.

Further research was conducted by Kortenhaus, Pearson, Bruce and Allsop (2004), to investigate what occurs at higher freeboard levels. It was determined that, as the water level rises to the height of the recurve wall, the recurve seawall is not as effective, because the water volume is no longer being captured and or trapped under the recurve wall (Kortenhaus *et al.*, 2004).

Figure 2.13 is a decision chart developed by Allsop, Bruce, Pearson and Besley (2005) to extend and refine the generic method recommended by Kortenhaus *et al.* (2004).

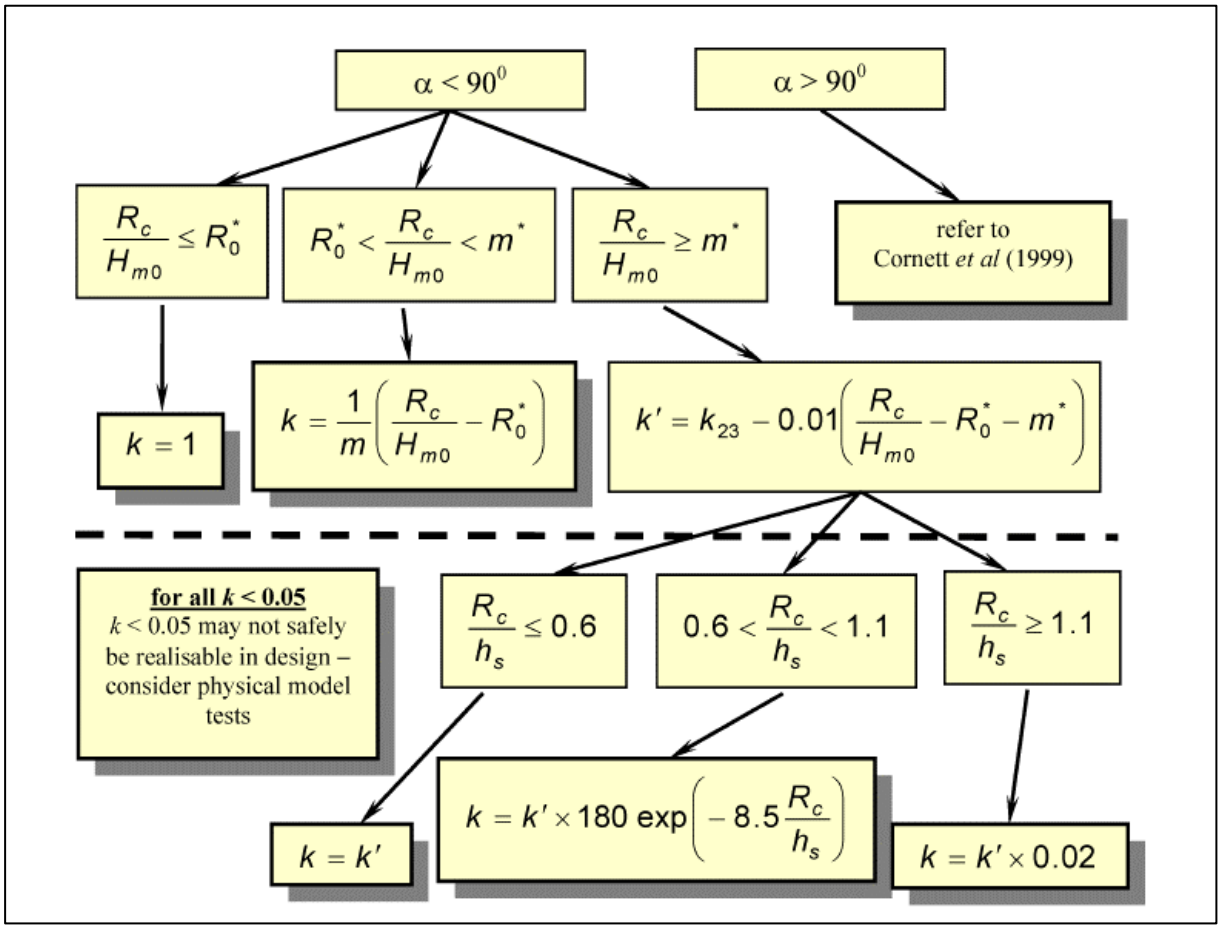

Figure 2.13: Generic method decision chart (Allsop *et al.*, 2005)

Where:

$$R_0^* = 0.25\frac{h_r}{B_r} + 0.05\frac{P_c}{R_c} \tag{2.13}$$

$$m^* = m(1 - k_{23}) \qquad k_{23} = 0.2 \tag{2.14}$$

$$m = 1.1\sqrt{\frac{h_r}{B_r}} + 0.2\frac{P_c}{R_c} \tag{2.15}$$

The decision chart and Equations (2.13) to (2.15) are validated for simple recurve profiles. The generic method is difficult to follow when the recurve profile is a complex structure, where the parameters become difficult to distinguish.

The method proposed by Kortenhaus, Haupt and Oumeraci (2002) under-predicts the reduction factors for high overtopping rates and delivers conservative overtopping reduction factors for low overtopping rates.

To improve this method and reduce the scatter, the large CLASH database was evaluated in combination with the VOWS project and no general trend emerged. Kortenhaus, Pearson Bruce and Allsop (2004) concluded that it is not possible to find a generic method. However, in order to determine a reduction factor approach for recurve seawalls, the results were grouped by their geometry, size and form. Kortenhaus *et al.* (2004) analysed photographs and videos to isolate the key physical process that reduce overtopping volumes.

The CLASH database data is often analysed by plotting the dimensionless overtopping parameter against the freeboard over significant wave height.

$$Dimensionless\ overtopping\ parameter = \frac{Q}{\sqrt{g\ {H_{mo}}^3}} \tag{2.16}$$

The scatter was not completely removed, which had been expected to some extent, considering the wide range of geometries that was compared. The approach of Kortenhaus *et al.* (2004) delivered conservative reduction factors, which indicate an overestimation of predictive reduction factors, and Kortenhaus *et al.* (2004) finally concluded that the level of the reduction factor is dependent on the magnitude of overtopping.

2.5.2 Flaring Shaped Seawall (FSS) (2003-2007)

The Flaring Shape Seawall is a deep circular seawall profile that was developed by Murakami, Irie and Kamikubo (1996) to completely withstand wave overtopping, by reflecting incoming waves back into the ocean. With the deep circular cross-section of the FSS as demonstrated in Figure 2.14, the crest level can be lower than for a vertical seawall. Additionally, there would be a large recreational area on top of the FSS.

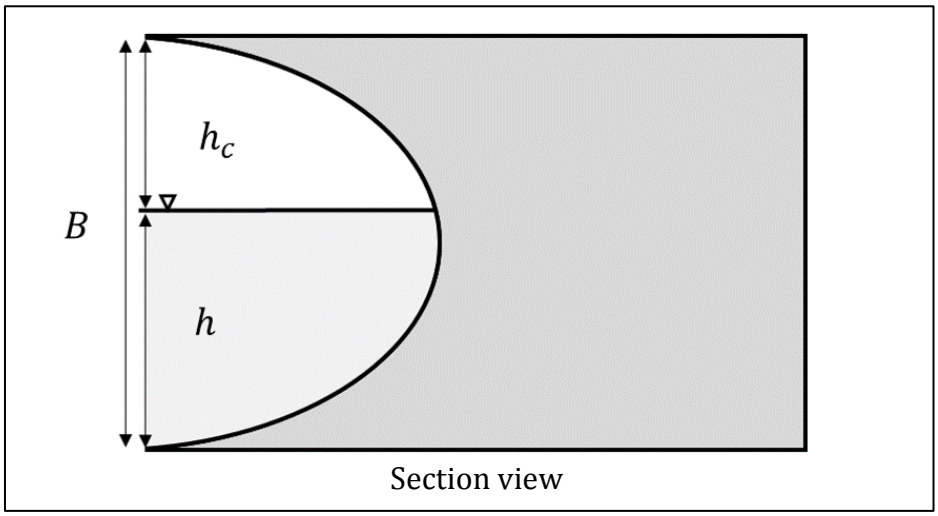

Figure 2.14: FSS definition illustration
Regenerated by author: (Kamikubo, Murakami, Irie, Kataoka & Takehana, 2003)

Murakami, Kamikubo and Takehana (2004) investigated the wave overtopping, reflection and the forces that were generated by the FSS. Critical crest evaluation was done for the four different FSS shapes that were tested with a constant crest level height for each, as shown in Table 2.8.

Table 2.8: FSS geometrical properties of experiments

FSS Geometrical properties		
B	225	mm
h	100, 150	mm
d	75, 150, 300	mm
H_{mo}	40, 60, 70, 80, 90	mm
L_O	1.1-7.5	m

It was determined by Murakami *et al.* (1996), that an FSS with a deep arc, in comparison to the incident wavelength, is effective for the reduction of wave overtopping. The point where the maximum pressure occurs on the FSS is just below the still water level (SWL).

Anand, Sundar and Sannasiraj (2010) investigated two types of recurve seawall namely a Flaring Shaped Seawall (FSS) recommended by Kamikubo *et al.* (2003), and a curved seawall

shape (CPS) investigated by Weber (1934). The focus of this study was the magnitude and location the pressure induced by the waves breaking against the seawall.

The tests were administered for a T_p of 1 and 3 seconds with a varying depth of 0.88 and 1 m (model values). The two different profiles are provided in Figure 2.15 indicating the locations the pressure transducers situated on the seawalls.

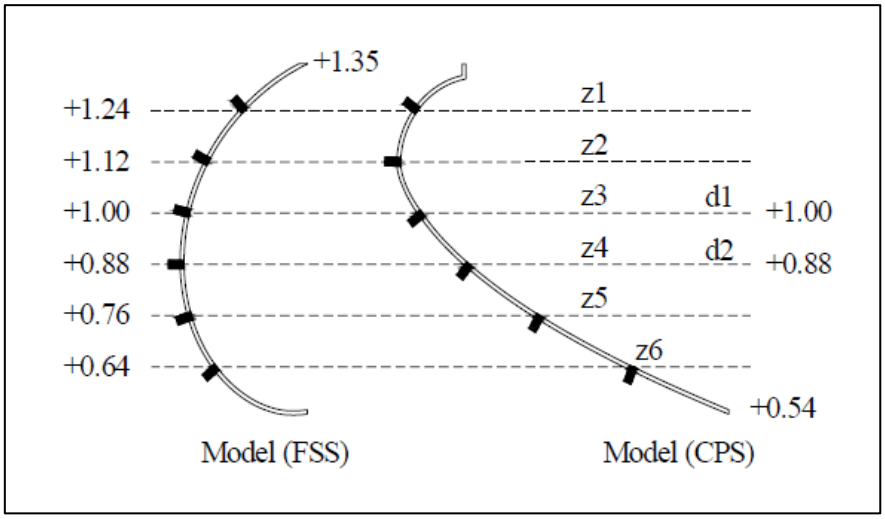

Figure 2.15: Pressure transducers on FSS and CPS profiles (Anand, Sundar & Sannasiraj, 2010)

Kamikubo *et al*. (2003) validated that the location on the profile where the greatest pressure was induced was just below the SWL. Plotting a dimensionless pressure parameter P_s ∗ the FSS experienced the largest pressures just below the SWL, delivering lower velocities. From that it was concluded that the FSS would have the least amount of scouring at the toe of the structure (Anand *et al.*, 2010). In the comparison of the two profiles, the FSS outperformed the CPS delivering no overtopping of waves.

Depending on the seabed profile or the sea depth, a rubble mound structure is required at the bottom of the structure (Murakami, Kamikubo & Kataoka, 2008). This is to dissipate energy and to tilt the incoming waves towards the structure.

Further research was employed to determine the effect that a vertical wall on top of the FSS would have on the amount of water spray that would move over the crest of the structure. As demonstrated in Figure 2.16, the FSS both with and without a crown wall was tested to compare the efficiency of each in the reduction of overtopping (Kamikubo *et al.*, 2003).

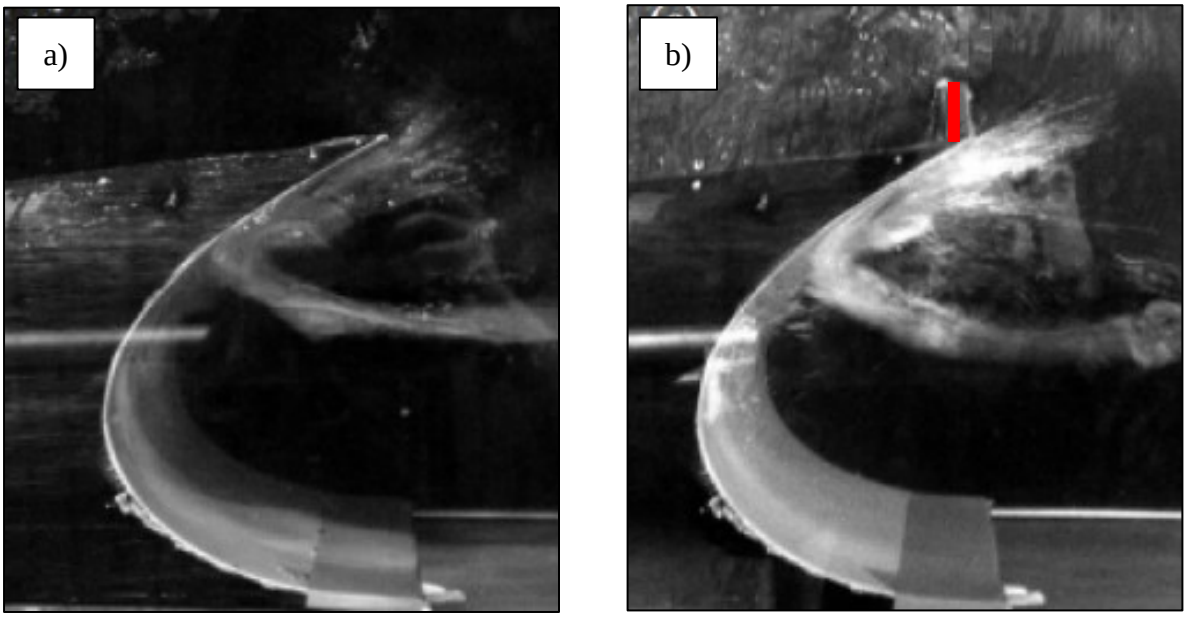

Figure 2.16a: FSS, b: FSS with vertical wall on top of structure (Kamikubo *et al.*, 2003)

Kamikubo *et al.* (2003) determined that the FSS outperformed a vertical upright seawall. It could further be concluded that the volume of water spray travelling across FSS crest significantly decreased when a crown wall was constructed on the top of the structure.

Murakami, Maki and Takehana (2011) conducted research with 11 FSS units to determine the effect of oblique wave attack on wave overtopping. This study concluded that the FSS improves the overtopping reduction performance of a vertical wall for oblique wave attack. A further conclusion was that the FSS is more efficient for short wave periods (Murakami *et al.*, 2011).

2.5.3 Allsop *et al.* (2005)

Allsop *et al.* (2005) did research mainly on the behaviour of overtopping of vertical walls. According to Allsop *et al.*, for vertical walls it is critical to determine whether the wave condition is pulsating or non-pulsating, to determine how to further assess the overtopping results. The impulsiveness parameter is defined by using Equation (2.17) and classified in Table 2.9.

$$h_* = 1.3 \frac{h_s \ \ 2\pi h_s}{H_{mo}\, g\, T_{m-1,0}^2} \tag{2.17}$$

Table 2.9: Classification of impulsiveness parameter (Allsop *et al.*, 2005)

Classification of h_*	
$h_* < 0.2$	Impulsive conditions
$0.2 < h_* < 0.3$	Breaking and non-breaking waves
$h_* > 0.3$	Non-impulsive conditions

It was determined that for the non-impulsive case, vertical walls with no freeboard (R_c = 0 m), the dimensionless overtopping parameter (Equation 2.16) can be used as 0.062 for probabilistic design purposes.

Allsop *et al.* (2005) recommended that for deterministic or safety assessment the dimensionless overtopping parameter should be taken as 0.068. Figure 2.17 is a comparison of CLASH datasets for the non-impulsive condition for a vertical wall.

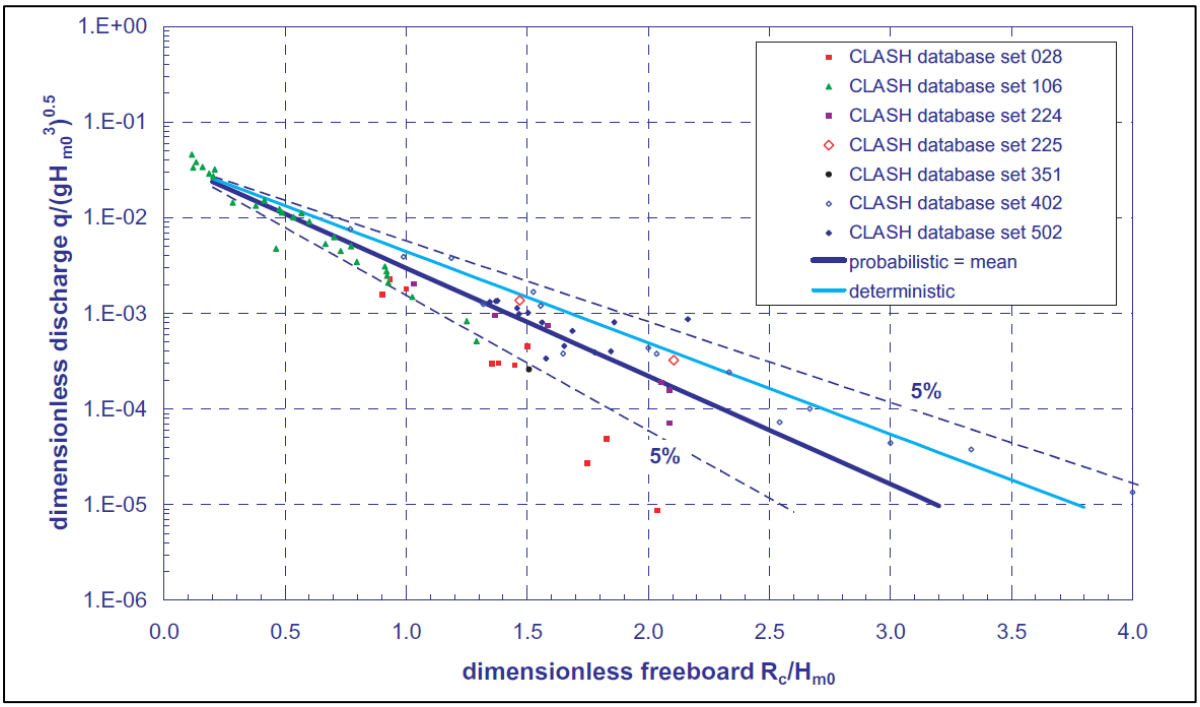

Figure 2.17: Non-impulsive condition for a vertical wall (Allsop *et al.*, 2005)

By extending the probabilistic trend from Figure 2.17 (indicated as the dark blue line), the trend line crosses the Y-axis with a dimensionless overtopping parameter of 0.04.

Allsop, Alderson and Chapman (2007) conducted research to reduce the overtopping along the coastline for both residential and commercial regions where the space was limited, to mitigate

the risk of property damage. Two recurve walls, as demonstrated in Figure 2.18, were investigated and their performances were compared with those of vertical seawalls.

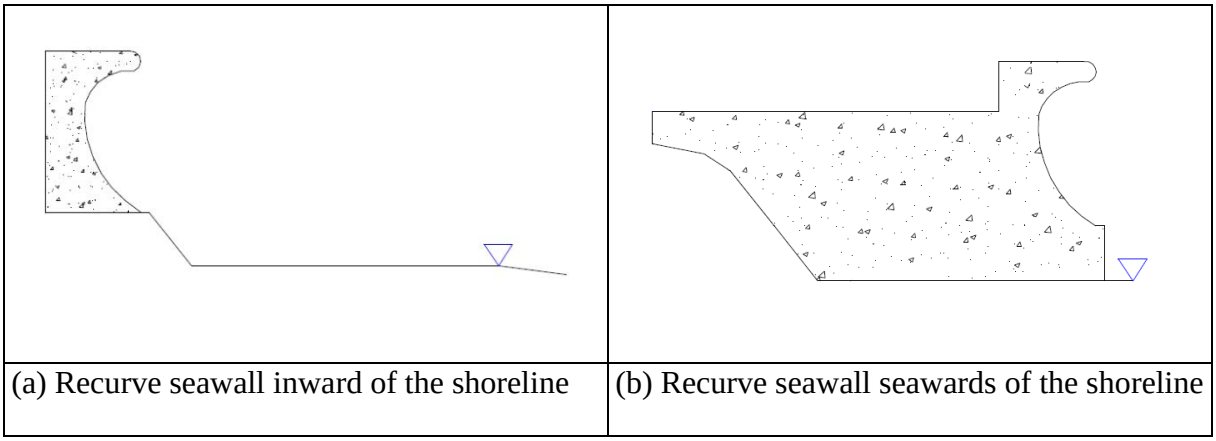

(a) Recurve seawall inward of the shoreline

(b) Recurve seawall seawards of the shoreline

Figure 2.18: Allsop *et al.* (2007) design profiles

The physical model results determined that the recurve walls would outperform the vertical walls; however, additional splash guards might be required if 0% overtopping is required.

The recurve wall inland of the shoreline (Figure 2.18 a) in comparison with the vertical walls proved to reduce the overtopping from two to nine times.

From this investigation it was concluded that if a recurve wall was positioned seaward, there should not be a vertical face for waves to break against, because the water then bypasses the recurve and the recurve wall acts as a vertical wall. This can be prevented by the construction of an angled wall below the recurve, creating a smooth transition to guide the water to fill the recurve (Allsop *et al.*, 2007).

From this investigation it was determined that in the design of the recurve seawall it is important to ensure that the recurve wall projects the overtopped water beyond the breaking point of the incoming waves, otherwise the projected water can be trapped in breaking waves and cause an air pocket to form (Allsop *et al.*, 2007).

2.5.4 Van Doorslaer and De Rouck (2011)

Van Doorslaer and De Rouck (2011) performed research on the modification of vertical walls on top of dikes in order to optimise the reduction in wave overtopping. A nose was added to the vertical wall, as demonstrated in the figure below, without increasing the total height of the parapet (h_t), to reflect water back into the sea instead of projecting water over the structure.

This paper investigates the effects that parapet nose angle and the height ratio $\lambda = \frac{h_n}{h_t}$ have on the reduction of wave overtopping rates. This is applicable only to a parapet constructed on top of smooth dike with a slope of 1:2 (V:H). The variations in geometrical properties that were tested are shown in Table 2.10.

Table 2.10: Van Dooslaer and De Rouck's definition sketch and parameters

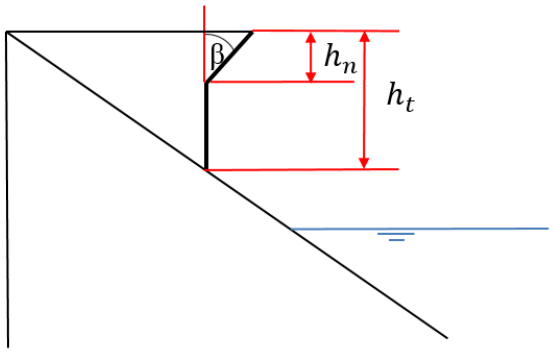

Geometrical properties		
h_t	20, 50, 80	mm
$\beta_{(1)}$	15, 30, 45, 60	°
λ	0.125 - 1	-

(1) Note that in this figure β is measured from the vertical axis

The results of the tests of the parapets, each with a vertical wall (VW) with a height of 50 mm, grouped by their nose angle, are provided in Figure 2.19. The dimensionless overtopping rate, as provided in Equation 2.17, is plotted against the dimensionless freeboard. Indicated on the Figure 2.19 is the correlation coefficient relating to each parapet nose angle.

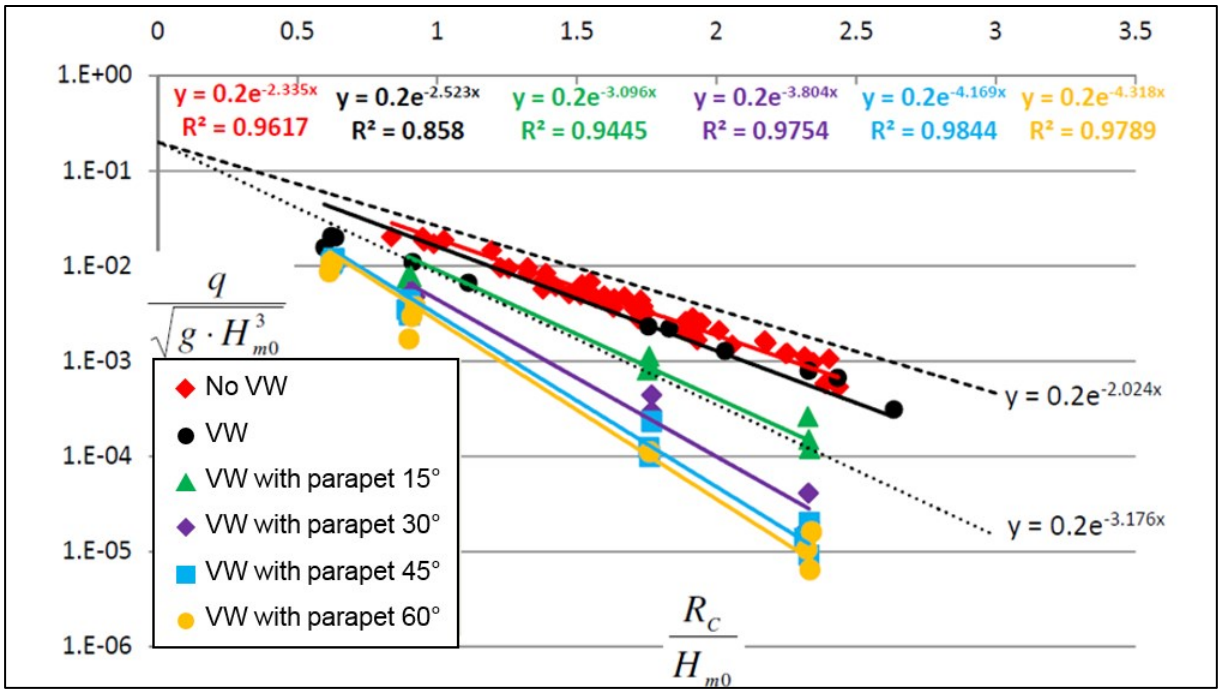

Figure 2.19: Sensitivity of parapet nose angle
(Van Dooslaer & De Rouck (2010) adapted by author)

The figure highlights that the 45° and 60° parapet angles deliver approximately the same reduction in overtopping. However, when considering the reduction factor versus the nose angle, it was determined that when the nose angle becomes greater than 50° it performs the same as a vertical wall.

From the investigation conducted by Van Dooslaer and De Rouck (2010) it was validated that a parapet with the same crest height as a smooth dike with no vertical wall improved the overtopping rates significantly. It was determined that a parapet with a nose angle of 45° performed the best, and a λ ratio of 1/3 is recommended.

It was also determined that a parapet with a ratio of $\frac{h_t}{R_c} < 0.25$ behaves differently, and a modified equation was suggested to predict overtopping in such cases. The individual conditions are difficult to isolate, making it almost impossible to determine which geometrical condition is responsible for any variation in results.

2.5.5 Veale *et al.* (2012)

Veale, Suzuki, Verwest, Trouw and Mertens (2012) investigated the optimal parapet geometry to reduce wave overtopping for the existing sea dike at Wenduine, Belguim. This reduction in overtopping must be accomplished while keeping the crest level of the dike as low as possible. Veale *et al.* (2012) used the recommendations of Van Doorslaer and De Rouck (2011), and investigated a parapet with a nose angle of 50°, resulting in approximately 150 wave overtopping tests. Figure 2.20 shows is the three profiles investigated by Veale *et al.* (2012).

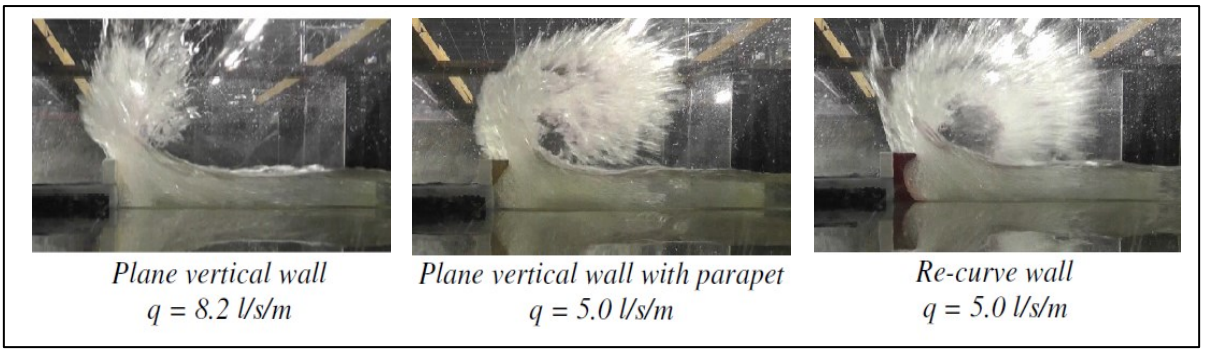

Figure 2.20: Experiment profiles (Veale *et al.*, 2012)

Note that in this study the parapet is a triangle fitted to vertical wall and Re-curve refers to the recurve shape as demonstrated in Figure 2.20.

As demonstrated in Figure 2.21 the seawall in position B performs slightly better than at position A; however, the combination of both positions outperforms either of the other design configurations.

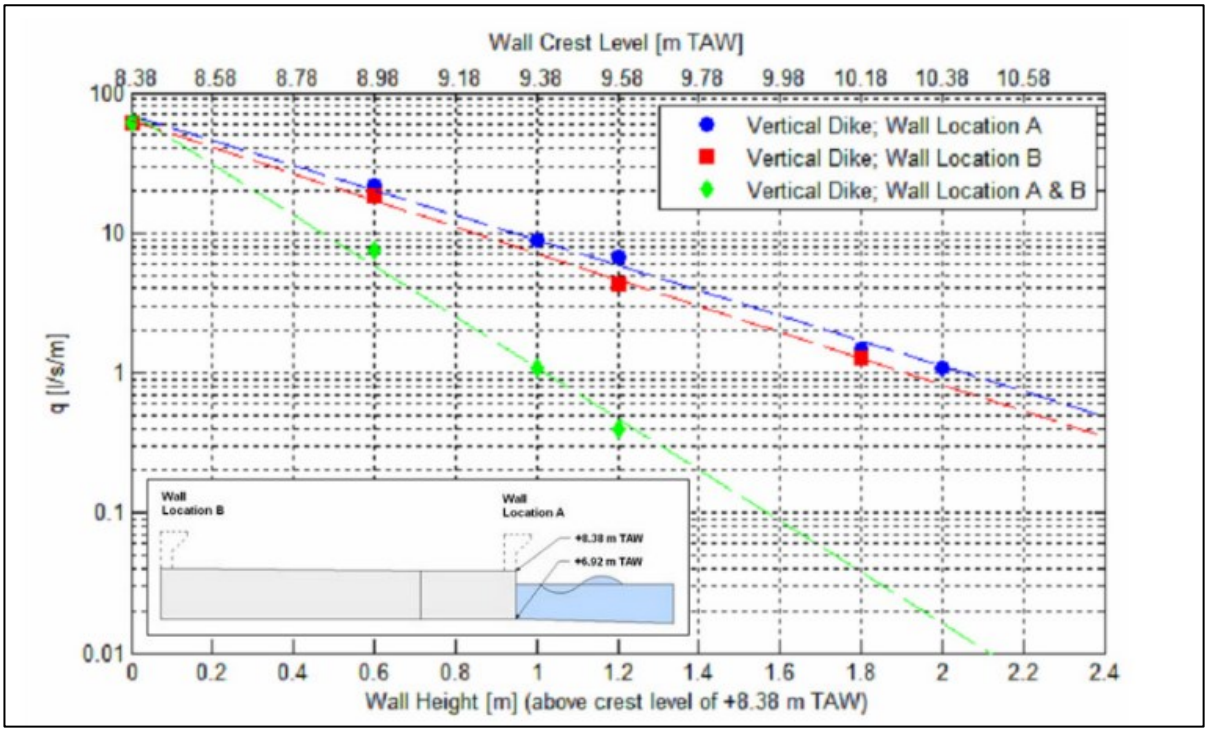

Figure 2.21: Influence of seawall position (Veale *et al.*, 2012)

However, the seawall that is further considered and discussed in this report is the one at location B.

The final design of the shore protection is as shown in Figure 2.22, with the primary overtopping reduction structure replacing the dike and forming a recurve shape. The secondary structure constrains the overtopping from flowing landward and forms a stilling basin for the flow to attenuate (Veale, 2012). The second structure is designed to also serve as a bench along the promenade for recreational purposes.

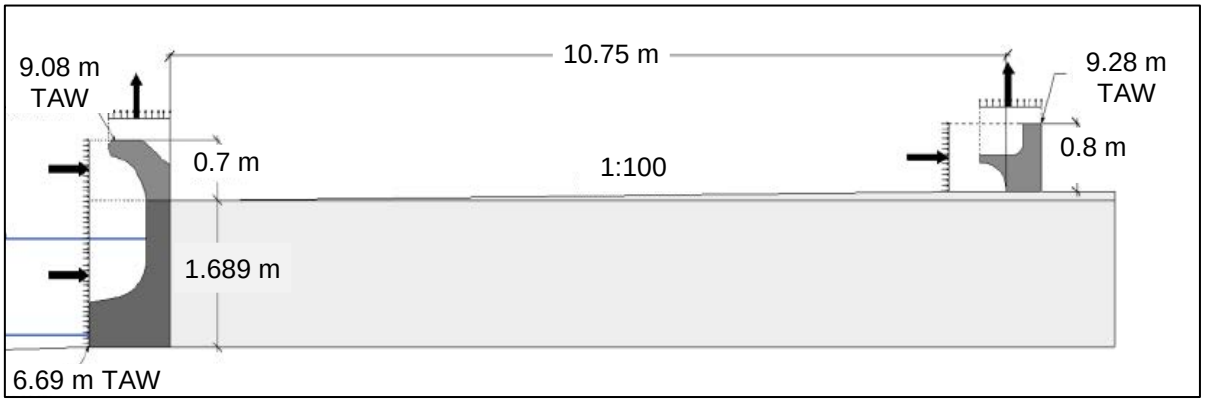

Figure 2.22: Promenade cross section (Veale *et al.* (2012) adapted by author)

2.5.6 Roux (2013)

Roux (2013) investigated the low crest level problem at Strand, South Africa by means of numerical and physical modelling. Roux conducted physical model tests on vertical as well as recurve walls to determine the effectiveness of the proposed design of a recurve wall.

Figure 2.23 shows the recurve wall designed and a side view of the physical model tested, which was manufactured from Perspex, with an overhang length of 50 mm (on a scale of 1:20).

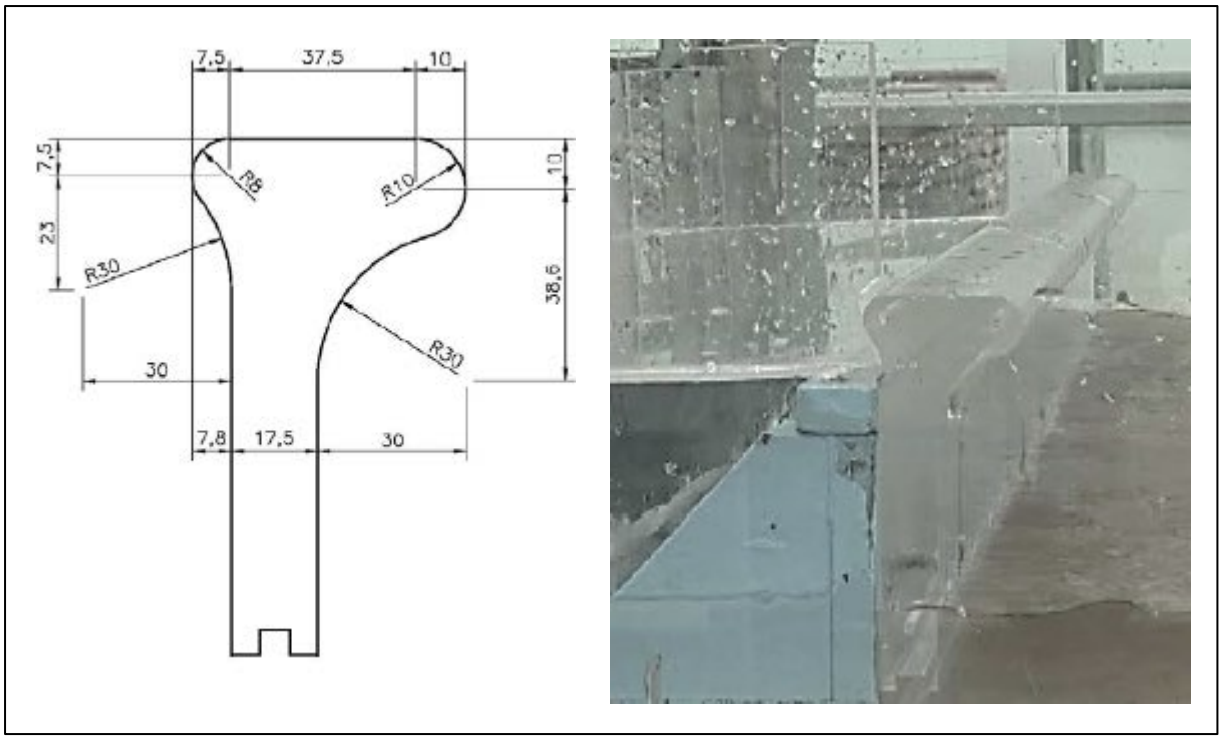

Figure 2.23: Design of recurve wall (left) Side view of recurve wall (right) (WML coast, 2011) (Roux, 2013)

Roux (2013) determined that when the beach slope was gentler the overtopping rate increased, as did the width of the beach. Less shoaling occurs as the distance available for the waves to propagate becomes shorter.

From the physical model tests, Roux determined that the wave period increased the overtopping rate up to a 12 second wave period, whereafter the overtopping rate declined, as shown in Figure 2.24.

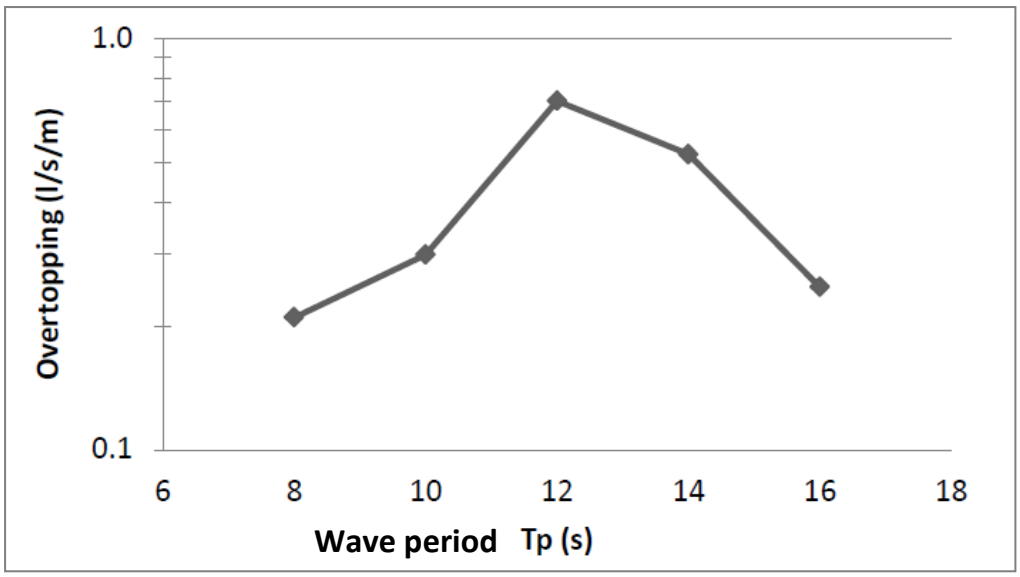

Figure 2.24: Influence of wave period on overtopping rate (Roux, 2013)

It was determined that the decline is attributable to the waves breaking before reaching the wall and thus losing energy which results in less water overtopping the crest of the recurve wall (Roux, 2013).

The addition of a recurve overhang to a vertical wall can reduce the overtopping considerably (Roux, 2013). Further, better reduction still can be achieved by increasing the freeboard. From the physical model tests Roux noted an average of 54% reduction in overtopping.

From the research dissimilarities were found between non-breaking (pulsating) and impulsive (breaking) wave conditions. The latter were found to be less sensitive to changes in freeboard.

2.5.7 Schoonees (2014)

Schoonees (2014) investigated the effect of recurve seawalls (Type 3) at the back of a beach to reduce overtopping as a measure to counteract the rise in sea level, without obstructing the sea view. Two recurve angles, as shown in Figure 2.25, were tested (one with a long and one with a short recurve overhang) and evaluated against a vertical seawall, to test the influence of overhang and determine the optimal design.

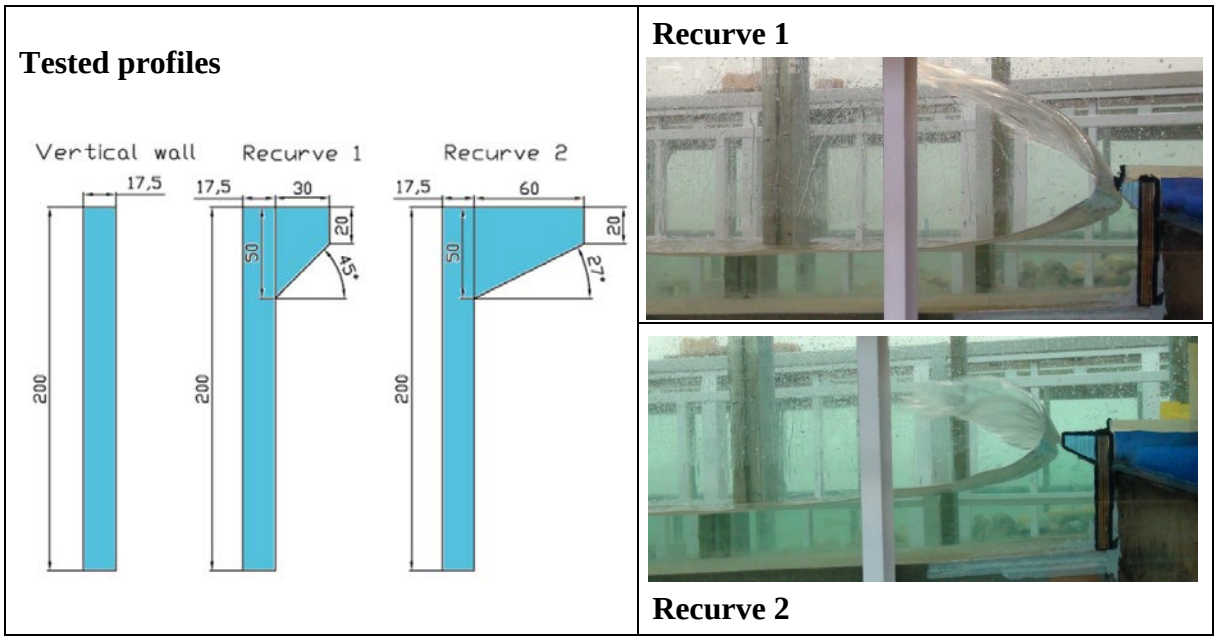

Tests were performed on physical model with breaking and non-breaking waves with a constant

Figure 2.25: Model geometries (Schoonees, 2014)

wall height and bed slope with variation in recurve angle, overhang length and freeboard level.

The test were performed with the geometrical properties given in Table 2.11, with a time series that was based on $1000T_P$.

Table 2.11: Geometrical properties of recurve wall (Schoonees, 2014)

Geometrical properties			
Freeboard	R_c	1.6, 2.0, 2.4, 3.0, 3.4	m
Parapet angle	β	0, 45, 60	°
Wave period	T_p	10	s

Figure 2.26 shows the influence of the overhang length on the mean overtopping rate. However, the primary objective of the research was not to create design curves for overhang lengths of recurve seawalls.

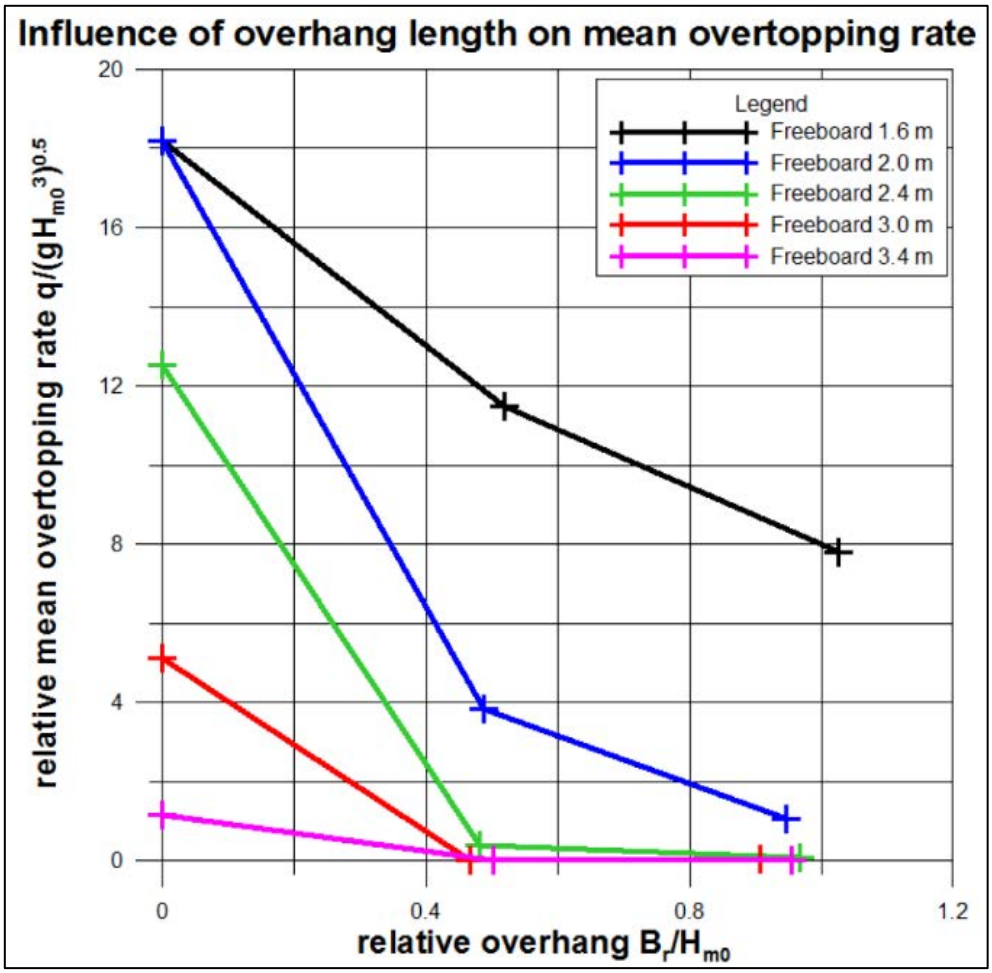

Figure 2.26: Influence of overhang length on mean overtopping rate (Schoonees, 2014)

The study determined that the recurve seawalls provided a reduction in mean overtopping compared against the vertical wall for high relative freeboard cases and low relative freeboard cases (Schoonees, 2014).

The tests conducted by Schoonees (2014) showed that recurve profile 2, with the longer sea facing overhang, was more efficient in reduction of wave overtopping. However, with higher freeboard levels where $\frac{R_c}{H_{m0}} > 2.2$, both recurve profiles perform equally well in reflecting the incoming waves, as the overhang length has less influence on overtopping reduction as for low freeboard cases. It was also shown that the effectivity was reduced as the freeboard decreased.

The results of the test were validated by the use of the EurOtop calculation tool. In contrast, for the case where $\frac{R_c}{H_{m0}} > 1.4$, the recurve wall substantially reduces wave overtopping.

One test was repeated with varying peak periods and the researcher concluded that the degree of overtopping was sensitive to peak wave period changes. It was recommended that further

tests be performed to validate the results and test other influences on the results. Larger varying overhang lengths should also be tested.

2.5.8 Summary

Research by Berkeley-Thorn and Roberts (1981) provides the greatest contribution to the fundamental development of recurved walls by recommending the geometry of a recurved seawall structure. Banyard and Herbert (1995) built on this to further develop a systematic approach to incorporating such a structure into the design process of a coastal defence.

The CLASH initiative contributed a great deal of attention to and research on wave overtopping. However, this was focused on the development of a formula to predict the wave overtopping rate with a given a set of parameters.

Van Doorslaer and De Rouck (2011) investigated the influence of the slope of the recurve wall feature that is necessary to effectively reduce wave overtopping. Recently Schoonees (2014) initiated a physical model test with a limited set of parameters to create a design guideline with various overhang lengths.

2.6 Physical modelling of wave overtopping

A physical model allows the researcher to develop a holistic view of nearshore processes without simplifying the process with assumptions, as is required with numerical models. One should, however, be cognisant in the design of any such model studies, of the need to take due account of any possible model scale effects. With a smaller scale, data collection is easier; however, with a model with a large scale, a better representation of actual events can be achieved (Hughes, 1995).

2.6.1 Similitude criterion

Generally there are four conditions, as stated by Hughes (1995), that should be conserved between the prototype and model conditions when administering short wave physical model are demonstrated in Table 2.12.

Table 2.12: Physical model similitude criterion (Hughes, 1995)

Physical model similitude criteria		
1	Froude number	$\frac{N_V}{\sqrt{N_g \times N_L}} = 1$
2	Strouhal number	$N_t = \sqrt{\frac{N_L}{N_g}}$
3	Reynolds number	$\frac{N_L \times N_V}{N_v} = 1$
4	Euler number	$\frac{N_p}{N_\rho \times {N_V}^2} = 1$

However, it is difficult to maintain both the Froude and Reynolds criteria in physical model studies. In this study, a physical model is executed with an undistorted scale in the Hydraulic Laboratory at Stellenbosch University. With an undistorted scale the inertial and gravitational forces are dominant and the model can be scaled according to the Froude criterion.

The general ratio of the scale ratio can be expressed visually by Equation (2.17) (Hughes, 1995):

$$N_x = \frac{X_p}{X_m} = \frac{Value\ of\ X\ in\ Prototype}{Value\ of\ X\ in\ Model} \tag{2.17}$$

The scale ratios under Froude's similarity law are provided in Table 2.13.

Table 2.13: Froude and Reynolds scaling laws (Hughes, 1995)

Characteristic	Dimension	Froude	Reynolds
Geometric			
Length	[L]	N_L	N_L
Area	[L^2]	$N_L{}^2$	$N_L{}^2$
Volume	[L^3]	$N_L{}^3$	$N_L{}^3$
Kinematic			
Time	[T]	$N_L^{1/2} N_\rho^{1/2} N_\gamma^{-1/2}$	$N_L{}^2 N_\rho N_\mu^{-1}$
Velocity	[LT^{-1}]	$N_L^{1/2} N_\rho^{-1/2} N_\gamma^{1/2}$	$N_L^{-1} N_\rho^{-1} N_\mu$
Acceleration	[LT^{-2}]	$N_\gamma N_\rho^{-1}$	$N_L^{-3} N_\rho^{-2} N_\mu{}^2$
Discharge	[L^3T^{-1}]	$N_L^{5/2} N_\rho^{-1/2} N_\gamma^{1/2}$	$N_L N_\rho^{-1} N_\mu$
Kinematic Viscosity	[L^2T^{-1}]	$N_L^{3/2} N_\rho^{-1/2} N_\gamma^{1/2}$	$N_\rho{}^{-1} N_\mu$
Dynamic			
Mass	[M]	$N_L{}^3 N_\rho$	$N_L{}^3 N_\rho$
Force	[MLT^{-2}]	$N_L{}^3 N_\gamma$	$N_\rho^{-1} N_\mu{}^2$
Mass Density	[ML^{-3}]	N_ρ	N_ρ
Specific Weight	[$ML^{-2}T^{-2}$]	N_γ	$N_L^{-3} N_\rho^{-1} N_\mu{}^2$
Dynamic Viscosity	[$ML^{-1}T^{-1}$]	$N_L{}^{3/2} N_\rho^{1/2} N_\gamma^{1/2}$	N_μ
Surface Tension	[MT^{-2}]	$N_L{}^2 N_\gamma$	$N_L^{-1} N_\rho^{-1} N_\mu{}^2$
Volume Elasticity	[$ML^{-1}T^{-2}$]	$N_L N_\gamma$	$N_L^{-2} N_\rho^{-1} N_\mu{}^2$
Pressure and Stress	[$ML^{-1}T^{-2}$]	$N_L N_\gamma$	$N_L^{-2} N_\rho^{-1} N_\mu{}^2$
Momentum, Impulse	[MLT^{-1}]	$N_L{}^{7/2} N_\rho^{1/2} N_\gamma^{1/2}$	$N_L{}^2 N_\mu$
Energy, Work	[ML^2T^{-2}]	$N_L{}^4 N_\gamma$	$N_L N_\rho^{-1} N_\mu{}^2$
Power	[ML^2T^{-3}]	$N_L{}^{7/2} N_\rho^{-1/2} N_\gamma^{3/2}$	$N_L^{-1} N_\rho^{-2} N_\mu{}^3$

A study by Schüttrumpf and Oumeraci (2005) determined that for normal test conditions the scale effects are minimised if the Weber and Reynolds numbers adhere to the limits of tolerance provided in Table 2.14.

Table 2.14: Tolerable scale limits (Schüttrumpf & Oumeraci, 2005)

Scaling laws	Tolerable limits	Influences
Weber number	30 - 3000	Surface tension
Reynolds	$Re_q > 10^3$	Viscosity

The Weber number is provided with Equation (2.18). However, if it falls outside the tolerable limit, surface tension will affect the test results.

$$We = \frac{(v_A h_A \rho_w)}{\sigma_0} \tag{2.18}$$

Where:

v_A – Wave run-up velocity at SWL

h_A – Layer thickness at SWL

ρ_w – Density of the fluid

σ_0 – Wave run-up height

The overtopping Reynolds number is calculated with Equation (2.19). However, if it falls below tolerable limit, viscosity will affect model results.

$$Re_q = \frac{2(R - R_C)^2}{vT} \tag{2.19}$$

Where:

R – Wave run-up height (m)

R_C – Freeboard (m)

v – Kinematic viscosity (m^2/s)

T – Wave period (s)

Important limitations of physical models are scale and model effects. These occur because it is not possible to achieve similitude of all relevant forces. The condition of the dominant forces, however, should be satisfied; in this case the gravitational and inertial force (Hughes, 1995).

2.6.2 Model effects

Laboratory effects are most often caused in short wave physical models by the following (Hughes, 1995):

- Physical limitations of the model boundaries on the flow;
- The use of a mechanical wave generator, which causes unintentional non-linear effects; and
- Simplification of the natural processes and forces.

The mechanical generation of waves can cause un-intended raised amplitudes, groups of waves or non-authentic long waves (Hughes, 1995).

The re-reflection of waves is a laboratory effect that is not as apparent as those already mentioned. Wave reflection occurs in the flume just as it would in nature; however, additionally, the wave flap which represents the seaward boundary; re-reflects the reflected waves back in the direction of the recurve seawall structure (Hughes, 1995). This effect can be mitigated by means of one of three methods:

- Energy dissipation beaches constructed with rubber mats in front of the wave flap;
- Experiments being executed with shorter wave periods, before the reflected wave reaches the wave flap; or
- Active wave absorption at the wave flap.

Romano, Bellotti, Briganti and Franco (2014) accounted for the wave reflection in the model by means of method developed by Goda and Suzuki (1976), rather than the use of absorption. This method was developed by measuring the two wave records at adjacent locations simultaneously and then analysing all amplitudes and Fourier components. The incident and reflected wave conditions are determined by modification of the estimated data sets (Goda & Suzuki, 1976).

The most obvious distortion that causes model effects is the absence of wind. The effect of wind on the overtopping is an important characteristic that should not be ignored, but should be additionally quantified after physical modelling is completed, especially in cases of strong winds, small overtopping volumes or pulsating conditions (Ward, Zhang, Wibner and Cinotto, 1998). According to Pearson, Bruce, Allsop and Gironella (2002) wind does not have such great

influence on large overtopping volumes, however more care should be taken for small overtopping volumes.

Another distortion, according to Pearson *et al.* (2002) is the use of fresh water instead of salt water in the model. The use of fresh water influences the concentration of air bubbles in the water, which has an influence on the wave pressures measured on the wall. However, there is no evidence that this has an effect on the overtopping processes (Pearson *et al.*, 2002)

2.6.3 Scale effects

Scale effects in physical models result from the assumption that the gravitational force is the governing force that influences the inertia forces in the model (Hughes, 1995). This incorrectly scales other physical factors.

According to De Rouck, Geeraerts, Troch, Kortenhaus, Pullen and Franco (2005), the influence of certain scale effects namely: surface tension and kinematic viscosity, increase as the flow decreases.

Le Méhauté (1976) provides a general rule of thumb that surface tension becomes significant if the wave period is smaller than 0.35 seconds or the water level lower than 20 mm.

For small overtopping volumes the hydraulic resistance on the slope increases, causing higher energy losses. This is as there is no turbulent boundary layer (De Rouck *et al.*, 2005).

A study by Pearson *et al.* (2002) compared physical model tests of small and large scale to determine whether there was a significant difference between the measured values in small-scale studies versus those in large scale studies. This study came to the conclusion that for peak and mean overtopping events under impulsive wave conditions the scale effects were insignificant, and also that scale effects for waves under pulsating condition are minimal (Pearson *et al.*, 2002).

From the OPTICREST project it was determined that wave run-up is greatly underestimated in small-scale tests (De Rouck *et al.*, 2005). Similarly, underestimation was expected from wave overtopping. Thus, as part of the CLASH project this was investigated by comparing full-scale tests at three locations with small-scale experiments. The three full-scale tests comprised:

- Low crested rubble mound breakwater with Antifer cubes in an armour layer (Zeebrugge, Belgium);

- Rock rubble mound breakwater (Ostia, Italy); and
- Vertical Wall (Samphire Hoe, United Kingdom)

Full-scale wave overtopping measurements were taken by placing an overtopping reservoir on top of each of the structures, as demonstrated in Figure 2.27 (De Rouck *et al.*, 2005).

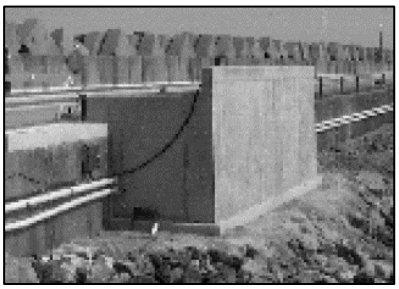		
Zeebrugge (Belgium) (De Rouck *et al.*, 2005)	Ostia (Italy) (De Rouck *et al.*, 2005)	Samphire Hoe (UK) (Pullen, Allsop, Bruce & Pearson, 2009)

Figure 2.27: Full-scale tests

De Rouck *et al.* (2005) determined that for vertical walls the prediction, prototype and laboratory results correlated well. The differences were attributed to wind effects. A method was also developed to minimize scale effects by considering scaling factors for various configurations considering the roughness and steepness of the slope, and considering the effect of the wind (De Rouck *et al.*, 2005).

From the experiments it was observed that the scale factor varies for different slopes, flat slopes having a larger scale factor (De Rouck *et al.*, 2005).

Further studies, in both 2D and 3D, were undertaken by Pullen *et al.* (2009), to compare the three full-scale tests to small-scale tests. This study validated that for vertical walls, the data points correlated well; however, there should be an adjustment made for the wind effects that was not included in the small-scale models. This has the largest influence on small overtopping volumes.

2.6.4 Mitigation of model effects

To minimise model effects (Wallingford, 1999) design the experiments with certain characteristics. Firstly, the physical model had two absorption channels, one on either side

constructed with perforated Perspex splitter walls to reduce the wave reflection model effects in the physical model.

Secondly, the wide range of design wave conditions in the flume was calibrated before the structure was built. The flume had the fixed design model bed and had a shingle spend beach at the end of the flume to reduce the re-reflection of waves (Wallingford, 1999).

2.6.5 Methods to measure overtopping

Overtopping is sensitive to change in the water level, as well as the incident wave characteristics and the structure geometry (Reis, Neves & Hedges, 2008). Therefore, care should be taken to keep the water level as constant as possible.

De Rouck *et al.* (2005) measured overtopping in full-scale by placing a reservoir behind the seawall to catch the overtopped water. The measurements were taken with the use of a submersible pump combined with a load cell, which was a transducer that quantifies the force measured, in this case the force caused by the water overtopped into the reservoir.

Romano *et al.* (2014) followed similar methods for determining overtopping measurements: a chute directs the overtopped water into a pipe that is connected to the bottom of the chute, where it runs into an overtopping tank connected to a load cell (Romano *et al.*, 2014).

At the Samphire Hoe full-scale test site six overtopping tanks were positioned behind the parapet structure to record the spatial distribution of the overtopped water. These tanks are V shaped so that they can measure small overtopping events more easily and accurately.

Each of the overtopping tanks was fitted with two recording devices that were connected to a control box sealed from storm conditions. The first device is a pressure transducer on the base of the tank and the second, overtopping detectors on one side of tank to document individual wave overtopping events as demonstrated in Figure 2.28.

Pearson *et al.* (2002), however, measured wave-by-wave events by suspending the measuring bucket from a load cell. This recorded the mass in the collection tank after each overtopping event. Metal tape was place at the crest of the structure to identify individual events. The mass increments were determined and converted to overtopping volumes (Pearson *et al.*, 2002).

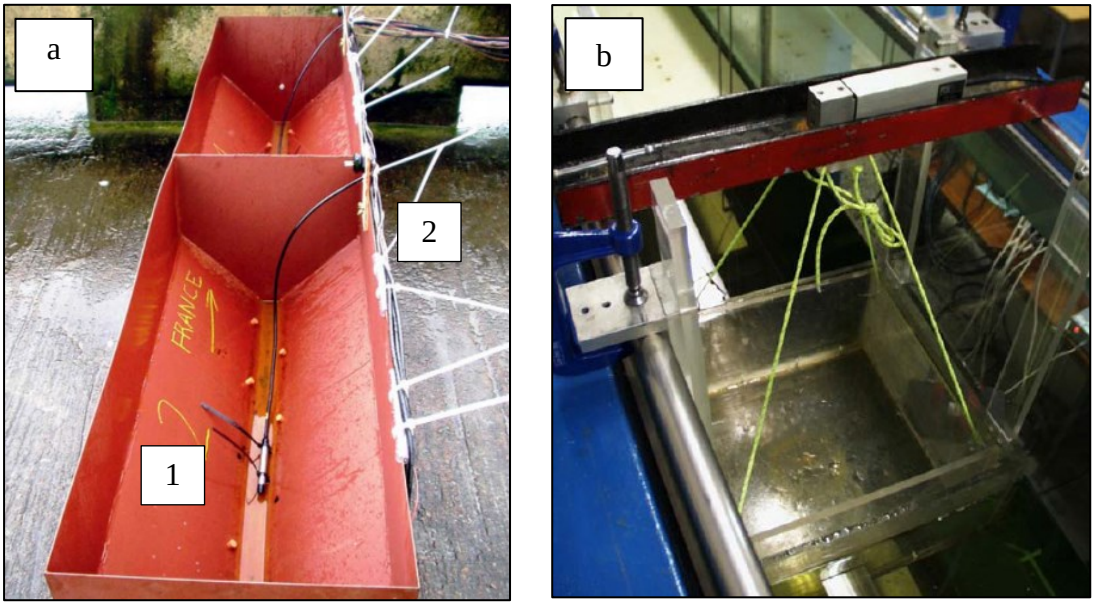

Figure 2.28a: Overtopping tank with 1) pressure transducers and 2) overtopping detectors; b: Overtopping tank suspended from load cell (Pullen *et al.*, 2009)

This measurement method was validated by filling the overtopping tank with known amounts of water to check the measurements. The results correlated well, and indicated that any variation was negligible (Pearson *et al.*, 2002).

The Pearson *et al.* (2002) 3D study was simplified to 2D and conducted in Edinburgh. The overtopping bin behind the seawall was divided into seven collection tanks in order to consider the spatial distribution of the overtopped water. The overtopping tank was similarly suspended from a load cell, and each compartment was equipped with a wire resistance gauge. The setup of overtopping compartments is provided in Figure 2.29.

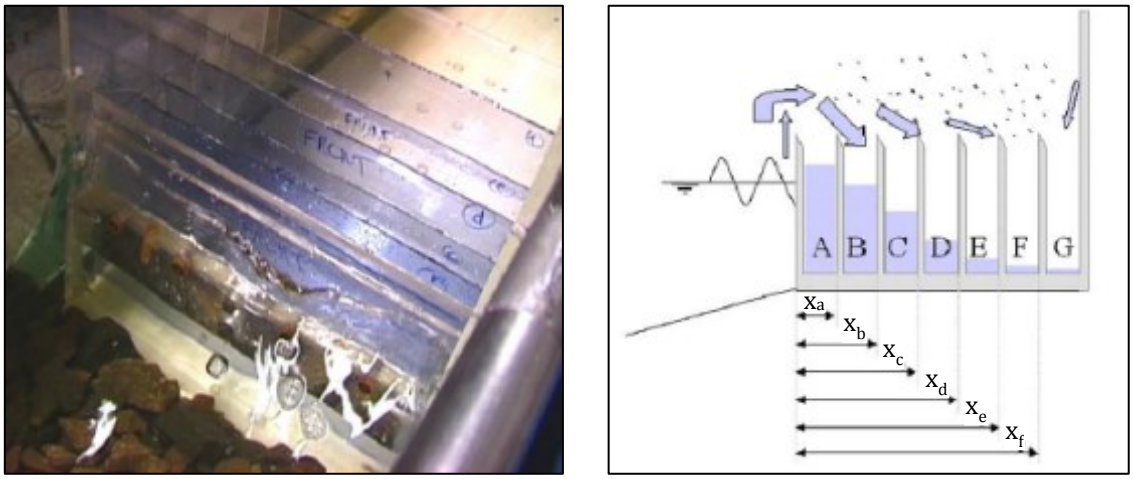

Figure 2.29: Spatial distribution of wave overtopping (Pearson *et al.*, 2002)

CHAPTER 3

PHYSICAL MODEL TESTS

3.1 General description of the model

3.1.1 Test facility

The physical model tests were performed in a 2D wave flume at the Hydraulic laboratory of the Civil Engineering Department of the University of Stellenbosch as provided in Figure 3.1, which has a width of 1 m, length of 30 m and a maximum operational depth of 0.8 m.

	
2D wave flume (Guerrero, n.d.)	Wave paddle in 2D flume (Guerrero, n.d.)

Figure 3.1: Test facility

The wave flume is equipped with a wave-maker, a piston-type paddle that moves horizontally to generate waves. The flume is fitted with an absorption beach behind the paddle to prevent splashing of water (HR Wallingford, 2010).

The wave paddle is fitted with a dynamic wave absorption system that compromises for the effect of the reflection of waves in the flume. This unit measures the water level and calculates the equivalent paddle position (EPP) signal. The EPP represents the position in which the paddle would have been without the effect of reflected waves (HR Wallingford, 2010).

The test setup, used by Schoonees (2014) in the wave flume in the hydraulic laboratory at the University of Stellenbosch was re-used to determine the influence that the overhang length of the recurve wall has on the effective reduction of overtopping. A detailed flume cross-section, indicating the elevations, is provided in Annexure B.

3.1.2 Bed slope

The bed slope in front of the structure will consist of two slopes, a deep-sea slope that is estimated at 1:50 and the nearshore slope characteristic southern African coasts. The slopes of five locations around South Africa's coast, around -1m to +1m MSL, were surveyed, as suggested by Schoonees (2014), to estimate an accurate nearshore slope. These slope calculations are provided in Table 3.1.

Table 3.1: Nearshore slope calculation

Location	Slope (-1m to +1m MSL)	Source
False Bay	1:16.5	(WNNR, 1983)
Grootbrak/Glentana	1:32	(Schoonees, *et al.*, 2008)
Richards Bay	1:42	(WSP Africa Coastal Engineers, 2012)
Saldanha Bay	1:11.5	(Schoonees & Theron, 2003)
Table Bay	1:14.5	(Soltau, 2009)
Average	**1:18.41**	

The deep-sea slope and the estimated nearshore slope are illustrated in Figure 3.2.

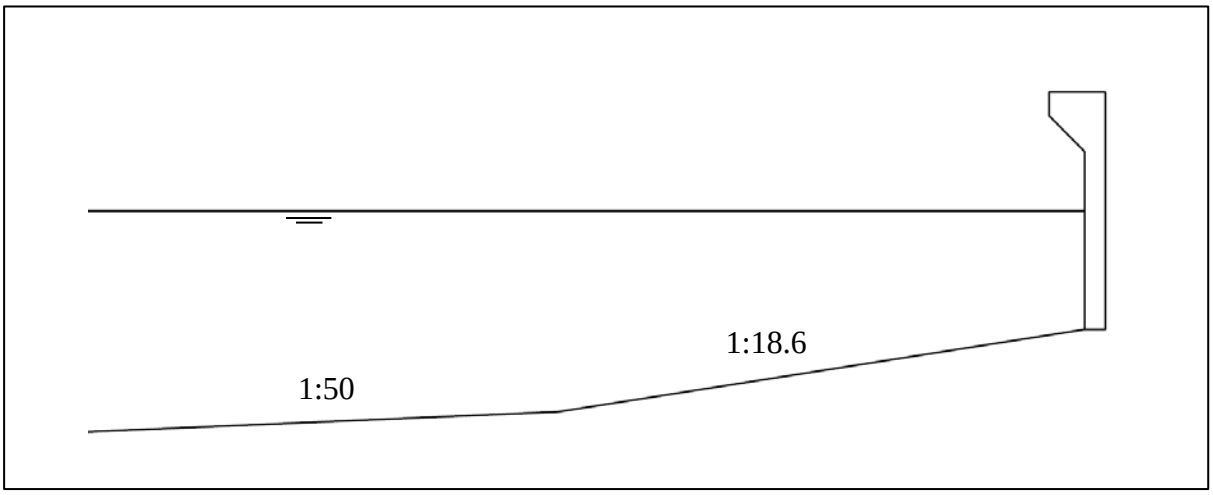

Figure 3.2: Estimated slopes in flume

A study by Bruce *et al.* (2005) proved that for vertical walls with impulsive wave conditions (where the shoaling water exposes the bed slope or the toe of the structure), the bed slope critically influences the incoming wave. However, for the purposes of this study only pulsating wave conditions were considered and thus the bed slope would not have had a substantial effect on this study.

3.1.3 Geometry of a recurve wall

To simplify the geometry of the recurve seawall, the geometry of a parapet is used. It was expected that the recurved shape of the seawall would further increase the reduction in overtopping; however, the order of this further reduction was not known. Limited research could be found on the design of parapet seawalls.

As illustrated in Figure 3.3, the overhang length B_r, which influences the angle β of the overhang, was varied in the tests in order to evaluate the influence is has on the reduction of overtopping.

The overhang length, B_r, varied in test conditions from 0 mm to 105 mm.

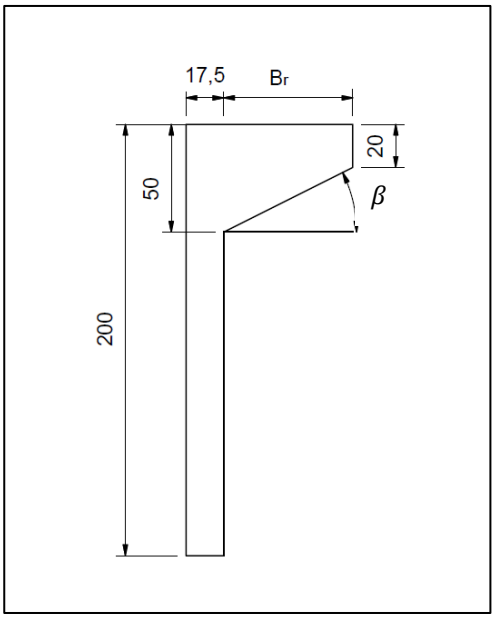

Figure 3.3: Generic recurve wall geometry of model tests

The 20 mm lip thickness is the minimum thickness allowed that provides enough space to place steel within the recurve form and still achieve adequate concrete coverage.

3.1.4 Wave period

Typically, wave periods that are found around the coast of South Africa range from 8 second to 12 second. To include possible storm conditions, a wave period of up to 16 second was included in the evaluation for overtopping reduction.

3.1.5 Wave spectra

The wave spectra that are characteristic around the coast South Africa (and also the North Sea) is the JONSWAP spectrum. This variation of the Pierson-Moskowitz spectrum originated out of the Joint North Sea Wave Project (JONSWAP) where Hasselmann, Barnett, Bouws, Carlson, Cartwright, Enke, Gienapp, Kruseman and Meerburg (1973) found that the wave spectrum is never fully developed. The spectrum continues to develop over long durations and distances by means of wave-to-wave interactions. In Figure 3.4 the JONSWAP spectrum is compared to the Pierson-Moskowitz spectrum.

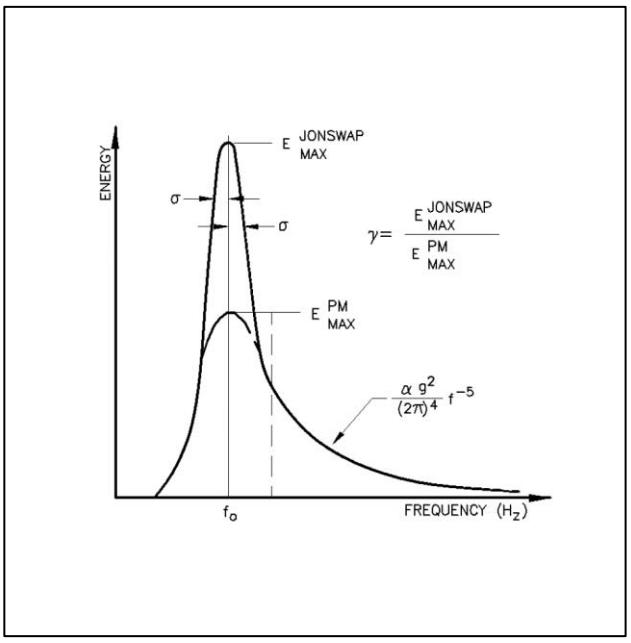

Figure 3.4: Pierson-Moskowitz versus JONSWAP spectra (U.S. Army Corps of Engineers, 2001)

The JONSWAP spectrum for fetch-limited seas can be expressed through equations (3.1) to (3.3).

$$E(f) = \frac{\propto g^2}{(2\pi)^4 f^5} exp\left[-1.25\left(\frac{f}{f_p}\right)^{-4}\right]\gamma^{exp\left[\frac{\left(\frac{f}{f_p}-1\right)^2}{2\sigma^2}\right]} \quad (3.1)$$

$$f_p = 3.5\left[\frac{g^2 F}{U_{10}^3}\right] \quad (3.2)$$

$$\propto = 0.076\left[\frac{gF}{U_{10}^2}\right]^{-0.22} \quad (3.3)$$

$$1 \leq \gamma \leq 7$$

$$\sigma = 0.07\, for\, f \leq f_p$$

$$\sigma = 0.09\, for\, f > f_p$$

Where:

$\propto -$ Equilibrium coefficient

$\sigma -$ Dimensionless spectral width parameter

$\gamma -$ Peak enhancement factor

$F -$ Fetch length

The peak enhancement factor is defined, and is demonstrated in Figure 3.4, as the ratio of the maximum energy density of the JONSWAP spectrum to the Pierson-Moskowitz spectrum.

The peak enhancement factor lies between one and seven in the North Sea; however, around South Africa's coast, it is between one and six. According to Rossouw (1989), the average 2.2 with a standard deviation of one. The peak enhancement factor was chosen as γ = 3.3 to enable the comparison of this study to other wave overtopping studies.

3.1.6 Length of wave sequence

Study by Reis *et al.* (2008) determined that for physical model testing the number of waves in a wave sequence is very important. Reis *et al.* suggests that for physical model tests with no provision for active wave absorption, more tests with the same design parameters, but with shorter wave period, should be executed. This would provide a more accurate account of mean wave overtopping. The shorter wave-time series would eliminate the possibility of energy buildup caused by the re-reflection of wave paddles and flume walls (Reis *et al.*, 2008).

Pearson *et al.* (2002) made the observation that a 500-wave sequence gives an accurate wave overtopping measurement, when compared to the 1000-wave sequence (EurOtop, 2007). This, however, is not the case for small wave overtopping measurements.

3.1.7 Data acquisition

The HR DAQ data acquisition software that works in conjunction with the HR wave paddle is equipped with reflection analysis, and the data analysis spectral density and zero crossing-up method data sequences (HR Wallingford, 2010). The incident and reflected wave heights are separated by the least squares method developed by Mansard and Funke (1980) for irregular waves. With this method, three wave height readings are required to be taken simultaneously. The four probes' H_{m0} values are averaged to determine the incident wave height.

The least squares method requires a constant water depth and probe spacing to calculate the range of allowable reflection frequency for each case. The wave sequence recorded is then analysed to determine the bulk reflection coefficient and the maximum and minimum reflections that occurred during that test condition. The Reflection Analysis interface is provided in Annexure P.

The least squares method is developed by equations (3.4) to (3.9); where the incident wave is separated from the reflected wave by the use of equation (3.9)

$$H_{mo}{}^2 = H_i{}^2 + H_r{}^2 \tag{3.4}$$

$$H_{mo} = \sqrt{(H_i{}^2 + H_r{}^2)} \tag{3.5}$$

$$H_r = K_r H_i \tag{3.6}$$

Substituting (3.5) in (3.6):

$$H_{mo} = \sqrt{(H_i{}^2 + K_r{}^2 H_i{}^2)} \tag{3.7}$$

$$H_{mo} = H_i \sqrt{(1 + K_r{}^2)} \tag{3.8}$$

$$H_i = \frac{H_{mo}}{\sqrt{(1 + K_r{}^2)}} \tag{3.9}$$

3.2 Model scale

The model scale of the physical model was chosen to be 1:20 and scaled according to the Froude similarity law, as discussed in Section 2.6.1. This was to minimise scale effects, taking into consideration the available flume volume, the wave-paddle capabilities, and to accommodate a realistic range of water levels.

The model scale, as demonstrated in Table 3.2, allows a wide range of parameters to be tested.

Table 3.2: Physical model scale (Schoonees, 2014)

Scale type	Parameter	Froude scale
Model scale	Water depth, wavelength, wave height	1:20
Time	Wave period, test duration	1:$\sqrt{20}$ = 4.472
Mass	Mass of overtopped water	1:20^3 = 8000

3.3 Test procedure

The process of the test schedule discussed in Section 3.6, is as follows:

1. Wait for the resounding waves and water level to even out;
2. The water level is raised or lowered to the desired water level;
3. The water is mixed by running a wave set with a duration of $100T_p$ to account for stratifying water;
4. Water level should settle out and probes in the flume are calibrated;
5. The water level in the overtopping bin and in flume is recorded;
6. The wave condition is initiated and absorption set; where-after the data acquisition is recorded for $1000T_p$;
   6.1. During the test the water in the overtopping bin is monitored, and if approximately 20 l water splashes out, 20 l is added behind the wave paddle in 5 l increments.
   6.2. If the water in the overtopping bin is close to capacity, it is pumped out of the bin to the weighing station and recorded.
7. Weigh the overtopping bucket, and measure the water level in the overtopping bin; and
8. Record the water level in the flume and in the overtopping bin.

9. Check that water level is within 2 mm of starting water level.

3.4 Measuring equipment and techniques

The steel overtopping bin with a see-through Perspex slot on the side is positioned behind the model recurve wall. Two pieces of steel are placed in the overtopping bin to ensure that the bin does not move. The water level in the overtopping bin is recorded before and after each test, with the use of a ruler fitted to the inside of the bin. The ruler is calibrated with predetermined volumes to streamline the data recording process. Plastic sheets are fitted around the bin to guide overtopped water into the overtopping bin.

A wooden frame was constructed and covered with plastic sheets for a distance of 4 metres from the structure towards the wave maker, thus sealing the edge of the flume to minimise water splashing and loss of water in the experiment, as demonstrated in Figure 3.5.

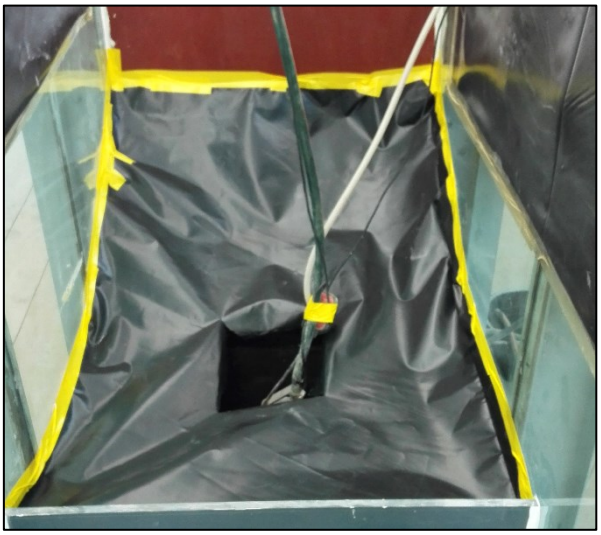

Plastic sheets to limit water loss

Guiding plastic water sheets

Figure 3.5: Plastic sheets

The smaller overtopping volumes were measured using only the overtopping bin. However, for overtopping volumes that would exceed the overtopping bin's capacity, a pump was used during the test, where-after the water mass was weighed and noted as demonstrated in Figure 3.6.

	
Pump in overtopping bin	Weighing and water refill station

Figure 3.6: Wave overtopping recording equipment

The pump that had initially been used burnt out, and eventually three different pumps were used during the course of the physical model tests. Each time a new pump was used, the overtopping bin was re-calibrated with the ruler.

To ensure that the incident wave was as designed and the effect of reflecting waves were accounted for, the four waves probes were spaced in front of the recurve wall structure. The spacing of the first three probes was determined by the Mansard and Funke (1980) method. The fourth probe was positioned one average wavelength away from the structure, as demonstrated in Table 3.3. This was to ensure that the wave readings were taken before the bed slope had an influence on the incident wave, and thus before wave breaking occurs. Reflection analysis was performed as discussed in Section 3.1.7.

Table 3.3: Average wavelength for calculation of probe spacing

Model wavelength (L_p) for corresponding wave period (T_p)		
T_p s		**L_p mm**
1.8		1542
2.2		1930
2.7		2316
3.1		2703
3.6		3089
AVERAGE	**2.7**	**2316**

The position of the probes in the wave fume is shown schematically in Figure 3.7.

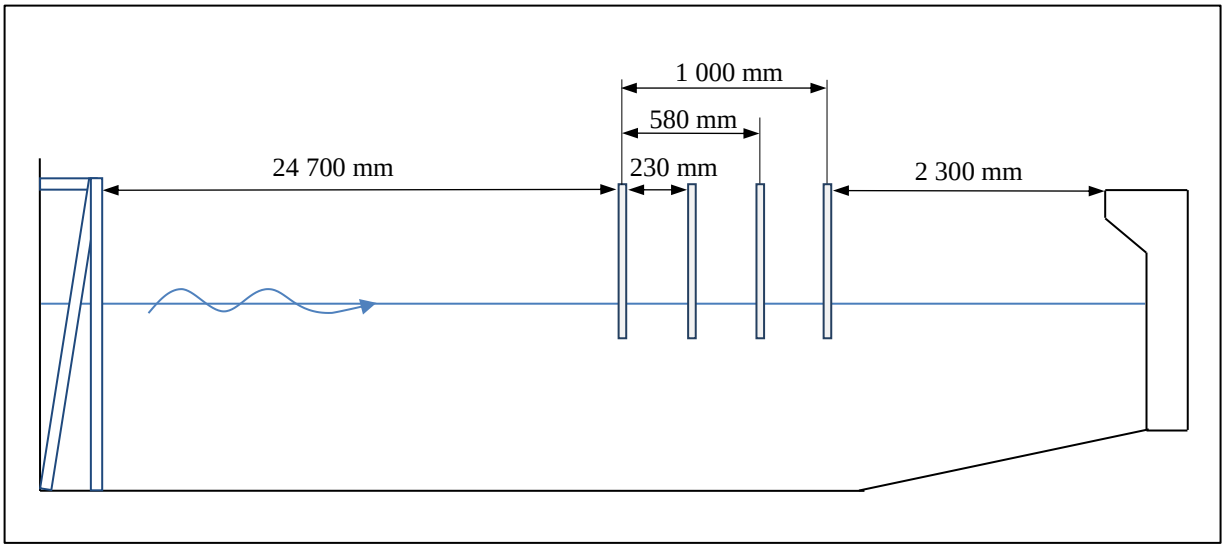

Figure 3.7: Probe spacing of physical model

To account for the water removed by violent overtopping volumes during the test, the overtopping volumes were closely monitored to ensure that a constant water level is maintained in the flume. If the overtopping bin filled with 20 l, approximately the same volume was added into the flume behind the wave flap. The water level at the start and end of the test were compared, to ensure that water was not lost from the system. If the water level dropped by more than 2 mm, the test was disregarded and the results removed from the dataset.

An analysis was done to determine the effect that the process of stratifying water had on the wave probes. This was done by mixing the water, and then after the wave paddle was switched off, the probes readings were taken for 6 hours, provided in Annexure Q.

3.5 Model limitations

The limitation of the physical model is predominantly the absence of wind and the influence it has on the initial overtopping measured. Without modelling the wind, the actual magnitude of the small overtopping volumes that are blown over the crest of the structure is not taken into account.

Additionally, one has to consider the implication of physical modelling in only two dimensions, where the effect of the incident angle of the incoming waves on the overtopping at structure is not considered. Lastly, there is the matter of the effect of wave re-reflection, as discussed earlier in Section 2.6.2.

3.6 Schedules

Provided in Table 3.4 are the nine sets of conditions (various combinations of recurve shapes, relative water level at the toe of the structure, as well as wave height and period) that were tested in the experimental programme.

Table 3.4: Test Schedule

Model		**Prototype**		
Test series	**Overhang length B_r mm**	**Significant wave height H_s m**	**Water level at toe m**	**Wave period T_p s**
A	0	1	0.6, 1, 1.6, 2, 2.4	8, 10, 12, 14, 16
B	7.5	1	0.6, 1, 1.6, 2, 2.4	8, 10, 12, 14, 16
C	15	1	0.6, 1, 1.6, 2, 2.4	8, 10, 12, 14, 16
D	30	1	0.6, 1, 1.6, 2, 2.4	8, 12, 14, 16
E	45	1	0.6, 1, 1.6, 2, 2.4	8, 10, 12, 14, 16
F	60	1	0.6, 1, 1.6, 2, 2.4	8, 10, 12, 14, 16
G	75	1	0.6, 1, 1.6, 2, 2.4	8, 10, 12, 14, 16
H	90	1	0.6, 1, 1.6, 2, 2.4	8, 10, 12, 14, 16
I	105	1	2, 2.4	8, 10, 12, 14, 16

After all tests had been completed, the most effective recurve wall overhang length was determined by comparing its overtopping volumes to the vertical wall (B_r = 0).

3.7 Summary of test conditions

Provided in Table 3.5 is a summary of the prototype test conditions of the experiments that were undertaken in this study.

Table 3.5: Summary of prototype test conditions

Geometrical properties		
Overhang length (B_r)	0, 0.15, 0.3, 0.6, 0.9, 1.2, 1.5, 1.8, 2.1	m
Wave period (T_p)	8, 10, 12, 14, 16	s
Freeboard (R_c)	0.6, 1, 1.6, 2, 2.4	m
Bed slope	1:18.6	-
Model scale	1:20	-

With the above-mentioned range of test conditions, with the repeated tests included, 240 experiments were done to create a comprehensive account of the overhang length that was most effective in the reduction of overtopping and, further, the freeboard height to which a recurve wall is most effective.

CHAPTER 4

RESULTS

4.1 Introduction

In this chapter the physical model test results are considered first, by giving a brief overview of the tests undertaken and their general performance. Secondly, the physical model results are compared against the results of previous research discussed in Chapter 2 Literature Review.

4.2 Physical model

During the course of this thesis, 240 tests were administered to compile a complete dataset in order to gain a better understanding of how the recurve wall performs under a wide set of sea-conditions. The behaviour of the recurve wall is considered by providing an overview of each series.

4.2.1 Test overview

The wave overtopping results are grouped by the recurve overhang length. The first test series, with the vertical wall with a 0 mm overhang length, is used as the basis dataset against which to compare the performance of each recurve shape to determine the efficiency of the relevant profile.

4.2.1.1 *Series A – 0 mm overhang*

In the vertical wall series with a 0 mm overhang, it was seen that a wave reflected from the recurve wall structure amplified the incoming wave and caused an amplified wave up-rush and overtopping volume over the crest of the structure. In certain instances, the reflective wave caused the incoming wave to break before reaching the structure, thus dissipating its energy and minimising the wave overtopping volume.

The waves from lower water levels break in front of the structure and a smaller wave overtopping volume splashed against the vertical wall and was thrown upward.

With higher freeboard levels, the non-impulsive waves appeared calmer and thus took longer to breach the crest of the vertical wall. However, when the wave overtopped over the crest of the structure, it was found that the overtopping volumes were significantly larger.

The dynamic wave absorption system was less effective for the 14 and 16 second wave periods, which resulted in higher wave heights. This had the most influence for the two lowest water levels. The overtopping events increased, as did the volume per event, however it should be noted that this was only a qualitative observation.

4.2.1.2 ***Series B – 7.5 mm overhang***

Series B, which has the smallest overhang length, provided a small reduction in wave overtopping, when compared to the vertical wall. This profile behaved similarly to those in Series A, with 0 mm overhang, as the small overhang did not shoot the wave uprush far enough seaward.

The small overhang restricts the small volumes that just overtopped the vertical wall. A small reduction in overtopping rate was seen.

However, with the more violent wave sequences (wave periods of 14 and 16 seconds) and at higher water levels, the overhang did not behave as designed and serves just as an obstruction for the incoming waves.

4.2.1.3 ***Series C – 15 mm overhang***

The 15 mm overhang behaved similarly to that in Series B with the 7.5 mm overhang length, providing a slightly greater reduction in overtopping at lower water levels than the vertical wall did.

However, the tests performed with the longer wave periods (14 and 16 seconds) and the two highest water levels, achieved poorer results than were recorded with the 7.5 mm overhang or the vertical wall.

As the waves with longer periods reached the structure, the wave curled into the recurve, and was trapped underneath the overhang, as the remainder of the oncoming wave pushes the trapped volume over the crest.

4.2.1.4 ***Series D – 30 mm overhang***

The 30 mm overhang was the first recurve shape with an overhang significant enough to direct the wave-uprush seaward. This overhang provided good overtopping reduction with the lower water levels.

During the experiments, it was observed that the 30 mm overhang length shoots the wave-uprush seaward at an extreme of 4 m physical model distance seaward (80 m prototype value seaward).

At the highest water level, the waves that curled into the recurve structure were minimal, thus the 30 mm overhang recurve provides small, if any, reduction in overtopping.

4.2.1.5 ***Series E – 45 mm overhang***

The 45 mm overhang provided a good reduction in overtopping for the lowest water levels. The overhang behaved similarly to the 30 mm overhang that shoots the wave-uprush a significant distance seaward. The wave uprush was shot back seaward over the crest of the incoming waves, and effectively cleared from underneath the seawall.

Further, when tested with a higher water level, this overhang length provided good reduction of wave overtopping compared with the shorter overhang lengths. While providing a reduction in the wave overtopping, this did not result in zero overtopping crossing crest level.

4.2.1.6 ***Series F – 60 mm overhang***

The recurve wall with the 60 mm overhang behaved similarly to that in Series H, providing good reduction in wave overtopping. This overhang length allowed the wave to curl into the shape and thus be thrown back seaward.

This overhang length was less effective at the two highest water levels tested, with the lowest freeboard. Although it did not provide zero overtopping, it nevertheless delivered a major reduction compared to the vertical wall results.

The zero overtopping results should, however, be interpreted carefully. The overtopping splashes were difficult to quantify. In some instances, the overtopping did not reach the water guiding plastic, but remained on the overhang ledge. There were splashes that were observed

during the test, that were too small to have had an effect on the overtopping bin water level (effectively less than $0.5l$ model value).

4.2.1.7 ***Series G – 75 mm overhang***

The 75 mm overhang recurve profile behaves similarly; however, it improved on the performance of the 60 mm overhang length.

The three lowest water levels provided good reduction in overtopping, allowing little, if any, overtopping over the crest of the recurve wall. The zero overtopping results should be interpreted carefully. The overtopping splashes were difficult to quantify, as discussed above.

4.2.1.8 ***Series H – 90 mm overhang***

Series H represents the second longest overhang length and, as expected, the lower water levels produced low overtopping volumes that were difficult to quantify, as discussed in Section 4.2.1.6.

The water splashes that were observed during the test were too small to have any effect on the overtopping bin water level (effectively less than $0.5l$ model value). In some instances, the overtopping did not reach the plastic water guide, but remained on the overhang ledge.

The lower water levels effectively reduced the wave overtopping as they allow the wave to curl into the wave recurve structure, which redirects the wave seaward.

4.2.1.9 ***Series I –105 mm overhang***

This profile represents the most extreme recurve profile, which was tested at only the two highest water levels. At the second highest water level, most of the waves hit the slanted component of the overhang length and the waves were cleared and shot back seaward at a small angle from the wall.

As the length of the overhang restricted the waves from overtopping the crest of the wall, the recurve wall had to withstand large forces as the wave collided with the seawall. In some instances, a void formed as the water level drops when the incoming wave reached the wall.

As the water level increased and the wave hit the perpendicular surface of the vertical wall, the wave overtopped the crest of the recurve wall.

4.2.1.10 ***Summary***

As expected, the performance of the recurve wall profiles in reducing the overtopping improved as the overhang length increased. The overhang length prevents the wave uprush from breaching the crest of the recurve wall. Up to a certain water level the longer overhang provides complete reduction in overtopping; however, the reduction is limited as the freeboard decreases.

The zero overtopping results in the series with overhang lengths of 45, 60, 75, 90 and 105 mm should be considered cautiously. Small overtopping volumes are difficult to quantify, because of the method used to measure the overtopping.

Series C, with a 15 mm overhang length, initially behaved similarly to the series with a 7.5 mm overhang length. However, with higher water levels, this profile reduction performance was less effective than that of the vertical wall. As the wave curls into the recurve, a portion of the wave is trapped beneath the overhang, and the remainder of the wave pushes this trapped volume over the crest.

The recurve seawalls achieved worse results with higher water levels and the longer wavelengths (14 and 16 seconds), which represented stormier conditions. These conditions submerged the recurve wall, which provided little or no resistance. During the study, results of the tests with a 16 second wave period were difficult to predict. This could be because the wave period lies on the outer boundary of the absorption gain value adjustment graph.

4.2.2 Overall performance

The physical model test results are provided in Annexure F per wave period, as the water level increases. The green represents the physical model values, with red representing the prototype volumes and overtopping rates.

The full dataset, comprising all wave periods, water levels and recurve overhang lengths provided below, was plotted with dimensionless overtopping parameter versus the freeboard over H_{mo} and is provided in Figure 4.1.

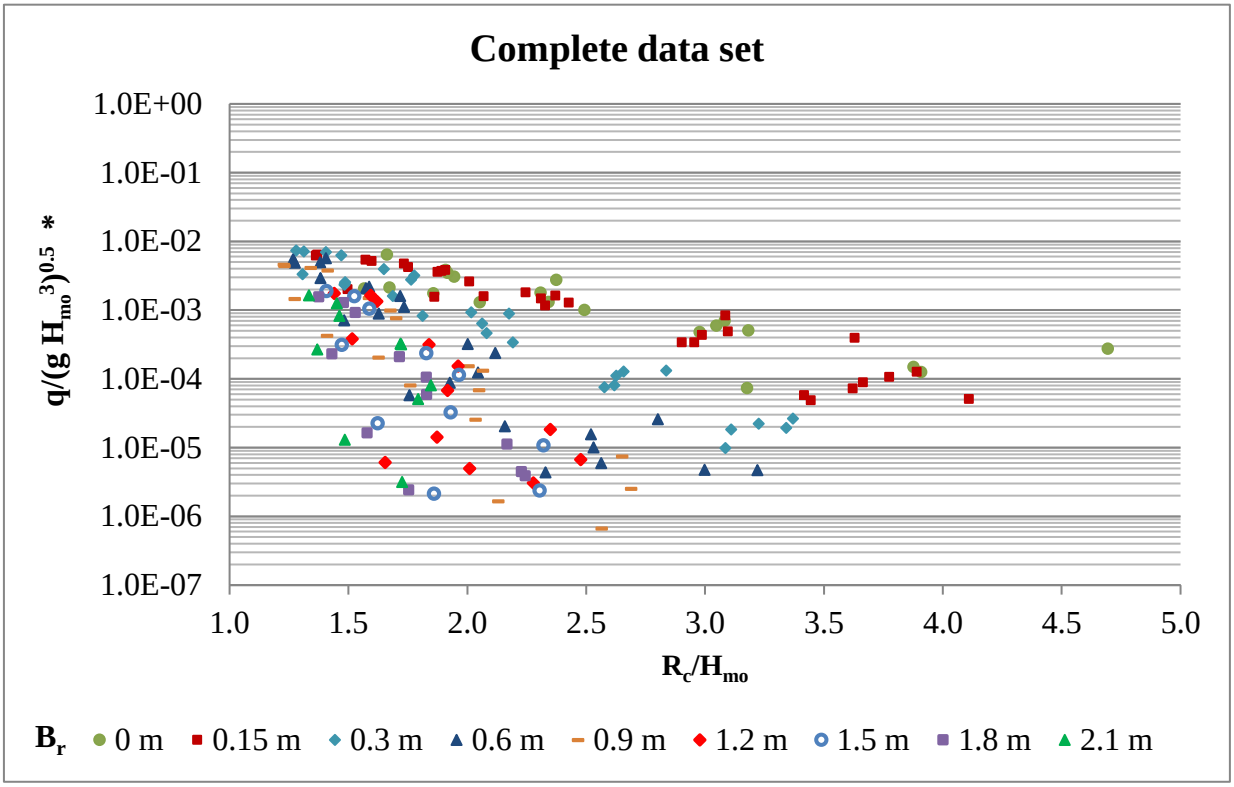

Figure 4.1: Complete data set overall performance

* Note the overtopping rate is in $m^3/s/m$

Tests that were repeated are shown on the figures as individual separate tests. The reference data plotted in Figure 4.1 are provided in Annexure F, per recurve overhang length. The small overtopping rates from the small and zero overtopping volumes at the 0.9, 1.2, 1.5 and 1.8 m overhang lengths are not represented on the graph, as 0 is not defined for a log scale.

Figure 4.1 indicates that all recurve wall shapes with overhang lengths larger than 0.15 m provide a clear reduction in wave overtopping. The 0.15 m overhang enhances the overtopping reduction in some cases; however, not in all conditions.

4.3 Results from EurOtop online calculation tool

The EurOtop overtopping calculation tool was evaluated with the measured data from the physical model tests. The data measured in the physical model tests are plotted against the probabilistic data provided in Figure 4.2.

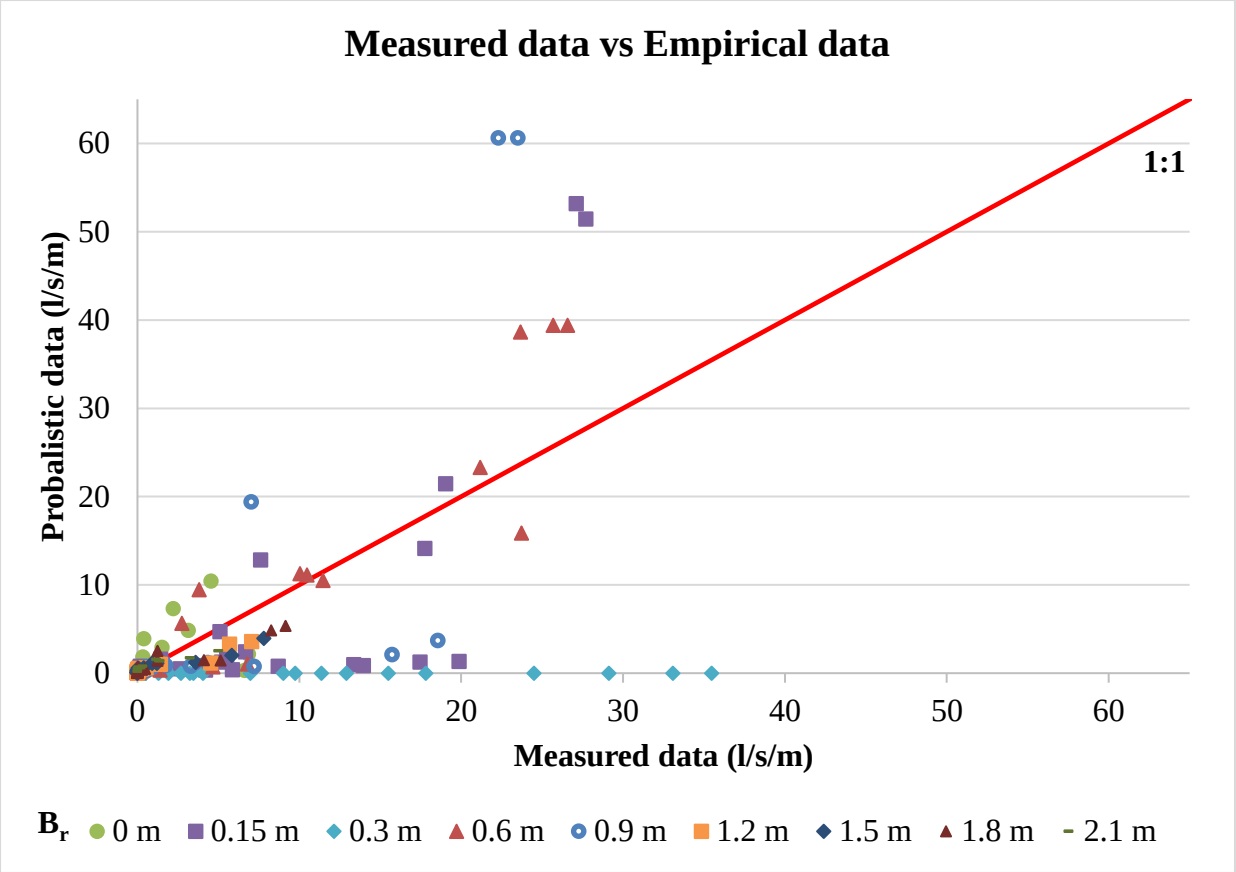

Figure 4.2: Measured versus Empirical data

It can be seen that with this wide spread of model test conditions, the empirical data does not fall on the 1:1 line, which represents a perfect relationship. The most critical finding is that the 15 mm overhang length was greatly under-predicted, delivering much larger overtopping rates than estimated.

The variability in the results is attributed to small overtopping volumes, extrapolated data, and limits within the dataset. This will be further discussed in Section 5.3.3.

4.4 Summary

All the overtopping lengths, except the 0.3 m overhang length (15 mm overhang length model value), improved the reduction performance of the vertical wall (0 m overhang length) under similar conditions.

The empirical data does not correspond to the measured physical model data in a 1:1 relationship as desired. This deviation and the remainder of the results are discussed and analysed in the following chapter.

CHAPTER 5

DATA DISCUSSION & ANALYSIS

5.1 Introduction

The data recorded during the physical model tests, the EurOtop online calculation tool, and previous research that was reviewed, will be compared, discussed and analysed in this chapter. Tests that were repeated to determine the accuracy are shown on graphs as two individual tests. The average of the repeated tests was used for calculation purposes in certain instances.

5.2 Physical model tests

The physical model tests were analysed by first commenting on the overall performance of the recurve walls.

Then considering, in the reduction of overtopping, the influence of

- overhang length,
- sensitivity of water level,
- wave period and
- wave height.

The accuracy and repeatability of the tests were considered and then, finally, the influence of the recurve on the recurve wall was examined. From here forward all overtopping rates are considered in *l*/s/m unless otherwise stated.

5.2.1 Overall performance of recurve walls

In the higher freeboard cases, the reflective wave collides with the incoming wave and the splashes travel over the crest of the structure. This collision also dissipates the energy of the incoming wave, as a mitigated wave hits the structure and then clears away from the wall.

As the waves hit the slanted component of the recurve wall, the waves are cleared from under the recurve wall. In some cases, the reflective wave amplifies the incoming wave so that wave

height increases and hits the recurve wall on the perpendicular surface of the overhang. The wave is thrown upward, falls on the overhang ledge and runs off behind the recurve wall.

Provided in Figure 5.1 is a comparison of the overall performance of the recurve walls.

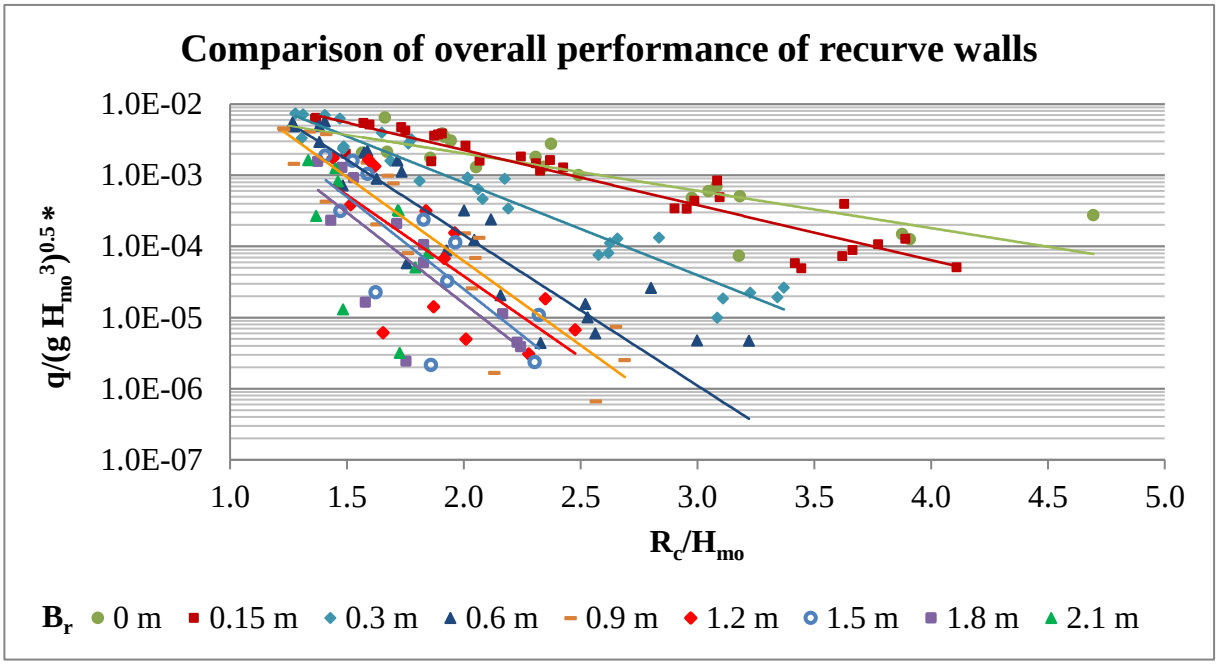

Figure 5.1: Comparison of overall performance of recurve walls

* Note the overtopping rate is in $m^3/s/m$

Comparing the performance in the reduction of overhang, it can be noted that as the overhang length increases, the trend lines have steeper slopes. This confirms that at low freeboard levels the overtopping rates increase rapidly. It should be noted that the zero overtopping results are not included in this graph, as these cannot be plotted on a log graph.

Kortenhaus *et al.* (2004) found that for $^{R_c}/_{H_{mo}} > 1.5$ the recurve reduces the overtopping rate, when compared with the vertical wall. However, for $^{R_c}/_{H_{mo}} < 1.2$, the recurve wall had no influence on overtopping.

Van Doorslaer and De Rouck (2011) determined that for a slope of 1:2 (V:H), the parapet angle of 60° (practically 30° and overhang of 0.3 m) performs the best. However, in this study it was found that overall the 0.3 m overhang provided worse results than the vertical wall. This is further discussed in Section 5.2.3.

Figure 5.1 illustrates that at the 0.6 m overhang length the slope becomes constant; however, the longer overhang lengths provided larger reduction (zero overtopping).

Van Doorslaer and De Rouck (2011) further found that at a 50° parapet angle (practically, an overhang of 0.15 and 0.3 m) overtopping reduction performance does not improve over that of a vertical wall. For this study, this result can be seen in the 0.15 m overhang length series. Provided in Figure 5.2 is a comparison of the 0, 0.15 and 0.3 m overhang lengths, magnified around the area of focus.

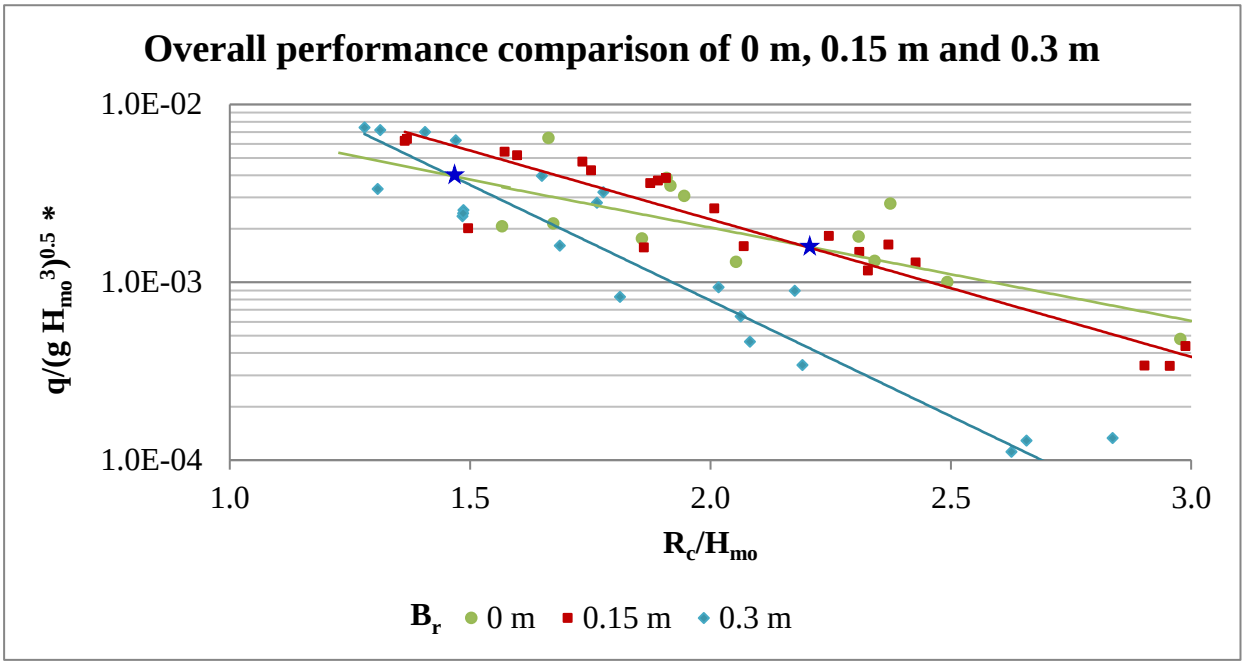

Figure 5.2: Overall performance comparison of 0 m, 0.15 m and 0.3 m

* Note the overtopping rate is in $m^3/s/m$

The intersections of lines are indicated on Figure 5.2 as dark blue stars. The mean of the 0.15 m series lies below the mean of the vertical wall, however for the $R_c/H_{mo} < 2$, the 0.15 m series intersects the 0 m mean. Similarly, the 0.3 m trend intersects the vertical wall at $R_c/H_{mo} < 1.5$. This illustrates that the 0.15 and 0.3 m overhang lengtdo not improve the reduction performance of the vertical wall.

5.2.2 Reduction of overtopping

The amount of the reduction in overtopping was evaluated by calculating the k-factor, as discussed in Section 2.5.1. To get a better understanding of the severity of the k-factor the overtopping rate of the vertical wall was plotted against the overtopping achieved for each overhang length, as provided in Figure 5.3.

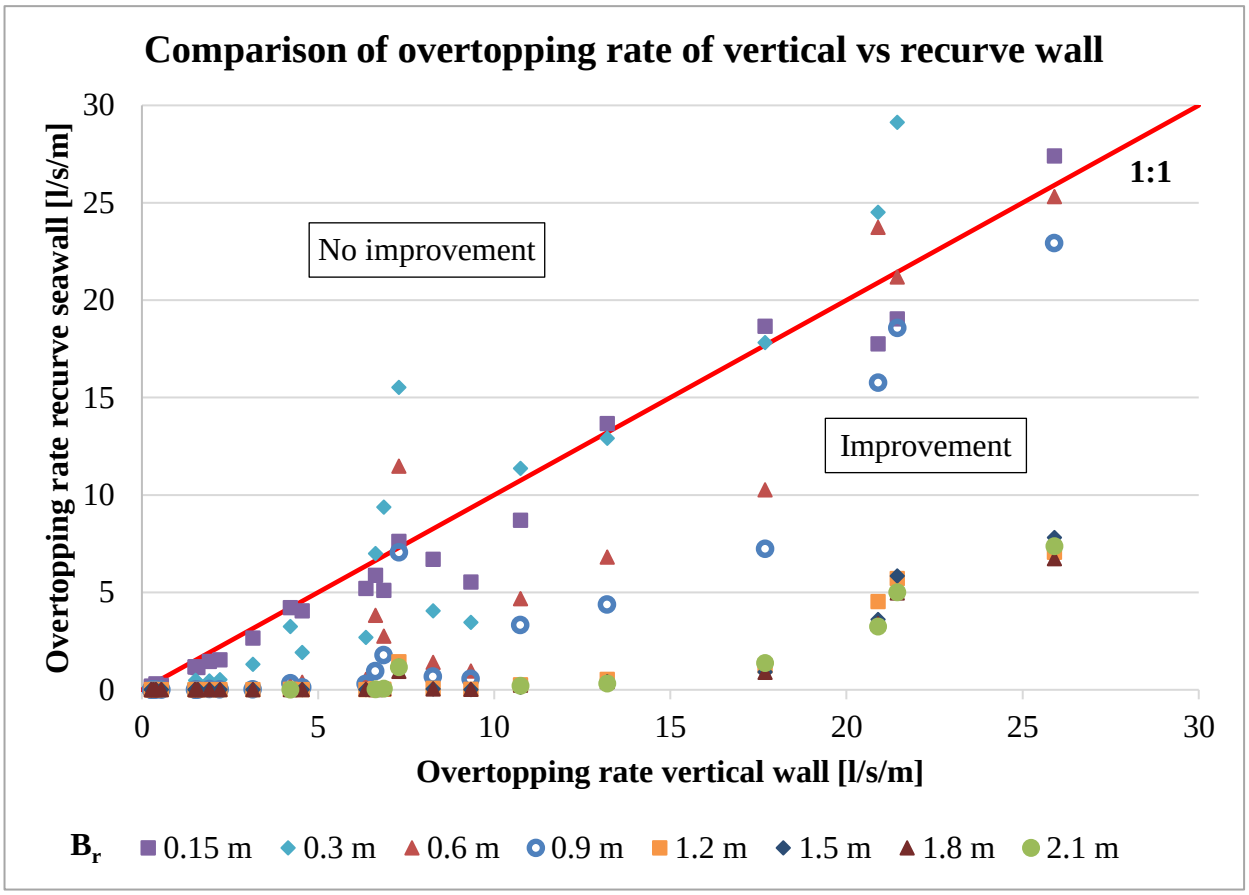

Figure 5.3: Comparison of overtopping rate of vertical versus recurve wall

Visually, Figure 5.3 may be interpreted as follows: If the data point lies below the red line, the recurve test improved the overtopping rate of the vertical wall. From Figure 5.3 it can be concluded that in most cases the recurve wall enhances the reduction in overtopping achieved by the vertical wall under similar conditions. The result of the 0.15 m overhang length test lies just below the line, indicating that this overhang length provided only a small reduction in overtopping rate and, in some instances, performed worse than the vertical wall.

There are individual tests in the 0.6 m overhang length series that perform worse than the vertical wall in similar conditions.

The 0.9 m overhang was the recurve with the longest overhang length before the wave height was adjusted, and it resulted in increased overtopping rates. This can be seen visually, as the 0.6 m overhang length outperformed the overtopping rate reduction of the 0.9 m overhang length, under similar conditions.

Furthermore, as the overhang length increases, the trend flattens, indicating that no further improvement occurs in the effectivity reduction. The lowest freeboard levels achieve large overtopping rate results.

To further refine the analysis to determine the freeboard height up to which the recurve wall would outperform the vertical wall, the k-factor (discussed in Section 2.5.1), is plotted against the freeboard over the significant wave height, in Figure 5.4.

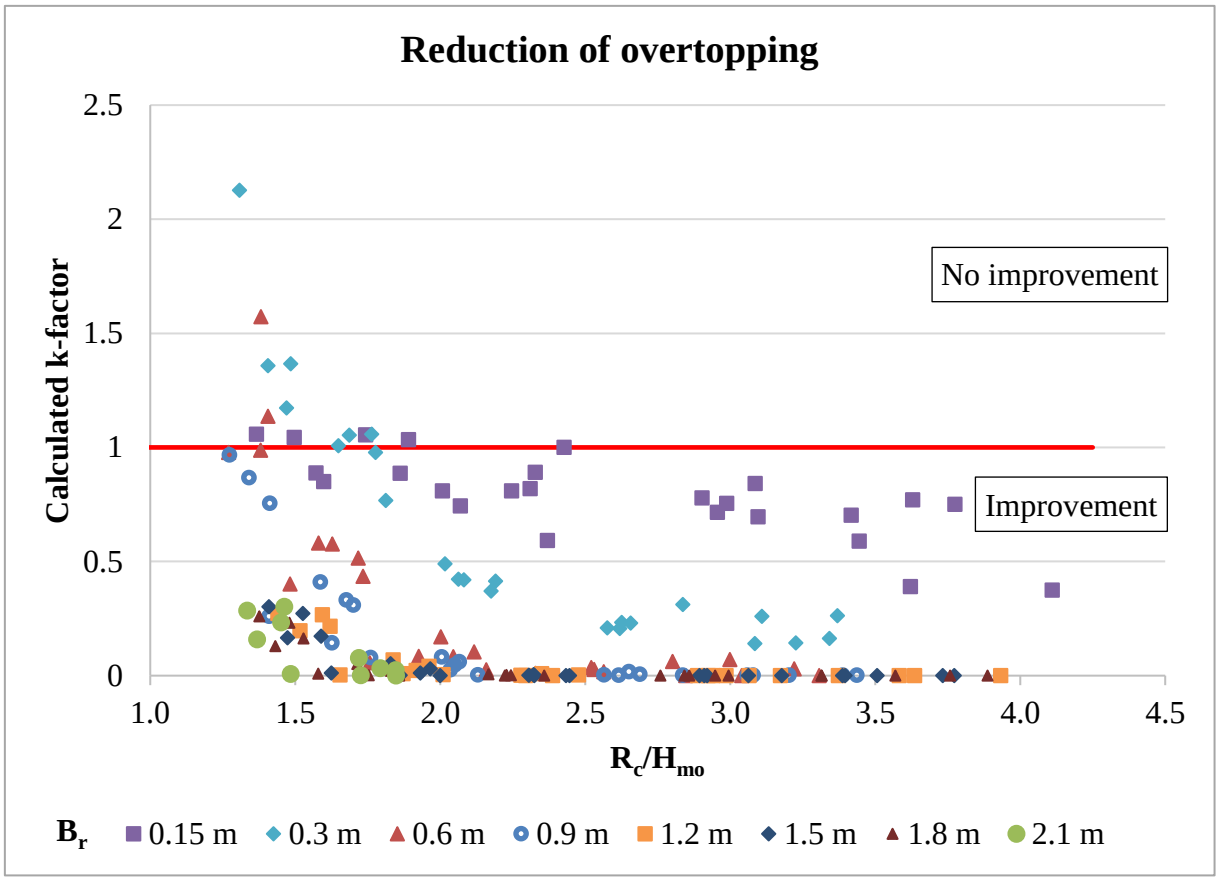

Figure 5.4: Reduction in overtopping: Full data set

Each recurve test is compared with the relevant vertical wall test with corresponding water level and wave period.

For the purposes of this study if a recurve wall achieved a k-factor equal to or more than one, the recurve wall fails in terms of improving the performance of the reduction of the overtopping of a vertical wall. This means that the recurve wall overtopping rate is equal to or greater than that of a vertical wall.

The k-factor per wave period for each recurve overhang length is provided in Annexure H. It should be noted that the zero k-factor results include scenarios where it was difficult to quantify small overtopping volumes or water splashes (green water). Kortenhaus *et al.* (2003) found that the magnitude of the k-factor depends on the degree of overtopping volume.

The overhang lengths that failed within the tested water levels are the recurve walls with overhang lengths of 0.15, 0.3 and 0.6 m. The reduction in overtopping for the recurve wall with the smallest overhang length of 0.15 m, is provided in Figure 5.5.

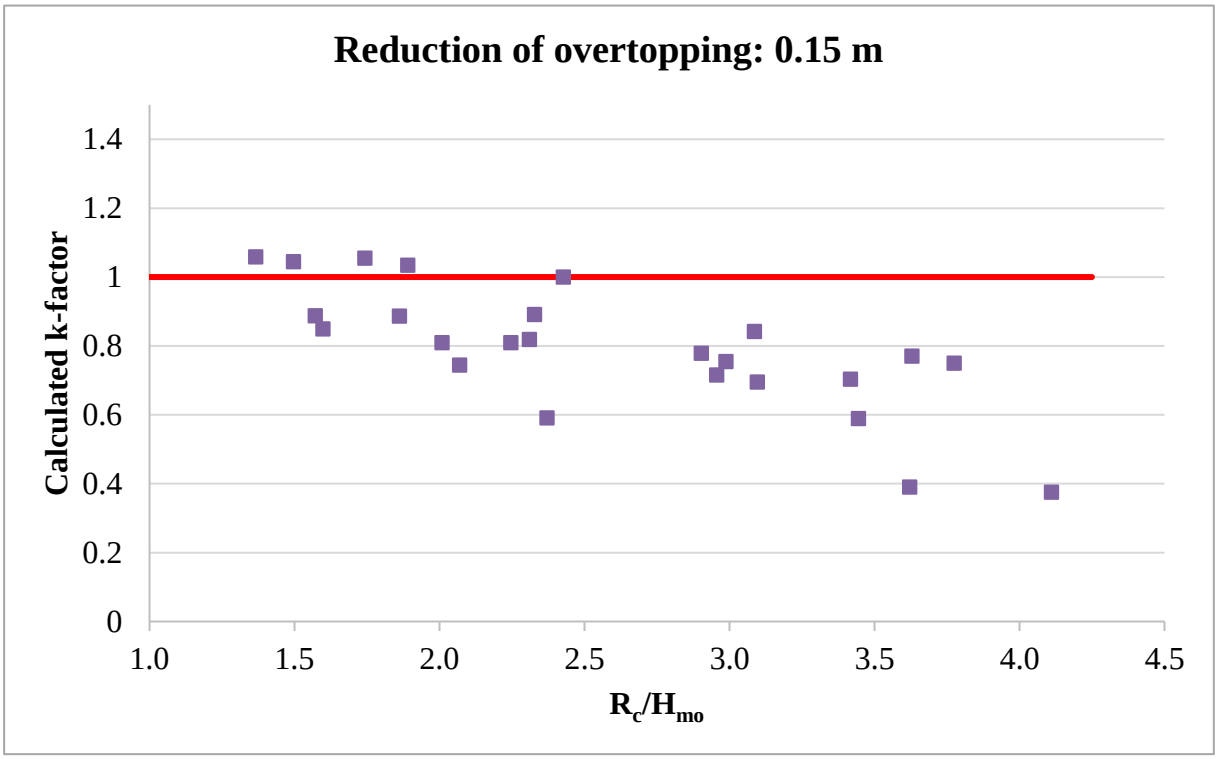

Figure 5.5: Reduction in overtopping: 0.15 m

For those cases where it does not fail, the 0.15 m overhang length provides only a slight improvement in the reduction of overtopping to that of the vertical wall. More than 50% of the data points lie in the 0.6 to 0.9 k-factor region, representing an improvement of only 10% to 40%. The failure pattern of the 0.15 m overhang length does not exhibit a well-defined clustering. To be certain that this recurve length provides a reduction in overtopping the use of this shape would be recommended only when $R_c/H_{mo} > 2.8$.

However, the 0.3 m overhang length provides a clearer failure relationship. The reduction of overtopping for the 0.3 m overhang is provided in Figure 5.6.

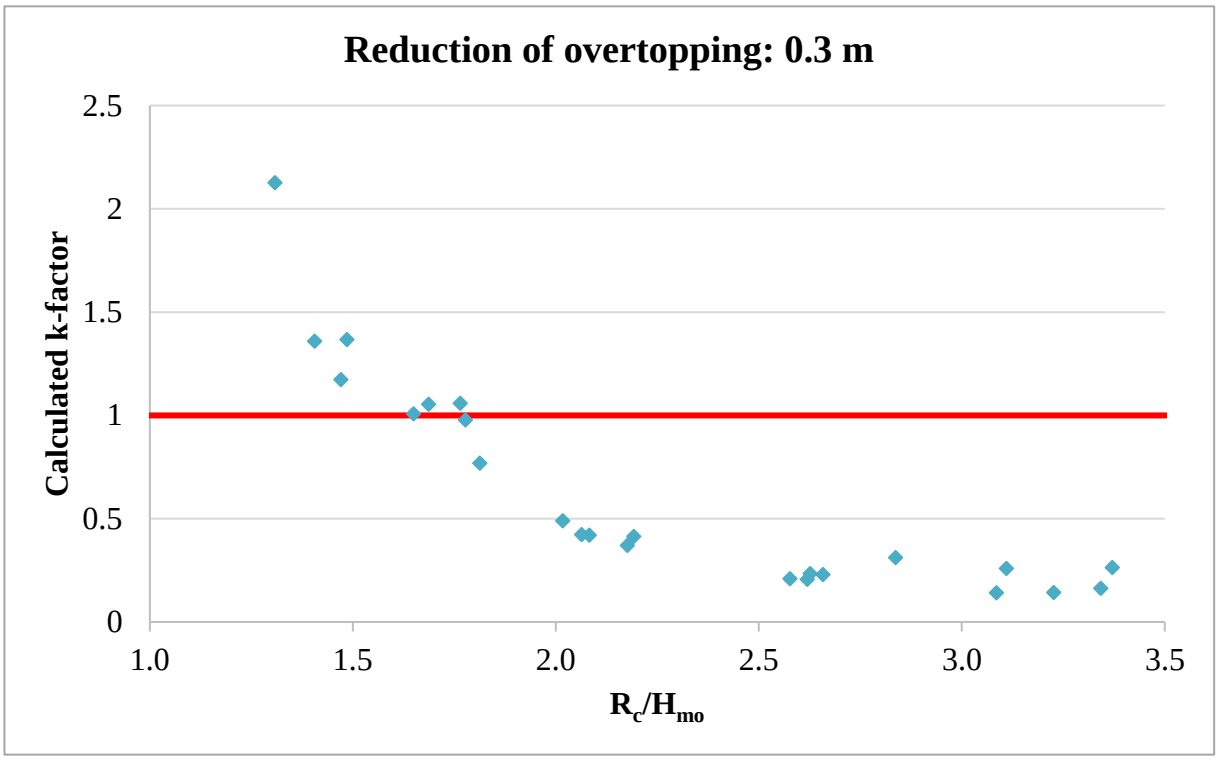

Figure 5.6: Reduction in overtopping: 0.3 m

Although this overhang length still fails at the low freeboard levels, it provides better reduction than the 0.15 m, with more than 50% of data in the 0.5 to 1 k-factor range. This represents 50%-100% reduction. The individual overhang lengths are provided in Annexure H.

5.2.3 Influence of the length of the overhang

The influence of overhang length on the overtopping rate is analysed per wave period. As the B_r/H_{mo} increases, it represents the increasing overhang length from 0 to 0.21 m. Figure 5.7 and Figure 5.12 demonstrate that the lower freeboard levels produce higher mean overtopping rates.

From research (Schoonees, 2014); (Roux, 2013), it was expected that a longer overhang length would increase the effectivity of the reduction of overtopping; however, only up to a point. Figure 5.7 illustrates that for a 10 second wave the 0.6 m overhang becomes trivial for all except the lowest freeboard water levels, for which a greater than 1.2 m overhang has no further influence on the reduction of overtopping.

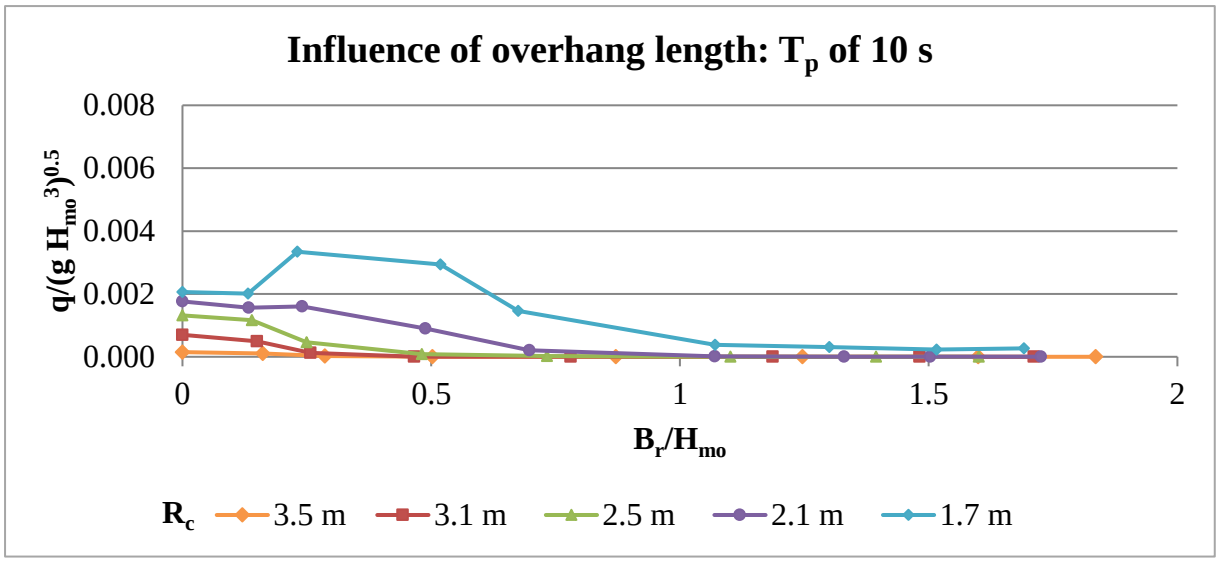

Figure 5.7: Influence of overhang length – T_p of 10 s

From Figure 5.7 it can be seen that the 2.5, 3.1 and 3.5 m freeboard levels achieve zero overtopping results for a B_r/H_{mo} > 0.25, which represents overhang lengths longer than 0.3 m. Similarly, this occurs for the 2.1 m freeboard level for a B_r/H_{mo} > 1.05, representing overhang lengths longer than 1.2 m. The overtopping rate at the highest freeboard level decreases as the overhang length increases, but never reaches zero overtopping.

There is a deviation from this trend in the lowest freeboard height, freeboard of 1.7 m, that is present in all wave periods. In Figure 5.7 the 0.15 m overhang provides a slight improvement in reduction of the overtopping rate compared with the 0 m overhang length, however, at a B_r/H_{mo} of 0.25, the 0.3 m overhang achieves worse overtopping results. This occurs as a volume is trapped under the 0.3 m overhang. This phenomenon is considered by analysing the overtopping reduction behaviour for the 10 second wave period with increasing overhang length in Figure 5.8 to Figure 5.10 (from 0 to 0.3 m overhang lengths).

For the first three data points, representing the 0, 0.15 and 0.3 m overhang lengths, the lowest two freeboard levels behave differently to the remainder of water levels. The vertical wall has more overtopping events than with the 0.15 and 0.3 m overhang lengths; however, this is mostly in small volumes.

The 0.15 m overhang length behaves similarly to the vertical wall, with a small lip of wave uprush overtopping crossing the crest of the recurve structure. The small recurve overhang restricts minimal overtopping, which results in the reduction of the dimensionless overtopping

parameter. Provided in Figure 5.8 and Figure 5.9 are the overtopping styles of the 0 and 0.15 m overhang lengths with arrows indicating the overtopping movement.

Figure 5.8: 0 m overtopping examples (A-17) (T_p = 10 s)

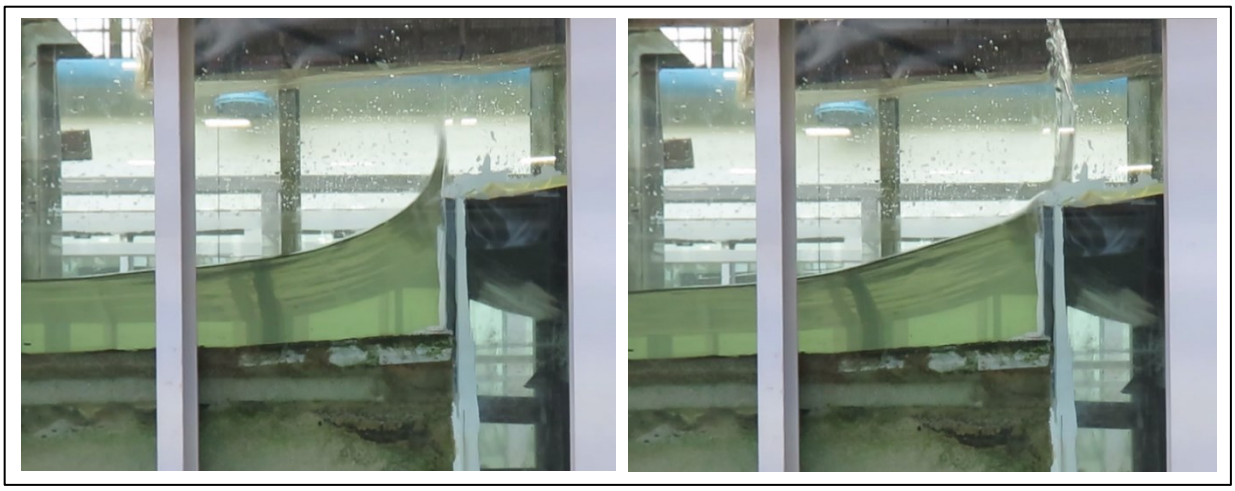

Figure 5.9: 0.15 m overtopping examples (B-17) (T_p = 10 s)

The 0.3 m overhang is the first recurve shape tested that changed the behaviour of the overtopping volume. The 0.3 m recurve shoots the wave uprush upward and a portion of the volume is trapped under the overhang component. As the remainder of the wave follows through, the volume trapped under the overhang is pushed over the crest of the recurve wall. Thus a larger volume breaches the crest of the structure than would without a recurve, as demonstrated in Figure 5.10, where arrows indicate overtopping movement.

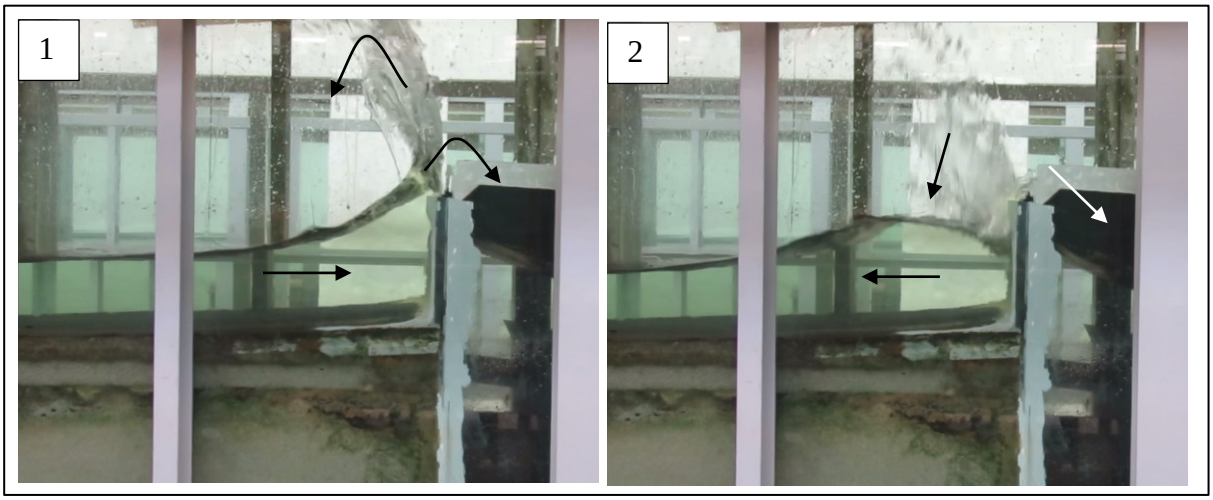

Figure 5.10: 0.3 m overtopping sequence (C-17) (T_p = 10 s)

The behaviour of the 0.3 m overhang length delivering worse overtopping reduction results than the vertical wall was observed in all wave periods. Schematisation of this phenomenon is provided in Figure 5.11, with arrows indicating the water movement.

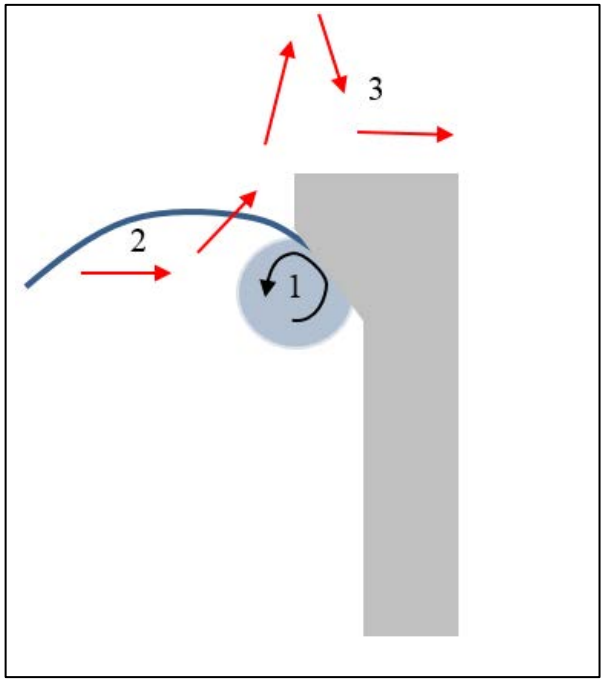

Figure 5.11: Schematic of 0.3 m overhang behaviour

It is clear that the various freeboard heights are not equally sensitive to the overhang length. This validates what Roux (2013) found: that the height of the crest level is critical and that great care should be taken when determining the crest level.

The influence the overhang length has on the reduction performance for the 14 and 16 second wave periods is as provided in Figure 5.12.

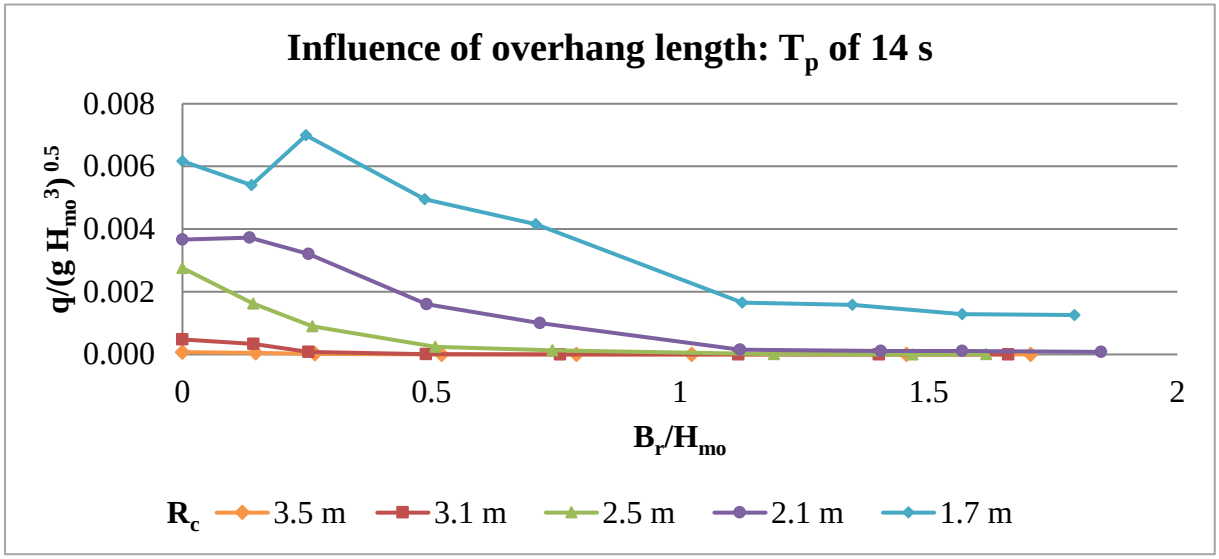

Figure 5.12: Influence of overhang length – T_p of 14 s

For the 2.5 and 3.1 m freeboard levels the overhang length becomes irrelevant from a B_r/H_{mo} of 0.5. The 1.7 m freeboard level flattens out from B_r/H_{mo} > 1.2, but does not reach zero overtopping.

The decline visible between the first two points of the 1.7 m freeboard level in Figure 5.12 demonstrates that the 0.15 m overhang length improves the reduction of overtopping for a vertical under similar conditions.

Figure 5.13 shows two examples of overtopping at the lowest freeboard level, for the vertical wall and for a 0.15 m overhang.

Figure 5.13: Vertical wall overtopping scenario (A-24) (Left)
0.15 m overhang length overtopping scenario (B-24) (Right)

The 0.15 m overhang length restricts overtopping minimally and therefore larger reflection occurs for the B-series. For the A series with a 0 m overhang, a larger volume is carried over the crest, visually represented as the decline in overtopping rate for the first two points in Figure 5.12.

The increase visible in Figure 5.12 for a R_c of 1.7 m is as discussed above for the 10 second wave period case. The overtopping scenario of the 14 second wave period in combination with the lowest freeboard level is shown in Figure 5.14.

Figure 5.14: 0.3 m overhang length overtopping scenario (C-24) (Left)
0.6 m overhang length overtopping scenario (D-24) (Right)

The tests series with a 0.3 and 0.6 m overhang lengths with a 14 second wave period are further analysed to understand the discrepancy in the overtopping rate trends that was seen to occur during this study. Although tests C-24 (0.3 m overhang) and D-24 (0.6 m overhang) have similar wave heights, the 0.6 m overhang provides greater reduction, however only slightly improves the 0.15 m overhang overtopping reduction. The 0.3 m overhang behaves as described in Figure 5.10, producing larger overtopping rates.

To recommend the overhang length that performs best overall the influence of the overhang length had to be examined for each water level. The wave periods for each freeboard level were plotted over each other, and are provided in Annexure K.

The maximum overhang length per water level was determined by allocating the point at which all the wave periods level out; thus the effect of increasing the overhang any further becomes insignificant. The minimum overhang length was identified by using an overtopping rate limit

of 0.1 *l*/s/m (the permissible overtopping rate for aware pedestrians provided by EurOtop (2007)). For the cases where this was not valid, the reduction of overtopping against a vertical wall was evaluated.

To determine the influence the freeboard level has on the overtopping rate, the 2.1 m freeboard height is provided in Figure 5.15.

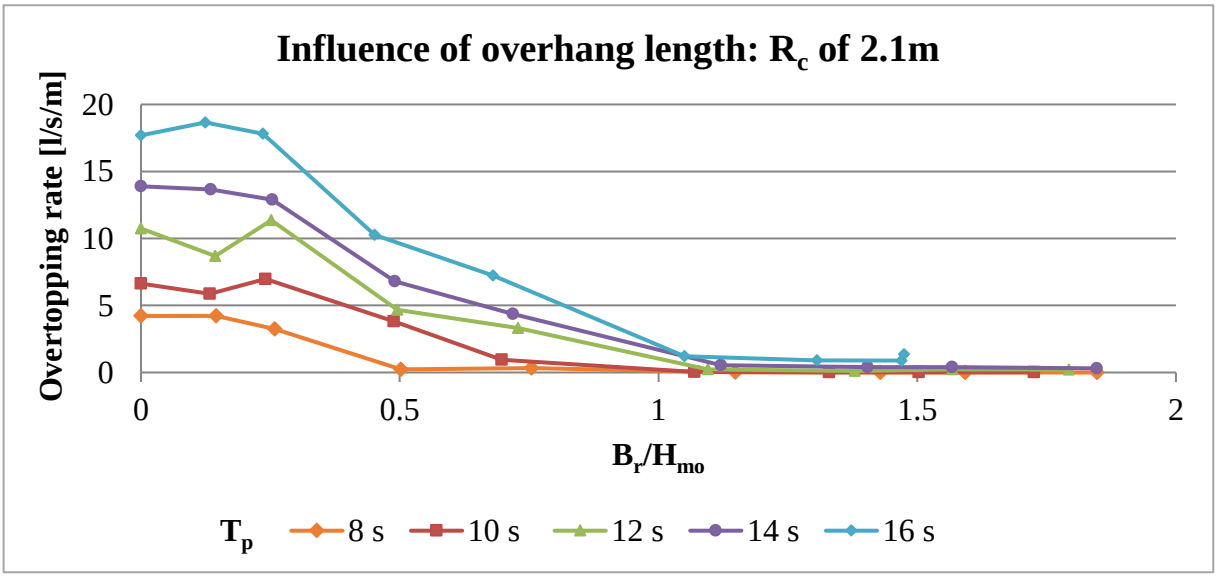

Figure 5.15: Influence of overhang length: R_c of 2.1m

From Figure 5.15 it can be observed that from $^{B_r}/_{H_{mo}} > 1$, the trends of all the wave periods flatten out, which indicates that the overhang length has no further impact on the overtopping rate. Only with the 0.6 m overhang does the overhang diminish the vertical wall overtopping rate. A similar procedure was followed to recommend a functional overhang length per water level, as provided in Table 5.1.

Table 5.1: Proposed overhang length per water level

Proposed overhang length per water level		
Water level at toe WL_{toe} [m]	**Freeboard R_c [m]**	**Overhang length B_r [m]**
0.6	3.5	0.15 - 0.6
1	3.1	0.15 - 0.9
1.6	2.5	0.3 - 1.2
2	2.1	0.6 - 1.5
2.4	1.7	0.9 - 1.2

5.2.4 Sensitivity to water depth

The sensitivity of the overtopping rate of recurve walls to water depth was investigated. The influence of the water depth below the vertical wall (0 m overhang), is provided in Figure 5.16.

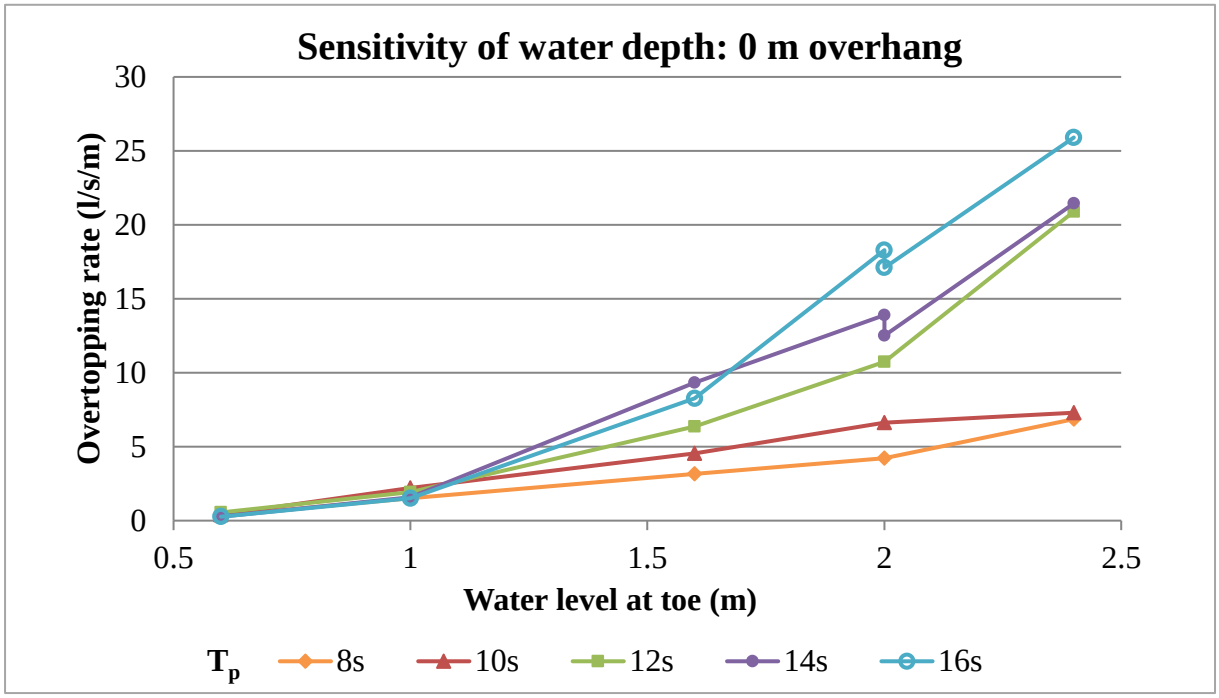

Figure 5.16: Sensitivity to the water depth of a vertical wall (0 m overhang)

Roux (2013) found, from empirical equations, that the change in water level at the toe of the seawall with 0 m overhang length is not critical. To the contrary, the present physical model results demonstrate that the overtopping rate is very sensitive to the change in water depth at the toe of the structure.

It can, however, be noted that the change in the overtopping rate is more critical for a 16 second wave than for the 8 second wave sequence. This is also true for the recurve walls, although the trend lines become steeper.

To determine the sensitivity of the overtopping rate of recurve wall to water depth, the 0.6 m overhang has been selected and the graph is provided in Figure 5.17.

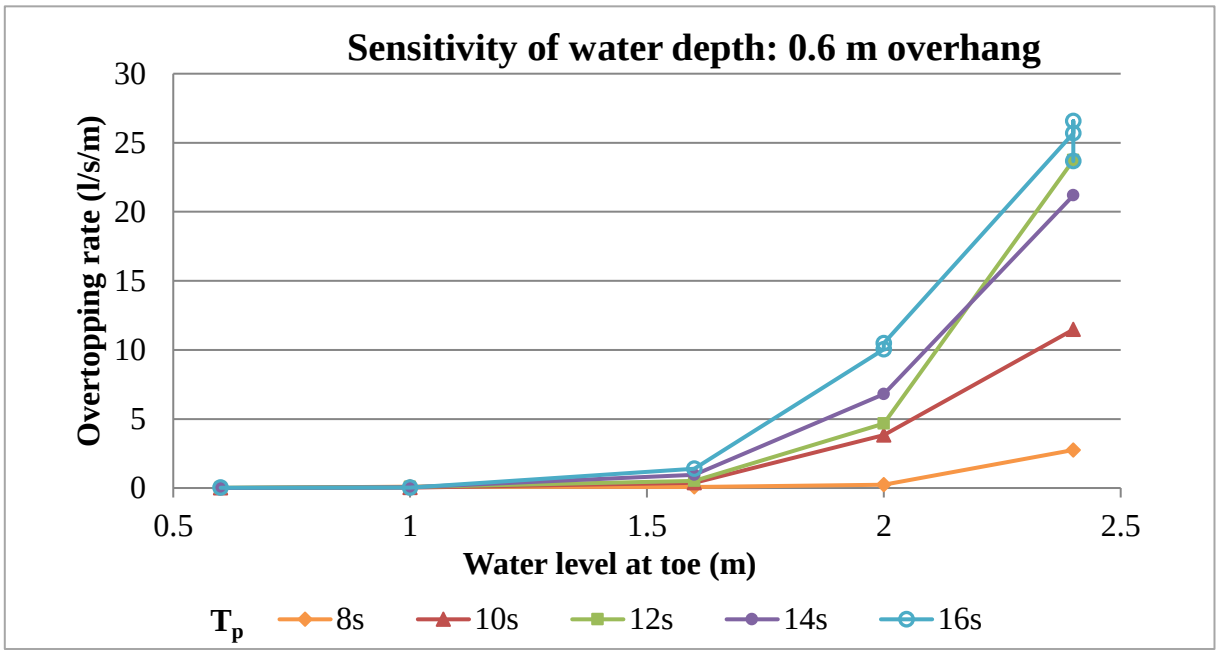

Figure 5.17: Sensitivity of a wall with 0.6 m overhang to water depth

Similarly, the wave period has an influence on the 0.6 m overhang only if the water level exceeds 1.6 m. The reason for the flattened graph and rightward shift is that, as the overhang length increases, the overtopping volumes that occur reduce. As the overhang length increases, the overtopping rate will be zero for greater water depths, and then rapidly increase.

For all the overhang lengths, in the scenarios in which the water level is less than the wave height, the wave period has no significant influence on the overtopping rate. Similarly, as for Figure 5.16, the slope of an 8 second wave is gentler than that of a 16 second wave. This indicates that the water depth is not the only dependent variable, and that the influence of the wave period should be researched.

5.2.5 Sensitivity of wave period

During the physical model tests the wave period was varied from 8 to 16 seconds, which influences the wavelength. To compare an 8 second wave with a 16 second, theoretically, with equal wave heights the 8 second wave crests would be more closely spaced than those of the 16 second wave. During this study variation was experienced because of influence of the wave maker and its influence on dynamic wave absorption, that will be further discussed in Section 5.2.8.

To determine the sensitivity of the overtopping rate to the wave period, each recurve wall was considered separately by plotting the overtopping rate against the wave period per water level

at the toe of the structure, as shown in Figure 5.18. The wave period sensitivity for each overhang length is provided in Annexure L.

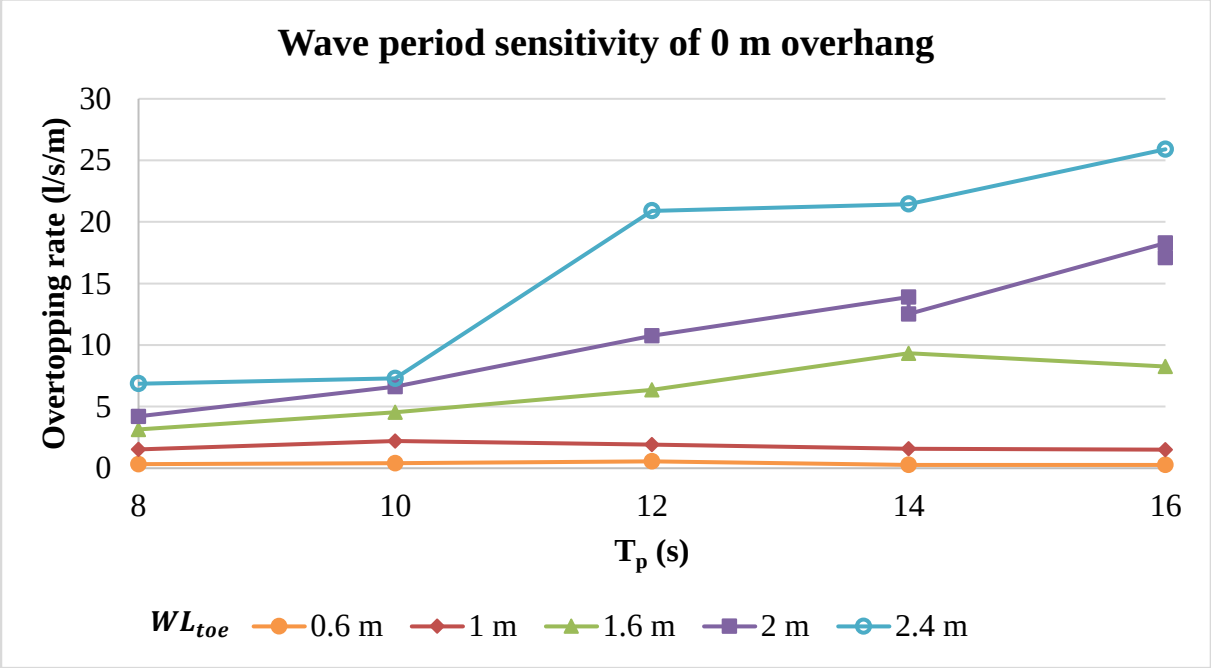

Figure 5.18: Vertical wall (0 m overhang) wave period sensitivity

As can be seen in Figure 5.18 and Figure 5.16, the wave period or water level cannot easily be isolated as the only dependent variable. The wave period and water level each have a large influence on the wave overtopping. For the vertical wall, with 0 m overhang length, with the lower water levels the wave period does not have as significant an influence on the overtopping rate. As the water level increases, the change in wave period becomes more critical in its influence on the overtopping rate.

In most cases where overtopping is not zero it can be seen that the longer wave periods produce larger overtopping rates. The shorter wavelengths comprise of smaller volumes of water, and clear easily from the wall. In some instances, with the larger wavelengths, the first wave is thrown seaward and becomes caught up in the second wave. This superimposes the waves, and a larger volume breaches the crest.

The recurve wall profiles with overhang lengths of 0.15, 0.3 and 0.6 m, are also more sensitive to wave periods at higher water levels. With the overhang lengths longer than 0.6 m, the wave period sensitivity is as provided in Figure 5.19.

The effect of the wave height on the wave overtopping on the recurve wall is further discussed in Section 5.2.6.

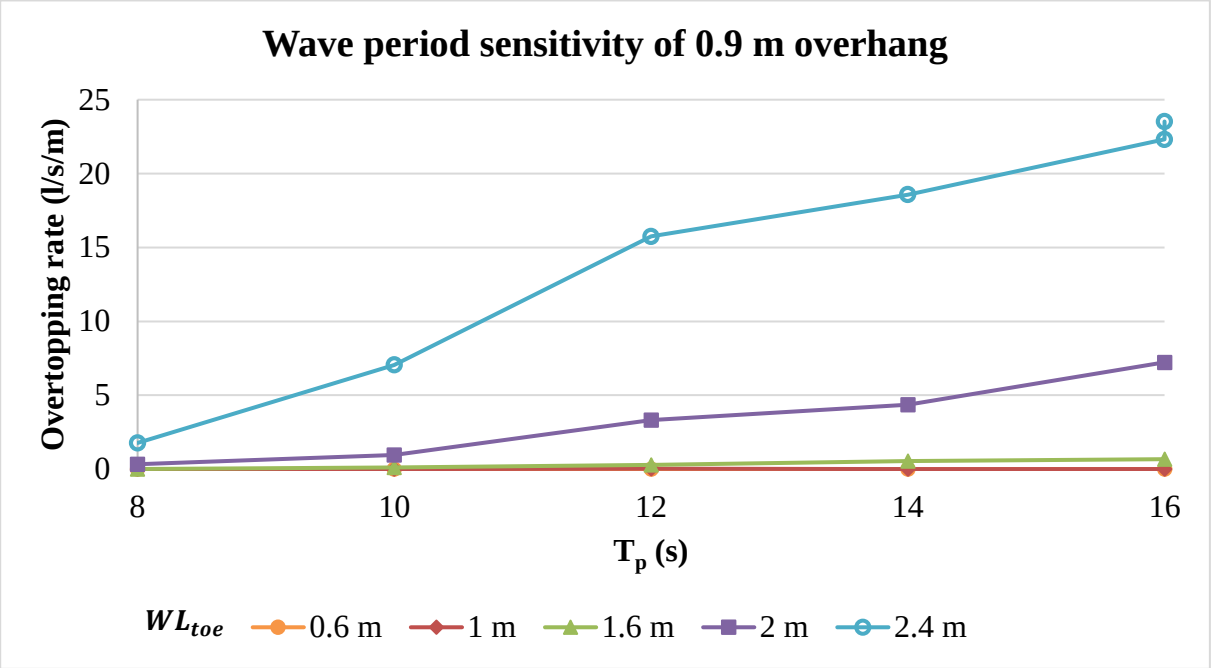

Figure 5.19: Sensitivity of 0.9 m overhang to wave period

As the overhang length increases, only the highest water level significantly increases the sensitivity of the wall to the wave period. This was in line with what had been expected for longer overhang lengths, as the recurve wall is more efficient in reducing overtopping. As a result, less water was breaching the crest of the recurve wall and thus less variability was visible in the overtopping rate.

For all the profiles, the overtopping rates increase as the wave period increases. This contradicts Roux (2013), who had found that the overtopping rate decreases beyond a T_p of 12 seconds.

The increased wave heights in physical model tests with 14 and 16 second wave periods resulted in increased overtopping rates. However, this increase would not be enough to explain the difference between model data and Roux's (2013) dataset.

5.2.6 Influence of wave height

For the purposes of the study it was chosen to keep the wave height constant. As a result of the differences noted in the wave height, with the other variables kept constant, the influence of the wave height on the overtopping rate is considered. This is further discussed in Section 5.2.7

The influence of both the maximum and incident wave heights were considered for the repeated tests, provided in Table 5.2.

Table 5.2: Influence of wave height on overtopping rate: T_p of 12 & 10 s

Influence of wave height on overtopping rate: T_p of 12 & 10 s									
Test		**A-3-3**	**A-3-4**	**A-3-5**	**A-3-6**	**A-22-1**	**A-22-2**	**A-22-3**	**A-22-4**
Overhang length (B_r)	**m**	0	0	0	0	0	0	0	0
Water level at toe	**m**	0.6	0.6	0.6	0.6	2.4	2.4	2.4	2.4
Maximum wave height	**m**	2.29	2.22	2.22	2.23	2.65	2.65	2.64	2.68
2% wave height	**m**	1.68	1.67	1.67	1.68	1.92	1.92	1.92	1.94
Incident wave height	**m**	0.97	0.99	0.97	0.97	1.11	1.10	1.10	1.10
$Volume_{measured}$	**l**	11	12	11	11	192	198	194	192
Overtopping rate	**l/s/m**	0.18	0.18	0.16	0.16	7.67	7.90	7.77	7.70

As provided in the table the H_{MAX}, $H_{2\%}$ and H_i are approximately equal. This corresponds with the overtopping rate recorded.

Difficulty was, however, experienced in achieving similar wave heights for the same test conditions for different overhang lengths. In Table 5.3 are two sets of data with the overhang length as the only variable.

Table 5.3: Influence of wave height on overtopping rate: T_p 14 & 16 s

Influence of wave height on overtopping rate T_p of 14 & 16 s									
Test		**A-24**	**B-24**	**C-24**	**D-24**	**A-25**	**B-25**	**C-25**	**D-25**
Overhang length (B_r)	**m**	0	0.15	0.3	0.6	0	0.15	0.3	0.6
Water level at toe	**m**	2	2	2	2	2.4	2.4	2.4	2.4
Maximum wave height	**m**	1.806	1.796	2.006	2.020	3.062	3.063	3.320	3.591
2% wave height	**m**	2.50	2.51	2.76	2.79	1.99	2.06	2.13	2.23
Incident wave height	**m**	1.07	1.11	1.21	1.21	1.19	1.24	1.29	1.34
$Volume_{measured}$	**l**	751	478	1019	741	1036	1096	1371	1012
Overtopping rate	**l/s/m**	21.45	19.03	29.12	21.18	25.90	27.40	33.09	25.31

Comparing the tests C-24 and D-24 (0.3 m versus 0.6 m overhang length), the H_{MAX}, $H_{2\%}$ and H_i should be similar. However, it can be seen that results from tests A-24 and B-24 are approximately the same, and similarly for tests C-24 and D-24. The exact influence this has on the physical model results is unknown.

During the course of the study it was observed that the maximum wave height influences the maximum volume that overtops the crest of the structure, although the volume per overtopping event was not measured. When comparing tests B-25 and C-25, the H_{MAX} is larger for test C-25, although this is not significantly noticeable in H_i.

In cases where the freeboard is at its lowest, the wave height has a great influence on the volume that overtops the crest of the recurve wall. This is at the lowest freeboard level (highest water level), where the wave height is greater than the available freeboard height (R_c = 0.6 m where H_i = 1 m). As the incoming wave hits the recurve wall, the wave submerges the wall and overtops the crest of the recurve wall.

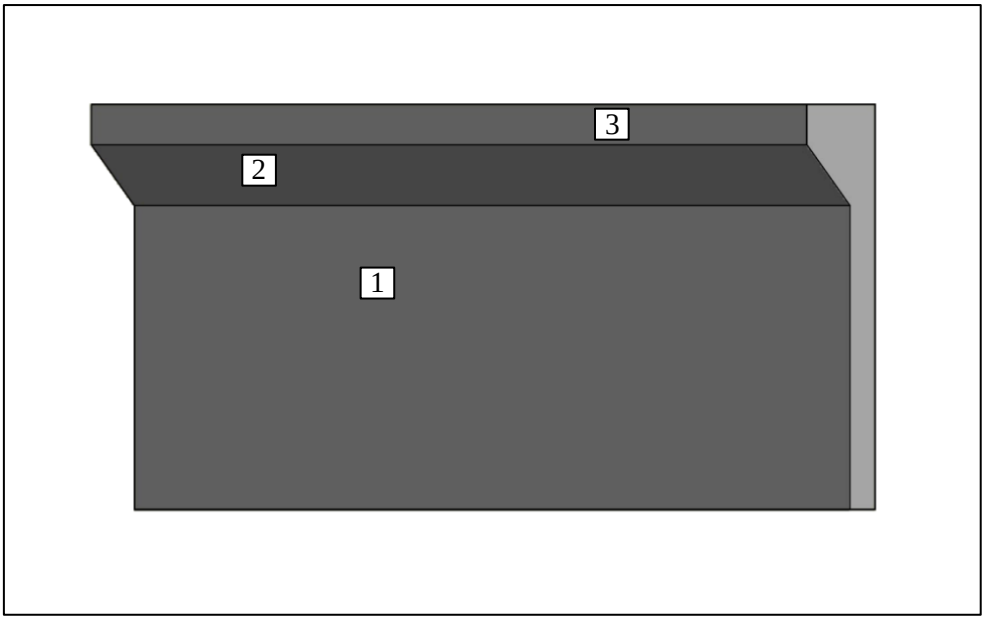

Figure 5.20: Illustration of recurve wall components

The recurve wall is designed so that the incoming wave hits the vertical wall and/or the slanted component of the wall (indicated as 1 and 2 on Figure 5.20). The waves are then reflected and cleared from the wall. In some cases, the incoming wave hits the recurve wall on the perpendicular face of the crest, above the recurve (indicated as 3 on Figure 5.20), and the wave is then thrown upward and a large quantity of water overtops the structure.

The effect of the wave height in the dimensionless overtopping parameter (Equation 2.16) is to the power of 1.5. This does not illustrate the influence of the wave height on the volume clearly.

5.2.7 Repeatability & accuracy

The accuracy of the tests was evaluated by repeating two sets of tests four times. To evaluate the variability in the overtopping rates with repeated conditions, the coefficient of variation (CoV) is calculated by using Equation (5.1).

$$CoV = \frac{\sigma}{\mu} \times 100 \tag{5.1}$$

Where:

σ – Standard deviation of prototype overtopping rates

μ– Average of the prototype overtopping rates

The first test was that where only the overtopping bin was used as an overtopping measuring technique as provided in Table 5.4. Second, the test with a higher water level, using the pump in combination with the overtopping bin as recording technique, as demonstrated in Table 5.5.

Table 5.4: Accuracy test with use of overtopping bin

Accuracy test with use of overtopping bin						
MODEL VALUES	**Test**		**A-3-3**	**A-3-4**	**A-3-5**	**A-3-6**
	WL_{paddle}	**m**	0.446	0.446	0.446	0.446
	WL_{toe}	**m**	0.03	0.03	0.03	0.03
	T_p	**s**	2.638	2.638	2.638	2.638
	Test duration	**s**	2638	2638	2638	2638
	$H_{mo\ AVG}$	**mm**	57.10	58.31	57.10	57.40
	H_i	**mm**	48.28	49.47	48.31	48.59
	$Volume_{measured}$	**l**	**11.00**	**11.50**	**10.93**	**11.00**
PROTOTYPE VALUES	**WL_{toe}**	**m**	0.6	0.6	0.6	0.6
	R_C	**m**	3.4	3.4	3.4	3.4
	T_p	**s**	12	12	12	12
	$H_{mo\ AVG}$	**m**	1.14	1.17	1.14	1.15
	H_i	**m**	0.97	0.99	0.97	0.97
	$Volume_{measured}$	**l**	**88000**	**92000**	**87467**	**88000**
	Overtopping rate	**l/s**	3.52	3.54	3.24	3.14
	Overtopping rate pm	**l/s/m**	0.18	0.18	0.16	0.16
	CoV	**%**	2.37			

Table 5.5: Accuracy tests with use of pump

Accuracy test with use of pump						
MODEL VALUES	**Test**		**A-22-1**	**A-22-2**	**A-22-3**	**A-22-4**
	WL_{paddle}	**m**	0.535	0.535	0.535	0.535
	WL_{toe}	**m**	0.12	0.12	0.12	0.12
	T_p	**s**	2.236	2.236	2.236	2.236
	Test duration	**s**	2236	2236	2236	2236
	$H_{mo\ AVG}$	**mm**	70.93	70.56	70.91	70.87
	H_i	**mm**	55.25	54.99	55.24	55.20
	$Volume_{measured}$	**l**	**191.71**	**197.61**	**194.20**	**192.38**
PROTOTYPE VALUES	**WL_{toe}**	**m**	2.4	2.4	2.4	2.4
	R_c	**m**	1.7	1.7	1.7	1.7
	T_p	**s**	10	10	10	10
	$H_{mo\ AVG}$	**m**	1.42	1.41	1.42	1.42
	H_i	**m**	1.11	1.10	1.10	1.10
	$Volume_{measured}$	**l**	**1533713**	**1580911**	**1553595**	**1539054**
	Overtopping rate	**l/s**	153.37	158.09	155.36	153.91
	Overtopping rate pm	**l/s/m**	7.67	7.90	7.77	7.70
	CoV	**%**	1.36			

The coefficient of variability (CoV) of the repeated tests is less than 5%, which is good coefficient of variability. As a result of the variations in wave heights and the maximum wave height that was experienced during the experiments, the CoV could not be further lowered. The CoV for the CLASH dataset was up to 13% (De Rouck *et al.*, 2005). This is allowable, as the data were recorded in different flumes and on variable scales. The CoV was expected to be lower in this case as the physical model setup was the same for all tests.

5.2.8 Influence of recurve wall on Dynamic Wave Absorption

As the physical model tests were executed, and the overhang length was increased, it was observed during the 1.2 m overhang series, series F, that the wave height increased gradually. Thus, indicating that the dynamic wave absorption system is not working as designed, as discussed in Section 2.6.2, and not removing the reflective outgoing wave from the wave paddle. This resulted in mean wave heights outside the tolerable range. Practically, this was seen by the height of the waves being much larger than the design wave height, which was

confirmed by the H_{mo} retrieved from the DAQ software. This occurred while the design parameters were being kept constant, as well as specifically keeping the water level constant throughout the test.

The dynamic wave absorption system designed by HR Wallingford (2010) for a 2D flume, was developed to enable adjustment of the wave height reflecting from the wave paddle, in order to generate wave heights more accurately to design conditions. It is known that the DWA is not as effective if applied to vertical structures, for example Series A, with 100% reflection. The application of the DWA concept on the recurve wall further worsens its performance.

When the recurve wall was functional in the flume, a larger percentage of the incoming wave was reflected back in the direction of the wave paddle. Thus no adjustment was made for the increased reflective wave and, therefore slowly the wave heights were amplified during the course of the experiment.

	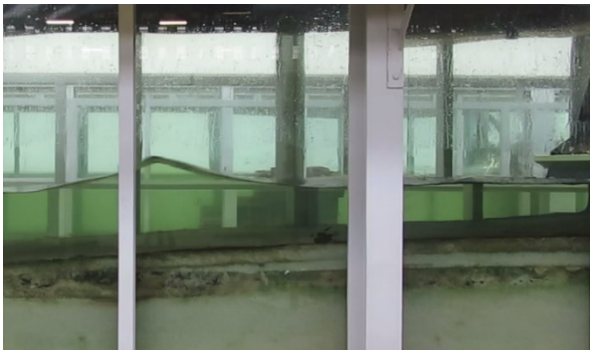
Reflective wave	Amplified reflective wave

Figure 5.21: Amplified reflective wave F-22

As the DWA is only a function of the water depth and wave period, an adjustment was made to use a lesser wave height to counteract this phenomenon. This delivered an average wave height that was similar to that of the other data series. Figure 5.22 illustrates the influence of wave adjustment on Test F-25.

	
F-25	F-25 with wave adjustment

Figure 5.22: Influence of wave adjustment F-25

The adjustment reduced the average H_i from 72 mm to 58 mm. It can be seen that large volumes overtopped the crest level of the recurve wall.

5.3 Comparison with previous results and EurOtop tool

The physical model results were compared with results obtained from Allsop *et al.* (2005), Schoonees (2014), as well as with those from the online EurOtop overtopping prediction tool.

5.3.1 Allsop *et al.* (2005)

The physical model results were compared with the research of Allsop *et al.* (2005) in two ways. First, by plotting the dimensionless overtopping parameter against the freeboard over wave height and, secondly, by evaluating the theoretically developed k-factor against the calculated k-factors.

Further, a theoretical k-factor was developed by Allsop *et al.* to provide an indication of what reduction in the overtopping rate could be expected from an overhang length.

The theoretical k-factor versus the calculated k-factor was plotted per overhang length, provided in Annexure L. Figure 5.23 shows results for the 0.6 m overhang length.

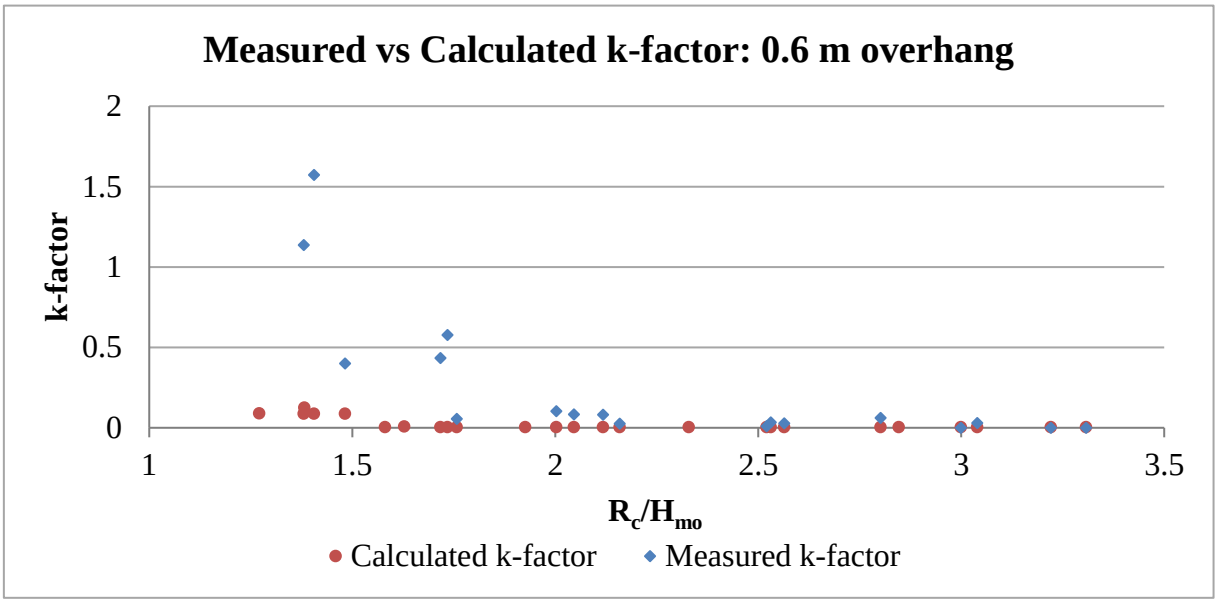

Figure 5.23: Measured versus Calculated k-factor: 0.6 m overhang

The theoretical k-factor equations deliver a maximum k-factor of one. Thus, the scenario of a recurve wall that does not improve the overtopping rate of a vertical wall is not taken into account of.

Practically, during the course of this study this highlights a shortcoming in the theoretical k-factor. Visually it can be seen from the figure by the calculated k-factor forming a horizontal line from $R_c/H_{mo} < 1.5$. The measured k-factor does include scenarios where recurve walls fail, resulting in k-factors larger than one.

The EurOtop database and k-factor method was developed with a recurve profile as demonstrated in Figure 5.24 on the right. However, the physical model recurve wall geometry is as provided on the left.

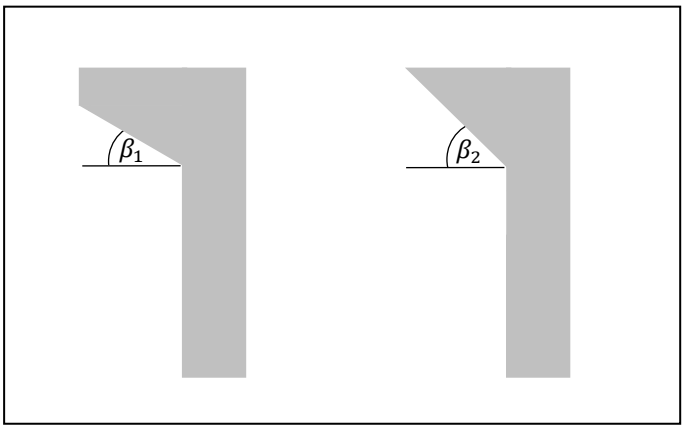

Figure 5.24: Physical model recurve wall (left);
EurOtop Wave return wall (right)

The calculated k-factor should predict increased overtopping rates, as a result of the difference in geometry. The opposite is visible in Figure 5.23, as all the calculated k-factors are lower than the measured k-factor. This implies that the reduction is over-predicted. Allsop *et al.* (2005) recommended that a physical model should be used if a reduction factor of 20 is required (k < 0.05).

As the overhang length becomes greater, the k-factor reduces as expected and correlates better with the calculated k-factors. The 0.3 m overhang series, as discussed in the previous section, does not improve the overtopping reduction performance of the vertical wall. The measured versus the calculated k-factor for the 0.3 m overhang series is provided in Figure 5.25.

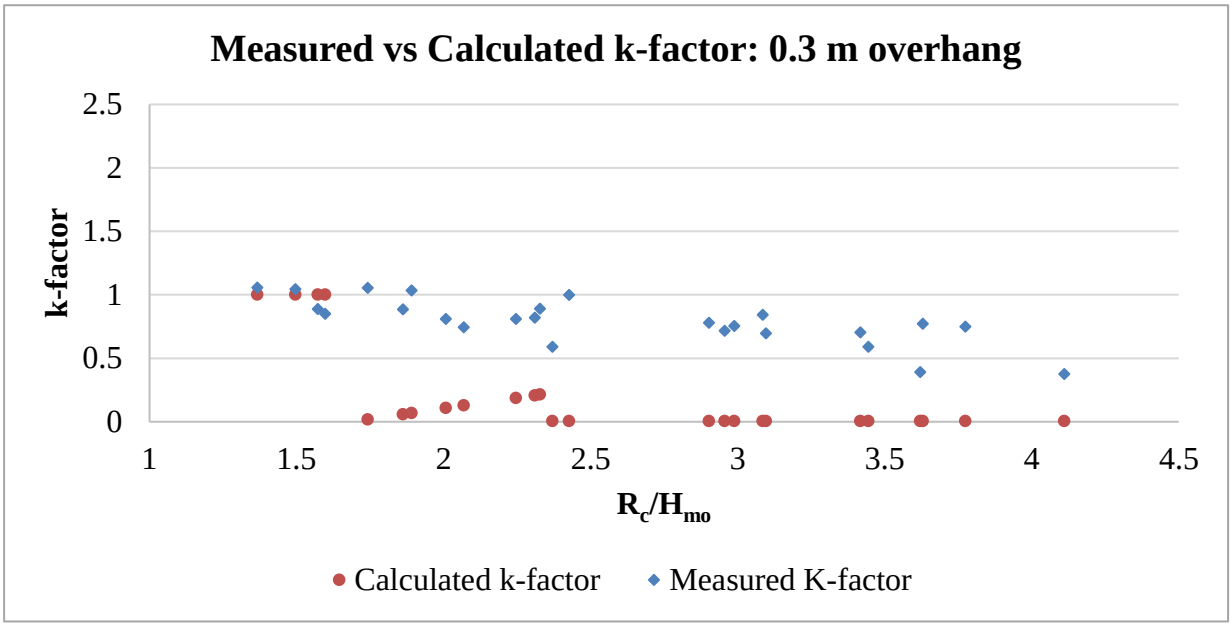

Figure 5.25: Measured versus Calculated k-factor: 0.3 m overhang

For all the overhang lengths, the calculated k-factor becomes constant at a certain point.

The theoretical k-factor equations (2.13) to (2.15) are dependent on the R_c and H_{mo}, the values of which vary for each series, but using the same variables causes similar k-factors, for example at $R_c/H_{mo} < 1.5$.

5.3.2 Schoonees (2014)

The dataset for this research project was designed to expand on Schoonees's (2014) research. Two datasets were repeated, to determine whether tests with overlapping conditions could be used. The first dataset was the 10 second wave period for the 0 m overhang recurve profile (i.e.

the vertical wall). The comparison of Schoonees's (2014) vertical wall dataset extract was compared against the model results, provided in Table 5.6.

Table 5.6: Comparison of Model results and Schoonees (2014) 0 m recurve profile

Extract Series A: 0 m overhang recurve profile						
Test		**A-2**	**A-7**	**A-12**	**A-17**	**A-22**
WL_{toe}	**m**	0.03	0.05	0.08	0.1	0.12
R_c	**m**	0.175	0.155	0.125	0.105	0.085
T_p	**s**	2.236	2.236	2.236	2.236	2.236
$H_{mo\ AVG}$	**m**	0.0451	0.0503	0.0534	0.0565	0.0543
Overtopped volume	**l**	10.00	55.25	113.77	165.72	182.39

Schoonees's (2014) 0 m overhang recurve profile						
Test		**AVG_{A6-7}**	**AVG_{A4-5}**	**AVG_{A2-3}**	**A-1**	**AVG_{A8-10}**
WL_{toe}	**m**	0.03	0.05	0.08	0.1	0.12
R_c	**m**	0.17	0.15	0.12	0.1	0.08
T_p	**s**	2.236	2.236	2.236	2.236	2.236
$H_{mo\ AVG}$	**m**	0.060	0.063	0.063	0.060	0.059
Overtopped volume	**l**	29.08	127.82	312.64	454.78	454.85

It can be seen that the model results are significantly lower than those in the Schoonees's (2014) dataset. This can be attributed to various factors, namely, the water level, crest level and wave height.

It was attempted to replicate Schoonees's (2014) model setup to achieve results that corresponded as closely as possible. Because of the uncontrollable variables present during the configuration of the wall into the flume, the vertical wall was a height of 0.205 m, compared to the designed 0.2 m. This provided an additional 0.005 m of freeboard, which would cause less water to travel over the crest of the recurve wall. Furthermore, to achieve the same water level at the toe of the recurve wall, the water level at the wave paddle was lowered by 0.005 m. This was taken into account in all calculations and should not have a great effect on the overtopping rate.

Although the discrepancies might seem large in comparison to the varying wave height, the two different datasets correlated well with the corresponding EurOtop datasets. A root mean squared analysis was performed and is provided in Annexure M. For the vertical wall, the physical

model tests delivered a root mean squared error of 1.47. Between Schoonees (2014) and the EurOtop a larger error of 3.805 was achieved; although it still indicates a small error.

The wave heights achieved in the physical model are closer to the designed wave height of 0.05 m than that achieved by Schoonees (2014). These deviations all contribute to a lower overtopping volume. This also applies to the 1.2 m recurve profile that is provided in Table 5.7.

Table 5.7: Comparison of model results and Schoonees (2014) 1.2 m recurve profile

Extract Series F: 1.2 m overhang recurve profile						
Test		**F-2**	**F-7**	**F-12**	**F-17**	**F-22**
WL_{toe}	**m**	0.03	0.05	0.08	0.1	0.12
R_c	**m**	0.175	0.155	0.125	0.105	0.085
T_p	**s**	2.236	2.236	2.236	2.236	2.236
$H_{mo\ AVG}$	**m**	0.048	0.051	0.054	0.056	0.056
Overtopped volume	**l**	0.00	0.00	0.00	1.32	35.75
Schoonees's (2014) 1.2 m overhang recurve profile						
Test		**C-5**	**C-4**	**AVG_{C1-3}**	**AVG_{C6-9}**	**AVG_{C10-12}**
WL_{toe}	**m**	0.03	0.05	0.08	0.1	0.12
R_c	**m**	0.17	0.15	0.12	0.1	0.08
T_p	**s**	2.236	2.236	2.236	2.236	2.236
$H_{mo\ AVG}$	**m**	0.063	0.066	0.062	0.063	0.059
Overtopped volume	**l**	0.42	1.22	2.23	26.16	153.30

With the 1.2 m overhang profile, the results for the lower water levels, where most of the water is reflected against the vertical wall and the bottom component of the overhang length. The deviation is thus not as significant as in the lower freeboard cases, where the crest level had a significant influence.

The error for the 1.2 m overhang length is lower than the error for the vertical wall. The RME for the physical model is 0.25, compared to a 1.76 error achieved by Schoonees (2014). This indicates that the data series error is smaller than that in Schoonees's (2014) dataset, although it still indicates a small error. The full root mean squared method analysis is provided in Annexure M.

A comparison of the physical model results and those of Schoonees (2014) can be seen in Figure 5.26.

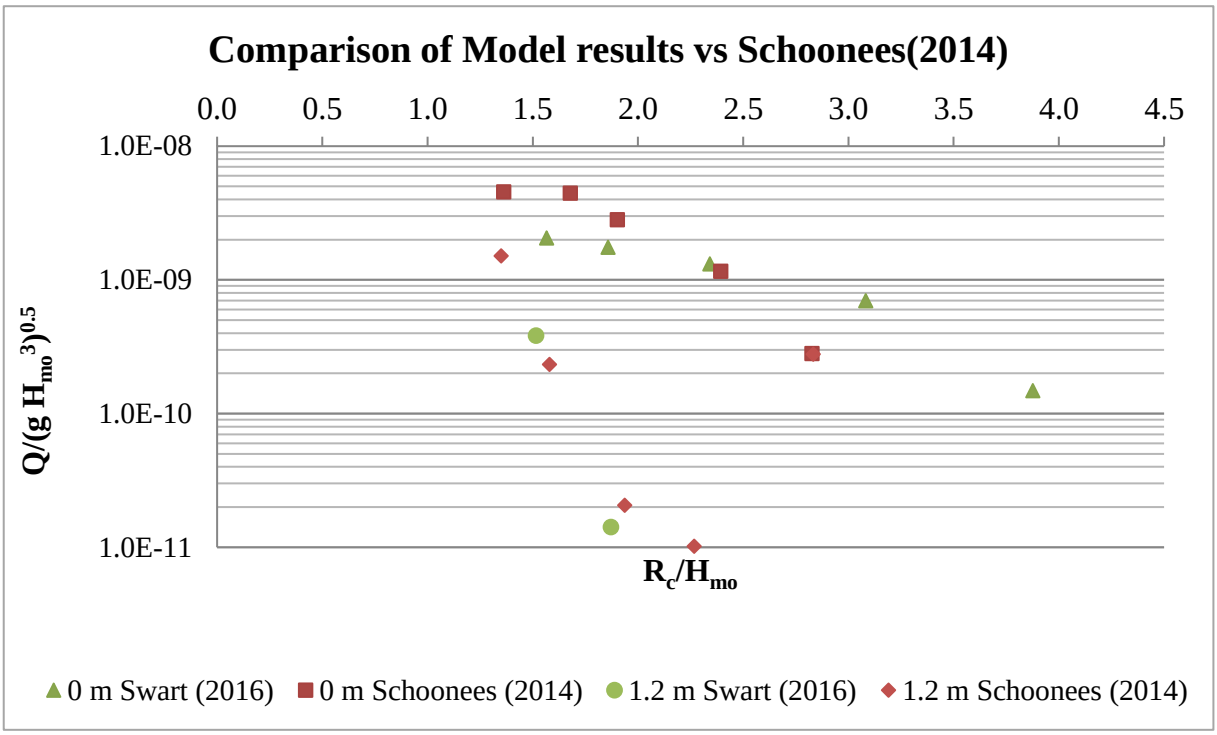

Figure 5.26: Comparison of Model results versus Schoonees (2014)

* Note the overtopping rate is in $m^3/s/m$

When the two datasets are compared in prototype values, with the wave height taken into account, the difference in results is not as significant. The 0 m for Swart (2016) and Schoonees (2014) follow the same trend. Similarly, for the 1.2 m overhang.

5.3.3 EurOtop online calculation tool

The online EurOtop overtopping calculation tool is used to evaluate the measured overtopping results, as described in Section 2.5.1 with the *vertical wall* and *vertical wall with wave return* interfaces. The vertical wall with the wave return is used as approximation, as the geometry of the recurve wall used in the physical model test would provide better results, as the wave return shoots the wave back seaward at a flatter angle. This is illustrated in Figure 5.24 by $\beta_1 < \beta_2$. Take note that the graphs' y-axes do not necessarily have the same scales.

The EurOtop tool provides the probabilistic and deterministic overtopping rate. The probabilistic plot is obtained by fitting a mean linear trend line to the dataset compiled by the CLASH initiative. The deterministic plot is one standard deviation from the probabilistic trend, this is to take account for variability of the dataset that is compiled from data with diverse model conditions. The data measured in the physical model should fall within the two boundaries.

The non-impulsive condition of the vertical wall (Series A) physical model results as well as the EurOtop results are compared with the data provided by Allsop *et al.* (2005) in Figure 2.17 (Section 2.5.3).

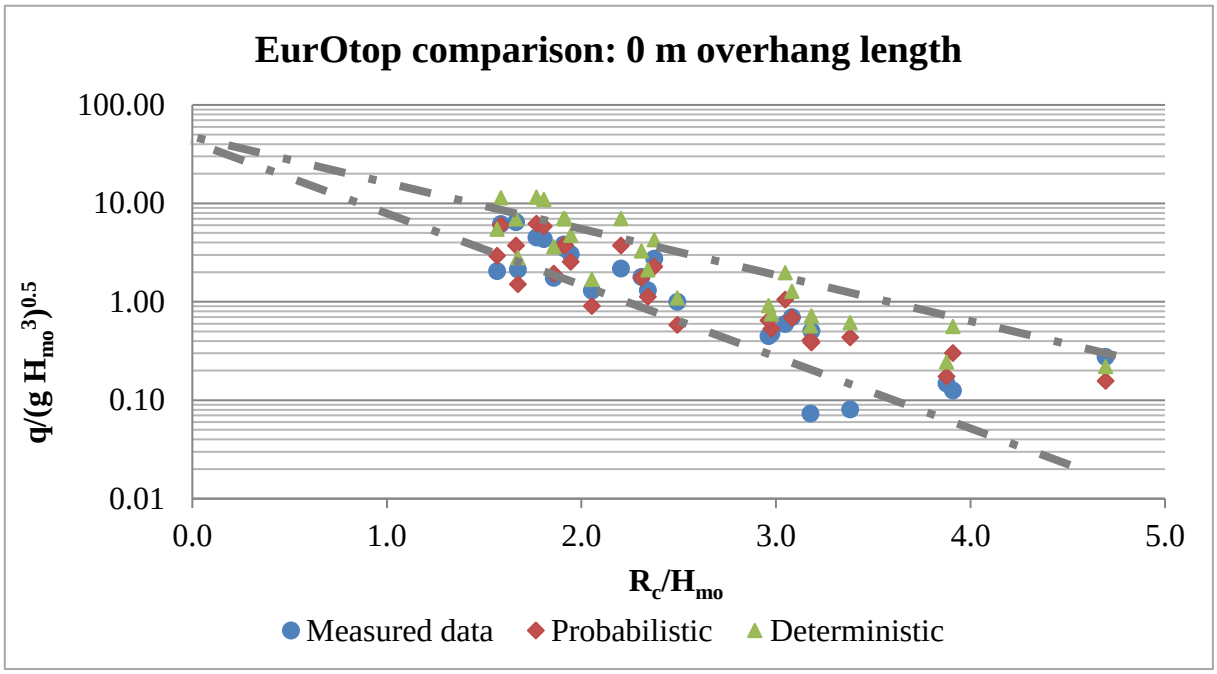

Figure 5.27: Comparison of EurOtop with physical model results 0 m

The data is plotted with the dimensionless overtopping parameter on a logarithmic scale versus the freeboard over incoming wave height on a linear scale.

The measured data of the vertical wall strives to a dimensionless overtopping parameter of 40 (0.04 if q is $m^3/s/m$), that corresponds with the trend found by Allsop *et al*. (2005).

The vertical wall with a wave period of 8, 10 and 12 second compares best with EurOtop probabilistic and deterministic data. Provided in Figure 5.28 is the 12 second wave period of the wall with a 0 m overhang length.

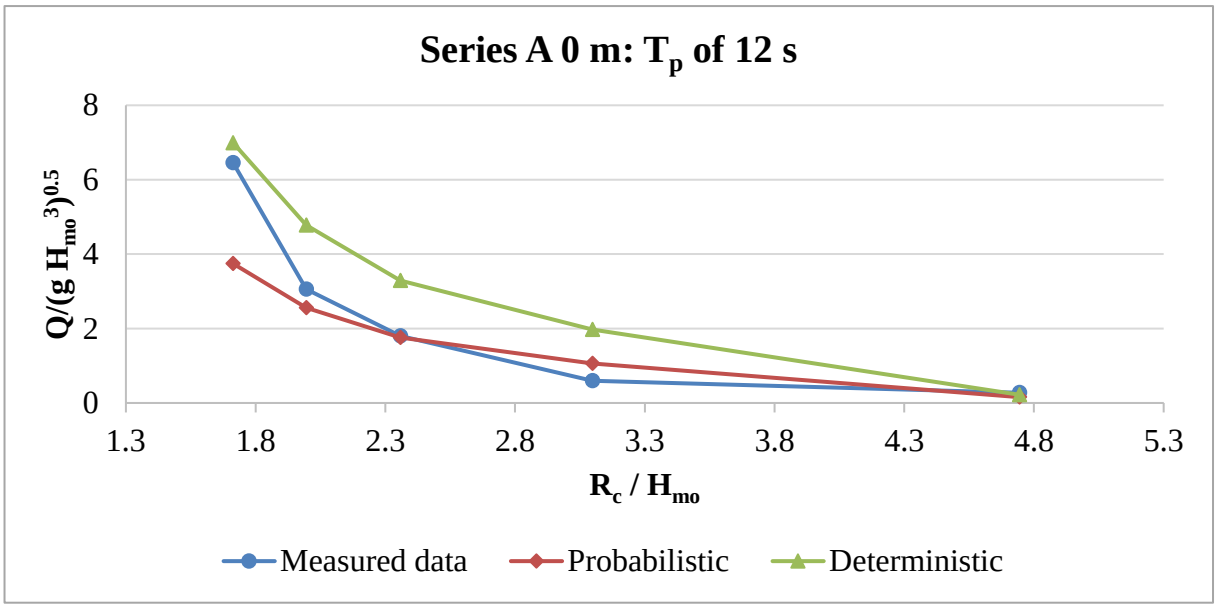

Figure 5.28: EurOtop comparison 0 m overhang – T_p of 12 s

Where the measured data falls below the empirical data is where $^{R_c}/_{H_{mo}} > 2.4$, representing the high freeboard levels. With these conditions the recurve wall is most effective and the low overtopping volumes are difficult to quantify in physical model conditions.

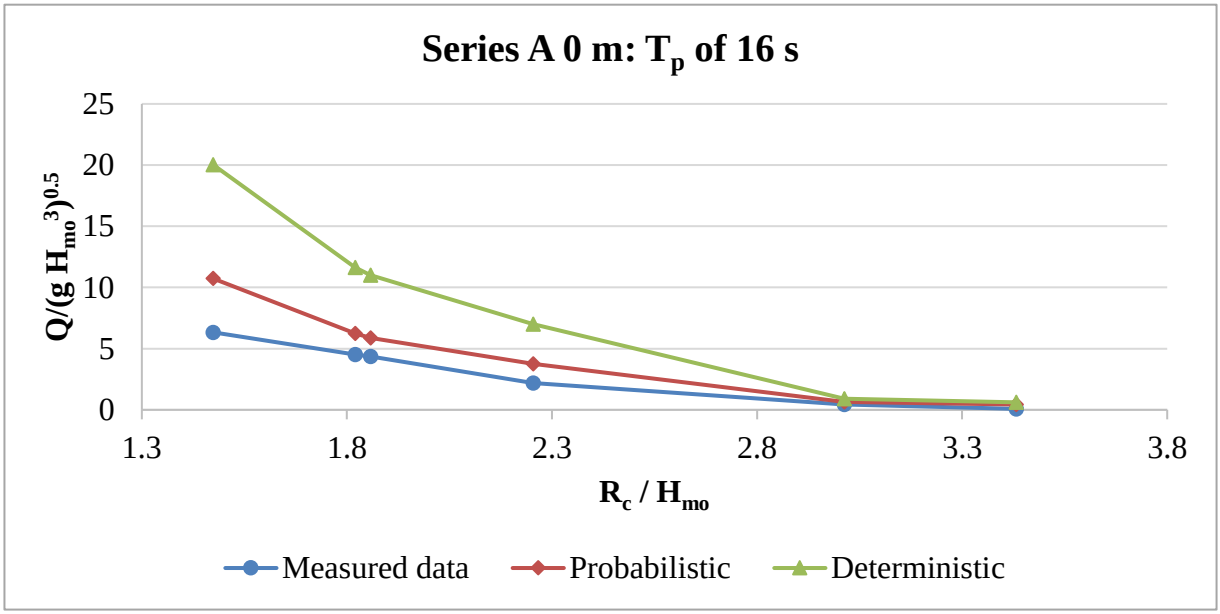

Figure 5.29: EurOtop comparison 0 m overhang – T_p of 16 s

Considering the higher wave periods for vertical walls, the measured data lies within two standard deviations from the probabilistic trend. This could be a result of the wave period being outside the allowable range, thus extrapolating data not based on actual tests. This results in the

tool over-predicting the overtopping rate for the 16 second wave period as indicated in Figure 5.29.

The wave recordings were taken before the slope of the recurve wall of the model, thus it was assumed that the beach slope had no significant influence on the wave height and, indirectly, on the wave overtopping.

When considering Series B to I, overhang lengths 0.15 to 2.1 m, the general trend was that cases with the higher freeboard where $^{R_c}/_{H_{mo}}$ > 2.3, the empirical method over-predicts and, for lower cases, under-predicts.

Although the empirical tool is suggested for the use of preliminary design, the 16 second wave period should be considered carefully when used with low freeboard water levels.

The recurve walls with the 0.15 and 0.3 m overhang lengths, behaved as shown in Figure 5.30. The comparisons of all the EurOtop datasets are provided in Annexure O.

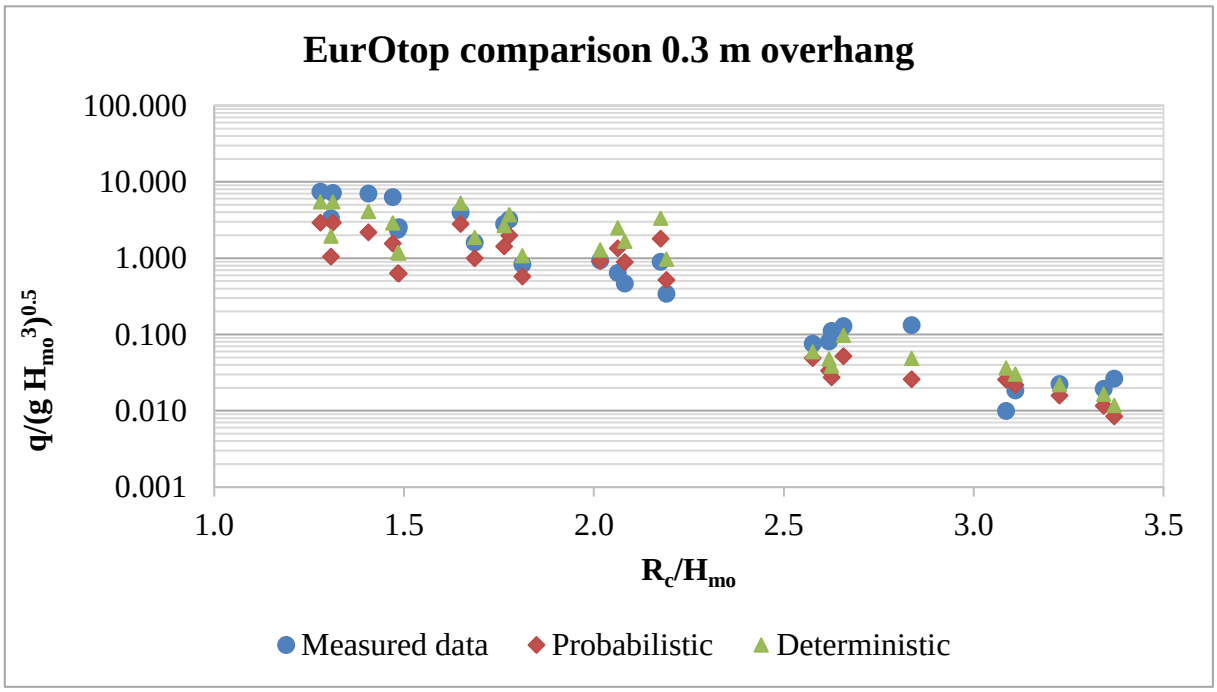

Figure 5.30: EurOtop comparison 0.3 m overhang

The measured data does not fall between the probabilistic and deterministic, but correlates better with the dataset. When considering only the 12 second wave period, a trend is more easily noticeable, as seen in Figure 5.31.

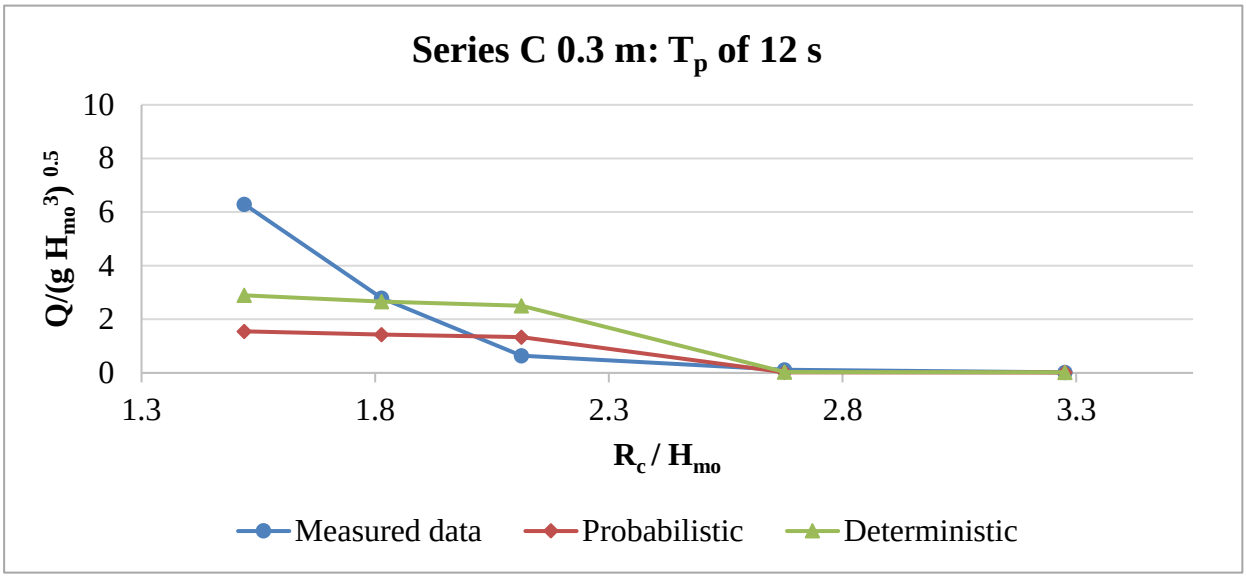

Figure 5.31: EurOtop comparison 0.3 m overhang – T_p of 12 s

For the higher freeboard cases, the empirical data suggests that the overtopping rate is not sensitive to the change in freeboard. This, however, is in contrast to what was found in the physical model. In the laboratory, as the freeboard decreased, the overtopping volumes increased, and are represented as the highest point of the measured data graph in Figure 5.31.

The empirical method correctly predicts only the lowest freeboard case for the recurve walls with longer overhang lengths (1.2 m and longer), as seen in Figure 5.32.

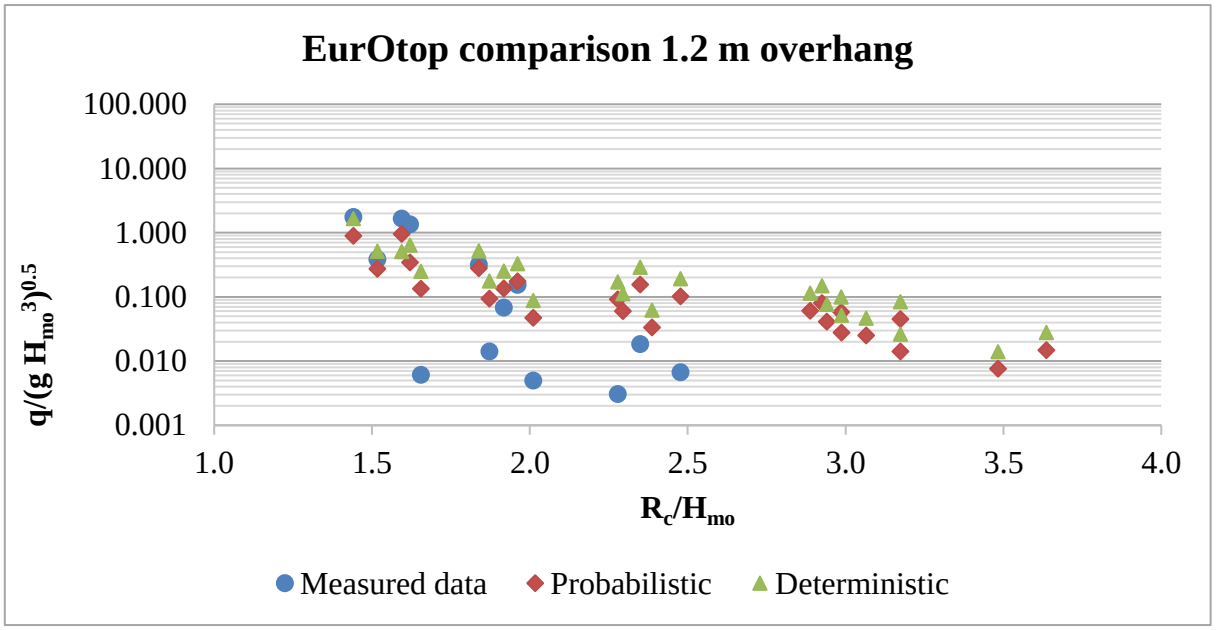

Figure 5.32: EurOtop comparison 1.2 m overhang

Furthermore, all wave periods follow the same trend, and the empirical data over-predicts the overtopping rate.

For the overhang lengths of 1.2 m and longer, the recurve wall achieves zero overtopping results where the wall allows little or no overtopping to breach the crest of the recurve wall. These instances of very little overtopping are not included in the figure in the region where $R_c/H_{mo} >$ 2.5.

From the online tool, it was found that there were discrepancies in the results, where the overtopping rate calculated was outside the expected range. These outliers were identified where the overtopping rate was outside range of wave periods at the same water level. This was found at an overhang length of 0.9 m, with wave periods of 10 and 16 second, as well as for an overhang length of 1.8 m with a 12 second wave period.

5.4 Summary

The analysis of the physical model's results illustrated that the overtopping rate is not only sensitive to the change in overhang length, but also strongly dependent on the change in water depth, freeboard level and wave height and period.

The research validated that for the recurve wall with a parapet angle greater than 50º, as defined by Section 2.5.4, does not improve the rate of prevention of overtopping of a vertical wall. If a recurve wall with 0.15 or 0.3 m overhang is considered, the design process should validate the results with a physical model designed with the exact parameters as design problem.

As the water level increased and freeboard decreased, it was found that the functionality of the recurve reduces, because the recurve wall is not a feature that is designed to function in a *drowned* state.

At the lowest freeboard levels, the overtopping is especially sensitive to changes in wave height. If the wave hits the slanted or perpendicular surface of the overhang of the recurve wall in the drowned state, the wall is no longer effectively reducing the overtopping, and would result in large overtopping rates.

The physical model results disproved Roux's (2013) conclusion that a wave period of greater than 12 seconds reduces the overtopping rate, as continuous growth of overtopping rate was observed under these conditions from test results.

For the lowest freeboard case, an overhang length greater than 1.2 m does not have a significant influence on the reduction of overtopping. In these cases, especially for the 12, 14 and 16 second wave periods, the volume overtopping is strongly dependent on the wave height. This occurs,

because the freeboard available is less than the wave height, and the waves thus overtops the wall regularly.

The physical model results correlate moderately well with previous research. For the EurOtop results, the high overtopping events are over-predicted and the low freeboard levels are under-predicted. As this is only recommended for preliminary design, the variability is acceptable.

It was found, in high freeboard cases of the physical model results, that the data recording method was not accurate enough to measure the small overtopping volumes and, as the EurOtop over-predicts the wave overtopping, the average of the two is required to achieve an authentic representative account of the performance of recurve walls.

CHAPTER 6

PROPOSED DESIGN PROCEDURE

6.1 Introduction

The reader should now have an in-depth knowledge of overtopping and the behaviour of recurve walls under various, yet specific, sea conditions. In this chapter more attention will be given to aiding the designer in the process of design and selection. First, the general design considerations will be discussed, then the selection of the recommended overhang length and finally, the importance of awareness of potential failure modes will be highlighted.

6.2 Design considerations

6.2.1 General comment

The recurve wall is designed to function so that the waves curl up into the recurve and shot back seaward. It is important to design the recurve wall to have enough freeboard so that it can function in this manner. As a rule of thumb, the design should allow for a freeboard of a minimum of 1.5 times the height of the design wave.

The designer should consider the effect that the recurve wall will have on the surrounding area. A 100% reflection of waves can change the wave climate and cause wave focusing at a different point. The public should not use the area beneath the recurve wall, as the waves that shoot seaward could cause harm if unexpected by people in the area.

The conclusions made from this study are valid only for the chosen design parameters as stipulated in Section 3.7.

6.2.2 Procedure

The main principles that should be followed in the process of designing a recurve wall can be divided into four steps:

1. **Determine the use of the facility:**

   The purpose the wall or area is designed for will determines the permissible overtopping rate that the recurve wall should be design for. EurOtop provides limits for various purposes, provided in Table 2.1 - 2.3. These tables allow the designer to choose to incorporate a safety factor by choosing a higher overtopping rate than required.

2. **Wave climate information:**

   The wave climate information required for this design process is the wave height and period (H_{mo} and T_p) of the identified area.

3. **Site-specific information:**

   To determine the crest level, the water level and freeboard levels are required. Most often more than one freeboard and crest level will be selected, to provide more alternatives.
   The crest level should be chosen so that the design water level falls within the vertical face of recurve wall (indicated as 1 on Figure 5.20) so that the incoming HMAX collides into the vertical face of the recurve wall.

4. **Select relevant chart:**

   The relevant design chart is chosen according to the site-specific wave period.

   The overtopping rate and H_{mo} are inserted in the dimensionless overtopping parameter, provided in Equation (2.16). Finally, the dimensionless overtopping parameter is used as a limit. All freeboard and overhang length combinations beneath the limiting parameter can be chosen.

   Note: The limitation of this study is that it is developed for an approach seabed slope of 1:18.6 and H_{mo} from 1 to 1.25 m.

6.2.3 Recommended overhang lengths

The overhang lengths, B_r as indicated in Figure 6.1, for each wave period are considered and the recommended overhang lengths are provided in Table 5.1.

The low freeboard and high freeboard levels should be interpreted differently. For the R_c of 1.7 and 2.1 m, a longer overhang length is required, as the recurve wall is functioning in a submerged state, with mostly large volumes overtopping the crest.

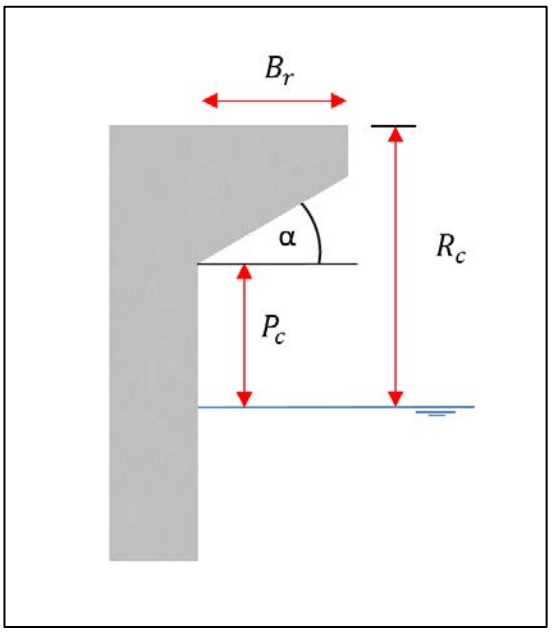

Figure 6.1: Input parameters

6.2.4 Potential failure modes

Identification of the potential failure modes was not the objective of this study; however, these were indirectly observed. From the results of the physical models test, the following were highlighted as the sites of possible problems: first, the areas between the precast units and, secondly, the connections between the vertical and diagonal faces.

The large forces observed in the physical model, resulted in practical problems of fixing the seawall to the flume walls; highlighted that the joint between the recurve wall units (indicated as 1 in Figure 6.2), is a weak point, and should be designed accordingly.

Secondly, considering the joint between the vertical and diagonal faces. As the incoming wave hits the structure, the wave is captured beneath the overhang, which then experiences a large force upward (indicated as 2 in Figure 6.2). This is more significant for longer overhang lengths. The joint between the overhang length and the upright section as should be considered.

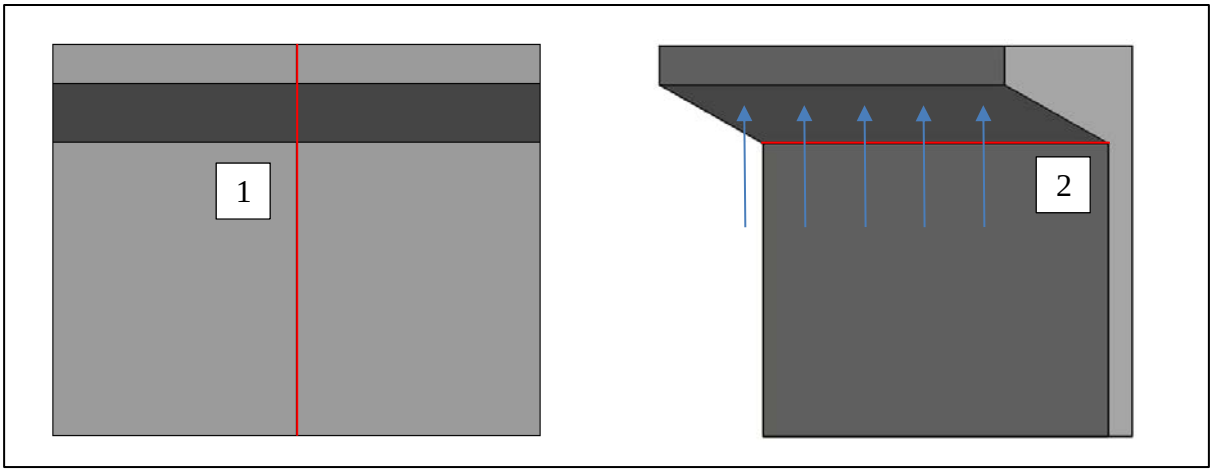

Figure 6.2: Failure modes schematic

6.3 Example

To illustrate the design procedure, an example of how to follow the four steps as provided in Section 6.2.2 is given below.

The wave climate input variables H_{mo} and T_p are chosen. The site that the recurve is being designed for, is accessible to the public. The overtopping rate is chosen from Table 2.3, as that which is safe for aware pedestrians.

Table 6.1: Procedure example input variables

Procedure example						
INPUT VARIABLES				**1. Facility use**	***Table 2.1***	
2. Wave climate			CHECKS	Q	0.1	l/s/m
T_p	12	s		Safe for aware pedestrians		
H_{mo}	1	m	√			
				4. OUTPUT VARIABLES		
3. Site-specific				Dimensionless overtopping parameter		
S_o	1:18.6	-	√	$\frac{Q}{\sqrt{g\ {H_{mo}}^3}}$	0.00319	
WL_{toe}	2.3	m				
R_c	1.7	m				

For the present design problem, the wave height and approach slope are within the allowable range. The relevant chart for the 12 second wave period is selected. The dimensionless overtopping parameter is used as a limiting variable (Figure 6.3).

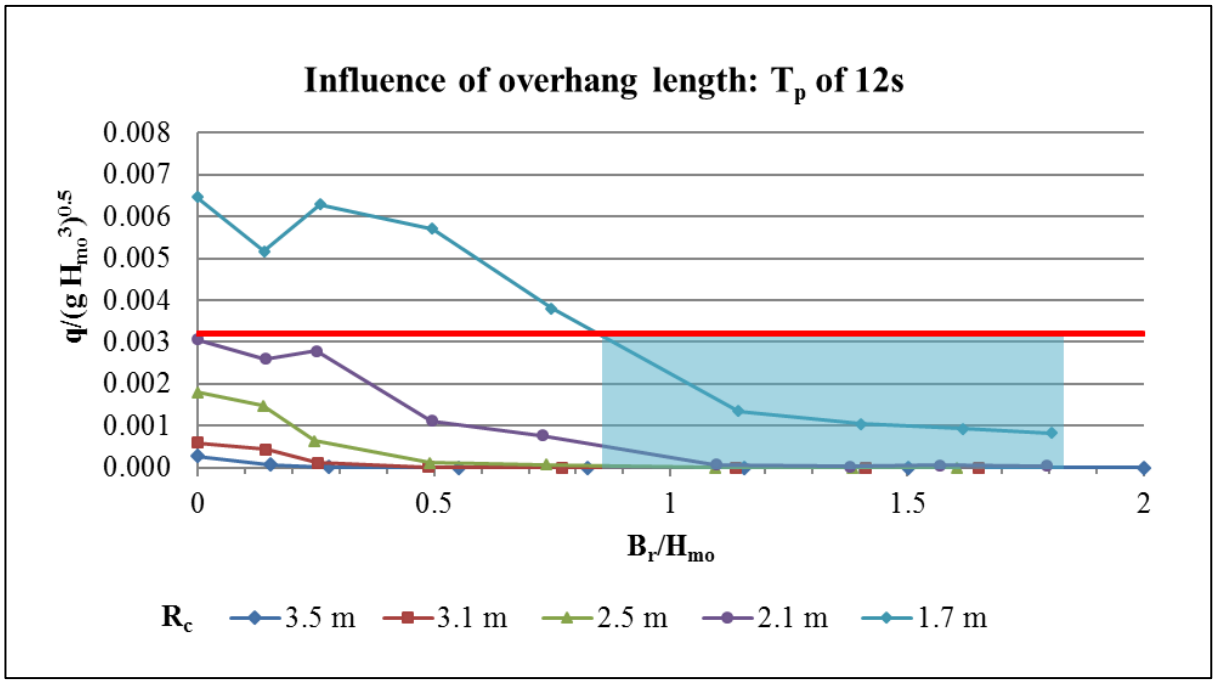

Figure 6.3: Example of how to use the design chart

To achieve the designed overtopping rate for the design scenario, any overhang length, in combination with a freeboard level beneath the red line can be chosen. For the chosen freeboard level of 1.7 m, the blue shaded area is the allowable design region. Freeboard levels should be interpolated on the chart to achieve a value between data points.

For this freeboard level, the 1.2, 1.5, 1.8 and 2.1 m overhang lengths are included. However, as no significant reduction effect can be seen between overhang lengths of 1.2 m and 2.1 m. The use of a 1.2 m overhang length is recommended.

6.4 Summary

The design procedure is schematically represented in Figure 6.4

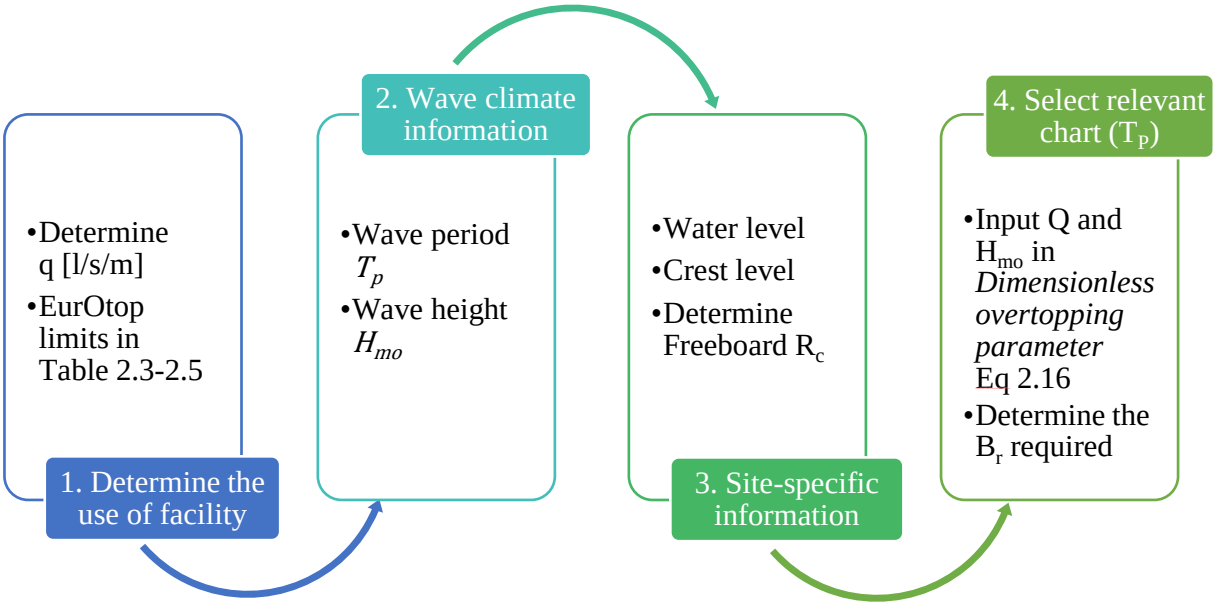

Figure 6.4: Schematic of design procedure

CHAPTER 7

CONCLUSIONS

7.1 Introduction

An extensive study was conducted on the effect of the length of the overhang on the reduction of overtopping when compared with the performance of a vertical wall under similar conditions. As a result, the knowledge base concerning the manner in which recurve seawalls behave and specifically, influence wave overtopping was significantly expanded.

The objectives of this study were to determine the effect of the overhang length on the reduction of overtopping, to compile a comprehensive set of design guidelines for the design of recurve seawalls, and to determine to the freeboard height to which the recurve seawall will outperform a vertical wall.

To achieve these objectives, a 2D physical model was designed and tests were conducted in a glass-walled wave flume equipped with a piston-type wave-generating paddle that was equipped with a dynamic wave absorption system. To provide a detailed design guideline, nine different recurve shapes were tested with five different water levels. Wave periods characteristic of the South African coast were chosen, while the seabed slope and wave height remained constant.

7.2 Findings from the literature

The literature reports remarkable research regarding the use of recurve walls to reduce wave overtopping; the detailed attention on this type of structure having started in the early stages of research on recurve walls by Berkeley-Thorn and Roberts (1981), who developed the now well-known recurve wall shape.

Owen (1993) conducted research to evaluate the performance of different types of recurve walls and concluded that the use of a recurve wall was more effective than raising the crest level of a vertical seawall. It was further concluded that the freeboard and crest level of a recurve seawall have a significant influence on the effectiveness of the wall.

Recent research administered through the European Union's CLASH programme (Crest Level Assessment of coastal Structures and Hazard analysis on permissible overtopping) has resulted

in the establishment of a substantial database. This dataset is now accessible through an online calculation tool that can be used to predict the reduction in overtopping. Allsop *et al.* (2005) developed a decision chart to aid in predicting the reduction in overtopping for the purposes of the design of feasibility studies.

Van Doorslaer and De Rouck (2011) conducted research on a vertical wall with a parapet nose on top of a 1:2 (V:H) slope and concluded that the if the nose angle increases by more than 50° the performance of the parapet is similar to that of a vertical wall. The research also determined that a parapet angle of 45° provides the best overtopping reduction (Van Doorslaer & De Rouck, 2011).

The Flaring Shape Seawall (FSS), a deep circular concrete section, was developed by Kamikubo *et al.* (2003). The FSS crest level can be significantly lower than that of a conventional vertical wall (Kamikubo *et al.*, 2003). However, this large seawall has to be constructed, using concrete shutters, as a single new structure and cannot be added to existing vertical walls. Kortenhaus *et al.* (2004) stated that the FSS is difficult to construct; however, there are now various commercial companies specialising in the design and construction of FSS structures.

In summary, the literature review showed that, although various components of the recurve seawall have been researched in detail to develop parameters to estimate the probable performance of the recurve seawall, there is currently limited validation of the theoretical parameters developed, and still no clear and extensive design approach in place for recurve seawalls.

Therefore, this physical model study was conducted to establish the extensive design guidelines necessary for recurve seawalls.

7.3 Wave overtopping results from this physical model study

This study highlighted the fact that the overtopping process is dependent on various parameters, with the most important influencing parameters being wave height, freeboard and crest level, and recurve geometry, including overhang length.

These dependencies emphasise the importance of the careful selection of design parameters during the feasibility and fundamental design process.

The impact of the variables tested on overtopping is highlighted in the following sub-sections (7.3.1 to 7.3.7).

7.3.1 Reduction in overtopping

The reduction in wave overtopping over a recurve wall is evaluated with the k-factor, as defined in Section 2.5.3 by Equation (2.17). As the length of the overhang increases, the trends flatten, indicating that at a certain point the length of the overhang is no longer significant in the further reduction of overtopping, as demonstrated in Figure 5.4.

Reference to Figure 5.3 shows that there are three recurve profiles that fail, with the 0.15 m, 0.3 m and 0.6 m overhang lengths delivering test results with a k-factor greater than one, indicating that the recurve wall does not improve the rate of reduction of overtopping for vertical walls, but actually makes it worse. In comparison with Figure 5.3, the magnitude of the individual cases can be evaluated and the severity determined.

7.3.2 Influence of the length of the overhang

For all the wave periods tested with the three lowest water levels, the reduction in overtopping increased up to a certain point, after which any increase in the length of the overhang had no further influences. This point varies with wave period and water level. For the highest water level (lowest freeboard level) the 0.3 m overhang did not improve the overtopping for the 0 m or the 0.15 m overhang length, as demonstrated in Figure 5.12.

It was found that the 0.15 m overhang length, but even more so the 0.3 m overhang length, was less effective than the vertical wall demonstrated in Figure 5.2. This occurred at the two lowest freeboard levels, and for all wave periods. The phenomenon is discussed in Section 5.2.3, and illustrated in Figure 5.11.

7.3.3 Sensitivity to water depth

It may be concluded that the rate of overtopping is exceedingly sensitive to any change in water level, as illustrated in Figure 5.16. With a 16 second wave period, this was particularly noticeable. However, the magnitude of the reduction in overtopping was different for each overhang length.

For all the overhang lengths the scenarios in which the water level was less than the wave height, the wave period had no significant influence on the overtopping rate.

Furthermore, the recurve wall is designed to function with the design water level no higher than the vertical section of the recurve wall, to ensure that it would not function in a submerged state. This highlights the importance of the accurate determination of the crest level of the structure.

7.3.4 Sensitivity to wave period

The volume of water associated with shorter wavelengths is less and is cleared easily from the wall. In some instances, with the larger wavelengths, the first wave is thrown seaward and caught up in second wave. This superimposes the first wave on the second and a larger volume breaches the crest.

The recurve wall profiles with 0.15, 0.3 and 0.6 m overhang lengths are also more sensitive to wave period at higher water levels, as shown in Annexure L.

It was found during the course of this investigation that for tests with 14 and 16 second wave periods it was difficult to control the output. This could be because the 16 second wave period is close to the limit of what can be generated in the small flume in the hydraulics laboratory, and the extent of the variability is unknown.

7.3.5 Influence of wave height

Due to specific and particular physical attributes of the physical model used in this study, differences were noted in the wave height while the other variables were kept constant. A dependency analysis was done to quantify the variance in wave height.

It was concluded that the wave height had a significant influence on the tests with the lowest freeboard level, as the wave height determines where on the recurve wall structure the incoming wave hits. The overtopping volume will be greater when the incoming wave hits the recurve wall on the perpendicular face of the curve (indicated as 3 on Figure 5.20), from where the wave is thrown upward and consequently substantial overtopping occurs.

The recurve wall is designed so that the incoming wave hits the vertical wall and/or the slanted component of the wall (indicated as 1 and 2 on Figure 5.20).

7.3.6 Repeatability and accuracy

The repeatability and accuracy were determined by repeating tests with and without the use of the pump. The coefficient of variance (CoV) for the tests repeated with the pump was 1.36% and for the tests without the pump 2.37%. These figures are both less than 5%, which indicates a good repeatability factor, compared to the CLASH database, which achieved a CoV of 13% (De Rouck *et al.*, 2005).

7.3.7 Influence of recurve wall on Dynamic Wave Absorption (DWA)

The Dynamic Wave Absorption system (DWA) was developed to adjust the wave height reflecting from the wave paddle, in order to generate wave heights more accurately to design conditions.

It was known that the DWA was not as effective when applied to vertical structures, for example, during test in Series A, with 100% reflection. The application of the DWA concept on the recurve wall further worsened the performance. An adjustment was made to the wave height for the recurve wall with overhang lengths longer than 1.2 m, to counteract this phenomenon.

7.4 Comparison of previous research

7.4.1.1 *Allsop et al. (2005)*

The physical model results for the vertical wall (0 m overhang was compared to the results obtained by Allsop *et al.* (2005), provided in Figure 5.27. The trend fitted to the dataset from this physical model study strives to 40 (0.04 if q is $m^3/s/m$), corresponding to the finding by Allsop *et al*. (2005).

Further, the theoretical k-factor obtained by using the decision chart developed by Allsop *et al.* (2005), which is provided in Figure 2.13, and which represents the reduction provided in overtopping provided by the recurve wall, was evaluated against the calculated k-factor, provided in Equation (7.1).

It was found that the selection of the test conditions for the investigation was such that the theoretical k-factor did not include cases where the overtopping rate of the vertical wall had not

been improved. Although there are discrepancies for different recurve wall geometries, the theoretical k-factor over-predicts the reduction of overtopping, as illustrated in Figure 5.24.

As it was intended that Figure 5.25 should be used to give an indication of the reduction in overtopping by the recurve wall, this would deliver a false k-factor and prediction of the reduction in overtopping.

7.4.1.2 ***Schoonees (2014)***

Schoonees (2014) did research on the effect that the overhang length of a recurve wall has on the overtopping reduction. Two recurve angles were investigated, and evaluated against the performance in overtopping reduction of a vertical wall.

This project's dataset was designed to expand on the Schoonees's (2014) research. Two datasets were repeated to determine whether tests with overlapping conditions could be used, results are provided in Table 5.6 and 5.9. Differences between the results, as found by Schoonees and results in the present study, can be attributed to various factors, namely, the water level, crest level and wave height.

A root mean squared analysis was performed to evaluate the correlation of dataset. The error for the 1.2 m overhang length was lower than the error for the vertical wall. The RME for the physical model is 0.25, compared to a 1.76 error achieved by Schoonees. This indicates that the data series error is smaller than that found by Schoonees's dataset. However, both the present study and that by Schoonees had an acceptably small margin of error. The full root mean squared method analysis is provided in Annexure M.

7.4.1.3 ***EurOtop online calculations***

Comparing the physical model results of this study with the EurOtop database, the EurOtop results under-predict the results for low freeboard cases. On the other hand, for higher freeboard cases it was found that the physical model delivers low or no overtopping results. However, the smaller overtopping rates obtained for specific combinations of parameters in the physical model are difficult to compare with the EurOtop database as it proved quite difficult to accurately measure small overtopping volumes.

It can therefore be concluded that the design guidelines as developed in this physical model study provide a valuable extension of the design capabilities available for recurve seawalls.

7.5 In conclusion

It was found in the physical model study that for all cases where the overhang is larger than 0.3 m, the reduction in overtopping was enhanced. Apart from its dependence on the overhang length, the overtopping rate is also sensitive to changes in wave height and wave period, as well as to the water level at the foot of the structure.

A recurve seawall with a parapet angle, as defined as in Section 2.5.4, that is greater than 50º will not improve the reduction rate of overtopping when compared to the results for a vertical wall under similar conditions.

The freeboard has been identified as the most critical parameter in determining overtopping. If sufficient freeboard is not provided, the recurve wall will be drowned and will not provide any reduction in overtopping. On the other hand, a combination of high freeboard and low water levels can produce up to a 100% reduction in overtopping.

Provided below in Table 7.1 is a summary of the recommended overhang length per freeboard level.

Table 7.1: Summary of proposed overhang lengths per freeboard level

Proposed overhang length per R_c			
R_c [m]	**B_r [m]**		
3.5	0.15	-	0.6
3.1	0.15	-	0.9
2.5	0.3	-	1.2
2.1	0.6	-	1.5
1.7	0.9	-	1.2

As a result of this study, design guidelines were developed to aid the designer in the conceptual design phase, with the wave height, wave period and tolerable overtopping rate as input variables. With the use of the charts provided in Annexure J and the input variable, the combination of overhang length and freeboard level is chosen. The design procedure is fully discussed in Chapter 6.

Referring to Section 1.2 it can be seen that all the objectives have been met during the course of this investigation.

CHAPTER 8

RECOMMENDATIONS

8.1 General

It is recommended that the results obtained in this study should be used in a step-by-step approach as outlined in Chapter 6, for designing recurve seawalls for practical applications. It is not recommended, at present, that the design procedure be used beyond the range of the design conditions stipulated in Section 3.7.

In cases where a large reduction in the overtopping rate (a factor of 20 or a $k < 0.05$) is required, it is recommended that physical model tests be conducted with the exact conditions needed, to validate the design predictions.

8.2 Recommendations for further study

The recommendations for further study are discussed, after first considering the physical model test conditions, which is followed by considering the physical model equipment.

8.2.1 Enhancing the Design Guidelines for recurve seawalls

A large range of parameters was tested during this investigation; however, additional tests are required to understand the amplification that occurs with the 0.3 m overhang, as discussed in Section 5.2.3. It is recommended that recurve walls with 0.2 and 0.4 m overhangs also be tested, to assist with the refinement of the critical range in which this occurs.

Further, it is suspected that the 16 second wave period was on the boundary of allowable wave periods achievable in the facility where the present study was conducted. Therefore, the 16 second wave period dataset should, for the moment, be used only for the preliminary design. In order to improve the predictive capability, it is recommended that tests should be conducted in a different facility where the scope of hydraulic parameters is such that it will be possible to validate the overtopping results for a 16 second wave period with a more constant range of wave heights.

Since the beach slope was kept constant for all conditions tested, it is essential that in further experimental work the influence of beach slope on the wave height and overtopping should be researched.

Any and all research done in line with the recommendations as listed above should be incorporated into the currently proposed set of design guidelines (see Chapter 6) and thus, over time, improve the accuracy of predictions and thus the design certainty, as well as expand the applicable range of the design guidelines.

8.2.2 Physical model equipment

Further research should be conducted to quantify the interactive reflections between the recurve wall, the piston-type wave-generating paddle, and the dynamic wave absorption in this interactive system. This would provide insight into the effect that the recurve wall has on the equipment and validate the adjustment made to the wave height during this research.

From observation during the tests in this physical model study, it was clear that water droplets on the plastic sheets and recurve wall were not accounted for. For the large overtopping volumes, this would not make any significant difference; however, for small volumes the effect, while unknown, could potentially be more significant.

Therefore, before any further tests are conducted, it would be advisable to improve the method of measuring small volumes of overtopping, to ensure accuracy.

On a practical note, some difficulties were experienced with the model setup during the present study. For the recurve walls with longer overhang lengths, the structure had to be monitored closely, as in some instances the recurve wall came loose during the test series as a result of the substantial hydraulic forces exerted on the structure. Research should be undertaken to investigate the forces that are exerted on these recurve walls. This would, on the one hand, provide more insight into the interaction between units for design purposes and, on the other offer suggestions as to how the structural stability of the model structures could be improved.

REFERENCES

Allsop, N.W.H., Alderson, J.S. and Chapman, A., 2007. Defending buildings and people against wave overtopping. *Proceedings: Conference on Coastal Structures*, Venice.

Allsop, W., Bruce, T., Pearson, J. & Besley, P. 2005. Wave Overtopping at Vertical and Steep Seawalls. *Proceedings of the ICE-Maritime Engineering*, **158**(3):103-114. Thomas Telford Ltd.

Allsop, N.W.H., Pullen, T.A., van der Meer, J.W., Bruce, T., Schüttrumpf, H. & Kortenhaus, A. 2008. Improvements in wave overtopping analysis: The EurOtop overtopping manual and calculation tool. *Proceedings: COPEDEC VII*, Dubai, UAE, (77).

Anand, K., Sundar, V. & Sannasiraj, S. 2010. Dynamic pressures on curved front seawall models under random waves. *Journal of Hydrodynamics, Ser.B*, **22**(5):538-544.

Berkeley-Thorn, R. & Roberts, A. 1981. *Sea Defence and Coast Protection Works: a guide to design.* Thomas Telford Ltd.

Besley, P. and Environment Agency. 1999. *Overtopping of seawalls*. Environment Agency, Bristol (United Kingdom).

Bradbury, A., Allsop, N. & Stephens, R. 1988. Hydraulic performance of breakwater crown walls. *HR Wallingford, Report No. SR146*.

Bruce, T., van der Meer, J., Pullen, T. and Allsop, W. (2009). Wave Overtopping at Vertical and Steep Structures. *Handbook of Coastal and Ocean Engineering*, 411-439.

CIRIA, CUR & CETMEF, 2007. *The Rock Manual. The use of rock in hydraulic engineering (2nd edition).* London (683), CIRIA.

Clifford, J. 1996. *Advances in coastal structures and breakwaters:* Proceedings: International conference organized by the institution of civil engineers and held in London on 27-29 April 1995. (7). Thomas Telford.

Concrete Groynes. 2006. [Online]. Available at: http://www.thisbrighton.co.uk/digicanvas/Images/UGraniteBoulders.jpg [9 August 2016].

Culture: Undercliff Walk. 2015. [Online] Available at: http://www.thisbrighton.co.uk/culture undercliff2.htm [13 October 2015].

Cycling Along Blackpool's Seafront. 2015. [Online] Available at: http://joylovestravel.com/ [13 October 2015].

De Rouck, J., Geeraerts, J., Troch, P., Kortenhaus, A., Pullen, T. & Franco, L. 2005. New results on scale effects for wave overtopping at coastal structures. *Proceedings of ICE Coastlines, Structures & Breakwaters*, **5**:29-43.

Evans, Rupert. 2015. Wave Return Wall Sea Palling. [Online] Available at: https://www.flickr.com/photos/evansriversandcoastal/4054750625 [13 October 2015].

EurOTop. 2007. *Wave Overtopping of Sea Defences and Related Structures–Assessment Manual.* UK [Online] Available at: www.overtopping-manual.com. [18 March 2015].

Goda, Y. & Suzuki, T. 1976. Estimation of Incident and Reflected Waves in Random Wave Experiments. *Coastal engineering proceedings*, **1**(15).

Google Maps, (2014). *Google Maps*. [Online] Available at: https://www.google.co.za/maps/@-34.3862413,21.4258414,3a,75y,331.83h,84.78t/data=!3m6!1e1!3m4!1s-Vl8ikNsoUrjs8eiPM_NCg!2e0!7i13312!8i6656 [19 August 2016].

Guerrero, F. n.d. *Wave Flumes Training*. HR Wallingford.

Hasselmann, K., Barnett, T.P., Bouws, E., Carlson, H., Cartwright, D.E., Enke, K., Ewing, J.A., Gienapp, H., Hasselmann, D.E., Kruseman, P. and Meerburg, A., 1973. *Measurements of wind-wave growth and swell decay during the Joint North Sea Wave Project* (JONSWAP). Deutches Hydrographisches Institut.

Hill, P. 2014. *Sandgate to Lydd via Hythe*. [Online] Available at: http://my.viewranger.com/route/details/NTUwNzM= [5 August 2016].

HR Wallingford. 2010. Flume Wave Generation System: User manual for University of Stellenbosch.

HR Wallingford 2010. Large Flume wave absorption System: User and Technical Manual Supplied to University of Stellenbosch.

Hughes, S.A. 1993. *Physical models and laboratory techniques in coastal engineering.* World Scientific. Vicksburg, USA: Coastal Engineering Research Center.

Kamikubo, Y., Murakami, K., Irie, I., Kataoka, Y. and Takehana, N., 2003. Reduction of wave overtopping and water spray with using flaring shaped seawall. In *The Thirteenth International Offshore and Polar Engineering Conference*. International Society of Offshore and Polar Engineers.

Kilmac construction. 2013. Arbroath Concrete Recurve Wall. [Online] Available at: http://www.kilmac.co.uk/kilmac-construction/Case+Studies/1101/+Angus+Council+Arbroath+Concrete+Recurve+Wall+2012/ [13 October 2015].

Kortenhaus, A., Haupt, R. and Oumeraci, H. 2002. Design aspects of vertical walls with steep foreland slopes. In *Breakwaters, Coastal Structures and Coastlines: Proceedings of the International Conference Organized by the Institution of Civil Engineers and Held in London, UK on 26-28 September 2001*. 221. Thomas Telford.

Kortenhaus, A., Pearson, J., Bruce, T. & Allsop, N.W. 2004. Influence of Parapets and Recurves on Wave Overtopping and Wave Loading of Complex Vertical Walls. Paper presented at *Coastal Structures* 2003. 363-381.

Kobe Steel Engineering, 2009. Collapse mechanism of seawalls Vol. 59, No. 2. Kobe Steel Engineering Reports.

Kolbeco. 2012. Flared seawall in Kunigami, Okinawa. [Online]. Available at: http://www.kobelco.co.jp/english/about_kobelco/csr/environment/2012/03.html [13 October 2015].

Lake Pontchartrain Basin Foundation. 2015. Old Beach, Bayou St John. [Online]. Available at: http://lpbf.maps.arcgis.com/apps/MapTour/?appid=4ad38306b21d46e89dfa85ca04e e6c 58 [13 October 2015].

Le Mehaute, B. 1976. Similitude in Coastal Engineering. *Journal of the Waterways Harbors and Coastal Engineering Division*, **102**(3):317-335.

Mail Online. 2014. *Sea crashed over Blackpool seafront*. [Online] Available at : http://news2.onlinenigeria.com/world/329606-storms-red-alert-homeowners-told-to-pack-their-bags-as-powerful-tidal-surge-threatens-to-overwhelm-battered-flood-defenses-as-britain-is-hit-with-new-gales-and-heavy-rain.html [8 August 2015].

Mansard, E.P. and Funke, E.R., 1980. The measurement of incident and reflected spectra using a least squares method. *Coastal Engineering Proceedings*, **1(**17).

Murakami, K., Irie, I. & Kamikubo, Y. 1996. Experiments on a non-wave overtopping type of seawall. *Coastal Engineering Proceedings*, **1**(25).

Murakami, K., Kamikubo, Y. & Takehana, N. 2004. Hydraulic efficiencies of non-wave overtopping type seawall installed on a mound. Paper presented at *Proc. of 6th International Conference on Hydrodynamics*. 255-260.

Murakami, K., Kamikubo, Y. & Kataoka, Y. 2008. Hydraulic performances of non-wave overtopping type seawall against sea level rise due to global warming. Paper presented at *The Eighteenth International Offshore and Polar Engineering Conference*. International Society of Offshore and Polar Engineers.

Murakami, K., Maki, D. & Takehana, N. 2011. Wave overtopping on flaring shaped seawall under oblique incident waves. *Proceeding of the Sixth International Conference, APAC.*

Owen, M. & Steele, A. 1993. Effectiveness of Recurved Wave Return Walls. Report SR 261: HR Wallingford.

Pearson, J., Bruce, T., Allsop, W. & Gironella, X. 2002. *Violent Wave Overtopping-Measurements at Large and Small Scale*. Paper presented at Coastal Engineering Conference. 2227-2238.

Pullen, T., Allsop, W., Bruce, T. & Pearson, J. 2009. Field and Laboratory Measurements of Mean Overtopping Discharges and Spatial Distributions at Vertical Seawalls. *Coastal Engineering*, **56**(2):121-140.

Reis, M.T., Neves, M.G. & Hedges, T. 2008. Investigating the Lengths of Scale Model Tests to Determine Mean Wave Overtopping Discharges. *Coastal Engineering Journal*, **50**(4):441-462.

Romano, A., Bellotti, G., Briganti, R. & Franco, L. 2014. Uncertainties in the physical modelling of the wave overtopping over a rubble mound breakwater: the role of the seeding number and of the test duration. Submitted to *Coastal Engineering*, (103):15-21.

Rossouw, J. 1989. *Design waves for the South African coastline.* PhD Thesis, Stellenbosch: University Stellenbosch.

Roux, G. B. 2013. *Reduction of seawall overtopping at the Strand.* Masters' Thesis, Stellenbosch: University of Stellenbosch.

Schüttrumpf, H. and Oumeraci, H. 2005. Scale and model effects in crest level design. Paper presented at *Proc. 2nd Coastal Symposium*. Höfn. Iceland.

Schoonees, T. 2014. *Impermeable recurve seawalls to reduce wave overtopping*. Masters' Thesis, Stellenbosch: University of Stellenbosch.

Schoonees, J. S., Lynn, B. C., le Roux, M. & Bouton, P. 2008. Development set-back line for southern beaches of Richards Bay, Stellenbosch: WSP.

Schoonees, J. S. & Theron, A. K., 2003. Shoreline stability and sedimentation in Saldanha Bay, Stellenbosch: CSIR.

Soltau, C., 2009. The cross-shore distribution of grain size in the longshore transport zone, Masters' Thesis, Stellenbosch: University of Stellenbosch.

Special Formwork. 2015. Folkstone defence. [Online] Available at: http://www.formwork.co.uk/our-projects/folkstone-sea-defence/ [13 October 2015].

Special formwork. 2015. Ilse of Wright sea defence. [Online] Available at: http://www.formwork.co.uk/our-projects/isle-of-wight-sea-defences/ [13 October 2015].

Special formwork. 2015. Lyme Regis sea defence. [Online] Available at http://www.formwork.co.uk/our-projects/lyme-regis-sea-defences/ [13 October 2015].

Stacey, A. 2009. Southwold to Kessingland via Easton Bavents and Cove hit 5 September 2009. [Online] The Geography Department. Available at: http://www.stacey.peak-media.co.uk/EastonBavents/EastonCovehitheSep2009/EastonCovehitheSep2009.htm [13 October 2015].

Swarzenski, P. 2014. *Waves overtopping the berm*. [Online] Available at: http://soundwaves.usgs.gov/2014/04/images/Pac7OverwashCR.jpg [8 August 2015].

Teign mouth seawall. 2015. [Online] Available at: http://www.dawlish.com/content/968/teign mouthseawall-1.jpg [13 October 2015].

U.S. Army Corps of Engineers, 2001. *Coastal Engineering Manual.* Engineer Manual 1110-2-1100 (in 6 volumes) ed. Washington, D.C.: U.S. Army Corps of Engineers.

Van Doorslaer, K. and De Rouck, J. 2011. Reduction on wave overtopping on a smooth dike by means of a parapet. *Coastal Engineering Proceedings*, ***1***(32):6.

Van Gent, M., Pozueta, B., Van den Boogaard, H. & Medina, J. 2005. D42 Final Report on Generic Prediction Method. *CLASH WP8—Report, WL| Delf Hydraulics and Polytechnic University of Valencia,*

Veale, W., Suzuki, T., Verwaest, T., Trouw, K. and Mertens, T. 2012. Integrated design of coastal protection works for Wenduine, Belgium.*Coastal Engineering Proceedings*, ***1***(33):70.

Wallingford, H. 1999. Overtopping of Seawalls: Design and Assessment Manual. *Environment Agency Technical Report W,* 178

Ward, D.L., Zhang, J., Wibner, C.G. and Cinotto, C.M., 1998. Wind effects on run-up and overtopping of coastal structures. PhD Thesis, Texas A&M University.

Weber C. Seawall. U.S. Patent 1,971,324, filed Jul. 18, 1934, issued Aug. 21, 1934.

WML Coast, 2011. Coastal Protection Works Strand. *Report submitted to PD Naidoo & Associates for CoCT. Cape Town*.

WNNR, 1983.*Valsbaai: Velddataverslag Volume II: Figure (C/SEA 8219/2),* Stellenbosch: WNNR.

WSP Africa Coastal Engineers, 2012. *Coastal processes setback line for the Duin & See development between Great Brak Rriver and Glentana,* Stellenbosch: WSP.

ANNEXURES

LIST OF ANNEXURES

A: Examples of recurve seawalls

Teighmouth, England (Teign mouth seawall, 2015)

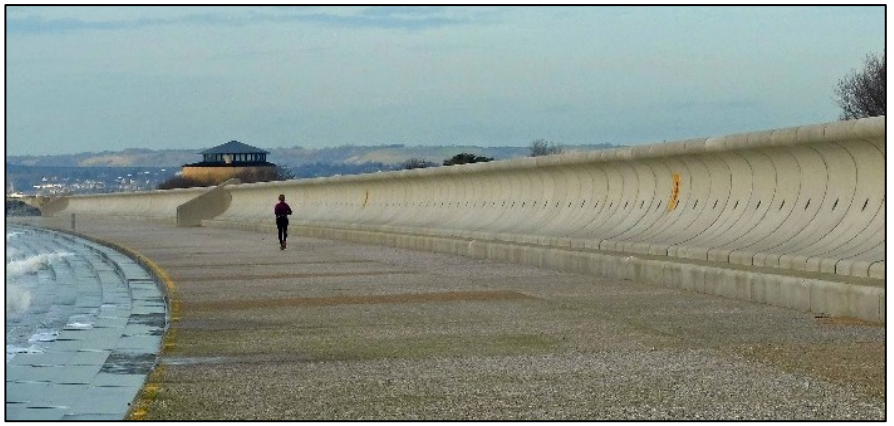

St Mary's bay, United Kingdom (Hill ,2014)

Lyme Regis Sea Defence, England (Special formwork, 2015)

Isle of Wright, England (Special formwork, 2015)

	
United Kingdom (Stacey, 2009)	Arbroath, Scotland (Kilmac construction, 2013)
	
Blackpool, England (Cycling Along Blackpool's Seafront, 2015)	Kunigami, Okinawa Japan (Kolbeco, 2012)

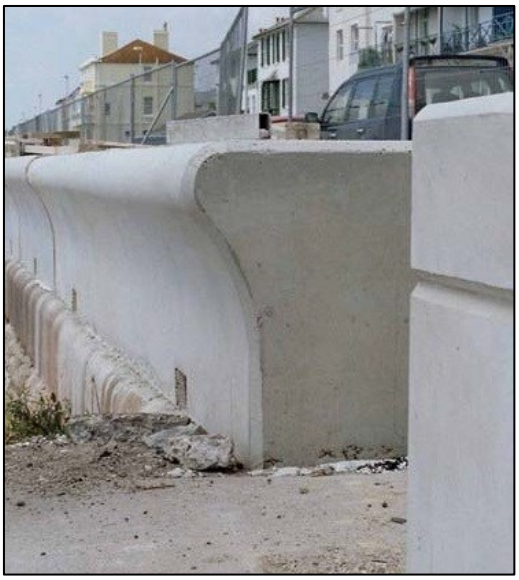	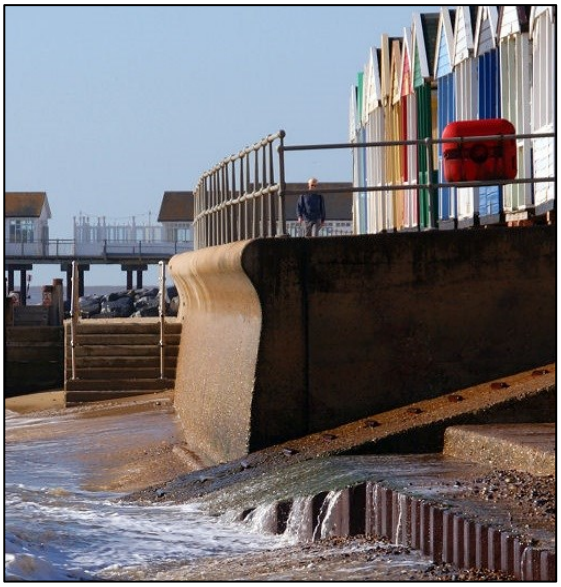
Folkstone Harbour Sea Defence, England (Special Formwork, 2015)	United Kingdom (Stacey, 2009)
	
(Concrete Groynes, 2006)	(Kolbeco, 2015)

	
Cape Town, South Africa (Schoonees, 2014)	Still Bay, South Africa (Google maps, 2014)
	
Damaged Strand recurved walls, South Africa (Schoonees, 2014)	Repaired Strand recurved walls, South Africa

B: Flume cross section

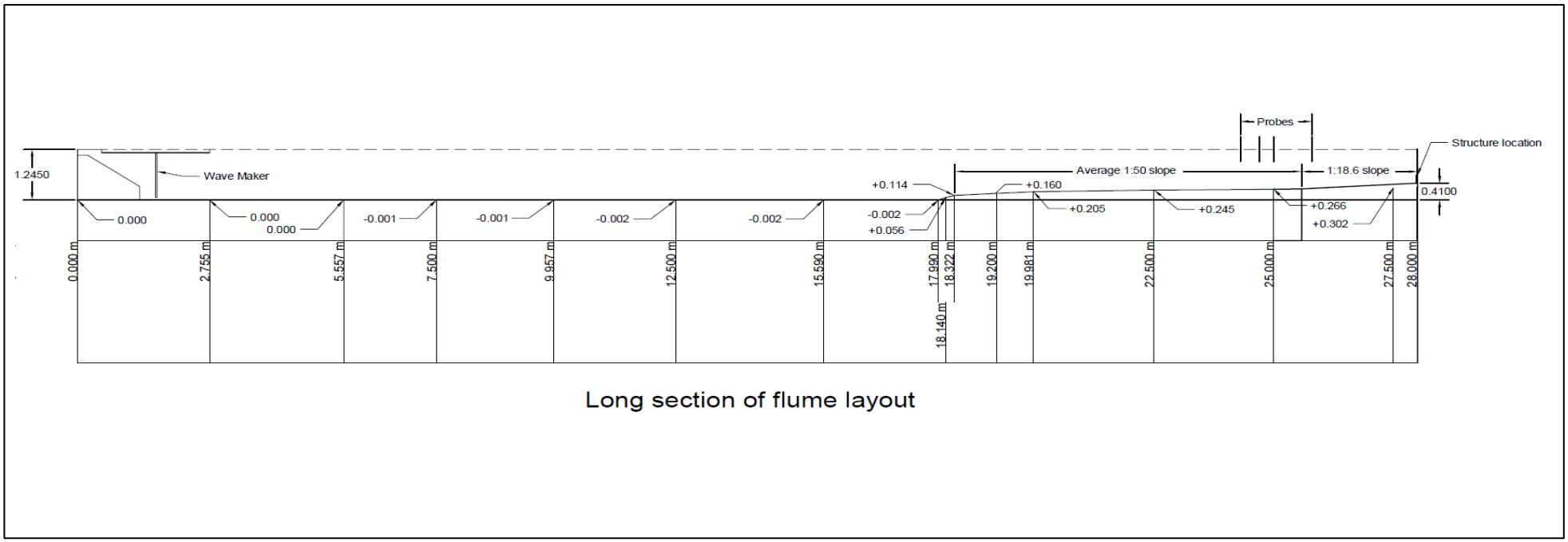

Long section of flume layout

C: Model recurve shapes

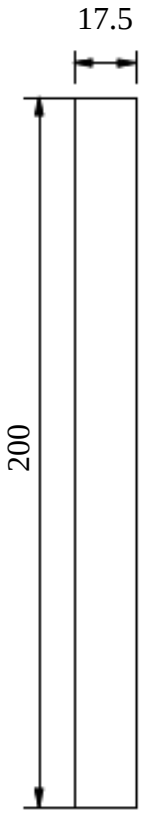	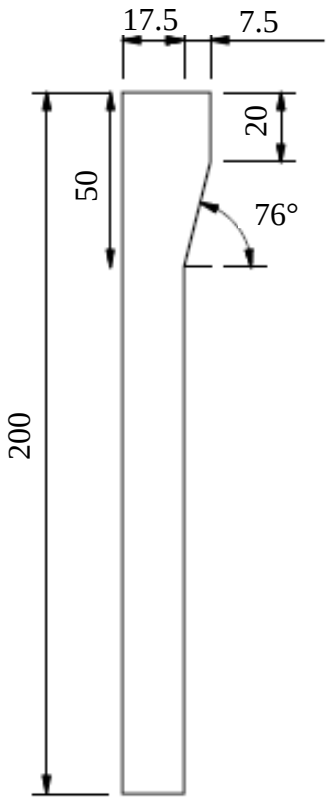	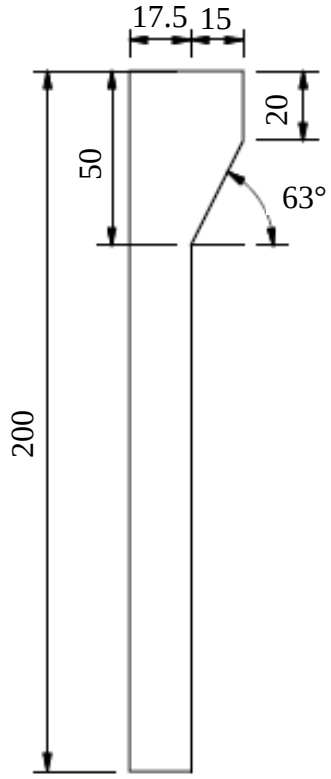
A: 0 mm overhang	B: 7.5 mm overhang	C: 15 mm overhang

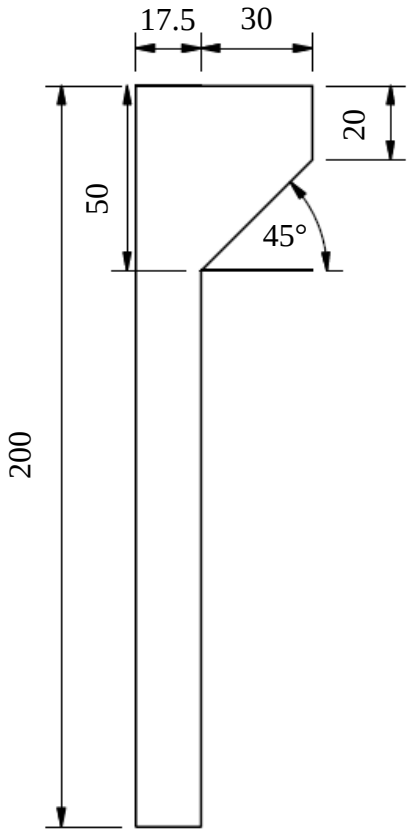	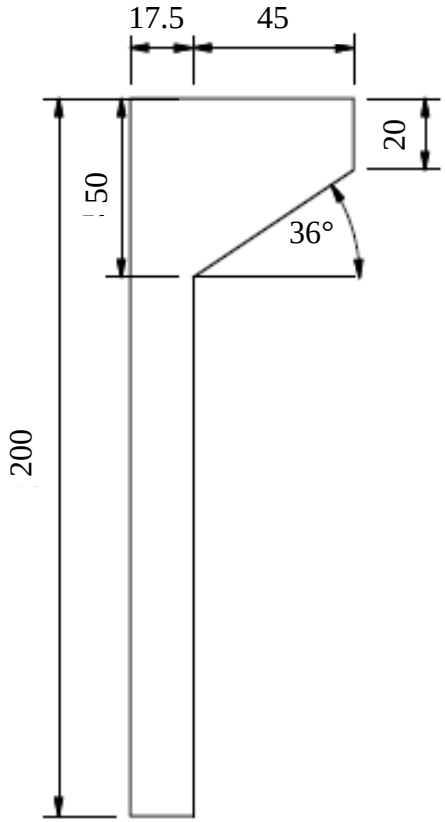	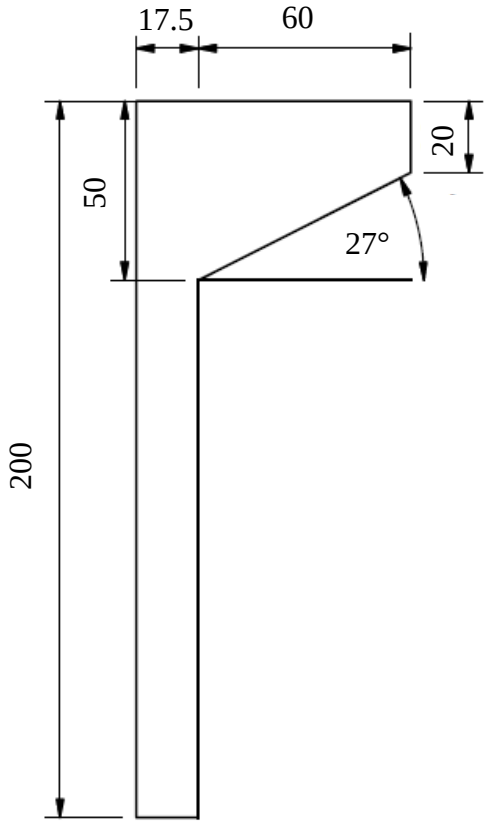
D: 30 mm overhang	E: 45 mm overhang	F: 60 mm overhang

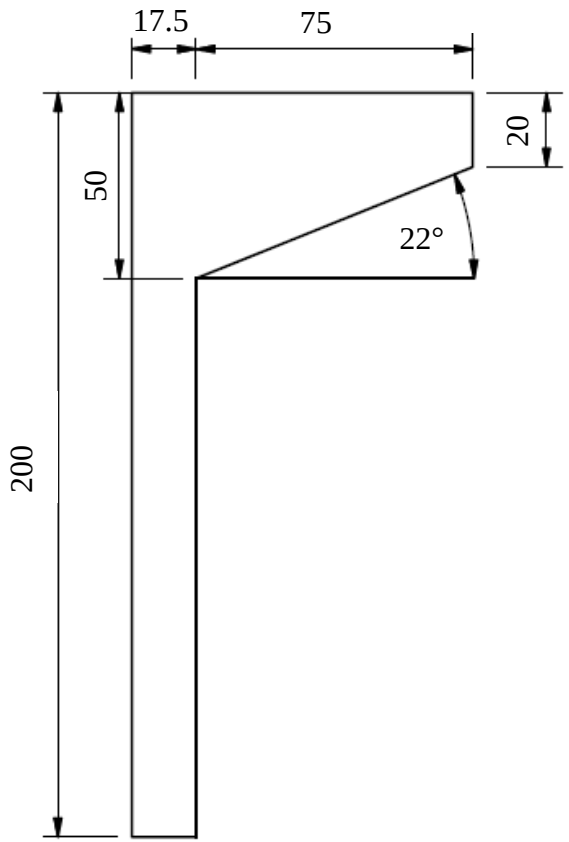	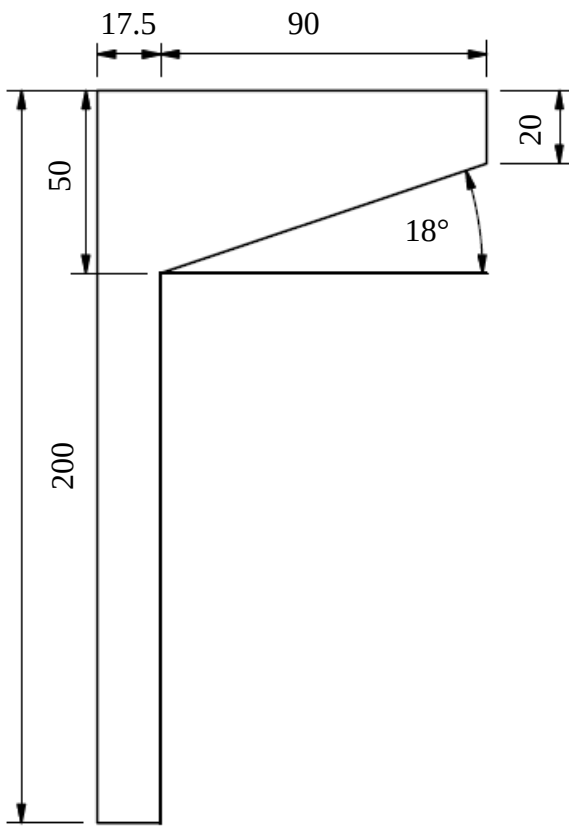	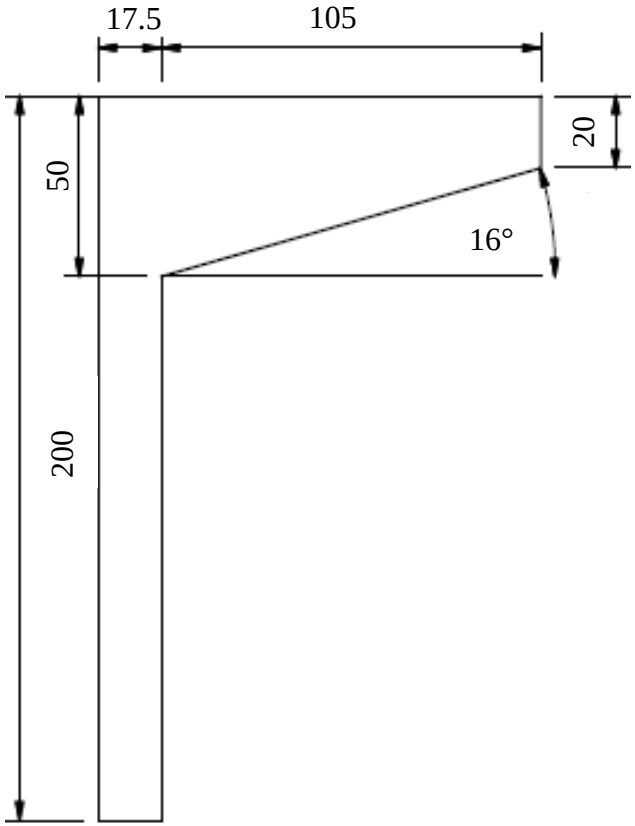
G: 75 mm overhang	H: 90 mm overhang	I: 105 mm overhang

D: Generation capacity curves for small and large flumes

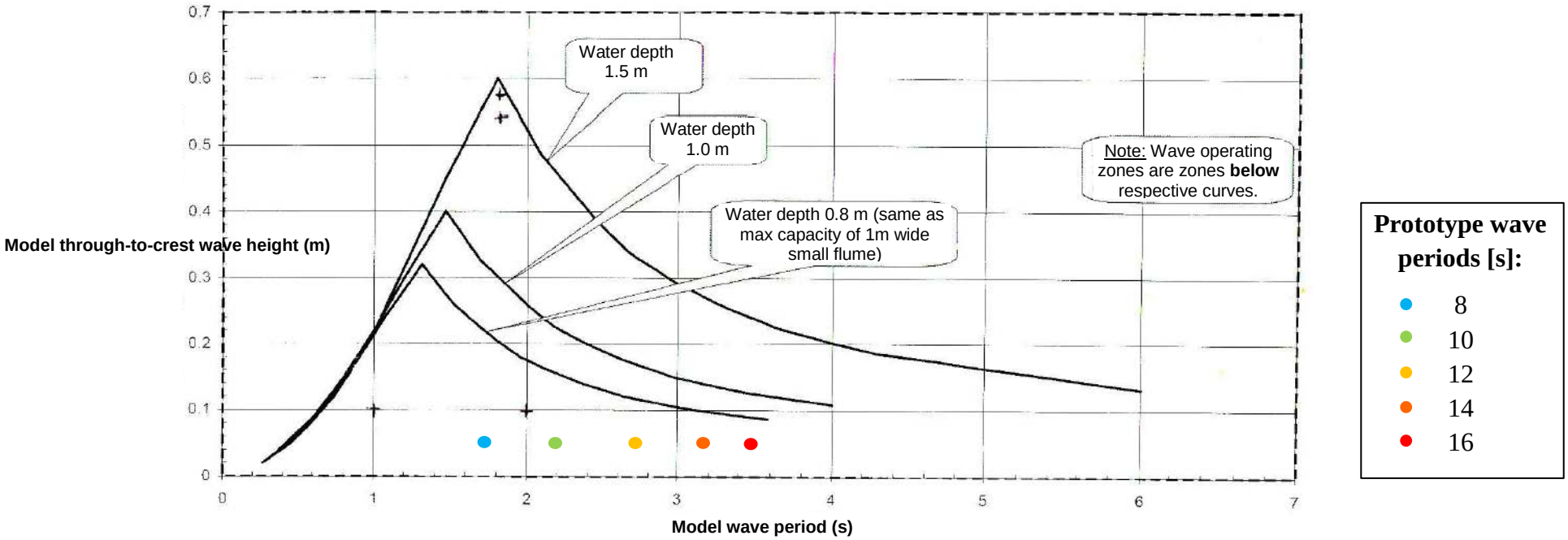

E: EurOtop online overtopping rate calculation tool interface

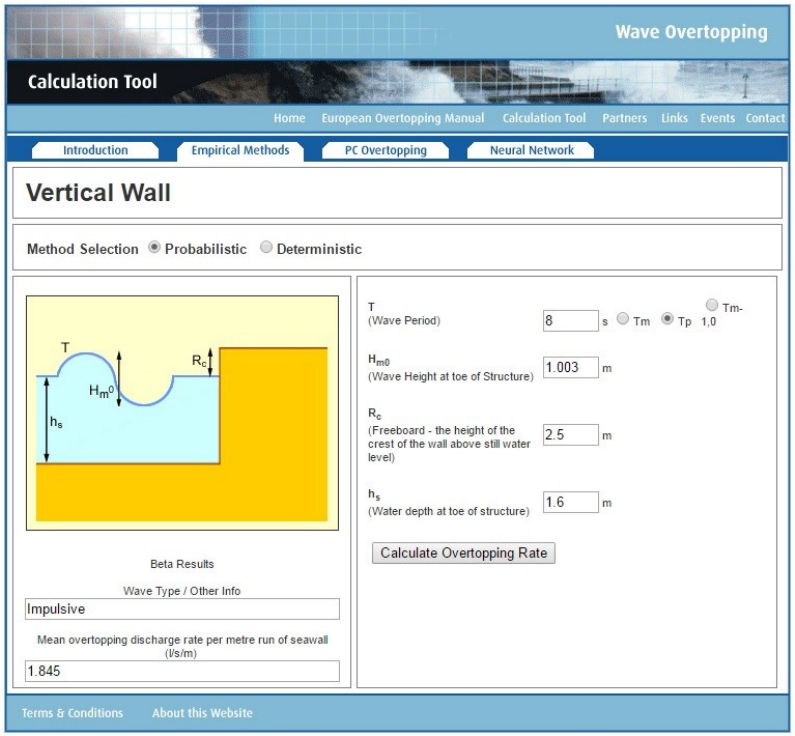

Vertical wall
(HR Wallingford, n.d.)

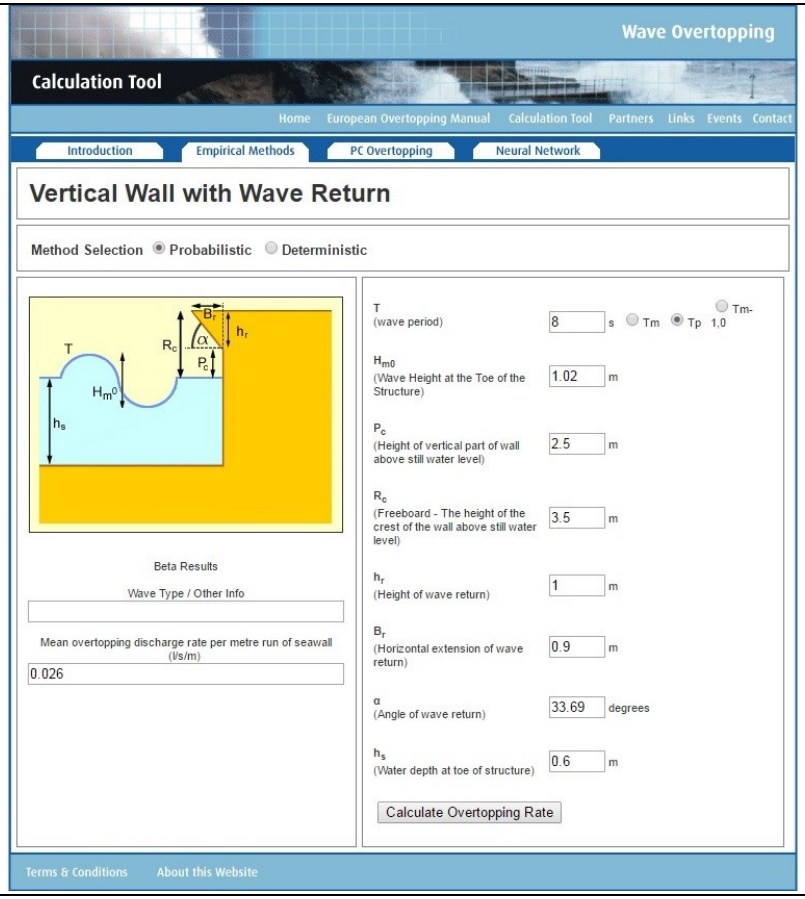

Vertical wall with wave return
(HR Wallingford, n.d.)

F: Model results

A 0 m Model results											
Test		**A-1**	**A-6**	**A-11**	**A-16**	**A-21**	**A-2**	**A-7**			
WL_{paddle}	**m**	0.445	0.465	0.495	0.515	0.535	0.445	0.465			
WL_{toe}	**m**	0.03	0.05	0.08	0.1	0.12	0.03	0.05			
T_p	**s**	1.789	1.789	1.789	1.789	1.789	2.236	2.236			
Test duration	**s**	1789	1789	1789	1789	1789	2236	2236			
$H_{mo\ AVG}$	**mm**	51.5	57.25	61.4125	64.695	66.04	52.25	60			
Hi	**mm**	44.76	48.70	50.15	51.14	50.79	45.14	50.28			
$Volume_{measured}$	**l**	6.67	30.50	63.00	84.34	137.24	10.00	55.25			
WL_{toe}	**m**	0.6	1	1.6	2	2.4	0.6	1			
R_c	**m**	3.5	3.1	2.5	2.1	1.7	3.5	3.1			
T_p	**s**	8	8	8	8	8	10	10			
$H_{mo\ AVG}$	**m**	1.03	1.15	1.23	1.29	1.32	1.05	1.20			
H_i	**m**	0.895	0.974	1.003	1.023	1.016	0.903	1.006			
$Volume_{measured}$	**l**	53333	244000	504000	674699	1097908	80000	442000			
Overtopping rate	**l/s**	6.67	30.50	63.00	84.34	137.24	8.00	44.20			
Overtopping rate pm	**l/s/m**	0.33	1.53	3.15	4.22	6.86	0.40	2.21			
Test		**A-12**	**A-17**	**A-22**	**A-3**	**A-8**	**A-13**	**A-18**	**A-23**	**A-4**	**A-9**
WL_{paddle}	**m**	0.495	0.515	0.535	0.445	0.465	0.495	0.515	0.535	0.445	0.465
WL_{toe}	**m**	0.08	0.1	0.12	0.03	0.05	0.08	0.1	0.12	0.03	0.05
T_p	**s**	2.236	2.236	2.236	2.638	2.683	2.683	2.683	2.683	3.13	3.13
Test duration	**s**	2236	2236	2236	2638	2683	2683	2683	2683	3130	3130
$H_{mo\ AVG}$	**mm**	65.985	71.265	69.6825	44.5	60	68.08	69.7975	67.8475	63.25	60.3875
H_i	**mm**	53.37	56.52	54.25	37.28	50.86	54.15	53.97	51.11	55.07	52.06
$Volume_{measured}$	**l**	113.77	165.72	182.39	16.67	57.50	190.68	322.38	626.91	9.33	55.67
WL_{toe}	**m**	1.6	2	2.4	0.6	1	1.6	2	2.4	0.6	1
R_c	**m**	2.5	2.1	1.7	3.5	3.1	2.5	2.1	1.7	3.5	3.1
T_p	**s**	10	10	10	12	12	12	12	12	14	14
$H_{mo\ AVG}$	**m**	1.32	1.43	1.39	0.89	1.20	1.36	1.40	1.36	1.27	1.21
H_i	**m**	1.067	1.130	1.085	0.746	1.017	1.083	1.079	1.022	1.101	1.041
$Volume_{measured}$	**l**	910124	1325768	1459150	133333	460000	1525459	2579067	5015311	74667	445333
Overtopping rate	**l/s**	91.01	132.58	145.92	11.11	38.33	127.12	214.92	417.94	5.33	31.81
Overtopping rate pm	**l/s/m**	4.55	6.63	7.30	0.56	1.92	6.36	10.75	20.90	0.27	1.59

A 0 m Model results											
Test		**A-14**	**A-19-1**	**A-19-2**	**A-24**	**A-5**	**A-10**	**A-15**	**A-20-1**	**A-20-2**	**A-25**
WL_{paddle}	**m**	0.495	0.515	0.515	0.535	0.445	0.465	0.495	0.515	0.515	0.535
WL_{toe}	**m**	0.08	0.1	0.1	0.12	0.03	0.05	0.08	0.1	0.1	0.12
T_p	**s**	3.13	3.13	3.13	3.13	3.578	3.578	3.578	3.578	3.578	3.578
Test duration	**s**	3130	3130	3130	3130	3578	3578	3578	3578	3578	3578
$H_{mo\ AVG}$	**mm**	66.705	70.89	70.385	70.8275	59.75	61.9475	71.4825	76.1325	74.5425	78.875
H_i	**mm**	52.65	55.01	54.77	53.59	51.75	52.32	56.72	59.33	58.09	59.71
$Q_{measured}$	**l**	326.78	486.27	438.19	750.59	10.67	60.30	330.45	731.43	684.01	1036.08
WL_{toe}	**m**	1.6	2	2	2.4	0.6	1	1.6	2	2	2.4
R_c	**m**	2.5	2.1	2.1	1.7	3.5	3.1	2.5	2.1	2.1	1.7
T_p	**s**	14	14	14	14	16	16	16	16	16	16
$H_{mo\ AVG}$	**m**	1.33	1.42	1.41	1.42	1.20	1.24	1.43	1.52	1.49	1.58
H_i	**m**	1.053	1.100	1.095	1.072	1.035	1.046	1.134	1.187	1.162	1.194
$Volume_{measured}$	**l**	2614264	3890170	3505547	6004724	85333	482400	2643603	5851415	5472040	8288605
Overtopping rate	**l/s**	186.73	277.87	250.40	428.91	5.33	30.15	165.23	365.71	342.00	518.04
Overtopping rate pm	**l/s/m**	9.34	13.89	12.52	21.45	0.27	1.51	8.26	18.29	17.10	25.90
B 0.15 m Model results											
Test		**B-1**	**B-6**	**B-11**	**B-16**	**B-21**	**B-2-1**	**B-2-2**	**B-7**		
WL_{paddle}	**m**	0.445	0.465	0.495	0.515	0.535	0.445	0.445	0.465		
WL_{toe}	**m**	0.03	0.05	0.08	0.1	0.12	0.03	0.03	0.05		
T_p	**s**	1.789	1.789	1.789	1.789	1.789	2.236	2.236	2.236		
Test duration	**s**	1789	1789	1789	1789	1789	2236	2236	2236		
$H_{mo\ AVG}$	**mm**	49.5	56.5	61.4	65.1	66.0	56.5	53.2	59.8		
H_i	**mm**	42.57	48.21	50.23	51.51	50.74	47.75	44.97	50.06		
$Q_{measured}$	**l**	2.50	23.50	53.05	84.30	102.08	6.50	8.50	38.40		
WL_{toe}	**m**	0.6	0.6	1	1.6	2	0.6	0.6	1		
R_c	**m**	3.5	3.5	3.1	2.5	2.1	3.5	3.5	3.1		
T_p	**s**	8	8	8	8	8	10	10	10		
$H_{mo\ AVG}$	**m**	0.99	1.13	1.23	1.30	1.32	1.13	1.06	1.20		
H_i	**m**	0.85	0.96	1.00	1.03	1.01	0.96	0.90	1.00		
$Volume_{measured}$	**l**	20000	188000	424400	674400	816635	52000	68000	307200		
Overtopping rate	**l/s**	2.50	23.50	53.05	84.30	102.08	5.20	6.80	30.72		
Overtopping rate pm	**l/s/m**	0.13	1.18	2.65	4.22	5.10	0.26	0.34	1.54		

B 0.15 m Model results											
Test		**B-12**	**B-17**	**B-3**	**B-8**	**B-13**	**B-18**	**B-23**	**B-4**	**B-9**	**B-14**
WL_{paddle}	**m**	0.495	0.515	0.445	0.465	0.495	0.515	0.535	0.445	0.465	0.495
WL_{toe}	**m**	0.08	0.1	0.03	0.05	0.08	0.1	0.12	0.03	0.05	0.08
T_p	**s**	2.236	2.236	2.638	2.683	2.683	2.683	2.683	3.13	3.13	3.13
Test duration	**s**	2236	2236	2638	2683	2683	2683	2683	3130	3130	3130
$H_{mo\ AVG}$	**mm**	66.4	71.0	57.1	61.4	68.1	67.7	70.3	57.4	61.4	66.8
H_i	**mm**	53.70	56.40	48.32	51.87	54.11	52.28	53.19	50.80	52.44	52.73
$Volume_{measured}$	**l**	101.33	146.90	6.50	43.40	156.06	261.01	532.61	5.50	39.85	193.19
WL_{toe}	**m**	1.6	2	0.6	1	1.6	2	2.4	0.6	1	1.6
R_c	**m**	2.5	2.1	3.5	3.1	2.5	2.1	1.7	3.5	3.1	2.5
T_p	**s**	10	10	12	12	12	12	12	14	14	14
$H_{mo\ AVG}$	**m**	1.33	1.42	1.14	1.23	1.36	1.35	1.41	1.15	1.23	1.34
Hi	**m**	1.07	1.13	0.97	1.04	1.08	1.05	1.06	1.02	1.05	1.05
$Volume_{measured}$	**l**	810667	1175206	52000	347200	1248489	2088072	4260895	44000	318800	1545544
Overtopping rate	**l/s**	81.07	117.52	4.33	28.93	104.04	174.01	355.07	3.14	22.77	110.40
Overtopping rate pm	**l/s/m**	4.05	5.88	0.22	1.45	5.20	8.70	17.75	0.16	1.14	5.52
Test		**B-19-1**	**B-19-2**	**B-24**	**B-5**	**B-10**	**B-15**	**B-20-1**	**B-20-2**	**B-25-1**	**B-25-2**
WL_{paddle}	**m**	0.515	0.515	0.535	0.445	0.465	0.495	0.515	0.515	0.535	0.535
WL_{toe}	**m**	0.1	0.1	0.12	0.03	0.05	0.08	0.1	0.1	0.12	0.12
T_p	**s**	3.13	3.13	3.13	3.578	3.578	3.578	3.578	3.578	3.578	3.578
Test duration	**s**	3130	3130	3130	3578	3578	3578	3578	3578	3578	3578
$H_{mo\ AVG}$	**mm**	70.9	72.2	71.4	59.5	63.3	70.2	77.2	77.9	81.9	82.1
H_i	**mm**	55.05	56.01	54.07	51.21	53.39	55.65	59.94	60.57	62.10	62.31
$Volume_{measured}$	**l**	488.56	467.62	666.18	7.50	46.95	267.42	698.08	794.56	1108.07	1084.13
WL_{toe}	**m**	2	2	2.4	0.6	1	1.6	2	2	2.4	2.4
R_c	**m**	2.1	2.1	1.7	3.5	3.1	2.5	2.1	2.1	1.7	1.7
T_p	**s**	14	14	14	16	16	16	16	16	16	16
$H_{mo\ AVG}$	**m**	1.42	1.44	1.43	1.19	1.27	1.40	1.54	1.56	1.64	1.64
H_i	**m**	1.10	1.12	1.08	1.02	1.07	1.11	1.20	1.21	1.24	1.25
$Volume_{measured}$	**l**	3908505	3740922	5329472	60000	375600	2139370	5584641	6356449	8864556	8673074
Overtopping rate	**l/s**	279.18	267.21	380.68	3.75	23.48	133.71	349.04	397.28	554.03	542.07
Overtopping rate pm	**l/s/m**	13.96	13.36	19.03	0.19	1.17	6.69	17.45	19.86	27.70	27.10

C 0.3 m Model results								
Test		**C-1**	**C-6**	**C-11**	**C-16**	**C-21-1**	**C-21-2**	**C-2**
WL_{paddle}	**m**	0.445	0.465	0.495	0.515	0.535	0.535	0.445
WL_{toe}	**m**	0.03	0.05	0.08	0.1	0.12	0.12	0.03
T_p	**s**	1.789	1.789	1.789	1.789	1.789	1.789	2.236
Test duration	**s**	1789	1789	1789	1789	1789	1789	2236
$H_{mo\ AVG}$	**mm**	60.4	64.2	70.1	72.8	73.7	73.5	62.5
H_i	**mm**	51.9	54.6	57.0	57.9	57.3	57.2	52.4
$Volume_{measured}$	**l**	1.75	9.50	26.07	64.75	180.30	194.82	1.63
WL_{toe}	**m**	0.6	1	1.6	2	2.4	2.4	0.6
Rc	**m**	3.5	3.1	2.5	2.1	1.7	1.7	3.5
T_p	**s**	8	8	8	8	8	8	10
$H_{mo\ AVG}$	**m**	1.21	1.28	1.40	1.46	1.47	1.47	1.25
H_i	**m**	1.04	1.09	1.14	1.16	1.15	1.14	1.05
$Volume_{measured}$	**l**	14000	76000	208571	518000	1442402	1558535	13000
Overtopping rate	**l/s**	1.75	9.50	26.07	64.75	180.30	194.82	1.30
Overtopping rate pm	**l/s/m**	0.09	0.48	1.30	3.24	9.02	9.74	0.07

Test		**C-7**	**C-12**	**C-17**	**C-22**	**C-3**	**C-8**	**C-13**	**C-18**	**C-23**	**C-4**
WL_{paddle}	**m**	0.465	0.495	0.515	0.535	0.445	0.465	0.495	0.515	0.535	0.445
WL_{toe}	**m**	0.05	0.08	0.1	0.12	0.03	0.05	0.08	0.1	0.12	0.03
T_p	**s**	2.236	2.236	2.236	2.236	2.638	2.683	2.683	2.683	2.683	3.13
Test duration	**s**	2236	2236	2236	2236	2638	2683	2683	2683	2683	3130
$H_{mo\ AVG}$	**mm**	69.8	74.0	77.8	82.2	65.1	70.6	76.4	76.3	75.8	65.5
H_i	**mm**	58.3	60.0	62.3	65.0	54.2	59.0	60.6	59.5	57.8	56.3
$Volume_{measured}$	**l**	12.67	47.75	174.48	387.79	2.38	13.42	80.50	340.91	735.25	2.42
WL_{toe}	**m**	1	1.6	2	2.4	0.6	1	1.6	2	2.4	0.6
R_c	**m**	3.1	2.5	2.1	1.7	3.5	3.1	2.5	2.1	1.7	3.5
T_p	**s**	10	10	10	10	12	12	12	12	12	14
$H_{mo\ AVG}$	**m**	1.40	1.48	1.56	1.64	1.30	1.41	1.53	1.53	1.52	1.31
Hi	**m**	1.17	1.20	1.25	1.30	1.08	1.18	1.21	1.19	1.16	1.13
$Volume_{measured}$	**l**	101333	382000	1395876	3102285	19000	107333	644000	2727289	5881971	19333
Overtopping rate	**l/s**	10.13	38.20	139.59	310.23	1.58	8.94	53.67	227.27	490.16	1.38
Overtopping rate pm	**l/s/m**	0.51	1.91	6.98	15.51	0.08	0.45	2.68	11.36	24.51	0.07

C 0.3 m Model results											
Test		**C-9**	**C-14**	**C-19**	**C-24**	**C-5**	**C-10**	**C-15**	**C-20**	**C-25-1**	**C-25-2**
WL_{paddle}	**m**	0.465	0.495	0.515	0.535	0.445	0.465	0.495	0.515	0.535	0.535
WL_{toe}	**m**	0.05	0.08	0.1	0.12	0.03	0.05	0.08	0.1	0.12	0.12
T_p	**s**	3.13	3.13	3.13	3.13	3.578	3.578	3.578	3.578	3.578	3.578
Test duration	**s**	3130	3130	3130	3130	3578	3578	3578	3578	3578	3578
$H_{mo\ AVG}$	**mm**	69.9	72.8	75.8	79.1	67.3	71.4	78.1	81.5	84.8	86.9
H_i	**mm**	59.2	57.5	59.1	60.5	56.7	60.2	62.0	63.7	64.7	66.4
$Volume_{measured}$	**l**	11.44	120.95	451.69	1019.30	1.50	12.56	161.77	712.58	1323.50	1418.96
WL_{toe}	**m**	1	1.6	2	2.4	0.6	1	1.6	2	2.4	2.4
R_c	**m**	3.1	2.5	2.1	1.7	3.5	3.1	2.5	2.1	1.7	1.7
T_p	**s**	14	14	14	14	16	16	16	16	16	16
$H_{mo\ AVG}$	**m**	1.40	1.46	1.52	1.58	1.35	1.43	1.56	1.63	1.70	1.74
H_i	**m**	1.18	1.15	1.18	1.21	1.13	1.20	1.24	1.27	1.29	1.33
$Volume_{measured}$	**l**	91556	967575	3613539	8154397	12000	100444	1294160	5700607	10587991	11351679
Overtopping rate	**l/s**	6.54	69.11	258.11	582.46	0.75	6.28	80.89	356.29	661.75	709.48
Overtopping rate pm	**l/s/m**	0.33	3.46	12.91	29.12	0.04	0.31	4.04	17.81	33.09	35.47

D 0.6 m Model results						
Test		**D-1**	**D-6**	**D-11**	**D-16**	**D-21**
WL_{paddle}	**m**	0.445	0.465	0.495	0.515	0.535
WL_{toe}	**m**	0.03	0.05	0.08	0.1	0.12
T_p	**s**	1.789	1.789	1.789	1.789	1.789
Test duration	**s**	1789	1789	1789	1789	1789
$H_{mo\ AVG}$	**mm**	61.5	65.1	70.4	74.5	73.6
H_i	**mm**	52.9	55.3	57.9	59.8	57.3
$Volume_{measured}$	**l**	0.00	1.90	1.60	4.75	55.04
WL_{toe}	**m**	0.6	1	1.6	2	2.4
R_c	**m**	3.5	3.1	2.5	2.1	1.7
T_p	**s**	8	8	8	8	8
$H_{mo\ AVG}$	**m**	1.23	1.30	1.41	1.49	1.47
H_i	**m**	1.06	1.11	1.16	1.20	1.15
$Volume_{measured}$	**l**	0	15200	12800	38000	440308
Overtopping rate	**l/s**	0.00	1.90	1.60	4.75	55.04
Overtopping rate pm	**l/s/m**	0.00	0.09	0.08	0.24	2.75

D 0.6 m Model results											
Test		**D-3**	**D-8**	**D-13**	**D-18**	**D-23**	**D-4**	**D-9**	**D-14**	**D-19**	**D-24**
WL_{paddle}	**m**	0.445	0.465	0.495	0.515	0.535	0.445	0.465	0.495	0.515	0.535
WL_{toe}	**m**	0.03	0.05	0.08	0.1	0.12	0.03	0.05	0.08	0.1	0.12
T_p	**s**	2.638	2.683	2.683	2.683	2.683	3.13	3.13	3.13	3.13	3.13
Test duration	**s**	2638	2683	2683	2683	2683	3130	3130	3130	3130	3130
$H_{mo\ AVG}$	**mm**	65.2	73.8	77.0	77.4	79.0	68.2	72.5	75.0	78.6	80.3
H_i	**mm**	54.3	61.5	61.1	60.5	60.5	57.6	61.2	59.0	61.1	61.6
$Volume_{measured}$	**l**	0.50	2.00	15.75	140.14	712.06	0.00	1.50	33.75	238.11	741.34
WL_{toe}	**m**	0.6	1	1.6	2	2.4	0.6	1	1.6	2	2.4
R_c	**m**	3.5	3.1	2.5	2.1	1.7	3.5	3.1	2.5	2.1	1.7
T_p	**s**	12	12	12	12	12	14	14	14	14	14
$H_{mo\ AVG}$	**m**	1.30	1.48	1.54	1.55	1.58	1.36	1.45	1.50	1.57	1.61
H_i	**m**	1.09	1.23	1.22	1.21	1.21	1.15	1.22	1.18	1.22	1.23
$Volume_{measured}$	**l**	4000	16000	126000	1121127	5696485	0	12000	270000	1904906	5930748
Overtopping rate	**l/s**	0.33	1.33	10.50	93.43	474.71	0.00	0.86	19.29	136.06	423.62
Overtopping rate pm	**l/s/m**	0.02	0.07	0.53	4.67	23.74	0.00	0.04	0.96	6.80	21.18

Test		**D-5**	**D-10**	**D-15**	**D-20-1**	**D-20-2**	**D-15**	**D-20-1**	**D-20-2**
WL_{paddle}	**m**	0.445	0.465	0.495	0.515	0.515	0.495	0.515	0.515
WL_{toe}	**m**	0.03	0.05	0.08	0.1	0.1	0.08	0.1	0.1
T_p	**s**	3.578	3.578	3.578	3.578	3.578	3.578	3.578	3.578
Test duration	**s**	3578	3578	3578	3578	3578	3578	3578	3578
$H_{mo\ AVG}$	**mm**	69.1	71.8	78.8	85.8	85.0	78.8	85.8	85.0
H_i	**mm**	58.4	60.5	62.4	66.7	66.1	62.4	66.7	66.1
$Volume_{measured}$	**l**	0.75	1.00	56.25	402.01	418.90	56.25	402.01	418.90
WL_{toe}	**m**	0.6	1	1.6	2	2	1.6	2	2
R_c	**m**	3.5	3.1	2.5	2.1	2.1	2.5	2.1	2.1
T_p	**s**	16	16	16	16	16	16	16	16
$H_{mo\ AVG}$	**m**	1.38	1.44	1.58	1.72	1.70	1.58	1.72	1.70
H_i	**m**	1.17	1.21	1.25	1.33	1.32	1.25	1.33	1.32
$Volume_{measured}$	**l**	6000	8000	450000	3216113	3351200	450000	3216113	3351200
Overtopping rate	**l/s**	0.38	0.50	28.13	201.01	209.45	28.13	201.01	209.45
Overtopping rate pm	**l/s/m**	0.02	0.03	1.41	10.05	10.47	1.41	10.05	10.47

E 0.9 m Model results											
Test		**E-1**	**E-6**	**E-11**	**E-16**	**E-21**	**E-2**				
WL_{paddle}	**m**	0.445	0.465	0.495	0.515	0.535	0.445				
WL_{toe}	**m**	0.03	0.05	0.08	0.1	0.12	0.03				
T_p	**s**	1.789	1.789	1.789	1.789	1.789	2.236				
Test duration	**s**	1789	1789	1789	1789	1789	2236				
$H_{mo\ AVG}$	**mm**	59.3	64.2	70.9	73.8	76.4	62.0				
H_i	**mm**	50.9	54.6	58.7	59.6	60.2	51.6				
$Volume_{measured}$	**l**	0.00	0.00	0.13	6.60	35.43	0.00				
WL_{toe}	**m**	0.6	1	1.6	2	2.4	0.6				
R_c	**m**	3.5	3.1	2.5	2.1	1.7	3.5				
T_p	**s**	8	8	8	8	8	10				
$H_{mo\ AVG}$	**m**	1.19	1.28	1.42	1.48	1.53	1.24				
H_i	**m**	1.02	1.09	1.17	1.19	1.20	1.03				
$Volume_{measured}$	**l**	0	0	1067	52800	283429	0				
Overtopping rate	**l/s**	0.00	0.00	0.13	6.60	35.43	0.00				
Overtopping rate pm	**l/s/m**	0.00	0.00	0.01	0.33	1.77	0.00				
Test		**E-7**	**E-12**	**E-17**	**E-22**	**E-3**	**E-8**	**E-13**	**E-18**	**E-23**	**E-4**
WL_{paddle}	**m**	0.465	0.495	0.515	0.535	0.445	0.465	0.495	0.515	0.535	0.445
WL_{toe}	**m**	0.05	0.08	0.1	0.12	0.03	0.05	0.08	0.1	0.12	0.03
T_p	**s**	2.236	2.236	2.236	2.236	2.638	2.683	2.683	2.683	2.683	3.13
Test duration	**s**	2236	2236	2236	2236	2638	2683	2683	2683	2683	3130
$H_{mo\ AVG}$	**mm**	69.0	75.5	80.3	83.8	65.6	69.9	76.8	78.7	78.0	66.2
H_i	**mm**	57.6	61.4	64.5	66.7	54.6	58.4	60.9	61.7	60.2	56.8
$Volume_{measured}$	**l**	0.24	2.75	23.64	176.19	0.00	0.89	8.73	99.46	472.41	0.00
WL_{toe}	**m**	1	1.6	2	2.4	0.6	1	1.6	2	2.4	0.6
Rc	**m**	3.1	2.5	2.1	1.7	3.5	3.1	2.5	2.1	1.7	3.5
T_p	**s**	10	10	10	10	12	12	12	12	12	14
$H_{mo\ AVG}$	**m**	1.38	1.51	1.61	1.68	1.31	1.40	1.54	1.57	1.56	1.32
H_i	**m**	1.15	1.23	1.29	1.33	1.09	1.17	1.22	1.23	1.20	1.14
$Volume_{measured}$	**l**	1956	22000	189143	1409493	0	7111	69867	795658	3779288	0
Overtopping rate	**l/s**	0.20	2.20	18.91	140.95	0.00	0.59	5.82	66.30	314.94	0.00
Overtopping rate pm	**l/s/m**	0.01	0.11	0.95	7.05	0.00	0.03	0.29	3.32	15.75	0.00

E 0.9 m Model results											
Test		**E-9**	**E-14**	**E-19**	**E-24**	**E-5**	**E-10**	**E-15**	**E-20**	**E-25-1**	**E-25-2**
WL_{paddle}	**m**	0.465	0.495	0.515	0.535	0.445	0.465	0.495	0.515	0.535	0.535
WL_{toe}	**m**	0.05	0.08	0.1	0.12	0.03	0.05	0.08	0.1	0.12	0.12
T_p	**s**	3.13	3.13	3.13	3.13	3.578	3.578	3.578	3.578	3.578	3.578
Test duration	**s**	3130	3130	3130	3130	3578	3578	3578	3578	3578	3578
$H_{mo\ AVG}$	**mm**	70.1	76.8	80.1	82.1	67.8	72.0	78.7	85.0	89.2	89.6
H_i	**mm**	59.2	60.5	62.6	63.4	57.2	60.4	62.3	66.1	69.0	69.1
$Volume_{measured}$	**l**	0.00	19.38	152.79	649.92	0.00	0.11	26.78	289.05	892.65	940.89
WL_{toe}	**m**	1	1.6	2	2.4	0.6	1	1.6	2	2.4	2.4
Rc	**m**	3.1	2.5	2.1	1.7	3.5	3.1	2.5	2.1	1.7	1.7
T_p	**s**	14	14	14	14	16	16	16	16	16	16
$H_{mo\ AVG}$	**m**	1.40	1.54	1.60	1.64	1.36	1.44	1.57	1.70	1.78	1.79
H_i	**m**	1.18	1.21	1.25	1.27	1.14	1.21	1.25	1.32	1.38	1.38
$Q_{measured}$	**l**	0	155022	1222337	5199396	0	889	214222	2312417	7141210	7527134
Overtopping rate	**l/s**	0.00	11.07	87.31	371.39	0.00	0.06	13.39	144.53	446.33	470.45
Overtopping rate pm	**l/s/m**	0.00	0.55	4.37	18.57	0.00	0.00	0.67	7.23	22.32	23.52

F 1.2 m Model results						
Test		**F-1**	**F-6**	**F-11**	**F-16**	**F-21**
WL_{paddle}	**m**	0.445	0.465	0.495	0.515	0.535
WL_{toe}	**m**	0.03	0.05	0.08	0.1	0.12
T_p	**s**	1.789	1.789	1.789	1.789	1.789
Test duration	**s**	1789	1789	1789	1789	1789
$H_{mo\ AVG}$	**mm**	52.0	57.6	63.7	65.2	65.7
H_i	**mm**	44.5	48.8	52.4	52.2	51.4
$Volume_{measured}$	**l**	0.00	0.00	0.00	0.33	0.40
WL_{toe}	**m**	0.6	1	1.6	2	2.4
Rc	**m**	3.5	3.1	2.5	2.1	1.7
T_p	**s**	8	8	8	8	8
$H_{mo\ AVG}$	**m**	1.04	1.15	1.27	1.30	1.31
H_i	**m**	0.89	0.98	1.05	1.04	1.03
$Volume_{measured}$	**l**	0	0	0	2667	3200
Overtopping rate	**l/s**	0.00	0.00	0.00	0.33	0.40
Overtopping rate pm	**l/s/m**	0.00	0.00	0.00	0.02	0.02

F 1.2 m Model results											
Test		**F-2**	**F-7**	**F-12**	**F-17-2**	**F-22**	**F-3**	**F-8**	**F-13**	**F-18**	**F-23**
WL_{paddle}	**m**	0.445	0.465	0.495	0.515	0.535	0.445	0.465	0.495	0.515	0.535
WL_{toe}	**m**	0.03	0.05	0.08	0.1	0.12	0.03	0.05	0.08	0.1	0.12
T_p	**s**	2.236	2.236	2.236	2.236	2.236	2.683	2.683	2.683	2.683	2.683
Test duration	**s**	2236	2236	2236	2236	2236	2.683	2683	2683	2683	2683
$H_{mo\ AVG}$	**mm**	57.2	60.4	67.4	70.2	71.4	58.9	62.6	68.6	70.2	69.2
H_i	**mm**	48.1	50.6	54.5	56.1	56.1	51.9	52.7	54.9	54.8	52.5
$Volume_{measured}$	**l**	0.00	0.00	0.00	1.32	35.75	0.00	0.00	0.33	7.32	135.71
WL_{toe}	**m**	0.6	1	1.6	2	2.4	0.6	1	1.6	2	2.4
R_c	**m**	3.5	3.1	2.5	2.1	1.7	3.5	3.1	2.5	2.1	1.7
T_p	**s**	10	10	10	10	10	12	12	12	12	12
$H_{mo\ AVG}$	**m**	1.14	1.21	1.35	1.40	1.43	1.18	1.25	1.37	1.40	1.38
H_i	**m**	0.96	1.01	1.09	1.12	1.12	1.04	1.05	1.10	1.10	1.05
$Volume_{measured}$	**l**	0	0	0	10571	286000	0	0	2667	58571	1085647
Overtopping rate	**l/s**	0.00	0.00	0.00	1.06	28.60	0.00	0.00	0.22	4.88	90.47
Overtopping rate pm	**l/s/m**	0.00	0.00	0.00	0.05	1.43	0.00	0.00	0.01	0.24	4.52
Test		**F-4**	**F-9**	**F-14**	**F-19**	**F-24**	**F-5**	**F-10**	**F-15**	**F-20**	**F-25**
WL_{paddle}	**m**	0.445	0.465	0.495	0.515	0.535	0.445	0.465	0.495	0.515	0.535
WL_{toe}	**m**	0.03	0.05	0.08	0.1	0.12	0.03	0.05	0.08	0.1	0.12
T_p	**s**	3.13	3.13	3.13	3.13	3.13	3.578	3.578	3.578	3.578	3.578
Test duration	**s**	3130	3130	3130	3130	3130	3578	3578	3578	3578	3578
$H_{mo\ AVG}$	**mm**	70.5	62.5	63.9	68.9	70.1	57.6	62.8	67.2	74.0	77.9
H_i	**mm**	58.6	53.7	50.5	53.5	53.3	48.8	53.0	53.2	57.1	59.0
$Volume_{measured}$	**l**	0.00	0.00	0.75	18.76	199.57	0.00	0.00	2.53	48.50	282.39
WL_{toe}	**m**	0.6	1	1.6	2	2.4	0.6	1	1.6	2	2.4
R_c	**m**	3.5	3.1	2.5	2.1	1.7	3.5	3.1	2.5	2.1	1.7
T_p	**s**	14	14	14	14	14	16	16	16	16	16
$H_{mo\ AVG}$	**m**	1.41	1.25	1.28	1.38	1.40	1.15	1.26	1.34	1.48	1.56
H_i	**m**	1.17	1.07	1.01	1.07	1.07	0.98	1.06	1.06	1.14	1.18
$Volume_{measured}$	**l**	0	0	6000	150095	1596578	0	0	20222	388000	2259154
Overtopping rate	**l/s**	0.00	0.00	0.43	10.72	114.04	0.00	0.00	1.26	24.25	141.20
Overtopping rate pm	**l/s/m**	0.00	0.00	0.02	0.54	5.70	0.00	0.00	0.06	1.21	7.06

G 1.5 m Model results											
Test		**G-1**	**G-6**	**G-11**	**G-16**	**G-21**					
WL_{paddle}	**m**	0.445	0.465	0.495	0.515	0.535					
WL_{toe}	**m**	0.03	0.05	0.08	0.1	0.12					
T_p	**s**	1.789	1.789	1.789	1.789	1.789					
Test duration	**s**	1789	1789	1789	1789	1789					
$H_{mo\ AVG}$	**mm**	54.0	57.5	62.8	65.5	66.7					
H_i	**mm**	46.39	48.77	51.36	52.49	52.32					
$Volume_{measured}$	**l**	0.00	0.00	0.00	0.00	1.50					
WL_{toe}	**m**	0.6	1	1.6	2	2.4					
R_c	**m**	3.5	3.1	2.5	2.1	1.7					
T_p	**s**	8	8	8	8	8					
$H_{mo\ AVG}$	**m**	1.08	1.15	1.26	1.31	1.33					
H_i	**m**	0.93	0.98	1.03	1.05	1.05					
$Volume_{measured}$	**l**	0	0	0	0	12000					
Overtopping rate	**l/s**	0.00	0.00	0.00	0.00	1.50					
Overtopping rate pm	**l/s/m**	0.00	0.00	0.00	0.00	0.08					
Test		**G-2**	**G-7**	**G-12**	**G-17**	**G-22**	**G-3**	**G-8**	**G-13**	**G-18**	**G-23**
WL_{paddle}	**m**	0.445	0.465	0.495	0.515	0.535	0.445	0.465	0.495	0.515	0.535
WL_{toe}	**m**	0.03	0.05	0.08	0.1	0.12	0.03	0.05	0.08	0.1	0.12
T_p	**s**	2.236	2.236	2.236	2.236	2.236	2.638	2.683	2.683	2.683	2.683
Test duration	**s**	2236	2236	2236	2236	2236	2638	2683	2683	2683	2683
$H_{mo\ AVG}$	**mm**	55.4	60.6	66.5	70.6	73.3	59.3	63.2	67.8	69.6	70.1
H_i	**mm**	46.88	50.60	53.79	56.40	57.66	49.90	53.07	54.21	54.37	53.47
$Volume_{measured}$	**l**	0.00	0.00	0.00	0.20	30.25	0.00	0.00	0.25	3.44	107.99
WL_{toe}	**m**	0.6	1	1.6	2	2.4	0.6	1	1.6	2	2.4
R_c	**m**	3.5	3.1	2.5	2.1	1.7	3.5	3.1	2.5	2.1	1.7
T_p	**s**	10	10	10	10	10	12	12	12	12	12
$H_{mo\ AVG}$	**m**	1.11	1.21	1.33	1.41	1.47	1.19	1.26	1.36	1.39	1.40
H_i	**m**	0.94	1.01	1.08	1.13	1.15	1.00	1.06	1.08	1.09	1.07
$Volume_{measured}$	**l**	0	0	0	1600	242000	0	0	2000	27556	863921
Overtopping rate	**l/s**	0.00	0.00	0.00	0.16	24.20	0.00	0.00	0.17	2.30	71.99
Overtopping rate pm	**l/s/m**	0.00	0.00	0.00	0.01	1.21	0.00	0.00	0.01	0.11	3.60

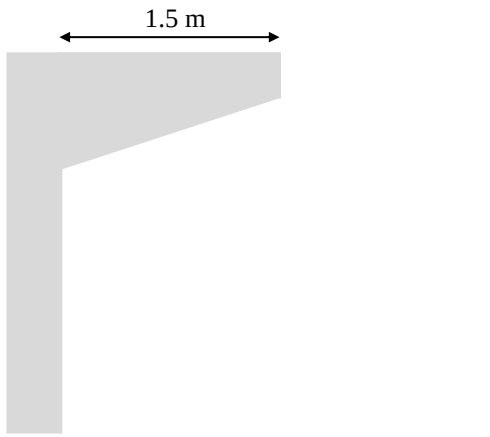

G 1.5 m Model results											
Test		**G-4**	**G-9**	**G-14**	**G-19**	**G-24**	**G-5**	**G-10**	**G-15**	**G-20**	**G-25**
WL_{paddle}	**m**	0.445	0.465	0.495	0.515	0.535	0.445	0.465	0.495	0.515	0.535
WL_{toe}	**m**	0.03	0.05	0.08	0.1	0.12	0.03	0.05	0.08	0.1	0.12
T_p	**s**	3.13	3.13	3.13	3.13	3.13	3.578	3.578	3.578	3.578	3.578
Test duration	**s**	3130	3130	3130	3130	3130	3578	3578	3578	3578	3578
$H_{mo\ AVG}$	**mm**	59.4	62.5	64.6	68.8	73.1	60.0	63.2	68.0	74.4	79.3
H_i	**mm**	51.52	53.56	51.10	53.41	55.69	51.66	53.24	53.82	57.40	60.31
$Volume_{measured}$	**l**	0.00	0.00	0.00	13.76	204.16	0.00	0.00	1.50	36.35	312.46
WL_{toe}	**m**	0.6	1	1.6	2	2.4	0.6	1	1.6	2	2.4
R_c	**m**	3.5	3.1	2.5	2.1	1.7	3.5	3.1	2.5	2.1	1.7
T_p	**s**	14	14	14	14	14	16	16	16	16	16
$H_{mo\ AVG}$	**m**	1.19	1.25	1.29	1.38	1.46	1.20	1.26	1.36	1.49	1.59
H_i	**m**	1.03	1.07	1.02	1.07	1.11	1.03	1.06	1.08	1.15	1.21
$Volume_{measured}$	**l**	0	0	0	110044	1633255	0	0	12000	290800	2499642
Overtopping rate	**l/s**	0.00	0.00	0.00	7.86	116.66	0.00	0.00	0.75	18.18	156.23
Overtopping rate pm	**l/s/m**	0.00	0.00	0.00	0.39	5.83	0.00	0.00	0.04	0.91	7.81

H 1.8 m Model results						
Test		**H-1**	**H-6**	**H-11**	**H-16-2**	**H-21-2**
WL_{paddle}	**m**	0.445	0.465	0.495	0.515	0.535
WL_{toe}	**m**	0.03	0.05	0.08	0.1	0.12
T_p	**s**	1.789	1.789	1.789	1.789	1.789
Test duration	**s**	1789	1789	1789	1789	1789
$H_{mo\ AVG}$	**mm**	54.2	60.4	64.2	70.3	67.8
H_i	**mm**	46.56	51.75	52.98	56.50	53.81
$Volume_{measured}$	**l**	0.00	0.00	0.00	0.00	1.15
WL_{toe}	**m**	0.6	1	1.6	2	2.4
R_c	**m**	3.5	3.1	2.5	2.1	1.7
T_p	**s**	16	16	16	16	16
$H_{mo\ AVG}$	**m**	1.08	1.21	1.28	1.41	1.36
H_i	**m**	0.93	1.04	1.06	1.13	1.08
$Volume_{measured}$	**l**	0	0	0	0	9200
Overtopping rate	**l/s**	0.00	0.00	0.00	0.00	1.15
Overtopping rate pm	**l/s/m**	0.00	0.00	0.00	0.00	0.06

H 1.8 m Model results											
Test		**H-2**	**H-7**	**H-12**	**H-17-2**	**H-22-2**	**H-3**	**H-8**	**H-13**	**H-18-2**	**H-23-2**
WL_{paddle}	**m**	0.445	0.465	0.495	0.515	0.535	0.445	0.465	0.495	0.515	0.535
WL_{toe}	**m**	0.03	0.05	0.08	0.1	0.12	0.03	0.05	0.08	0.1	0.12
T_p	**s**	2.236	2.236	2.236	2.236	2.236	2.638	2.683	2.683	2.683	2.683
Test duration	**s**	2236	2236	2236	2236	2236	2638	2683	2683	2683	2683
$H_{mo\ AVG}$	**mm**	58.3	62.8	69.3	74.8	75.2	53.5	64.9	70.3	73.2	72.3
H_i	**mm**	49.03	52.58	56.22	59.87	59.38	45.02	54.54	56.08	57.38	55.60
$Volume_{measured}$	**l**	0.00	0.00	0.00	0.25	23.43	0.00	0.00	0.50	6.83	101.89
WL_{toe}	**m**	0.6	1	1.6	2	2.4	0.6	1	1.6	2	2.4
R_c	**m**	3.5	3.1	2.5	2.1	1.7	3.5	3.1	2.5	2.1	1.7
T_p	**s**	10	10	10	10	10	12	12	12	12	12
$H_{mo\ AVG}$	**m**	1.17	1.26	1.39	1.50	1.50	1.07	1.30	1.41	1.46	1.45
H_i	**m**	0.98	1.05	1.12	1.20	1.19	0.90	1.09	1.12	1.15	1.11
$Volume_{measured}$	**l**	0	0	0	2000	187429	0	0	4000	54667	815083
Overtopping rate	**l/s**	0.00	0.00	0.00	0.12	18.74	0.00	0.00	0.33	4.56	67.92
Overtopping rate pm	**l/s/m**	0.00	0.00	0.00	0.01	0.94	0.00	0.00	0.02	0.23	3.40
Test		**H-4**	**H-9**	**H-14**	**H-19-2**	**H-24-2**	**H-5**	**H-10**	**H-15**	**H-20-2**	**H-25-2**
WL_{paddle}	**m**	0.445	0.465	0.495	0.515	0.535	0.445	0.465	0.495	0.515	0.535
WL_{toe}	**m**	0.03	0.05	0.08	0.1	0.12	0.03	0.05	0.08	0.1	0.12
T_p	**s**	3.13	3.13	3.13	3.13	3.13	3.578	3.578	3.578	3.578	3.578
Test duration	**s**	3130	3130	3130	3130	3130	3578	3578	3578	3578	3578
$H_{mo\ AVG}$	**mm**	61.0	63.7	68.3	73.6	74.5	62.6	66.7	73.0	79.0	80.4
H_i	**mm**	52.78	54.21	55.71	57.42	57.43	52.79	56.16	57.68	61.24	61.76
$Volume_{measured}$	**l**	0.00	0.00	0.50	14.25	173.76	0.00	0.00	1.75	35.60	268.85
WL_{toe}	**m**	0.6	1	1.6	2	2.4	0.6	1	1.6	2	2.4
R_c	**m**	3.5	3.1	2.5	2.1	1.7	3.5	3.1	2.5	2.1	1.7
T_p	**s**	14	14	14	14	14	16	16	16	16	16
$H_{mo\ AVG}$	**m**	1.22	1.27	1.37	1.47	1.49	1.25	1.33	1.46	1.58	1.61
H_i	**m**	1.06	1.08	1.11	1.15	1.15	1.06	1.12	1.15	1.22	1.24
$Volume_{measured}$	**l**	0	0	4000	114000	1390104	0	0	14000	284800	2150796
Overtopping rate	**l/s**	0.00	0.00	0.29	8.14	99.29	0.00	0.00	0.88	17.80	134.42
Overtopping rate pm	**l/s/m**	0.00	0.00	0.01	0.41	4.96	0.00	0.00	0.04	0.89	6.72

I 2.1 m Model results							
Test		**I-1**	**I-6**	**I-2**	**I-7**	**I-3**	**I-8**
WL_{paddle}	**m**	0.515	0.535	0.515	0.535	0.515	0.535
WL_{toe}	**m**	0.1	0.12	0.1	0.12	0.1	0.12
T_p	**s**	1.789	1.789	2.236	2.236	2.683	2.683
Test duration	**s**	1789	1789	2236	2236	2683	2683
$H_{mo\ AVG}$	**mm**	70.7	71.9	75.8	78.4	74.4	74.7
H_i	**mm**	56.83	57.26	60.84	62.08	58.54	58.14
$Volume_{measured}$	**l**	0.00	1.00	0.33	29.00	6.06	97.31
WL_{toe}	**m**	2	2.4	2	2.4	2	2.4
R_c	**m**	2.1	1.7	2.1	1.7	2.1	1.7
T_p	**s**	8	8	10	10	12	12
$H_{mo\ AVG}$	**m**	1.41	1.44	1.52	1.57	1.49	1.49
H_i	**m**	1.14	1.15	1.22	1.24	1.17	1.16
$Volume_{measured}$	**l**	0	8000	2667	232000	48444	778492
Overtopping rate	**l/s**	0.00	1.00	0.27	23.20	4.04	64.87
Overtopping rate pm	**l/s/m**	0.00	0.05	0.01	1.16	0.20	3.24

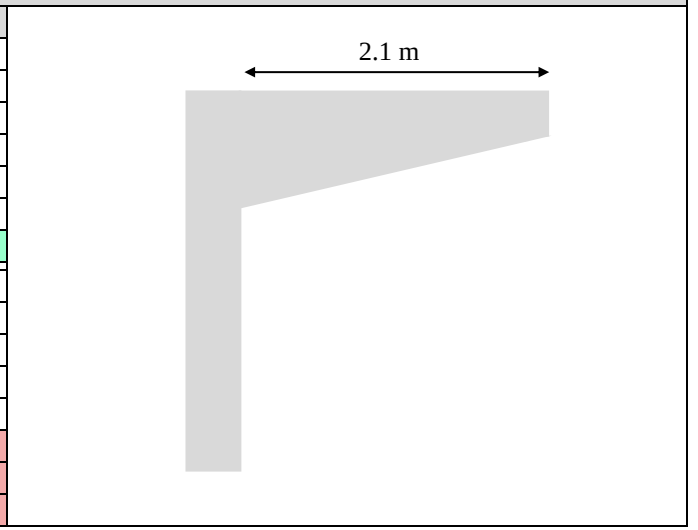

Test		**I-4**	**I-9**	**I-5-1**	**I-5-2**	**I-10**
WL_{paddle}	**m**	0.515	0.535	0.515	0.515	0.535
WL_{toe}	**m**	0.1	0.12	0.1	0.1	0.12
T_p	**s**	3.13	3.13	3.578	3.578	3.578
Test duration	**s**	3130	3130	3578	3578	3578
$H_{mo\ AVG}$	**mm**	72.9	75.9	78.9	78.8	82.7
H_i	**mm**	56.85	58.56	61.09	60.98	63.70
$Volume_{measured}$	**l**	10.78	174.86	55.00	53.75	294.92
WL_{toe}	**m**	2	2.4	2	2	2.4
R_c	**m**	2.1	1.7	2.1	2.1	1.7
T_p	**s**	14	14	16	16	16
$H_{mo\ AVG}$	**m**	1.46	1.52	1.58	1.58	1.65
H_i	**m**	1.14	1.17	1.22	1.22	1.27
$Volume_{measured}$	**l**	86222	1398871	440000	430000	2359327
Overtopping rate	**l/s**	6.16	99.92	27.50	26.88	147.46
Overtopping rate pm	**l/s/m**	0.31	5.00	1.38	1.34	7.37

G: Schoonees(2014) recurve results

		B Recurve with 30 mm overhang													
		Test number		B-4	B-3	B-2	B-6	B-7	B-1	B-5	B-5_2	B-5_3	B-5_4	B-8	B-9	B-10
PROTOTYPE	MEASURED	Water level	m	9	9.4	10	10	10	10.4	10.4	10.4	10.4	10.4	10.8	10.8	10.8
		Water depth at toe	m	0.6	1	1.6	1.6	1.6	2	2	2	2	2	2.4	2.4	2.4
		Freeboard R_c	m	3.4	3	2.4	2.4	2.4	2	2	2	2	2	1.6	1.6	1.6
		Wave period	s	10	10	10	10	10	10	10	10	10	10	10	10	10
		Duration of wave attack	s	10000	10000	10000	10000	10000	10000	10000	10000	10000	10000	10000	10000	10000
		$H_{s\ probes}$	m	1.195	1.288	1.273	1.242	1.223	1.268	1.223	1.213	1.227	1.210	1.165	1.162	1.145
		Overtopping	l/s per m	0.00004	0.02	0.4136	0.4224	0.312	4.4632	3.763	3.650	3.178	4.059	10.769	12.12	11.526
	CLASH	Probabilistic	l/s per m	0.065	0.126	0.461	0.417	0.389	0.694	0.586	0.566	0.607	0.566	11.697	11.42	10.877
		Deterministic	l/s per m	0.091	0.177	0.861	0.778	0.727	1.295	1.094	1.057	1.133	1.057	21.835	21.318	20.304
MODEL	MEASURED	Water level	m	0.45	0.47	0.5	0.5	0.5	0.52	0.52	0.52	0.52	0.52	0.54	0.54	0.54
		Water depth at toe	m	0.03	0.05	0.08	0.08	0.08	0.1	0.1	0.1	0.1	0.1	0.12	0.12	0.12
		Freeboard R_c	m	0.17	0.15	0.12	0.12	0.12	0.1	0.1	0.1	0.1	0.1	0.08	0.08	0.08
		Wave period	s	2.236	2.236	2.236	2.236	2.236	2.236	2.236	2.236	2.236	2.236	2.236	2.236	2.236
		Duration of wave attack	s	2236	2236	2236	2236	2236	2236	2236	2236	2236	2236	2236	2236	2236
		H_s (generator)	m	0.05	0.05	0.05	0.05	0.05	0.05	0.05	0.05	0.05	0.05	0.05	0.05	0.05
		H_s (probes)	m	0.060	0.064	0.064	0.062	0.061	0.063	0.061	0.061	0.061	0.061	0.058	0.058	0.057
		Overtopping	l	0.001	0.5	10.34	10.56	7.8	111.58	94.08	91.26	79.44	101.48	269.22	303	288.14

		C Recurve with 60 mm overhang												
		Test number		C-5	C-4	C-1	C-2	C-3	C-6	C-7	C-8	C-9	C-10	C-11	C-12
PROTOTYPE	MEASURED	Water level	m	9	9.4	10	10	10	10.4	10.4	10.4	10.4	10.8	10.8	10.8
		Water depth at toe	m	0.6	1	1.6	1.6	1.6	2	2	2	2	2.4	2.4	2.4
		Freeboard R_c	m	3.4	3	2.4	2.4	2.4	2	2	2	2	1.6	1.6	1.6
		Wave period	s	10	10	10	10	10	10	10	10	10	10	10	10
		Duration of wave attack	s	10000	10000	10000	10000	10000	10000	10000	10000	10000	10000	10000	10000
		$H_{s\ probes}$	m	1.20024	1.3236	1.21615	1.20741	1.29462	1.254	1.25827	1.27242	1.28059	1.1846	1.17751	1.19335
		Overtopping	l/s per m	1.148	0.0488	0.0632	0.0952	0.1096	1.1992	0.8264	1.3752	0.784	6.1744	5.64	6.5816
	CLASH	Probabilistic	l/s per m	1.335	0.126	0.389	0.376	0.492	0.649	0.671	0.694	0.717	2.197	2.197	2.277
		Deterministic	l/s per m	1.879	0.177	0.727	0.702	0.919	1.212	1.253	1.295	1.339	4.1	4.1	4.251
MODEL	MEASURED	Water level	m	0.45	0.47	0.5	0.5	0.5	0.52	0.52	0.52	0.52	0.54	0.54	0.54
		Water depth at toe	m	0.03	0.05	0.08	0.08	0.08	0.1	0.1	0.1	0.1	0.12	0.12	0.12
		Freeboard R_c	m	0.17	0.15	0.12	0.12	0.12	0.1	0.1	0.1	0.1	0.08	0.08	0.08
		Wave period	s	2.236	2.236	2.236	2.236	2.236	2.236	2.236	2.236	2.236	2.236	2.236	2.236
		Duration of wave attack	s	2236	2236	2236	2236	2236	2236	2236	2236	2236	2236	2236	2236
		H_s (generator)	m	0.05	0.05	0.05	0.05	0.05	0.05	0.05	0.05	0.05	0.05	0.05	0.05
		H_s (probes)	m	0.060	0.066	0.061	0.060	0.065	0.063	0.063	0.064	0.064	0.059	0.059	0.060
		Overtopping	l	28.7	1.22	1.58	2.38	2.74	29.98	20.66	34.38	19.6	154.36	141	164.54

H: Overtopping reduction

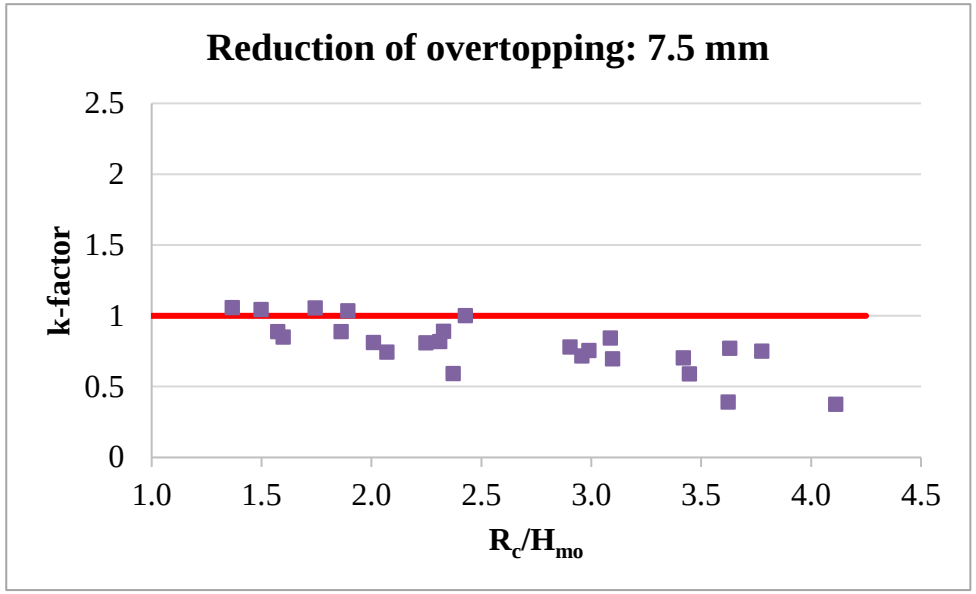

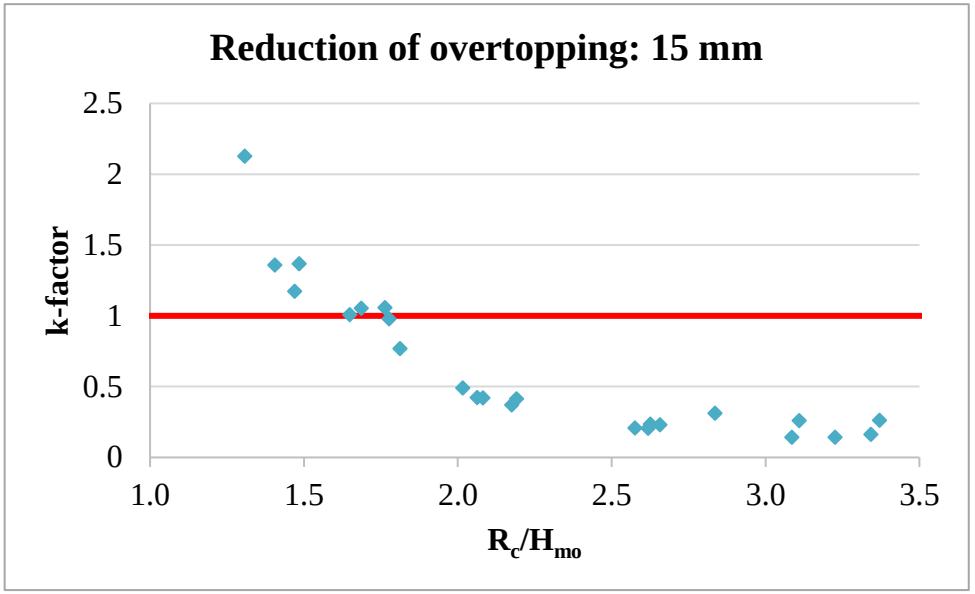

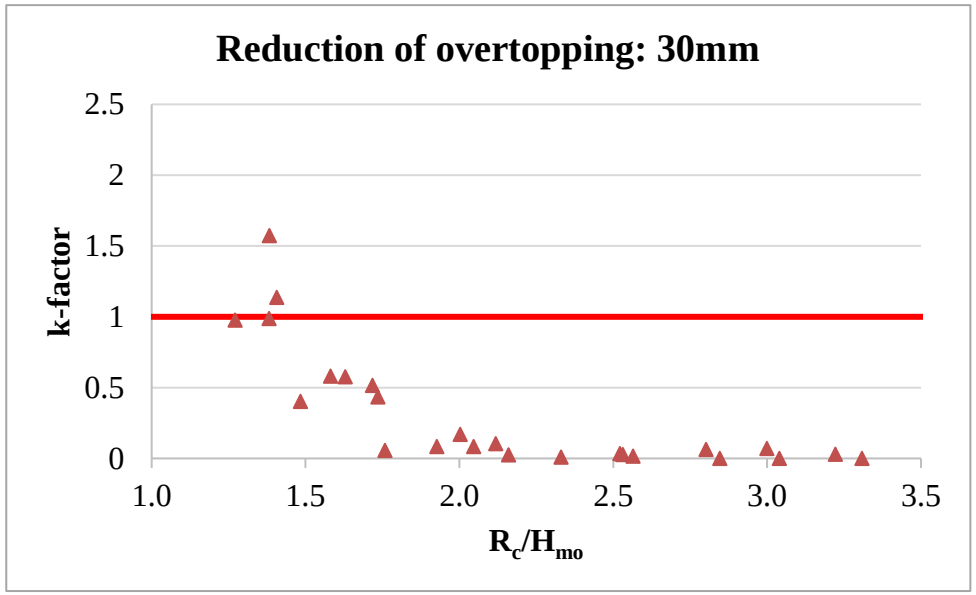

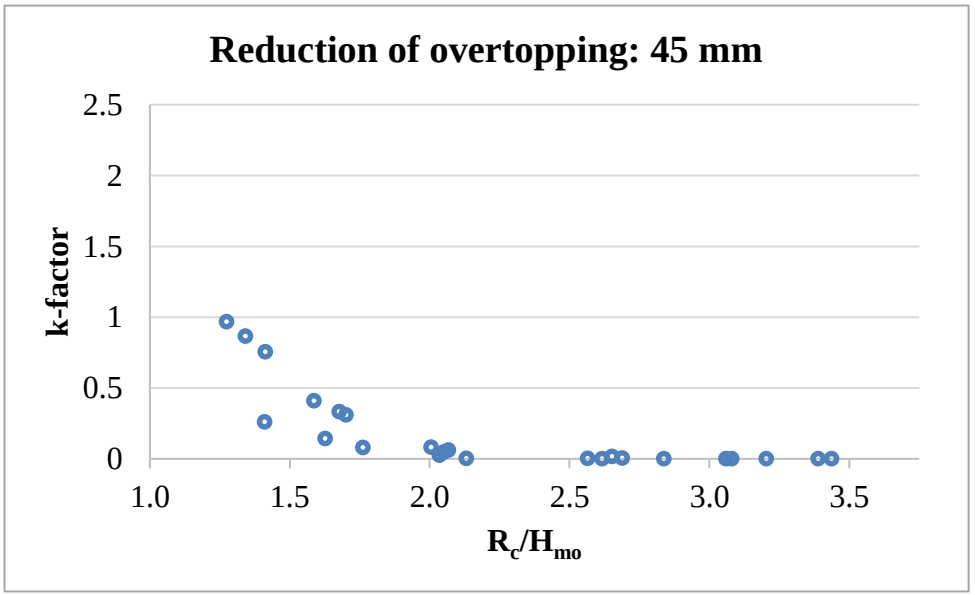

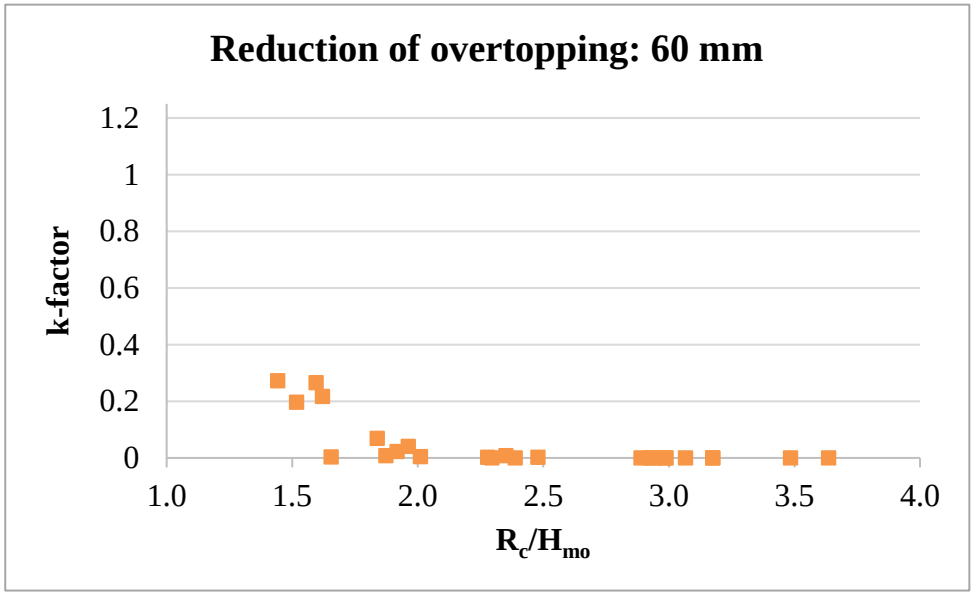

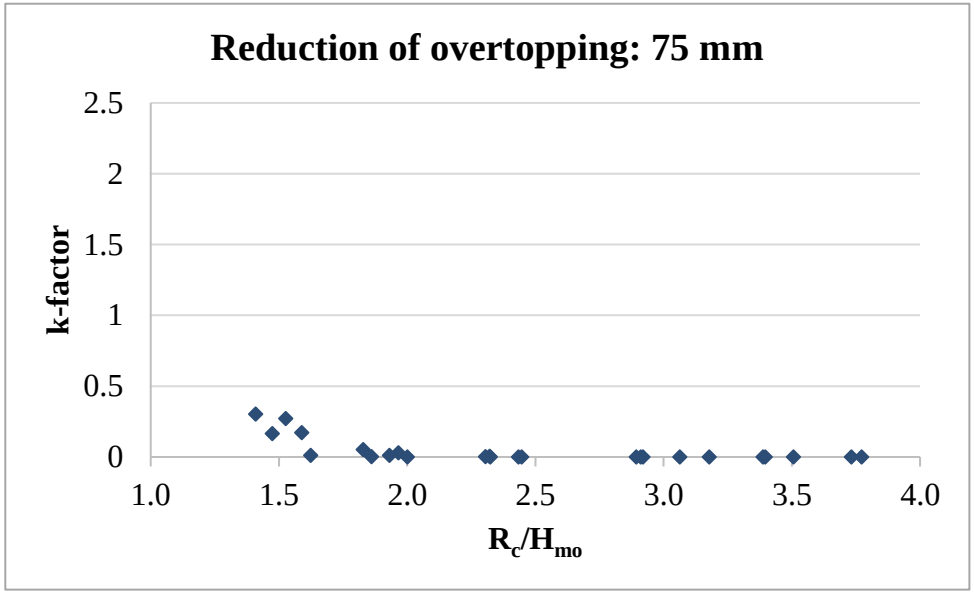

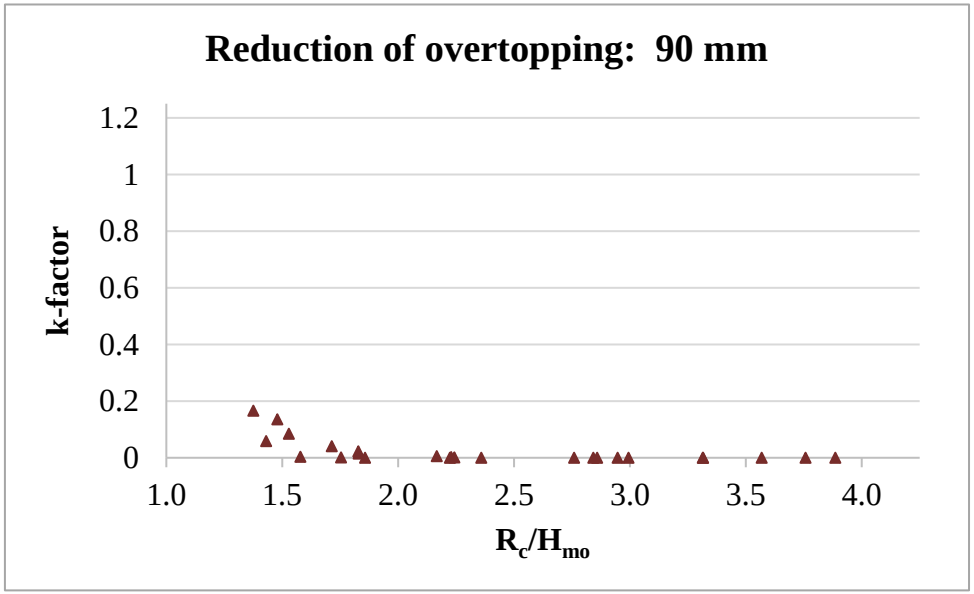

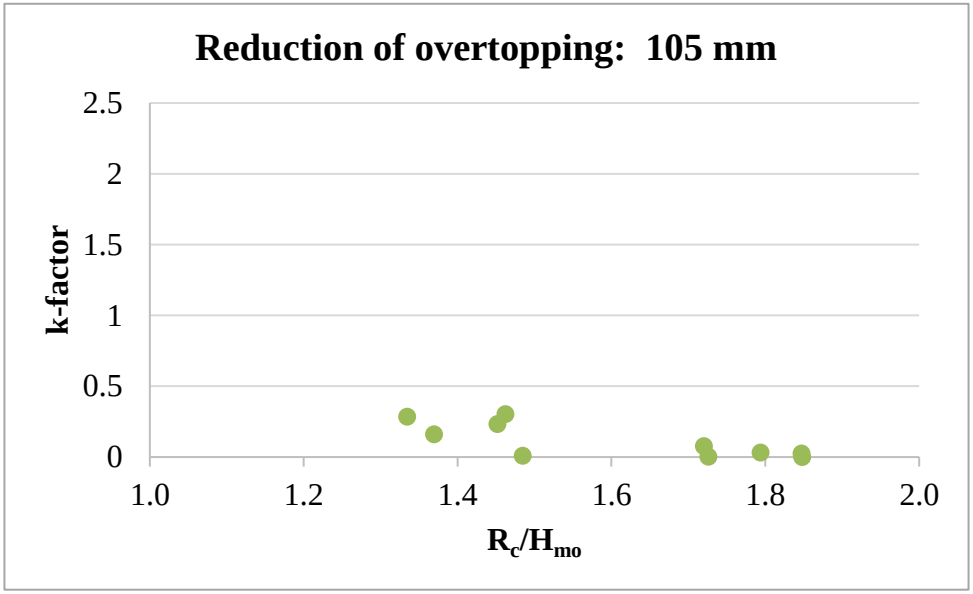

I: K-factor per wave period

		Wave period (s)									
		8					10				
		Freeboard water level (m)					Freeboard water level (m)				
Overhang length (m)		1.7	2.1	2.5	3.1	3.5	1.7	2.1	2.5	3.1	3.5
	0.15	0.375	0.770	0.842	1.000	0.744	0	0	0.75	0.695	0.891
	0.3	0.263	0.311	0.414	0.768	1.367	0.163	0.229	0.420	1.053	2.126
	0.6	0	0.062	0.025	0.056	0.401	0.0001	0.009	0.084	0.577	1.572
	0.9	0	0	0.002	0.078	0.258	0	0.004	0.024	0.143	0.966
	12	0	0	0	0.004	0.003	0	0	0	0.008	0.196
	1.5	0	0	0	0	0.011	0	0	0	0.001	0.166
	1.8	0	0	0	0	0.003	0	0	0	0.002	0.128
	2.1	0	0	0	0	0.007	0	0	0	0.002	0.159

		12					14				
		Freeboard water level (m)					Freeboard water level (m)				
Overhang length (m)		1.7	2.1	2.5	3.1	3.5	1.7	2.1	2.5	3.1	3.5
	0.15	0.886	1.044	0.39	0.755	0.818	0.810	0.850	0.589	0.716	0.591
	0.3	0.143	0.233	0.422	1.057	1.173	0.259	0.206	0.370	0.977	1.358
	0.6	0.03	0.035	0.083	0.435	1.136	0	0.027	0.103	0.515	0.988
	0.9	0	0.015	0.046	0.309	0.754	0	0	0.059	0.331	0.866
	12	0	0	0.002	0.023	0.216	0	0	0.002	0.041	0.266
	1.5	0	0	0.001	0.011	0.172	0	0	0	0.030	0.272
	1.8	0	0	0.003	0.021	0.163	0	0	0.002	0.031	0.232
	2.1	0	0	0	0.032	0.302	0	0	0	0.023	0.233

		16				
		Freeboard water level (m)				
Overhang length (m)		1.7	2.1	2.5	3.1	3.5
	0.15	0	0	1.034	0.888	0.703
	0.3	0.141	0.208	0.490	1.007	1.323
	0.6	0.070	0.017	0.170	0.580	0.977
	0.9	0	0.002	0.081	0.408	0.885
	12	0	0	0.008	0.069	0.273
	1.5	0	0	0.005	0.051	0.302
	1.8	0	0	0.005	0.050	0.259
	2.1	0	0	0	0.077	0.285

J: Influence of overhang length

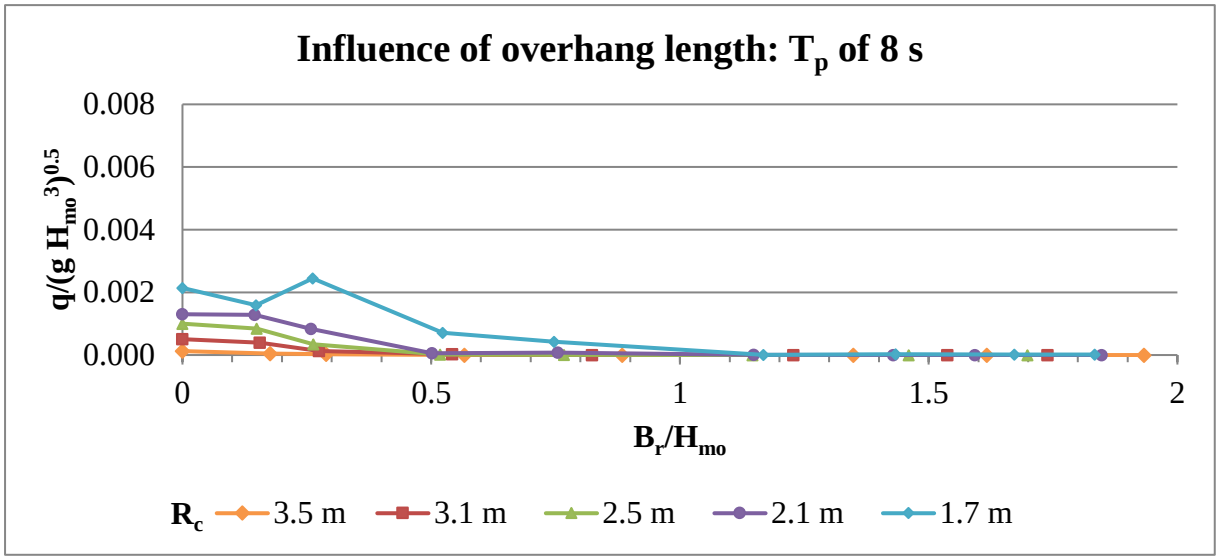

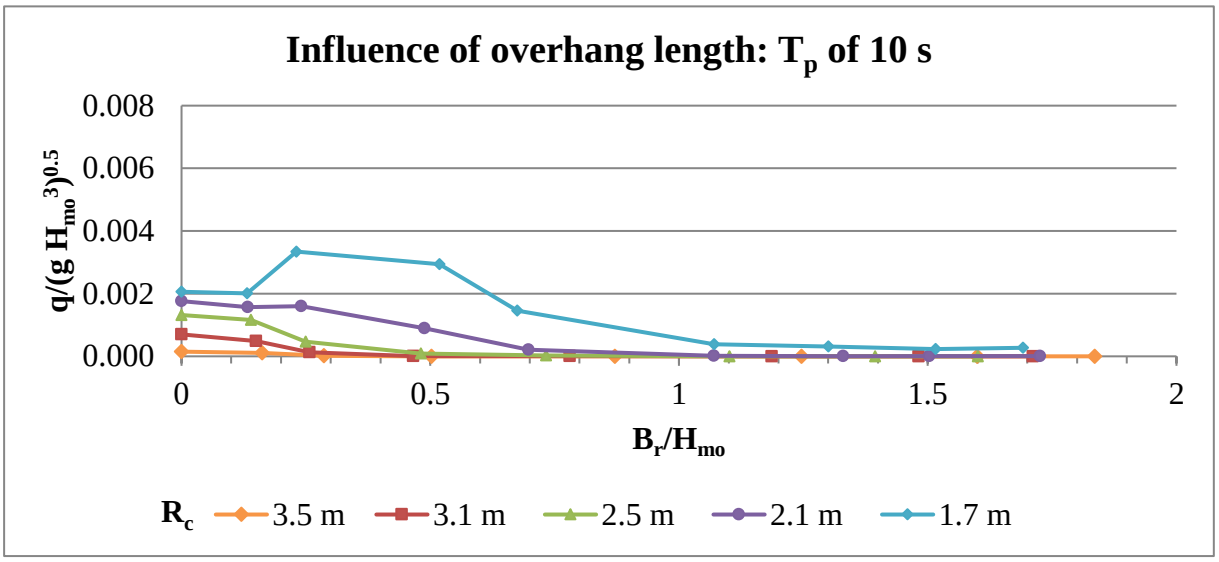

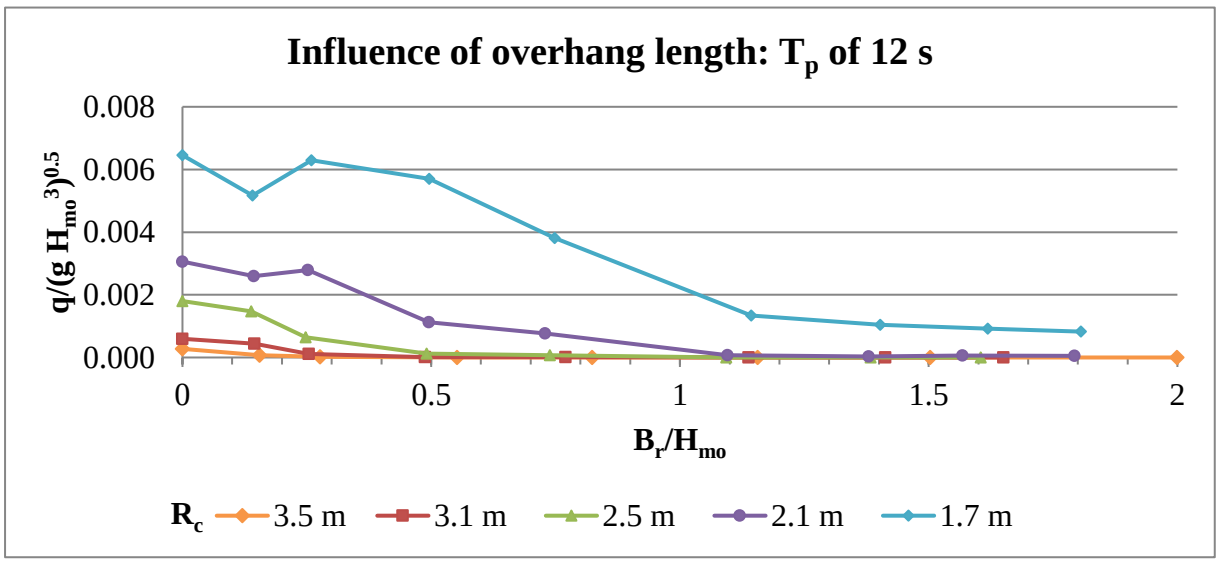

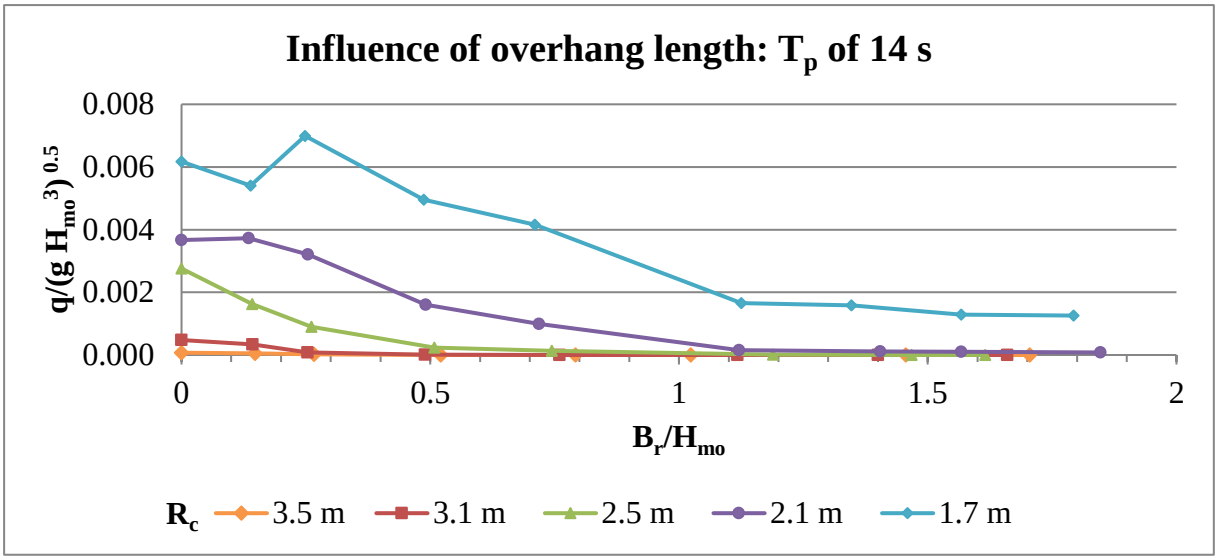

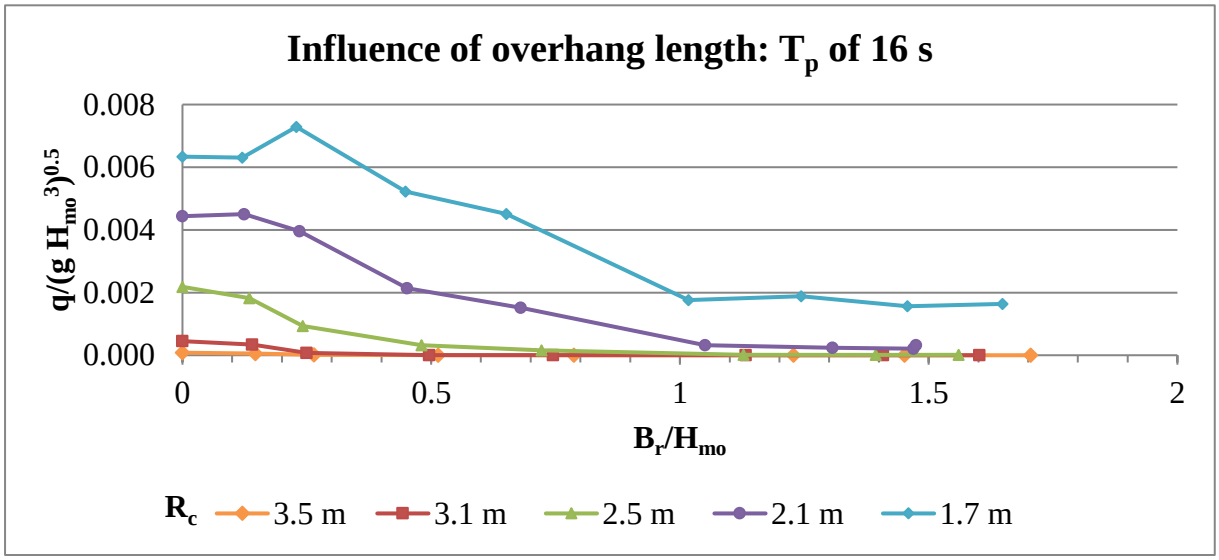

K: Influence of overhang length per R_c

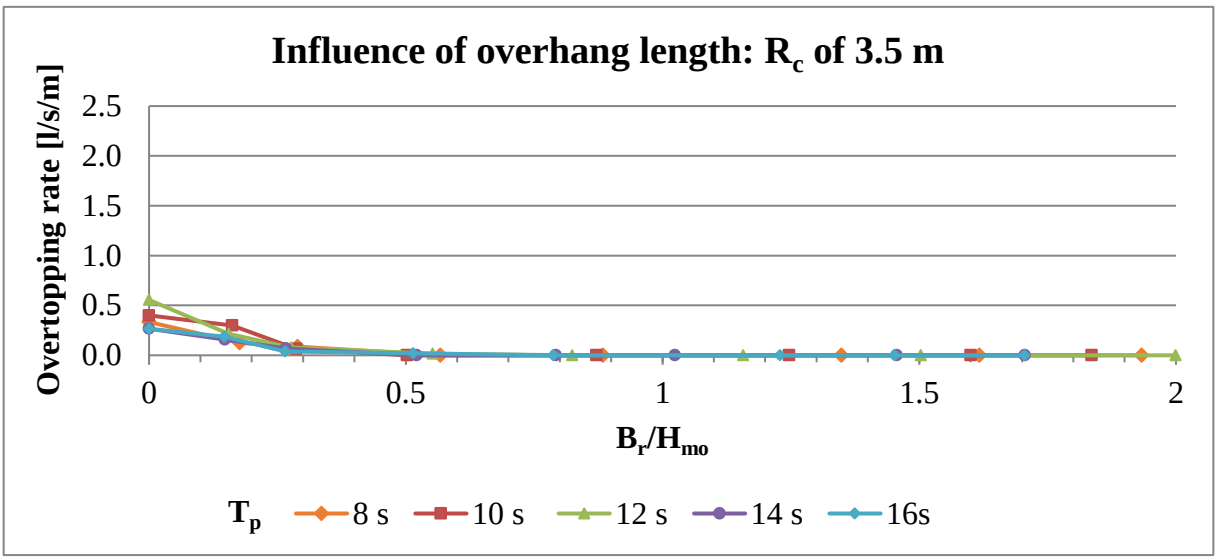

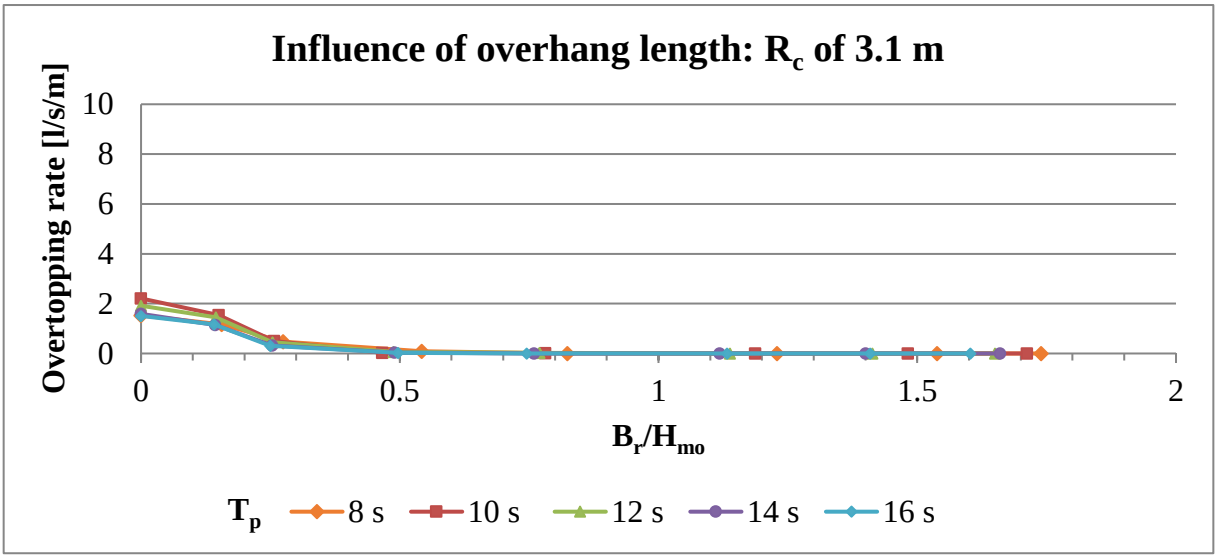

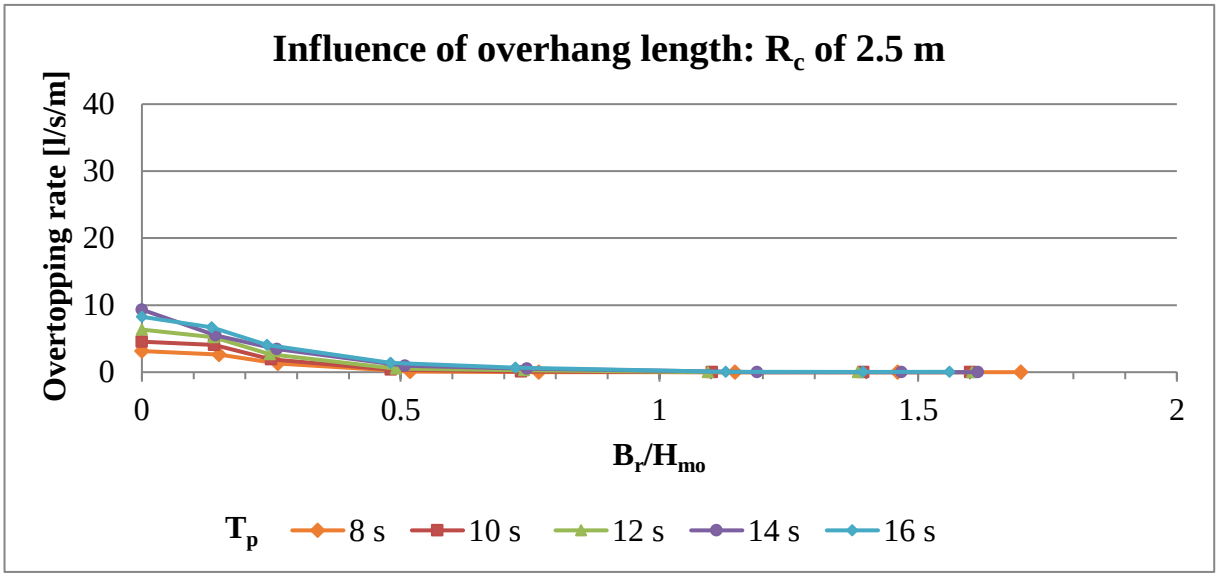

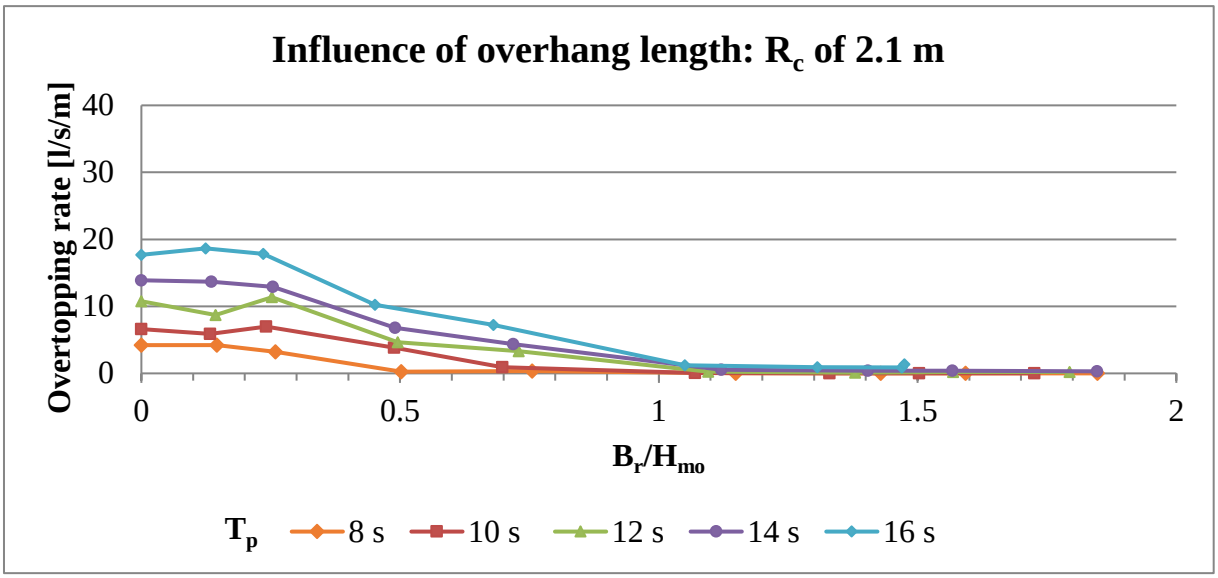

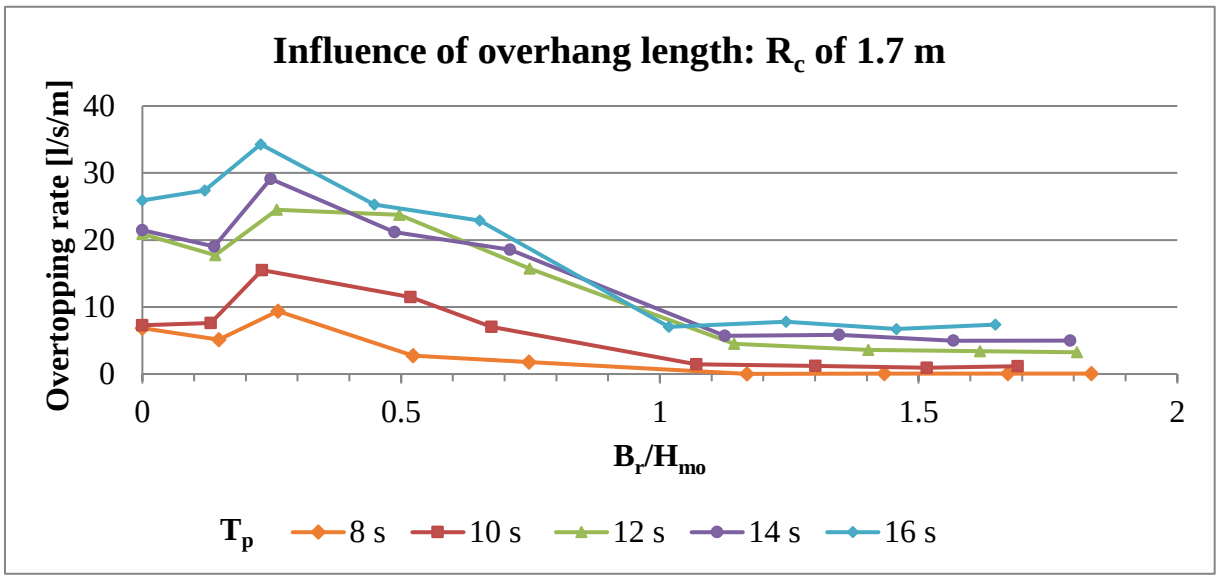

L: Wave period sensitivity per overhang length

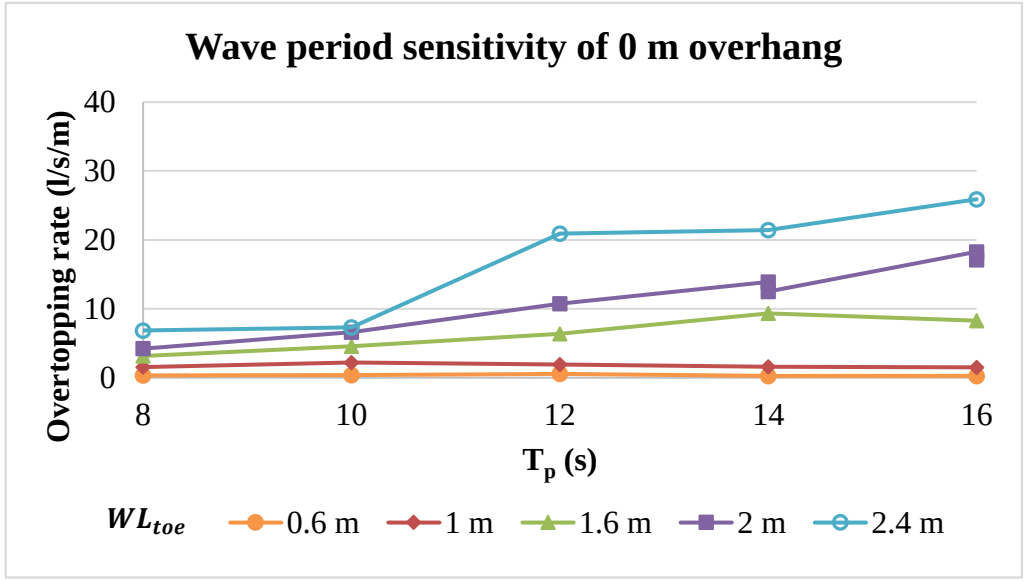

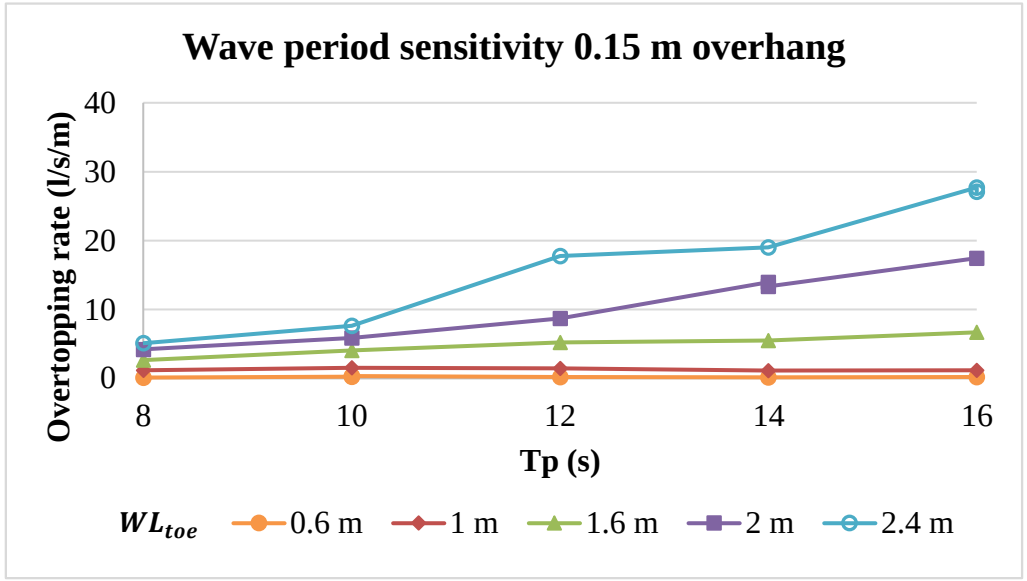

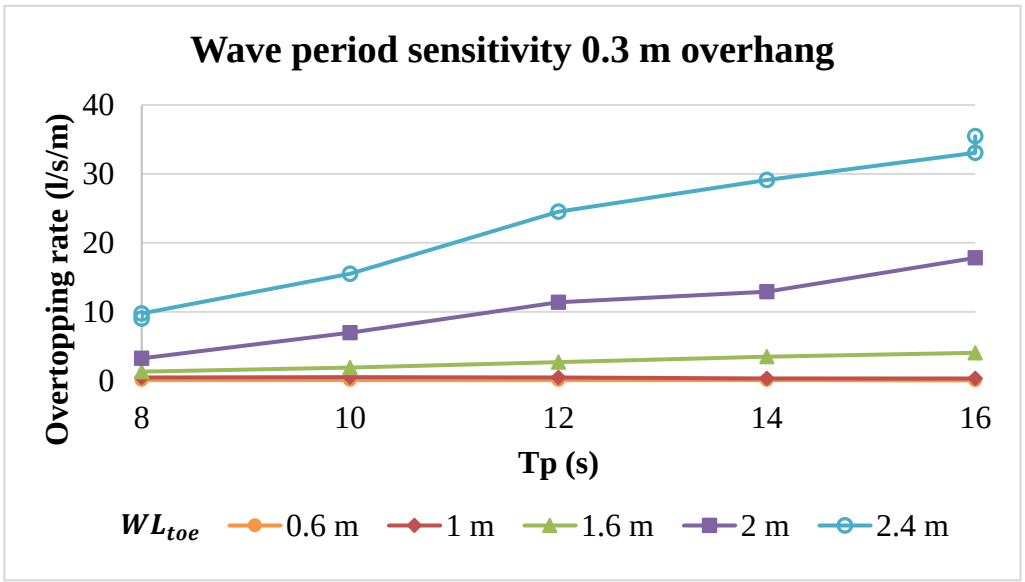

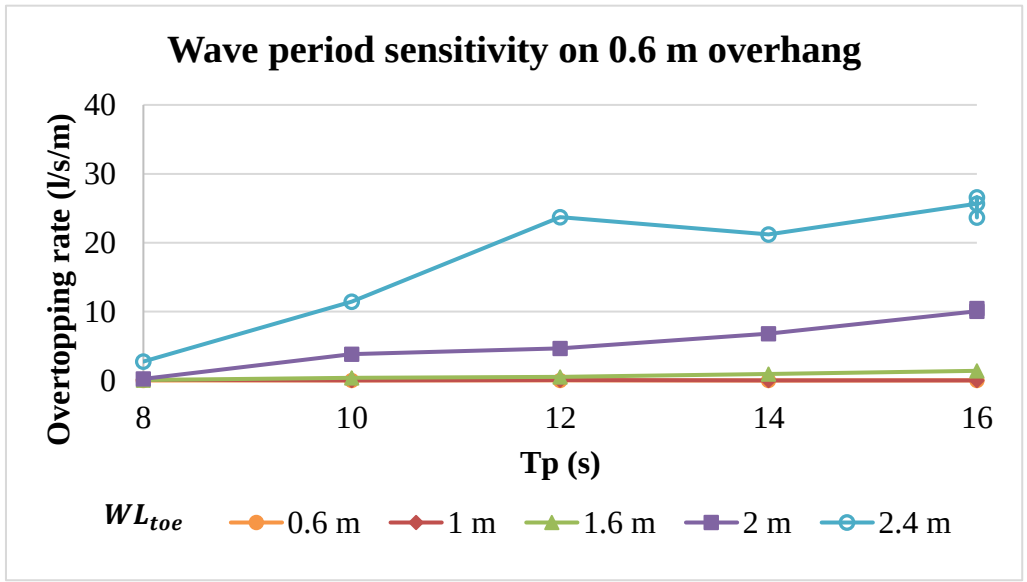

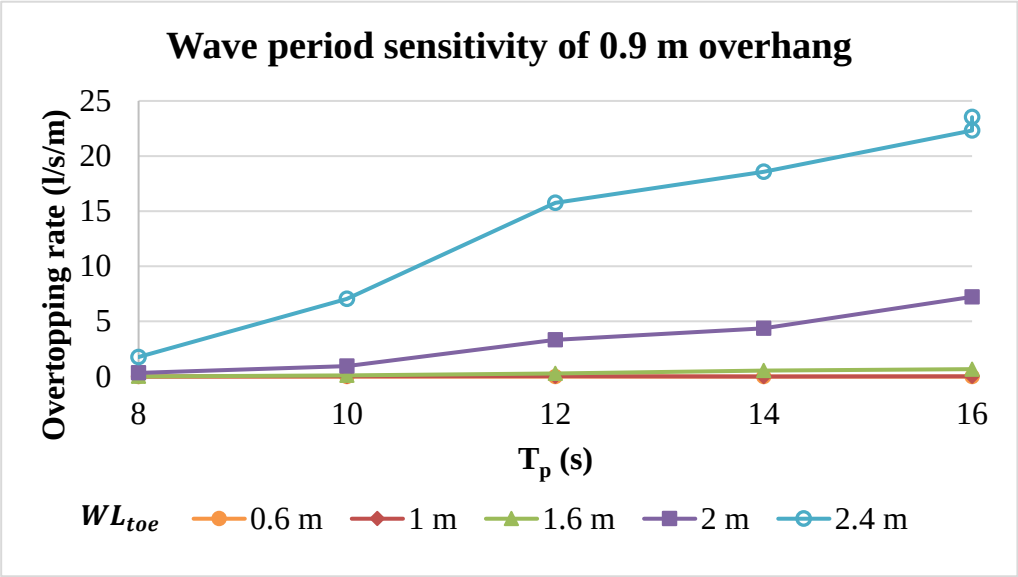

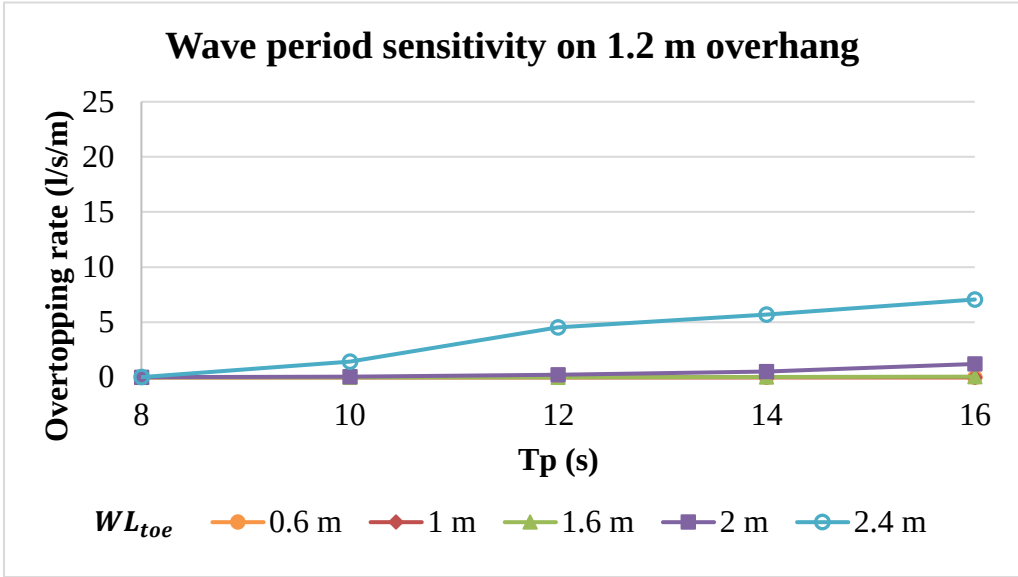

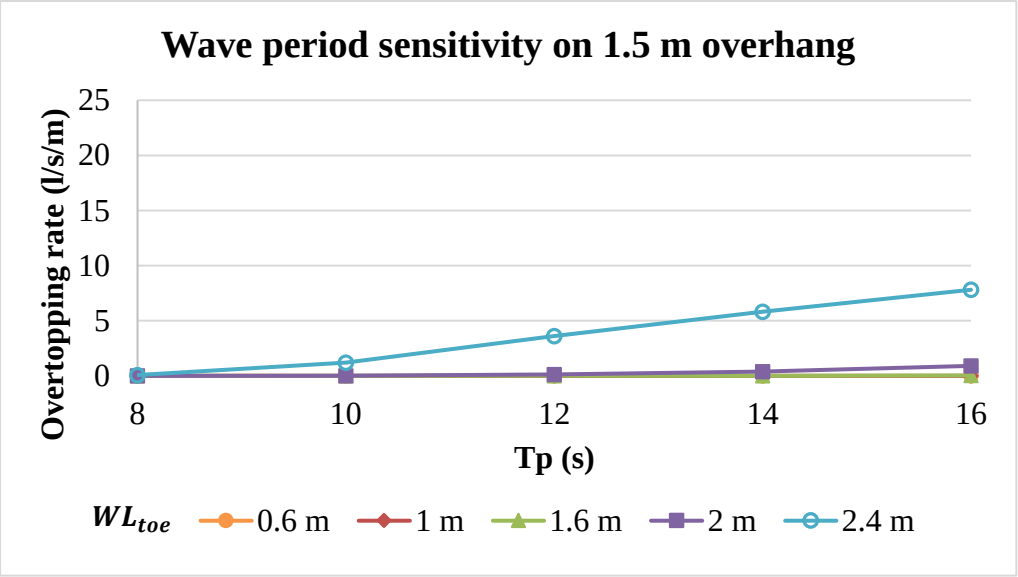

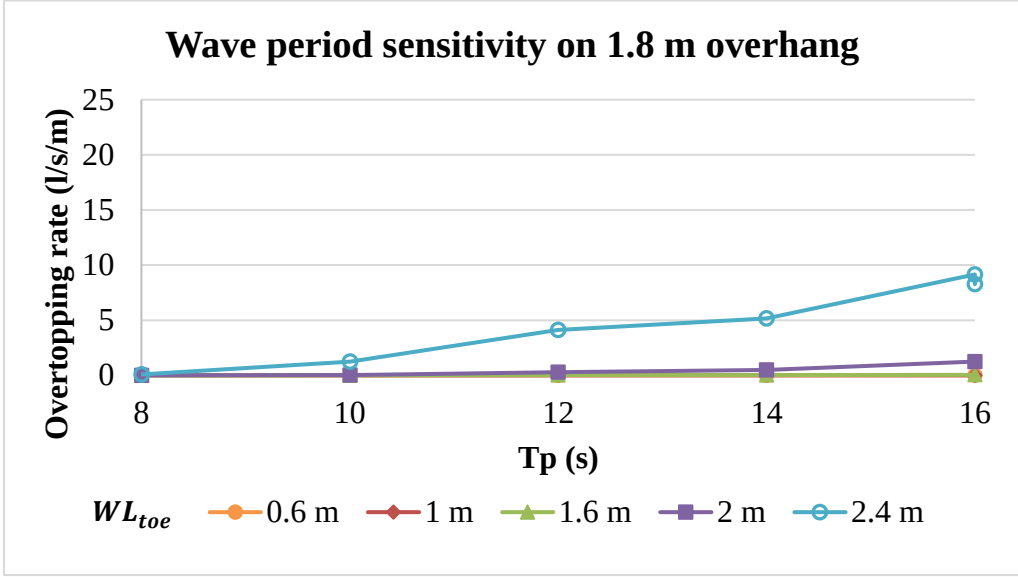

M: Analysing the accuracy of results using the Root Mean Squared Method

To further investigate the variability between the physical model tests and the EurOtop dataset the Root Mean Squared (RMS) method is used.

The physic model results are compared to the corresponding probabilistic EurOtop data overtopping rate as shown below.

Extract Series F: 1.2 m overhang length							
Test number		**F-2**	**F-7**	**F-12**	**F-17**	**F-22**	
Water depth at toe	**m**	0.6	1	1.6	2	2.4	
Freeboard	**m**	3.5	3.1	2.5	2.1	1.7	
Wave period	**s**	10	10	10	10	10	
H_s (probes)	**m**	0.96	1.01	1.09	1.12	1.12	
Overtopping rate	**l/s/m**	0.00	0.00	0.00	0.05	1.43	
Probabilistic	**l/s/m**	0.044	0.08	0.214	0.352	1.02	
Deterministic	**l/s/m**	0.082	0.149	0.399	0.657	1.905	
Root Mean Square		0.002	0.006	0.046	0.090	0.170	**0.25**

The delivers a Root Square Error (RME) of 0.25. Similarly, Schoonees (2014) dataset is compared with the same method. These test were conducted under similar conditions, as discussed in Section 2.5.7.

Schoonees (2014) 1.2 m overhang length							
Test number		**C-5**	**C-4**	**AVG_{C1-3}**	**AVG_{C6-9}**	**AVG_{C10-12}**	
Water depth at toe	**m**	0.6	1	1.6	2	2.4	
Freeboard	**m**	3.4	3	2.4	2	1.6	
Wave period	**s**	10	10	10	10	10	
H_s (probes)	**m**	1.200	1.324	1.239	1.266	1.185	
Overtopping rate	**l/s/m**	0	0.049	0.0893	1.046	6.132	
Probabilistic	**l/s/m**	0.08	0.126	0.419	0.688	2.224	
Deterministic	**l/s/m**	0.11	0.177	0.783	1.275	4.150	
Root Mean Square		0.006	0.006	0.109	0.132	15.28	**1.76**

A higher RME is achieved by Schoonees (2014), however the RME is still low indicating a small error. The same process is followed for the vertical wall (0 m overhang).

Extract Series A: vertical wall (0 m overhang length)							
Test number		**A-2**	**A-7**	**A-12**	**A-17**	**A-22**	
Water depth at toe	**m**	0.6	1	1.6	2	2.4	
Freeboard	**m**	3.5	3.1	2.5	2.1	1.7	
Wave period	**s**	10	10	10	10	10	
H_s (probes)	**m**	0.903	1.006	1.067	1.130	1.085	
Overtopping rate	**l/s/m**	0.40	2.21	4.55	6.63	7.30	
Probabilistic	**l/s/m**	0.47	2.18	3.91	7.31	10.44	
Deterministic	**l/s/m**	0.661	4.065	7.298	13.637	19.483	
Root Mean Square		0.00476	0.00102	0.4104	0.45854	9.87373	**1.47**

Schoonees (2014) vertical wall (0 m overhang)							
Test number		**AVG $_{A6-7}$**	**AVG$_{A4-5}$**	**AVG$_{A2-3}$**	**A-1**	**AVG$_{A8-10}$**	
Water depth at toe	**m**	0.6	1	1.6	2.0	2.4	
Freeboard	**m**	3.4	3	2.4	2.0	1.6	
Wave period	**s**	10	10	10	10.0	10	
H_s (probes)	**m**	1.203	1.254	1.261	1.191	1.174	
Overtopping rate	**l/s/m**	1.2	5.1	12.5	18.2	18.2	
Probabilistic	**l/s/m**	1.354	4.164	8.899	10.56	17.721	
Deterministic	**l/s/m**	1.906	7.238	16.946	19.71	33.079	
Root Mean Square		0.04	0.901	13.008	58.22	0.224	**3.80**

The vertical wall for the physical model tests as well as for Schoonees (2014) provides a larger RME, however still indicates a small error between the two datasets. As the EurOtop is based on results conducted in a large variety of conditions.

N: Measured versus calculated k-factor per overhang length

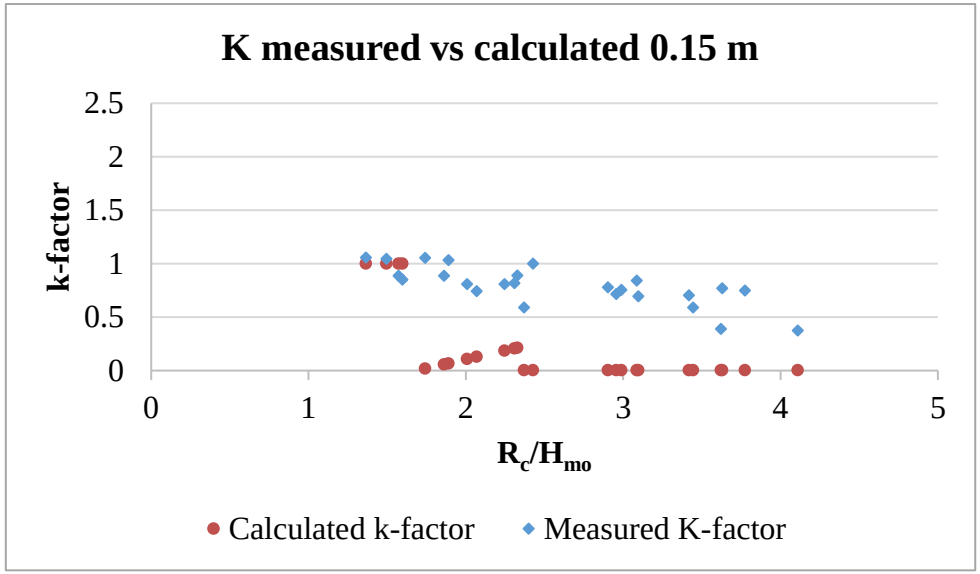

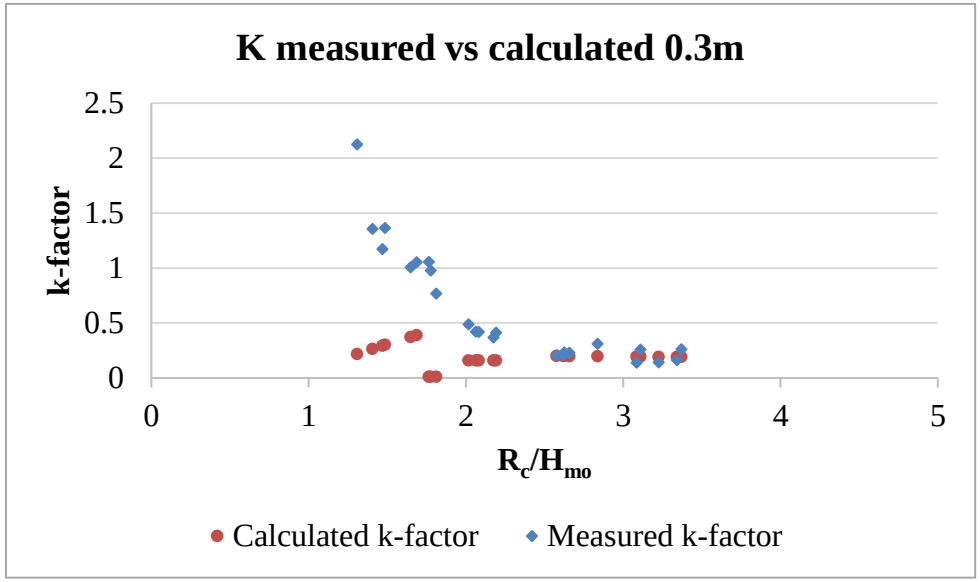

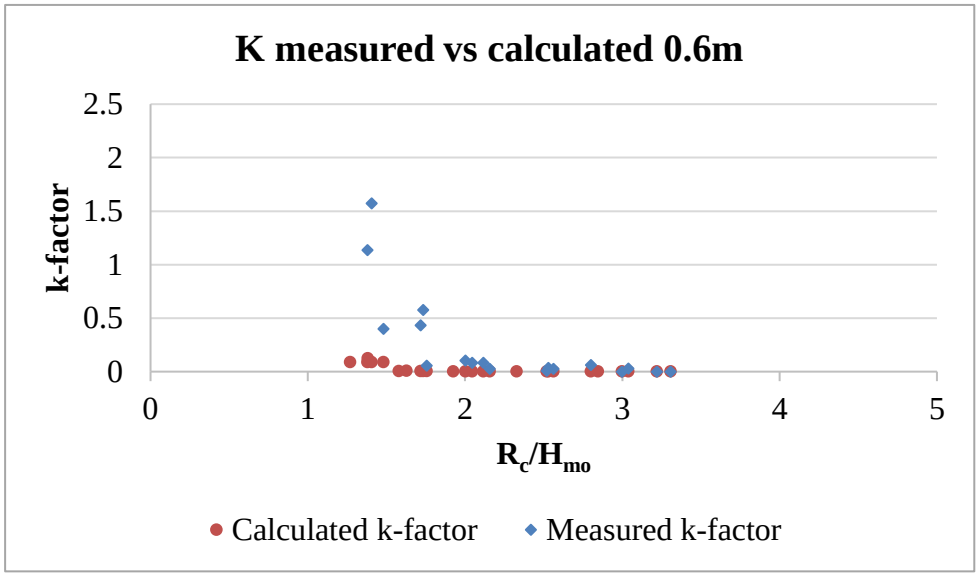

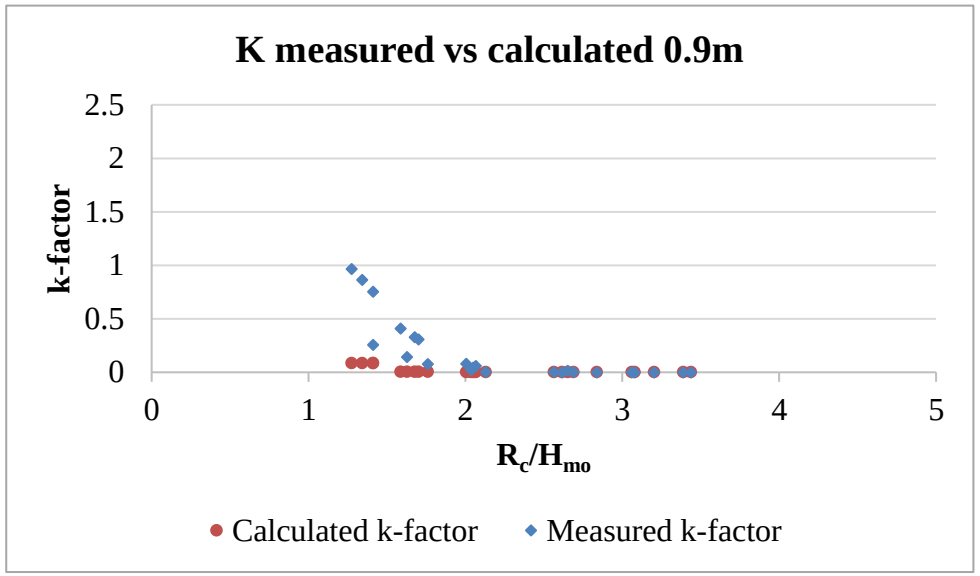

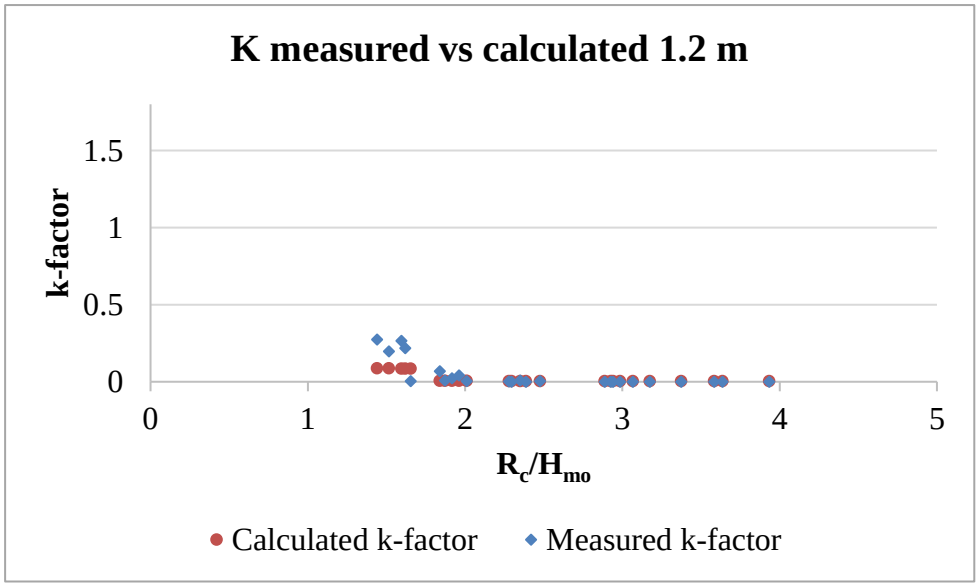

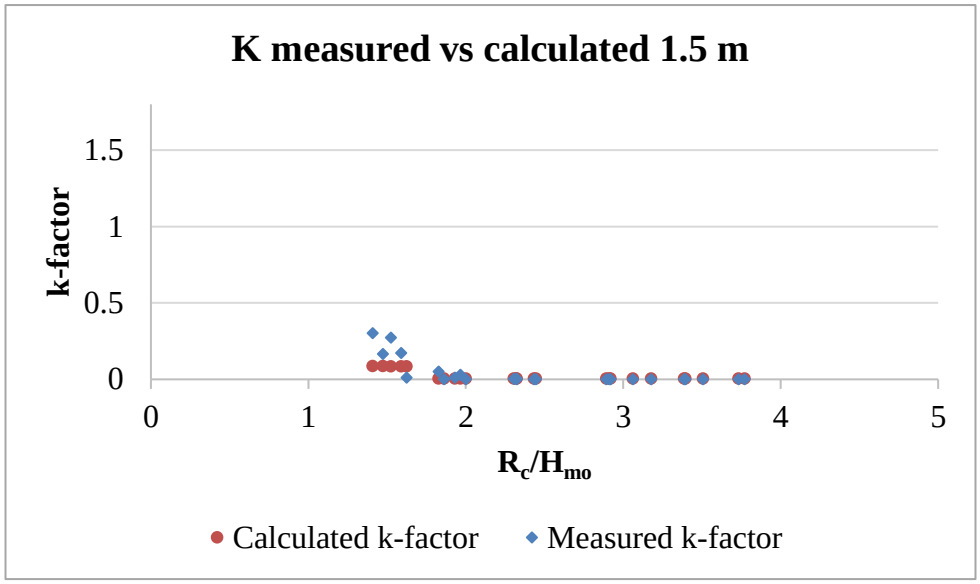

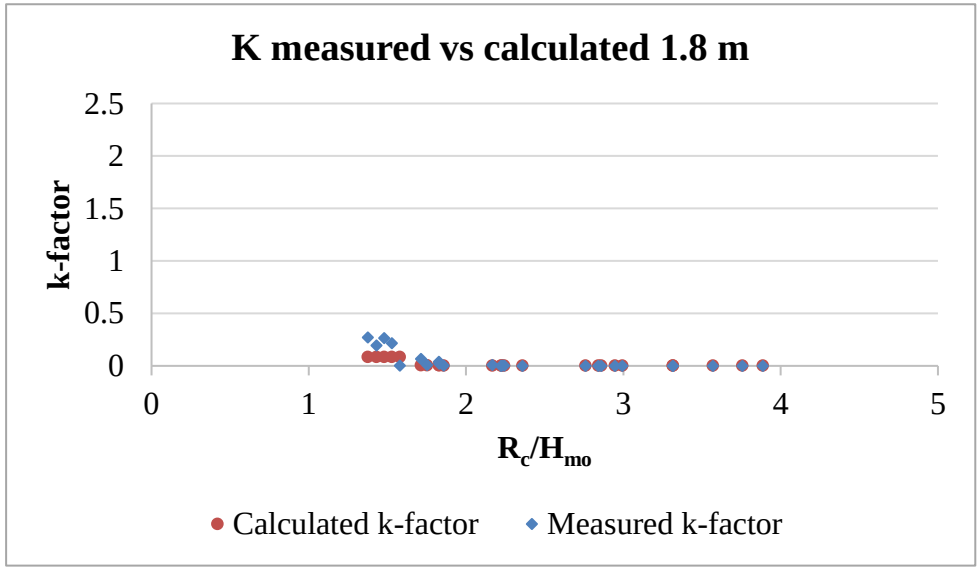

O: EurOtop comparison per overhang length

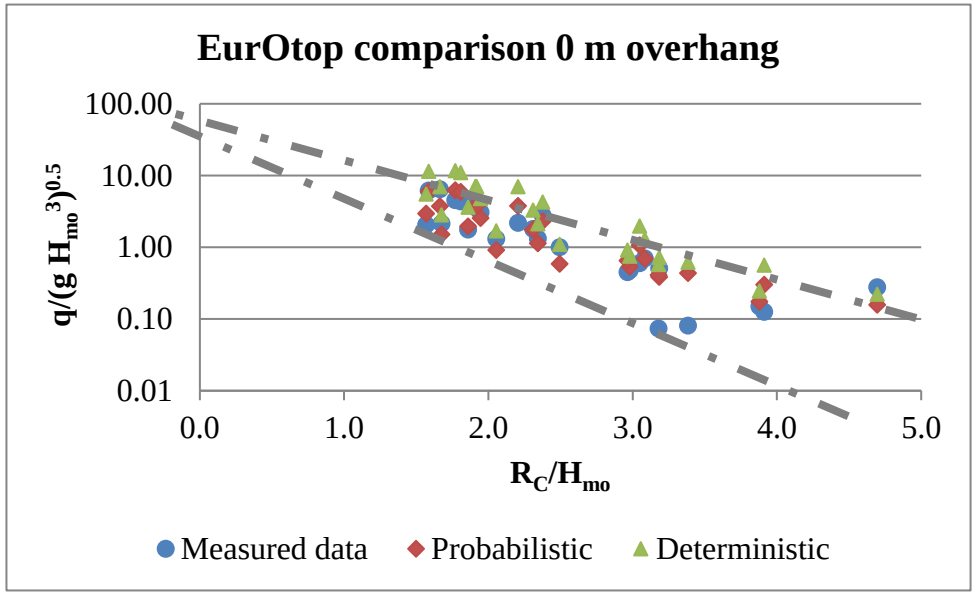

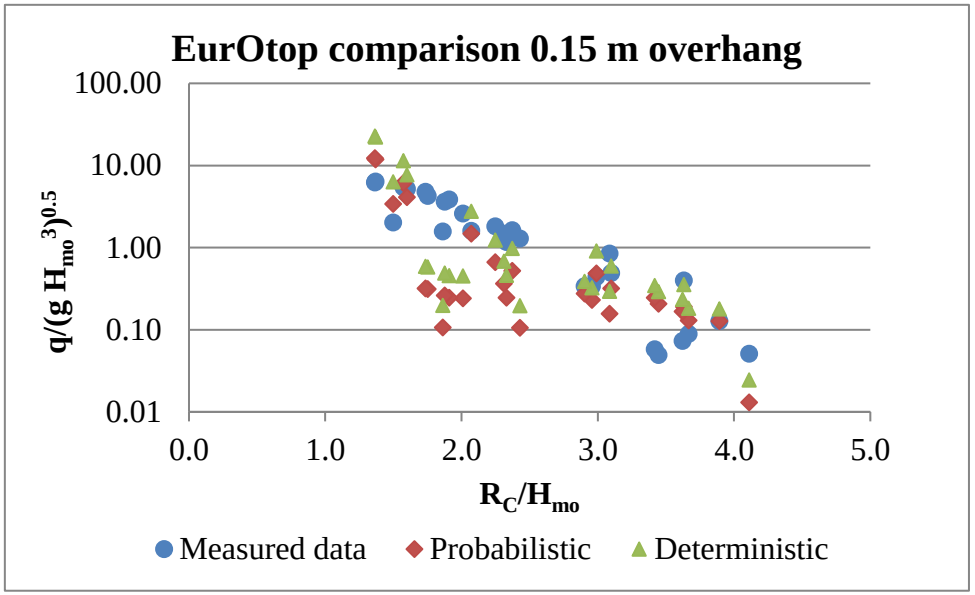

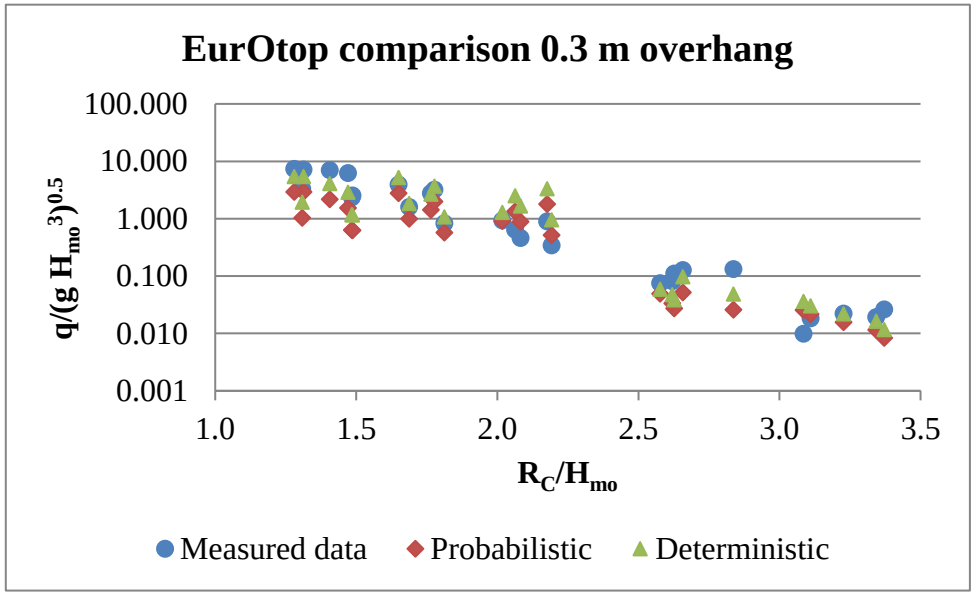

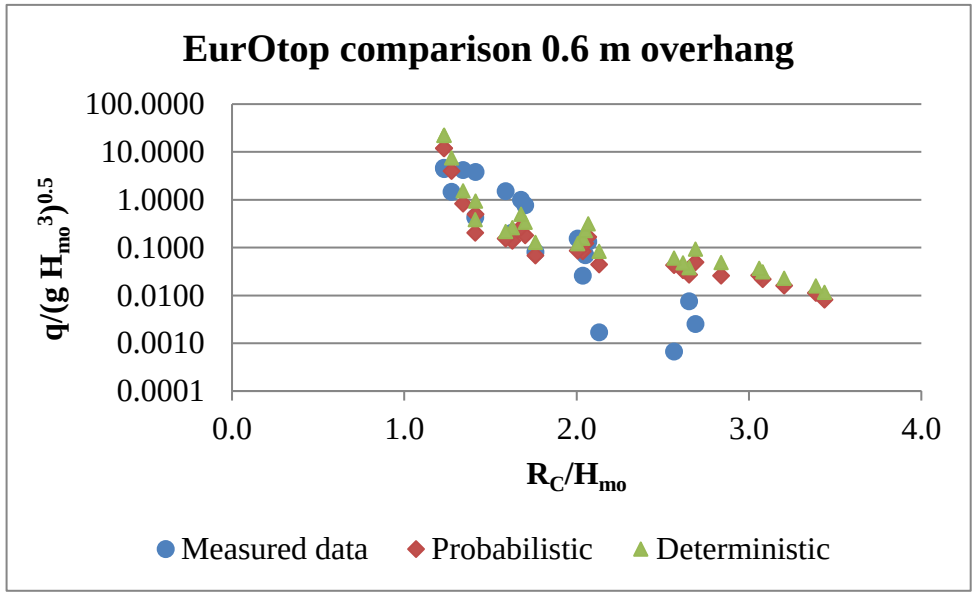

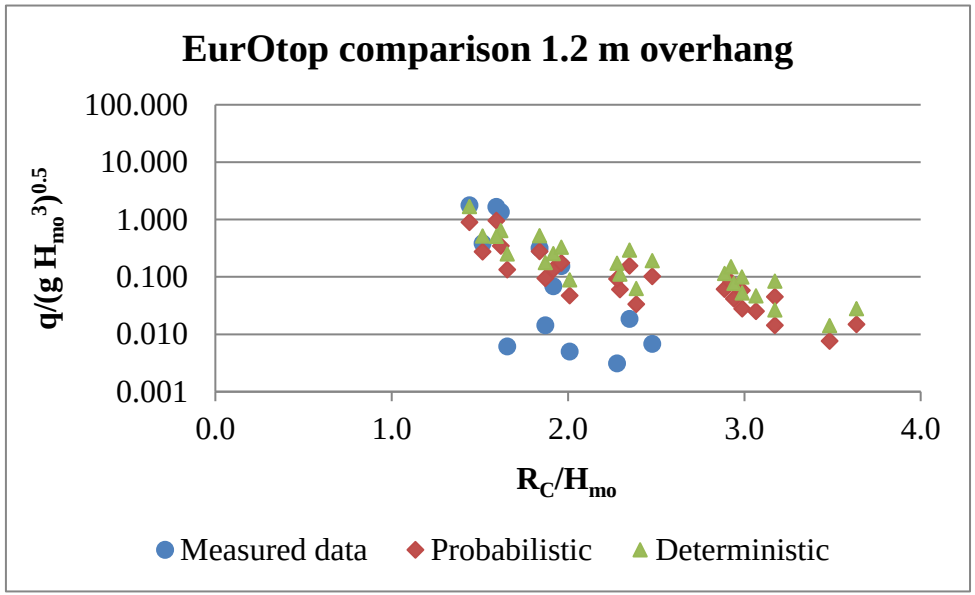

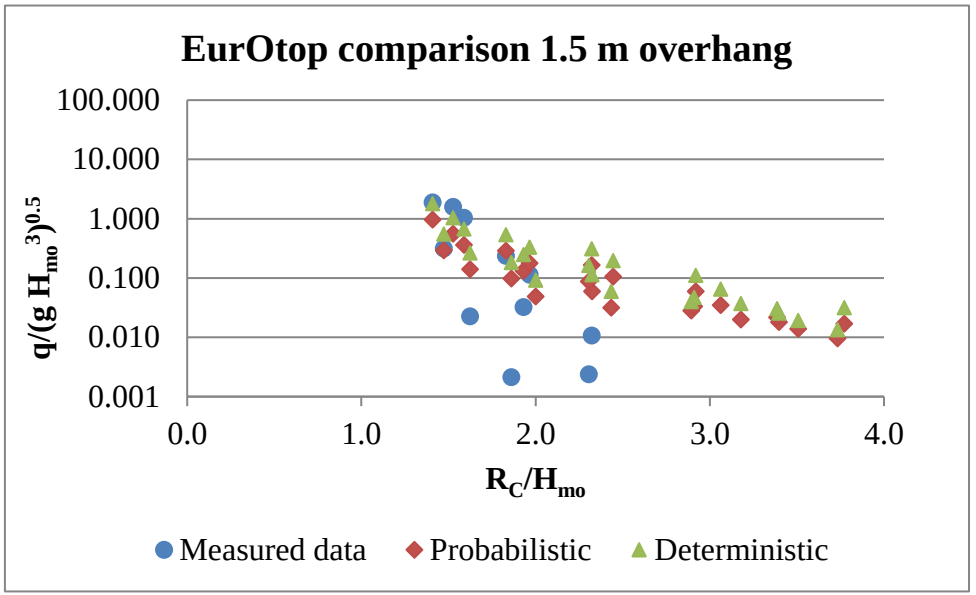

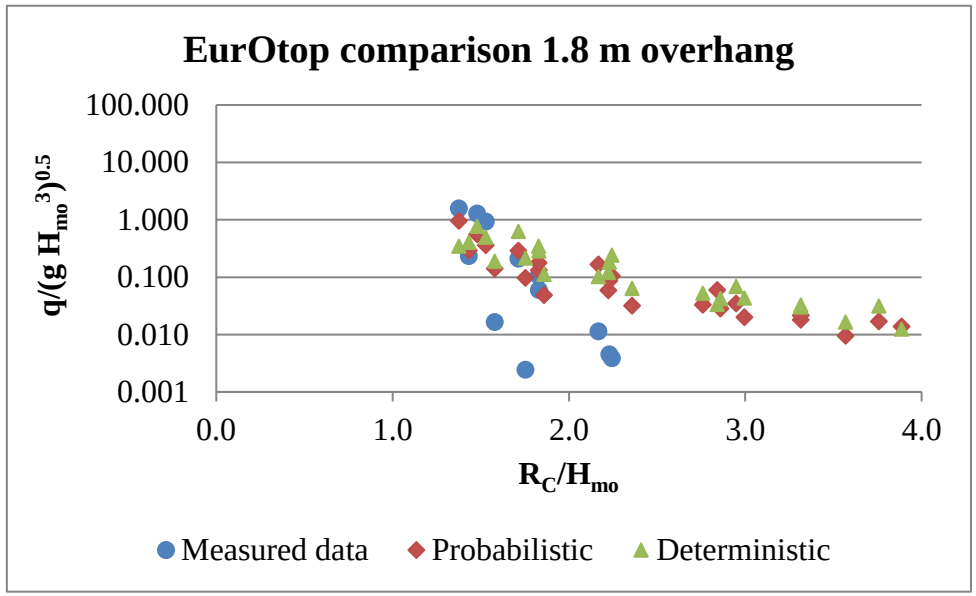

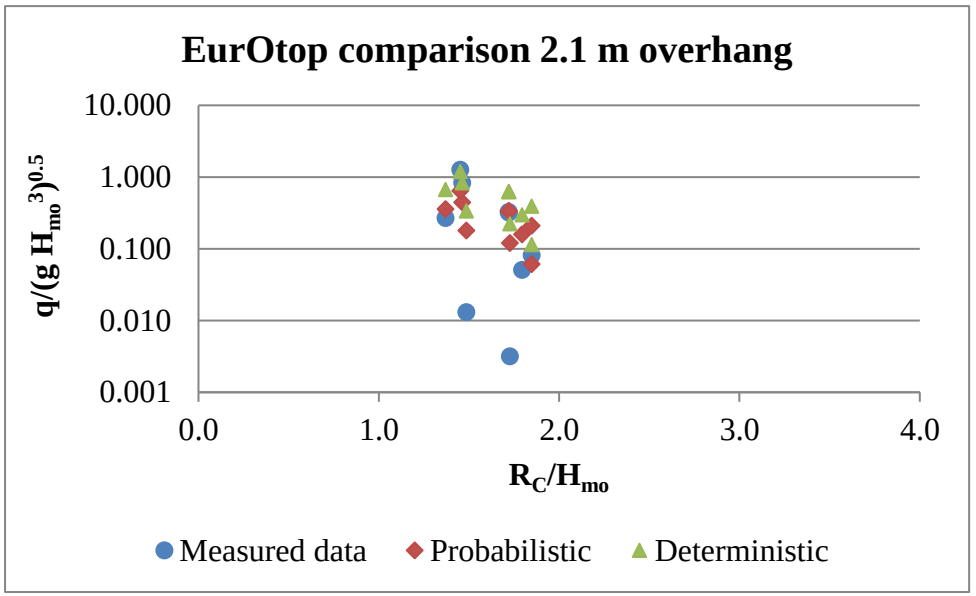

P: Reflection Analysis interface

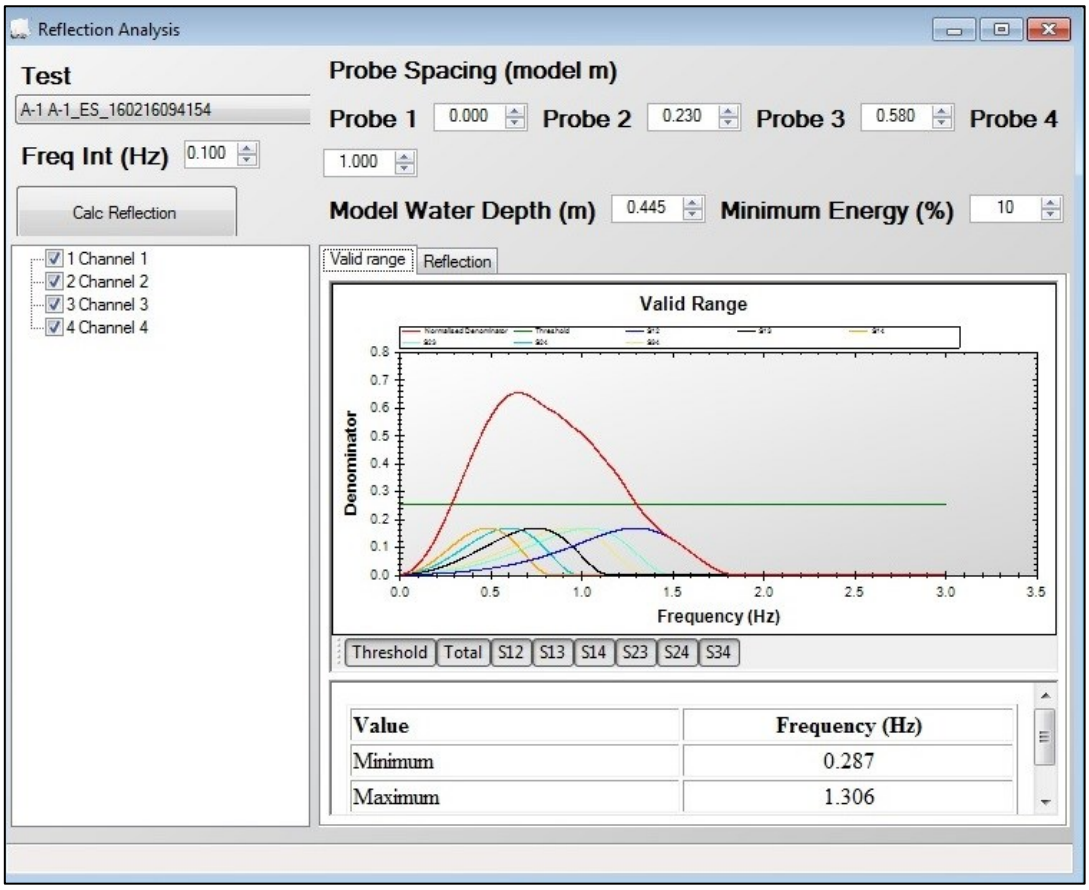

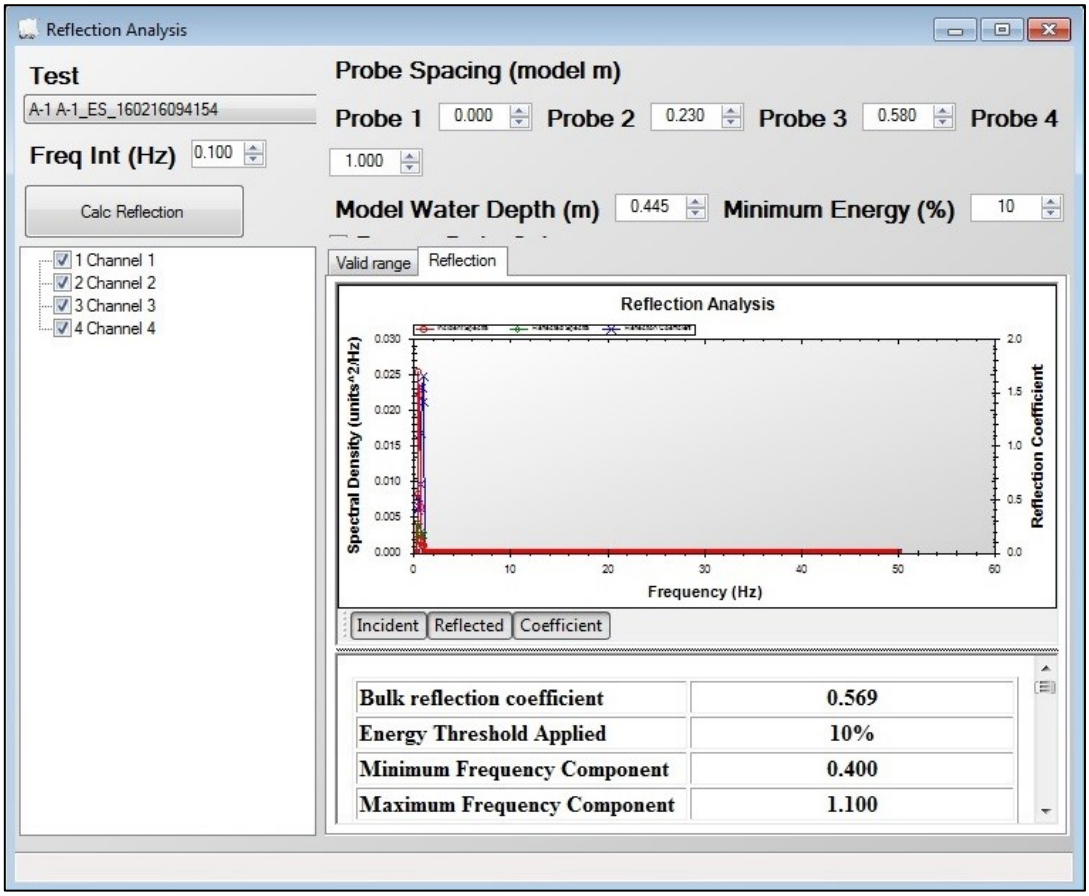

P: Probe temperature influence